

**AN IMPROVED SLIDING MODE CONTROL FOR VOLTAGE SOURCE
INVERTERS USING OPTIMAL SURFACE SELECTION MECHANISM**



FAHEEM HAROON
01-281172-005

A thesis submitted in fulfilment of the
requirements for the award of degree of
Doctor of Philosophy (Electrical Engineering)

Department of Electrical Engineering
BAHRIA UNIVERSITY ISLAMABAD

02 September, 2024

Approval for Examination

Scholar's Name : Faheem Haroon

Registration Number: 8261

Enrollment: 01-281172-005

Program of Study: PhD in Electrical Engineering

Thesis Title: AN IMPROVED SLIDING MODE CONTROL FOR VOLTAGE

SOURCE INVERTERS USING OPTIMAL SURFACE SELECTION MECHANISM

It is to certify that the above scholar's thesis has been completed to my satisfaction and, to my belief, its standard is appropriate for submission for examination. I have also conducted plagiarism test of this thesis using HEC prescribed software and found similarity index 11 %. that is within the permissible limit set by the HEC for the MS/M.Phil degree thesis. I have also found the thesis in a format recognized by the BU for the MS/M.Phil thesis.



Principal Supervisor Signature: _____

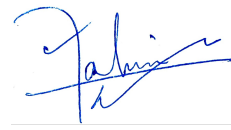
Date: 02 September, 2024

Name: Dr. Asad Waqar

Author's Declaration

I, **Faheem Haroon** hereby state that my PHD thesis titled "AN IMPROVED SLIDING MODE CONTROL FOR VOLTAGE SOURCE INVERTERS USING OPTIMAL SURFACE SELECTION MECHANISM" is my own work and has not been submitted previously by me for taking any degree from Bahria University, or anywhere else in the country/world.

At any time if my statement is found to be incorrect even after my graduation, the University has the right to withdraw/cancel my PHD degree.



Name of Scholar: Faheem Haroon

Date: 02 September, 2024

Plagiarism Undertaking

I, solemnly declare that research work presented in the thesis titled "AN IMPROVED SLIDING MODE CONTROL FOR VOLTAGE SOURCE INVERTERS USING OPTIMAL SURFACE SELECTION MECHANISM" is solely my research work with no significant contribution from any other person. Small contribution / help wherever taken has been duly acknowledged and that complete thesis has been written by me.

I understand the zero tolerance policy of the HEC and Bahria University towards plagiarism. Therefore I as an Author of the above titled thesis declare that no portion of my thesis has been plagiarized and any material used as reference is properly referred / cited.

I undertake that if I am found guilty of any formal plagiarism in the above titled thesis even after award of MS/M.Phil degree, the university reserves the right to withdraw / revoke my MS/M.Phil degree and that HEC and the University has the right to publish my name on the HEC / University website on which names of scholars are placed who submitted plagiarized thesis.

Scholar/Author's Sign:  _____

Name of Scholar: Faheem Haroon

List of Publications

- i. **Faheem Haroon**, Muhammad Aamir, and Asad Waqar. "Second-Order Rotating Sliding Mode Control with Composite Reaching Law for Two Level Single Phase Voltage Source Inverters." IEEE Access 10 (2022): 60177-60188.
[Impact Factor: 3.746]
- ii. **Faheem Haroon**, Muhammad Aamir, Assad Waqar, Saeed Mian Qaisar, Syed Umaid Ali, and Abdulaziz Turki Almaktoom. "A Composite Exponential Reaching Law Based SMC with Rotating Sliding Surface Selection Mechanism for Two Level Three Phase VSI in Vehicle to Load Applications." Energies 16, no. 1 (2022): 346. **[Impact Factor: 3.252]**

Dedication

To my beloved Mother and Father, with heartfelt gratitude and endless love.

Acknowledgements

During the course of preparing this thesis, I had the privilege of working with a diverse group of people, including researchers, academics, and practitioners. I am filled with profound gratitude for the invaluable contributions made by these individuals, which have significantly shaped my understanding and ideas. I am especially indebted to my thesis supervisors, Dr. Asad Waqar and Dr. Muhammad Aamir for their unwavering support, guidance, constructive criticism, their valuable guidance, and motivation.

In addition, I express my sincere gratitude for the valuable assistance provided by the Library and Laboratory staff at Bahria University for providing me with the necessary literature and technical resources. I am also grateful to Dr. Abdulaziz Turki Almaktoom and Dr. Saeed Mian Qaisar for their technical support during this journey and to my fellow postgraduate students, especially Engr. Syed Umaid Ali for their support, and to my colleagues and others who have provided me with helpful tips and insights along the way. While it is impossible to name each one of them, individually, I want to extend my appreciation to all of them.

I am also deeply grateful to U.S.-PAKISTAN Center For Advanced Studies In Energy (USPCASE), National University of Sciences and Technology (NUST). They not only provided me the opportunity to work in the Energy Conversion Lab (ECL) but also offered unwavering support throughout the implementation and analysis of the proposed system. Without their assistance, it would have been exceedingly challenging to carry out the experimental work successfully.

Finally, I am deeply grateful to my family members for their constant love and support throughout this journey. Without the support of all these individuals, this thesis would not have been possible.

Abstract

In the present era, the integration of Distributed Generation (DG) into power systems has become possible through power electronic interfaces like Voltage Source Inverters (VSIs). With the integration of effective control strategies, VSIs serve to provide reliable and high-quality power supply that meets the needs of various applications in today's dynamic world, including Uninterruptible Power Supplies (UPS), Electric Vehicles (EVs), power quality improvement, motor drives, active power filters, grid-tied solar inverters, laboratory power supplies and lifesaving equipment in hospitals or at emergency fields. This dissertation presents a cutting-edge approach for regulating output voltage in AC microgrids (MGs), using the robust control technique i.e. Sliding Mode Control (SMC). Despite the recognized feature of robustness, SMC is prone to a phenomenon called chattering along the sliding surface, which manifests as rapid and unwanted oscillations. Chattering can result in increased power losses and decreased efficiency in the VSIs, leading to higher energy consumption and reduced system effectiveness. To address this concern, an adaptive sliding surface selection mechanism is implemented here, that incorporates the advantages of the Rotating Sliding Surface (RSS) technique, along with a novel reaching law based on the magnitude of state variables, which enables the adjustment of the control gain value. The composite reaching law proposed in the study integrates three distinct functions i.e. exponential, power, and difference functions. The intelligent mix of these functions makes the law more effective in achieving both high-speed convergence rate of system states and significant reduction in chattering. In this approach, the sliding surface is selected using a time-varying slope based on error variables. The effectiveness of the proposed SMC method, that uses a Composite Exponential Reaching Law with a Rotating Sliding Surface (C-ERL-RSS) has been studied in comparison to two existing methods i.e. Cosine Exponential Reaching Law (Cos-ERL) SMC and Fractional Power Rate Reaching (FPRRL) SMC. The study was conducted on a single-phase VSI with varying load followed by input voltage and parametric disturbances, and the results showed that the new method outperformed the existing ones, with very low percentage of Total Harmonic Distortion %THD i.e. 0.25% and high voltage regulation of 99.9%, reduced chattering, and minimum tracking time. Moreover, the proposed C-ERL-RSS SMC, along with the Power Rate Exponential Reaching Law (PRERL) SMC, Enhanced Exponential Reaching Law (EERL) SMC, and Repetitive Reaching Law (RRL) SMC, are implemented on a two-level three-phase VSI under variable load conditions. The comparative analysis highlights the efficiency and authenticity of the proposed reaching law in achieving a stable output voltage with improved robustness, reduced chattering, low %THD of 1.1% and high voltage regulation of 99.83%. On top of it, the performance of the proposed C-ERL-SMC is evaluated experimentally on Hardware In Loop (HIL) setup comprising Opal-RT and MicroLabBox-dSPACE 1202. The proposed technique responded exceptionally well in voltage regulation of 99.8% under extreme conditions with fast transient response and low %THD of 3.23%.

TABLE OF CONTENTS

AUTHOR’S DECLARATION	ii
PLAGIARISM UNDERTAKING	iii
LIST OF PUBLICATIONS	iv
DEDICATION	v
ACKNOWLEDGEMENTS	vi
ABSTRACT	vii
LIST OF TABLES	xi
LIST OF FIGURES	xii
LIST OF SYMBOLS	xvii
LIST OF APPENDICES	xviii
1 INTRODUCTION	xix
1.1 Research Gaps	xxi
1.2 Research Problem	xxii
1.3 Research Objectives	xxii
1.4 Key Contributions	xxii
1.5 Thesis Organization	xxiv
2 LITERATURE REVIEW	2
2.1 Voltage Source Inverters (VSI)	3
2.1.1 Single Phase/Three Phase Voltage Source Inverters	4
2.2 Control for Voltage Source Inverters	5
2.3 Classification of VSIs	6
2.3.1 Grid Forming Voltage Source Inverters (GF-VSI)	6
2.3.2 Grid Feeding Voltage Source Inverters (GFe-VSI)	7
2.3.3 Grid Supporting Voltage Source Inverters (GS-VSIs)	9
2.4 Robust Control	10
2.4.1 Robust Control vs Conventional Control:	12
2.4.2 Robust Control Methods for VSIs	19

2.4.2.1	State Space Control Methods	19
2.4.2.2	Hierarchical control methods:	20
2.4.3	Robust Proportional Integral Derivative (PID) Controller:	21
2.4.3.1	H_{∞} based control method:	21
2.4.3.2	Backstepping-Based Control Methods:	22
2.4.3.3	Droop Control Method:	22
2.4.3.4	Sliding Mode Control (SMC)-Based Control Methods:	23
2.5	Sliding Mode Control (SMC)	27
2.5.1	Variable Structure Control	27
2.5.2	SMC Fundamental Theory and Methodologies	28
2.5.3	Lyapunov Stability Condition	29
2.5.3.1	Reachability Condition	29
2.5.4	Sliding Mode Control Design	30
2.5.4.1	Sliding Surface Design	30
2.5.5	Salient Features of SMC	33
2.5.6	Challenges Associated with SMC Design	33
2.6	Chattering Reduction Techniques	34
2.6.1	Boundary Layer Approach	34
2.6.2	Dynamic SMC Approach	35
2.6.3	Second Order SMC (SoSMC)	35
2.6.4	Super Twisting Algorithm Approach	36
2.6.5	Higher Order SMC (HoSMC)	37
2.6.6	Terminal SMC (TSMC)	39
2.6.7	Intelligent SMC Approach	41
2.6.8	State Observer Approach	42
2.6.9	Reaching Law Approach	43
2.6.9.1	Seminal Gao and Hung Reaching Laws	43
2.6.9.2	Exponential Reaching Law	44
2.6.9.3	Cos-Exponential Reaching Law	45
2.6.9.4	Power Rate Exponential Reaching Law	45
2.6.9.5	Enhanced Exponential Reaching Law	46
2.6.9.6	Fractional Power Rate Reaching Law	46
2.6.9.7	Hybrid Reaching Law	46
2.6.9.8	Piecewise Double Power Reaching Law	47
2.7	SMC for AC VSIs	47
2.7.1	Stand-alone VSI	47
2.7.2	Grid-tied AC VSIs	48
2.7.3	Critical Review	49
2.7.3.1	Sliding Surface Design/Sliding coefficient Selection	50
2.7.3.2	Reaching Law Design	52
2.7.4	Practical Applications of SMC based VSIs	55
2.7.5	Summary	56

3 RESEARCH METHODOLOGY

3.0.1	Step-I : Sliding Surface Design	58
3.0.1.1	Optimal Surface based on Rotating Sliding Surface (RSS)	59
3.0.2	Step-II : Reaching Law Design:	59
3.0.2.1	Proposed Composite Exponential Reaching Law(C-ERL)	60
3.0.2.2	Working Principle	60
3.0.2.3	Stability Analysis	60
3.0.3	Comparative Analysis of C-ERL With Other State-of-the Art Reaching Laws	61
3.1	Proposed C-ERL-RSS SMC for single phase VSI	65
3.1.1	System Modeling	66
3.1.2	Proposed SMC with C-ERL-RSS	67
3.2	Proposed C-ERL-RSS SMC for three phase VSI	69
3.2.1	System Modeling	69
3.2.2	Proposed SMC with C-ERL and RSS	70
3.3	Summary	73
4	RESULTS AND ANALYSIS	75
4.1	Performance analysis of the proposed C-ERL-RSS SMC for VSIs under disturbance conditions	75
4.1.1	Performance Analysis of Single Phase VSI on MATLAB Simulink	75
4.1.2	Performance Analysis of Three Phase VSI on MATLAB Simulink	84
4.1.3	Experimental validation of proposed C-ERL-RSS for VSI on Hardware in Loop (HiL) setup	90
4.2	Performance analysis of optimal surface selection	93
4.2.1	Surface selection analysis for Single Phase VSI	93
4.2.2	Surface selection analysis for Three Phase VSI	95
4.3	Performance analysis under input voltage disturbances	97
4.4	Performance analysis under filter and input voltage disturbances	100
4.5	Summary	108
5	SUMMARY , CONCLUSION AND FUTURE PROSPECTS	116
5.1	Summary	116
5.2	Conclusion	118
5.3	Future Prospects	118
	REFERENCES	119
A	APPENDIX ONE	141

LIST OF TABLE

2.1	Comparison of Grid Forming (GS), Grid-Feeding (GFe) and Grid Supporting (GS)-VSIs	11
2.2	Comparison of robust controllers and conventional controllers	18
2.3	Robust Control methods for AC VSIs.	25
2.4	Comparision of three different SMC methods	40
2.5	SMC applications for VSIs (islanded and grid-connected).	49
3.1	Reaching Laws with parametric values	62
3.2	Comparison of reaching laws in terms of robustness and chattering.	63
3.3	Comparison of Proposed C-ERL-RSS With Cos-ERL[1] and FPRRL[2]	66
4.1	Parameters of controllers.	76
4.2	Circuit Specifications.	81
4.3	Comparison of proposed C-ERL-RSS SMC [3] with Cos-ERL [1], FPRRL [2] and RSS [4] SMC.	85
4.4	Circuit Specifications for three phase.	90
4.5	Comparison of the proposed composite reaching law with other state-of-the art reaching laws.	91
4.6	Robust behavior under extreme conditions of input voltage disturbances and load disturbances.	100
4.7	Robust behavior of proposed C-ERL-RSS SMC under extreme conditions of input voltage disturbances of 400V till 0.045 secs that changes to 450V from (0.045 secs to 0.105 secs) and finally shifts to 500V from 0.105 secs to 0.15 secs, load disturbances of FL to NL and NL to FL and filter inductor disturbances of $\pm 10\%$ of rated values of filter capacitor and inductor.	108

LIST OF FIGURE

2.1	Block Diagram: Microgrid system’s classification [5]	3
2.2	Voltage Source Inverter (VSI)	3
2.3	Single Phase Voltage Source Inverter (SPVSI)	4
2.4	Three Phase Voltage Source Inverter	5
2.5	Voltage Source Inverter with Control	6
2.6	Grid Forming Inverter [6]	7
2.7	Grid Feeding Inverter [6]	8
2.8	Grid Supporting Inverter-Current Source [6]	9
2.9	Grid Supporting Inverter-Voltage Source [6]	10
2.10	Variable Structure Control	28
2.11	Phases Associated With SMC [7]	30
2.12	Time Varying Sliding Coefficient [7]	32
2.13	Dynamic SMC Approach [8]	35
2.14	Super Twisting Algorithm Approach [9]	37
2.15	State Observer Approach [10]	43
2.16	Block Diagram of AC Microgrid with SMC System [11]	48
3.1	Comparison of Reaching Laws Gain variation w.r.t distance from surface.	61
3.2	Tradeoff-tracking time vs chattering for Cos-ERL[1] with low value of gain.	63
3.3	Tradeoff-tracking time vs chattering for Cos-ERL[1] with high value of gain.	64
3.4	Tradeoff-tracking time vs chattering for FPRRL[2] with low value of gain.	64
3.5	Tradeoff-tracking time vs chattering for FPRRL[2] with high value of gain.	64
3.6	Trade-off-tracking time vs chattering for proposed C-ERL-RSS with low value of gain.	65
3.7	Trade-off-tracking time vs chattering for proposed C-ERL-RSS with high value of gain.	65
3.8	Single phase Voltage Source Inverters(VSIs).	66
3.9	Block diagram of single phase VSI with proposed C-ERL-RSS.	67
3.10	SMC with proposed C-ERL-RSS.	67
3.11	Three phase VSI with the proposed reaching law based SMC.	69
4.1	SPVSI output voltage and non-linear load current with Cos-ERL (Full Load to No Load) [1].	77
4.2	Voltage output reference tracking with Cos-ERL (Full Load to No Load) [1].	77

4.3	Output Voltage waveform-Tracking Evolution with Cos-ERL (Full Load to No Load Zoomed View) [1].	77
4.4	FFT analysis of output voltage with Cos-ERL[1].	78
4.5	SPVSI output voltage and non-linear load current with FPRRL (Full Load to No Load) [2].	78
4.6	Voltage output reference tracking with FPRRL (Full Load to No Load) [2].	78
4.7	Output Voltage waveform-Tracking Evolution with FPRRL (Full Load to No Load Zoomed View) [2].	79
4.8	FFT analysis of output voltage with FPRRL [2].	79
4.9	SPVSI output voltage and non-linear load current with proposed C-ERL-RSS [3] (Full Load to No Load)	79
4.10	FFT analysis of output voltage with CERLRSS [3].	80
4.11	Voltage output reference tracking with proposed C-ERL-RSS [3] (Full Load to No Load).	80
4.12	Output Voltage waveform-Tracking Evolution with proposed C-ERL-RSS [3] (Full Load to No Load Zoomed View)	80
4.13	SPVSI output voltage and non-linear load current with Cos-ERL (No Load to Full Load) [1]	81
4.14	Voltage output reference tracking with Cos-ERL (No Load to Full Load) [1].	82
4.15	Output voltage waveform-Tracking Evolution with Cos-ERL (No Load to Full Load Zoomed View)[1].	82
4.16	Voltage output reference tracking with FPRRL (No Load to Full Load) [2].	82
4.17	Voltage output reference tracking with FPRRL (No Load to Full Load) [2].	83
4.18	Output voltage waveform-tracking evolution with FPRRL SMC [2].	83
4.19	SPVSI output voltage and non-linear load current with proposed C-ERL-RSS [3] (No Load to Full Load).	83
4.20	Voltage output reference tracking with proposed C-ERL-RSS [3] (No Load to Full Load).	84
4.21	Output voltage waveform-tracking evolution with C-ERL-RSS [3]. (No Load to Full Load).	84
4.22	(a) PRERL[12], output voltage-reference tracking trajectory and voltage regulation. (b) PRERL[12], load current-step response under no load to full load condition.	85
4.23	(a) RRL[13], output voltage-reference tracking trajectory and voltage regulation. (b) RRL[13], load current-step response under no load to full load condition.	86
4.24	(a) EERL[14], output voltage-reference tracking trajectory and voltage regulation. (b) EERL[14], load current-step response under no load to full load condition.	87
4.25	(a) Proposed C-ERL-RSS, output voltage-reference tracking trajectory and voltage regulation. (b) Proposed C-ERL-RSS, load current-step response under no load to full load condition [15].	87

4.26 (a) PRERL[12], output voltage-reference tracking trajectory and voltage regulation. (b) PRERL[12], load current-step response under full load to no load condition.	88
4.27 (a) RRL[13], output voltage-reference tracking trajectory and voltage regulation. (b) RRL[13], load current-step response under full load to no load condition.	88
4.28 (a) EERL[14], output voltage-reference tracking trajectory and voltage regulation. (b) EERL[14], load current-step response under full load to no load condition.	89
4.29 (a) Proposed C-ERL-RSS, output voltage-reference tracking trajectory and voltage regulation. (b) Proposed C-ERL-RSS, load current-step response under full load to no load condition [15].	89
4.30 Experimental setup: Hardware in Loop (HiL) comprising Opal-RT 4200 and microLabBox dSPACE 1202	91
4.31 Response of the proposed C-ERL-RSS for sudden voltage reference variation from 200v to 100v	92
4.32 Response of the proposed C-ERL-RSS for load disturbance of full load to no load at 4.59 sec.	92
4.33 Response of the proposed C-ERL-RSS for load disturbance of no load to full load at 1.195 sec	93
4.34 Surface selection analysis for cos-ERL [1] (No Load to Full Load).	94
4.35 Surface selection analysis for cos-ERL [1] (Full Load to No Load).	94
4.36 Surface selection analysis for FPRRL [2] (No Load to Full Load).	94
4.37 Surface selection analysis for FPRRL [2] (Full Load to No Load).	95
4.38 Surface selection analysis for proposed C-ERL-RSS (No Load to Full Load).	95
4.39 Surface selection analysis for proposed C-ERL-RSS (Full Load to No Load).	96
4.40 Surface selection analysis for RRL [13] (No Load to Full Load).	96
4.41 Surface selection analysis for RRL [13] (Full Load to No Load).	96
4.42 Surface selection analysis for PRERL [12] (No Load to Full Load).	97
4.43 Surface selection analysis for PRERL [12] (Full Load to No Load).	97
4.44 Surface selection analysis for EERL [14] (No Load to Full Load).	98
4.45 Surface selection analysis for EERL [14] (Full Load to No Load).	98
4.46 Surface selection analysis for proposed C-ERL-RSS (No Load to Full Load).	98
4.47 Surface selection analysis for proposed C-ERL-RSS (Full Load to No Load).	99
4.48 Input Voltage with disturbances.	100
4.49 Output voltage behaviour under input voltage disturbances i.e. 400 V at 0-0.045 secs, 450V at 0.045 secs to 0.105 secs and 550V at 0.105 secs to 0.15secs	101
4.50 Output voltage and current behaviour of the CosERL SMC [1] under input voltage disturbances (400V at (0-0.045secS), 450V at (0.045secs-0.105sec) and 500V at (0.105secs-0.15secs). With FL to NL and NL to FL conditions at 0.045secs and 0.105secs, respectively.	102

4.51	Output voltage and current behaviour of the FPRRL SMC [2] under input voltage disturbances (400V at (0-0.045secS), 450V at (0.045secs-0.105sec) and 500V at (0.105secs-0.15secs). With FL to NL and NL to FL conditions at 0.045secs and 0.105secs, respectively.	103
4.52	Output voltage and current behaviour of the proposed C-ERL-RSS SMC under input voltage disturbances (400V at (0-0.045secS), 450V at (0.045secs-0.105sec) and 500V at (0.105secs-0.15secs). With FL to NL and NL to FL conditions at 0.045secs and 0.105secs, respectively.	104
4.53	Output voltage and current behaviour of the CosERL SMC[1] under input voltage disturbances (400V at (0-0.045secS), 450V at (0.045secs-0.105sec) and 500V at (0.105secs-0.15secs). With NL to FL and FL to NL conditions at 0.045secs and 0.105secs, respectively.	105
4.54	Output voltage and current behaviour of the FPRRL SMC [2] under input voltage disturbances (400V at (0-0.045secS), 450V at (0.045secs-0.105sec) and 500V at (0.105secs-0.15secs). With NL to FL and FL to NL conditions at 0.045secs and 0.105secs, respectively.	106
4.55	Output voltage and current behaviour of the proposed C-ERL-RSS SMC under input voltage disturbances (400V at (0-0.045secS), 450V at (0.045secs-0.105sec) and 500V at (0.105secs-0.15secs). With NL to FL and FL to NL conditions at 0.045secs and 0.105secs, respectively.	107
4.56	Output voltage and current behaviour of the proposed C-ERL-RSS SMC under filter disturbances at rated value of 15mH of inductor and +10% of 48uF (52.8uF) of a capacitor along with input voltage disturbances (400V at (0-0.045secS), 450V at (0.045secs-0.105sec) and 500V at (0.105secs-0.15secs). With FL to NL and NL to FL conditions at 0.045secs and 0.105secs, respectively.	109
4.57	Output voltage and current behaviour of the proposed C-ERL-RSS SMC under filter disturbances of +10% of 15mH (16.5mH) inductor and 48uF of rated capacitor along with input voltage disturbances (400V at (0-0.045secS), 450V at (0.045secs-0.105sec) and 500V at (0.105secs-0.15secs). With FL to NL and NL to FL conditions at 0.045secs and 0.105secs, respectively.	110
4.58	Output voltage and current behaviour of the proposed C-ERL-RSS SMC under filter disturbances of -10% of 15mH (13.5mH) inductor and value of 48uF of a capacitor along with input voltage disturbances (400V at (0-0.045secS), 450V at (0.045secs-0.105sec) and 500V at (0.105secs-0.15secs). With FL to NL and NL to FL conditions at 0.045secs and 0.105secs, respectively.	111
4.59	Output voltage and current behaviour of the proposed C-ERL-RSS SMC under filter disturbances 15mH inductor and -10% 48uF (43.2uF) of a capacitor along with input voltage disturbances (400V at (0-0.045secS), 450V at (0.045secs-0.105sec) and 500V at (0.105secs-0.15secs). With FL to NL and NL to FL conditions at 0.045secs and 0.105secs, respectively. .	112

4.60	Output voltage and current behaviour of the proposed C-ERL-RSS SMC under filter disturbances -10% of 15mH inductor (13.5mH) and -10% 48uF (43.2uF) of a capacitor along with input voltage disturbances (400V at (0-0.045secS), 450V at (0.045secs-0.105sec) and 500V at (0.105secs-0.15secs). With FL to NL and NL to FL conditions at 0.045secs and 0.105secs, respectively.	113
4.61	Output voltage and current behaviour of the proposed C-ERL-RSS SMC under filter disturbances +10% of 15mH (16.5mH) inductor and +10% 48uF (52.8uF) of a capacitor along with input voltage disturbances (400V at (0-0.045secS), 450V at (0.045secs-0.105sec) and 500V at (0.105secs-0.15secs). With FL to NL and NL to FL conditions at 0.045secs and 0.105secs, respectively.	114

LIST OF ABBREVIATIONS

SMC	–	Sliding Mode Control
DG	–	Distributed Generation
EES	–	Electrical Energy Storage
VSC	–	Voltage Source Converter
DER	–	Distributed Energy Resources
PCC	–	Point of Common Coupling
MG	–	Microgrids
UPS	–	Uninterrupted Power Supply
PLL	–	Phase Locked Loop
RES	–	Renewable Energy Sources
BESS	–	Battery Energy Storage System
VSS	–	Variable Structure Systems
VSC	–	Variable Structure Control
LTI	–	Linear Time Invariant
SoSMC	–	Second order Sliding Mode Control
HoSMC	–	Higher order Sliding Mode Control
TSMC	–	Terminal Sliding Mode Control
ERL	–	Exponential Reaching Law
PRERL	–	Power Rate Exponential Reaching Law
EERL	–	Enhanced Exponential Reaching Law
FPRRL	–	Fractional Power Rate Reaching Law Reaching Law
FTSMC	–	Fast Terminal Sliding Mode Control
RSS	–	Rotating Sliding Surface
C-ERL	–	Composite Exponential Reaching Law
VSI	–	Voltage Source Inverter
RRL	–	Repetitive Reaching Law

LIST OF APPENDICES

APPENDIX ONE

141

CHAPTER 1

INTRODUCTION

Voltage Source Inverter(VSI) is the most momentous element of several advanced applications. That covers wide range of utilization starting from tiny car adopters, households, many industrial applications to large grid systems. Speedy and frequent advances in the field of science and technology, aerospace, communication, defense sector,hospitals and power storage system requires high quality power supply. Moreover, an unexpected interruptions and outages may lead to storage loss, program destruction or even malfunctioning of power system equipment. Therefore, a well-regulated, clean and continuous power supply is of great importance. Several type of Voltage Source Inverters have been applied so far to achieve controlled quality power exchange between different energy sources in Distributed Generation (DG) like photovoltaic (PV) and wind generation systems. According to a report presented by the International Energy Agency (IEA) at the World Economic Forum in March 2023 [16], renewable energy capacity is projected to account for 35% of global power generation by 2025. Pakistan, in particular, has significant potential for generating solar and wind power. The World Bank reports that utilizing just 0.071 percent of Pakistan's area for solar PV power generation could meet the country's current electricity demand. Furthermore, Pakistan aims to increase the share of renewable energy in its electricity mix to 20% by 2025 and 30% by 2030 [17]. The 2030 Agenda for Sustainable Development, adopted by all United Nations Member States in 2015, provides a shared blueprint for achieving peace and prosperity for people and the planet. Central to this agenda are the 17 Sustainable Development Goals (SDGs), which call for urgent action by all countries [18]. This study specifically focuses on SDGs 7.1, 7.2, and 7.3.

DGs plays pivotal role in the development of today's power systems. However, constrains, primarily associated with supplied voltage stability and power flow limitations, raises serious concerns regarding reliability of such mechanism of generation with increasing integration of DGs into the power system [19]. This is due to one of the major facts that DGs have been initially treated as supplementary generating units, comprising minimal level of control from the transmission and distribution system operators. That leads to principally passive and least flexible distribution networks, having no chance of insulating particular section to operate as microgrids (MG) when grid encounters faults and unforeseen incidents. However, the operation of grid can be achieved in more flexible and efficient manner through integration of DGs into the system. Furthermore, smart integration of DGs equipped with proper control and energy storage devices pave ways and

widens the scope of associated services, along with ensuring uninterrupted power supply, through creation of active islands, termed as MG, activated by local generating units [20]. Therefore, it is highly anticipated that MG are going to perform key role in shaping future electrical grids, through addition of DGs at low voltage distribution networks.

A Microgrid (MG) can be envisioned as a small-scale grid, formed by the electrical integration of Distributed Generation (DG) systems, storage devices, and loads, all managed by a hierarchical control mechanism. It is worth noting here that among available renewable sources, PVs and wind are considered more suitable generators for integration in MG, that is due to their smaller size and scalability than central power plants, with a potential to be connected at any part of power systems [21]. Similarly, other non-renewable sources like diesel or gas fuelled etc., can also be integrated into the MG [22]. Moreover, MG has the capability to operate in both grid connected and islanded mode [23]. In either mode of operation, it is always desired that MG must operate to achieve high degree of reliability to ensure stable and constant power supply.

All these applications and sensitivity associated with the reliable and safe performance of MG generally and VSIs specifically calls for exceptionally reliable control and an effective response mechanism to handle any credible contingency. Therefore, an efficient control mechanism for VSI must be designed to fulfill multiple objectives, first of all, the controller must guarantee flawless reference tracking with good disturbance rejection capability. This results in a well-regulated output voltage with minimal %THD under both linear and non-linear loads. Secondly, good dynamic response during load varying conditions is highly desired [21]. It is a common observation that under the condition of heavy load for VSIs, the transient response of the controller is severely affected [24]. Thus, the controller for Voltage Source Inverter must be capable of achieving the above-mentioned objectives during unexpected output load variations.

Moreover, in order to cater financial and environmental concerns VSI based systems are working very near to stability constraints. However, ensuring a stable, reliable, and effective VSI's output for sensitive systems, especially MG, is still a challenging task. Therefore, a control system for VSIs must be designed to achieve the aforementioned objectives. Thus, to serve the purpose, a well-known effective control methods have been extensively applied on VSI based-system, specially MG. Conventional controllers, such as Proportional Integral (PI), Proportional Resonant (PR), Proportional Integral Derivative (PID), and various robust controllers like H_∞ , Back-stepping control, and Model Predictive Control (MPC), are notably used for VSIs. A detailed comparative analysis of these control techniques and the significance of robust controllers for VSIs is discussed in Table 2.3 and Table 2.2. From the available robust control techniques, to the best of our knowledge, Sliding Mode Control (SMC) is found to be the most effective control technique for VSIs. SMC is a non-linear controller derived from the continuous-time variable structure control theory and was introduced initially in 1950 in Russia by Emelyanov and several other co-researchers [25], [26]. SMC has some inherent properties like simple design, reduced order, and exceptional robustness. Moreover, SMC is insensitive to external disturbances and parametric variations, finite time convergence, and excellent dynamic behavior. Due to exponential robustness, SMC has been studied extensively for the first time in the theoretical research domain [27] and later on applied to industrial applications

[28]. Due to its inherent characteristics, SMC is a widely adopted technique in several non-linear systems, including VSI applications. In SMC, the sliding surface is selected such that states of the system are compelled to reach the sliding surface in a limited time. With this, system dynamics become linear time-varying stable, having negligible internal or external disturbances. Irrespective of asymptotic convergence of states to the sliding surface, like other non-linear control techniques, SMC suffer from few imperfections.

In this perspective, two major areas need utmost attention. The first major shortcoming that SMC suffers is related to a fixed sliding surface that restricts the dynamic behavior of the feedback system. The fixed value of the sliding surface slope is a compromise between tracking time under output current disturbances and the reaching time of the system states to the sliding surface [4]. The second shortcoming is that SMC often uses a high value of switching gains to achieve robustness. The choice of high gains can lead to severe problems related to chattering [29]. As a matter of fact, chattering has extremely adverse effect of overheating on VSI switches. To handle these challenges, several state-of-the-art scholarly works have been done so far. However, the reaching law technique is found to be the most effective in achieving fast reaching time and guaranteeing robustness, while causing chattering along the surface if the reaching gain is not managed properly.

1.1 Research Gaps

Multiple limitations found in existing SMC techniques are discussed at length in the literature review section. The most relevant of these limitations are listed below. These challenges motivate the development of a new and improved version of SMC to further enhance the convergence rate of system states to the equilibrium point with maximum chattering reduction and low %THD.

- i. Research contributions introduced to target draw backs associated with fixed sliding surface through emphasizing sliding surface design by adjusting the sliding coefficient value to maintain optimal balance between reaching time and tracking time. However, the well-known features of interest for VSI applications like %THD, robustness and voltage regulation along with unwanted chattering at the sliding surface that causes overheating at the inverter switches, were overlooked.
- ii. Scholarly efforts have primarily focused on crafting reaching laws to attain robustness and fast transient response, while minimizing chattering magnitude along the surface to achieve enhanced voltage regulation with high %THD. Nevertheless, concentrating solely on the design of reaching laws with a fixed sliding surface gives rise to shortcomings such as constraining the dynamic response of the closed-loop control mechanism for VSIs. In other words, a smaller sliding coefficient value leads to extended tracking time, whereas higher reaching time is encountered with elevated sliding coefficient values. Similarly, an excessively high sliding coefficient value can result in overshooting of the output voltage.
- iii. To fully harness the inherent advantages of SMC for VSIs, it's crucial to concurrently address both sliding surface design and reaching law formulation. However,

this comprehensive approach is notably absent in the existing scholarly endeavors.

1.2 Research Problem

The shortcomings highlighted under the section of research gaps leads to the formulation of following research problem:

”The efficiency of SMC for VSI applications is compromised due to exclusive concentration on one of its crucial design phases, either the sliding surface design or the reaching law formulation.”

1.3 Research Objectives

Based on the insights gained from an extensive review of the existing body of literature, the identified gaps have led to the establishment of the research objectives, which are as follows:

- i. Develop an optimal sliding surface selection mechanism for enhanced stability with improved balance between Tracking Time and Reaching Time for single phase and three phase VSI.
- ii. Devise an effective reaching law technique that optimally balances robustness, fast transient response and voltage regulation in single phase and three phase VSI, thereby mitigating chattering effect while ensuring low %THD.
- iii. Develop an integrated approach to achieve an improved SMC that addresses both optimal sliding surface design mechanism and effective reaching law formulation in VSI applications.

1.4 Key Contributions

Motivated by the limitations found in existing scholarly work related to SMC for VSIs and MG, salient contributions of this dissertation can be summarized as:

- i. A composite SMC technique is proposed using rotating sliding coefficient selection method based on single input fuzzy logic control (SIFLC) and exponential reaching law comprising cos function integrated with difference and power function. The smart integration of these functions results in achieving improved convergence rate to guarantee robustness without effecting chattering mitigation. The proposed SMC termed as Composite Exponential Reaching Law with Rotating Siding Surface (C-ERL-RSS) is extremely adaptive concerning the distance of system states from the sliding surface, i.e. at a longer distance, the magnitude of gain is higher to achieve robustness. While, as the system states approach the equilibrium point, the proposed law ensures that the gain magnitude is reduced to prevent chattering along the sliding surface. Behavior of the proposed C-ERL-RSS SMC control is tested on a second order system to examine responses with a high and low value of gains. Moreover, Cos-ERL[1] and FPRRL[2] were also tested on the same system, and

it is shown that at different values of gains, the proposed system behaves best in achieving fast convergence rate with reduced chattering i.e. 1212% increase in the convergence rate with just 10% increase in chattering, when applied to high and low value of gain.

- ii. The proposed C-ERL-RSS SMC technique is designed and applied on single phase VSI system under variable non-linear load conditions with input voltage and parametric disturbances to achieve extremely fast convergence with little chattering and reduced %THD on Matlab Simulink. Keeping %THD to the minimum possible level is of core importance for VSI systems, this is due the facts highlighted by many scholarly works like [30] and [31]. Which states that harmonics causes over sizing of VSIs and cables due to de-rating of equipment. Moreover, harmonics reduces effective lifetime of inverter's equipment and cables. In addition to this, harmonics increase input apparent power demand increasing utility line losses. Last but not the least, voltage harmonics cause excessive temperature rise in motors, transformers, inductive load, and electrical noise to trip sensitive equipment. As per the IEEE Standards (IEEE 519-2022), Table-1 on page 17 specifies that systems with bus voltages of 1kV or lower have an acceptable %THD limit of 8% [32]. Following which, Cos-ERL[1] and FPRRL[2] were also implemented on the same single phase VSI system and their performances are compared with the proposed SMC. The comparative analysis revealed that the extremely low value of %THD, compared to the allowable limit of 8% and tracking time of 0.25% and 1msec, respectively, along with improved voltage regulation of 99.9% is achieved. Moreover, in order to examine the behavior and validate the performance of the proposed SMC technique, experimental tests are conducted using Hardware in Loop (HIL) setup comprising Opal-RT and MicroLabBox-dSPACE 1202 platform. The results obtained from these experiments, demonstrate promising performance and validates the effectiveness of the proposed SMC approach in demanding scenarios i.e. quite encouraging voltage regulation of 99.8% with low %THD of 3.23% is achieved.
- iii. The proposed C-ERL-RSS SMC approach is implemented on a three-phase VSI/Grid-forming MG system with a nonlinear rectifier load conditions to achieve extremely fast convergence with little chattering and reduced %THD on Matlab Simulink. The objective is to test and validate the dynamic and robust behavior of the proposed SMC. Additionally, advanced techniques like PRERL[12], RRL[13] and EERL[14] are also implemented on the same system to compare and evaluate the dynamic and robust behavior of the proposed SMC. The comparative analysis of the proposed SMC with aforementioned state-of-the art SMC approaches are performed under extreme conditions. Analysis endorsed the performance efficiency and effectiveness of the proposed technique to ensure robustness and achieve reduce transient and tracking time of 0.05msec and 0.08msec, respectively, with mitigated chattering along the sliding surface along with low %THD of 1.1% and improved voltage regulation of 99.83%.

1.5 Thesis Organization

The rest of the thesis is organized as:

Chapter 2 presents a comprehensive overview of VSIs, their fundamentals and importance of control mechanism. Based on which classification of VSIs is presented to explain well-known grid forming, feeding and supporting VSIs. Along with the discussion of their operations, major challenges associated with the operations of VSI based systems are discussed. Following which, vitality of robust control is justified through its comparison with conventional controllers. Moreover, an overview of state-of-the art robust control methods implementation on MG are discussed. Comparative analysis is presented, based on which supremacy of SMC established among other robust controllers due to its inherent characteristics.

In chapter 3, SMC is comprehensively discussed, starting from its fundamental theory and design basics to latest developments. Based on which major challenges associated with SMC are listed down. Moreover, applications of SMC for VSIs are comprehensively discussed to summarise the pitfalls deduced from existing scholarly work. After which, discussion on critical review of SMC for VSIs is presented. At last, proposed SMC design for VSI applications is introduced. The design of which constitute two major parts of the SMC i.e. initially, sliding surface based on Single Input Fuzzy Logic (SIFL) is applied to design Rotating Sliding Surface(RSS), and in the second step composite exponential reaching law is proposed that embraces the properties of exponential function tailored with difference, power and cos functions to achieve an improve and more efficient SMC for the said objectives. The well-known Lyapunov stability function is applied to validate the stability constraint. Moreover, comparative performance analysis for setting the reaching gain value of the proposed reaching law along with other state-of-the art reaching laws is also presented, that strongly advocates the effective and adaptive nature of the proposed reaching law. In addition to this, the proposed SMC is implemented on second order system to further analyze it's behavior in order to achieve minimum possible reaching time while ensuring mitigated chattering along the sliding surface. Other state-of-the art SMCs along with proposed SMC are also tested on the same system for different gain values, comparison of their behavior under same conditions shows that the proposed SMC is the most effective technique in achieving required objective of robustness with minimum possible chattering along the sliding surface.

In chapter 4, the proposed SMC is designed, implemented and tested for a single phase VSI. Reference voltage tracking along with robust behavior of the proposed SMC with other state-of-the art SMC(s) i.e. Cos-ERL[1] and FPRRL[2] are critically analysed for variable rectifier non-linear load on MATLAB Simulink platform. Extremely encouraging response in-terms of minimum reaching time, low %THD, very low chattering and tracking time is witnessed through proposed SMC. Moreover, competency and authenticity of the proposed SMC for single phase VSI is demonstrated experimentally through implementation on HIL setup comprising Opar-RT and MicroLabBox dSPACE 1202. Moreover, the proposed SMC is designed following RSS and composite exponential reaching law for three phase VSI. Voltage reference tracking and step response of

the proposed SMC with other state-of-the art SMC techniques like PRERL[12], RRL[13] and EERL[14] are analysed through implementation on same three phase VSI system for variable non-linear load on MATLAB Simulink. Comparative analysis of which proves that the proposed SMC has improved %THD, tracking and transient time with impressive % voltage regulation. Addition to this, the optimal surface selection behaviour of the proposed C-ERL-RSS is also presented for load disturbance conditions of no load to full load and full load to no load conditions for single phase and three phase VSIs.

The chapter 5 is the final chapter of the thesis that presents a comprehensive summary of the research work conducted for SMC for Voltage Source Inverters and its applications, followed by a detailed discussion on the conclusions that can be drawn from the research work. The chapter also highlights the limitations and challenges that were encountered during the research process. Furthermore, this chapter provides insights into the potential research areas that can be explored in the future based on the findings of the study. The overall aim of this chapter is to provide a clear and concise summary of the research work presented in the thesis, while emphasizing its significance and potential impact on the field.

CHAPTER 2

LITERATURE REVIEW

The concept of centralized power generation with unidirectional power flow and demand-based operations are the salient features associated with conventional power system since its invention. In recent decades, the traditional power systems have been undergoing a transformation with the introduction of modern solutions such as Distributed Generation (DG) that utilizes Renewable Energy Sources (RES), Electrical Energy Storage (EES), adoptive AC transmission systems, and active demand management (ADM). These modern solutions are often integrated with Communication Technologies (CTs), which further enhances their effectiveness in improving the performance of power systems. With increase in penetration of DGs, raises question about the reliability of power generation scheme, effected by technical constraints associated with voltage stability and power flow limitations. However, vast integration of DG systems, can result in efficient and flexible operation of grid. Moreover, DG systems are connected closer to the consumer's end, which results in reduction of overall transport losses [33]. DG systems powered by appropriate control scheme with integration of ESS, enhances the scope of ancillary services along with ensuring continuous power supply, hence, pave way for the creation of microgrid (MG). Therefore, it is foreseen that MG are going to play a key role in setting the direction of future grid. Conceptually, one can consider MG as a small-scale grid, which constitutes DG systems integrated with EES devices to derive loads, which are interconnected electrically and controlled hierarchically [6]. In addition to this, MGs are capable of operating either in grid connected or is landed mode when desired. Renewable energy sources like wind and Photovoltaic (PV) are considered the most suitable generators for integration with MG. That is due to a fact that they are smaller in size and are more scale-able as compared to central power plants, with flexibility of addition to power system at any desired point [33] and [34].

Nowadays, modern DG systems offers higher level of controllability and operability than conventional generators. Being a major player of MG, DG systems have a key role in ensuring stability of the electrical networks. Initially, it was common practice to disconnect DG systems from the grid in the event of a fault. While, this standard is no longer allowed in today's MG. For example, it can be observed in wind power systems, where low voltage ride through requirement demands that wind power system must remain connected to the grid under fault condition to support particular grid services [35]. Following which, PV systems are also bound to stay connected with grid under fault condition [36]. However, during network outage condition, many countries around the

world do not allow to form energized islands. This is probably to avoid any possible risk during maintenance operations or for the protection of electrical equipment. Therefore, irrespective of obvious benefits of feeding power to the isolated parts of the grid in black-out conditions, most VSIs are forced to shut down, as a result of which energy supply is interrupted for consumers, thus local generators fulfill power requirements of consumers. However, advancements in control schemes for DG and MG systems, tailored with the integration of communication system for DG plants and loads, allows intentional is-landing, following near future grid codes [37], [36]. Figure 2.1 provides an general overview of the

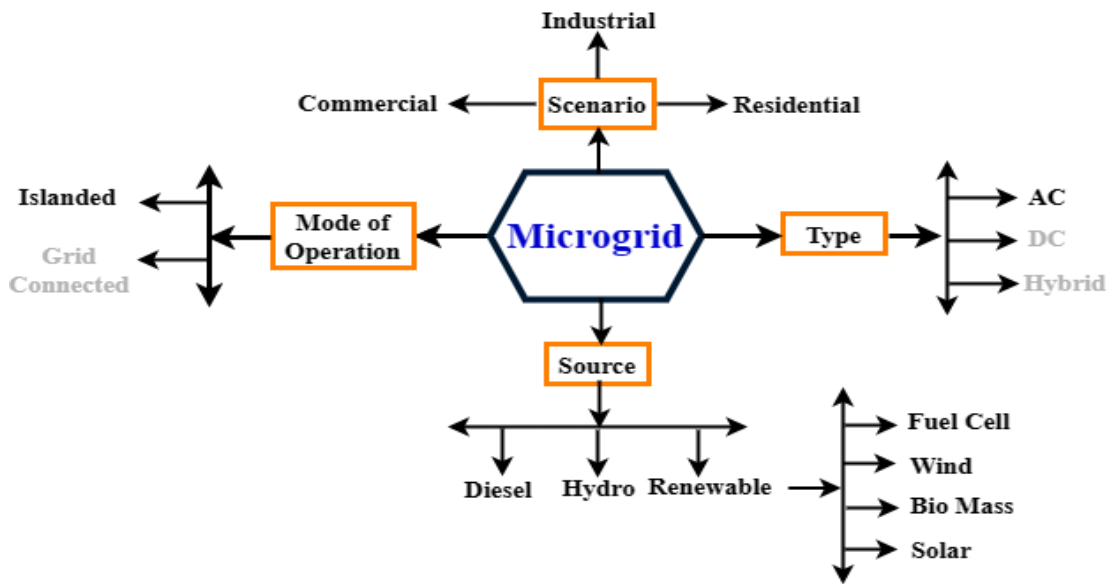


Figure 2.1: Block Diagram: Microgrid system's classification [5]

MG system, offering insights into its operational modes, energy sources, output supply characteristics, system configuration, and the connected consumers it serves.

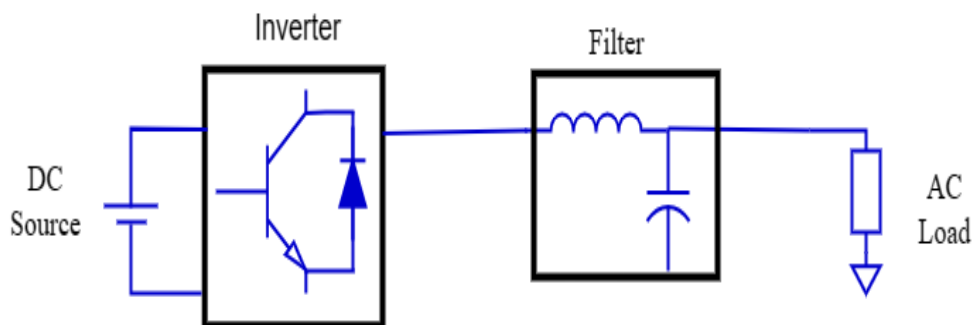


Figure 2.2: Voltage Source Inverter (VSI)

2.1 Voltage Source Inverters (VSI)

Voltage Source Inverters (VSIs) play a crucial role in linking renewable energy sources (RES) like solar panels, wind turbines, and energy storage units to AC loads.

VSI ensure that the necessary AC power is supplied both to and within the MG. Figure 2.2 illustrates a typical VSI system, which can be used in both single-phase and three-phase setups. Insulated-Gate Bipolar Transistors (IGBTs) are commonly employed in VSI configurations, although Si-MOSFETs can be a viable alternative in certain cases [38]. Power semiconductor components, such as IGBTs and diodes, are essential for allowing bidirectional power flow, as shown in Figure 2.2. IGBTs are preferred over Metal-Oxide-Semiconductor Field-Effect Transistors (MOSFETs) due to their superior power amplification, reduced power losses, and suitability for higher voltage operations.

2.1.1 Single Phase/Three Phase Voltage Source Inverters

The three-phase inverter finds extensive utility in industrial systems and electricity distribution. Nevertheless, the utilization of single-phase inverters has experienced substantial growth [39]. This increased usage is attributed to its features and the eventual production cost advantages it offers. Furthermore, three-phase Voltage Source Inverters (VSI) are the preferred choice for powering heavy loads, while single-phase VSIs find extensive use in domestic applications. The demand for these utilities is steadily growing, driven by the integration of DER and standalone power systems [40]. The basic VSIs can be classified into two categories: single-phase and three-phase VSIs. Figure 2.3 and Figure 2.5 depict the most common configurations with bridge inverter switch circuits, customized with LC filters for single-phase and three-phase applications, respectively.

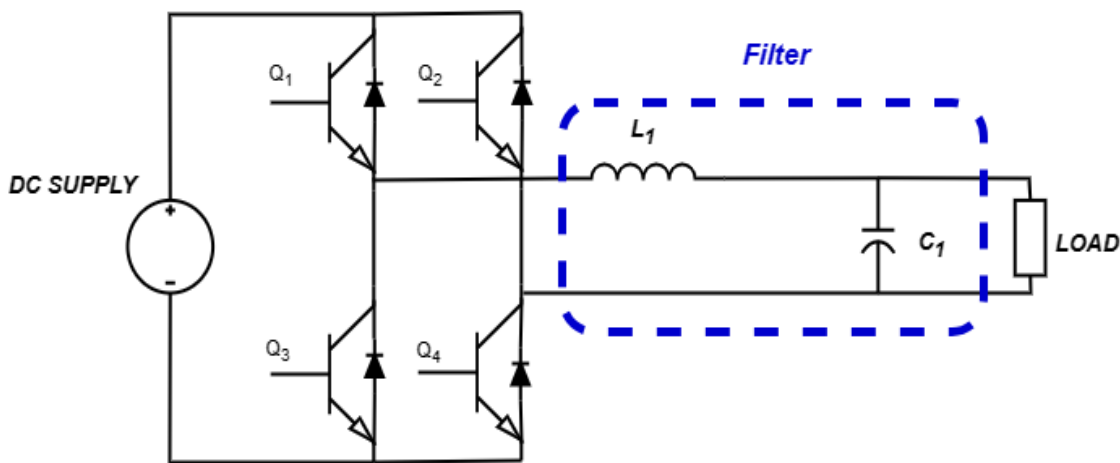


Figure 2.3: Single Phase Voltage Source Inverter (SPVSI)

The quality of power delivered to the Load can undergo changes when inverters employ Pulse Width Modulation (PWM) techniques. Enhancing power quality, minimizing the size and cost of the output filter, simplifying control, and ensuring reliability and availability present significant challenges in the selection of inverter configurations [41]. A comprehensive summary of various inverter topologies available in the literature is provided in [42]. The key distinctions among these topologies primarily revolve around the number of legs, PWM levels, and the type of filters employed. Extensive scholarly work has been done so far in each section of VSI i.e. inverter's switches topologies, filter design and PWM techniques to achieve efficient and regulated required ac output voltage [43], [44].

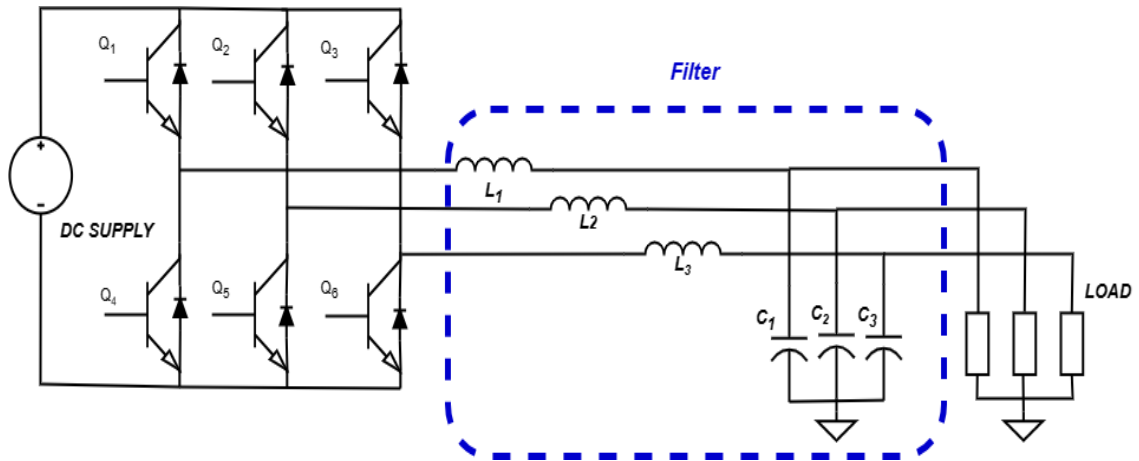


Figure 2.4: Three Phase Voltage Source Inverter

2.2 Control for Voltage Source Inverters

The primary goal of a VSI is to guarantee a consistent supply of AC output at the necessary amplitude and frequency for powering critical loads. Achieving this objective is contingent on an efficient control system that continuously observes and promptly response to adjust the output to attain referenced parameters, especially during exceptional circumstances such as extreme load variation. Moreover, in order to achieve optimal performance of VSI, includes achieving low %THD, good voltage regulation and fast transient response in sudden load changes [45]. The way an inverter operates and the control strategies it employs can differ based on the types of loads and MG modes. As of now, there are no universally established control and operation standards for inverter-based systems, and it might not be feasible to create such standards. The existing literature reviews on the control and operation of DG units concentrate on primary control strategies due to the complexities associated with power sharing [46], [47], [48].

When a MG operates independently without relying on the utility grid supply, it becomes essential to establish the reference voltage and frequency. In islanded MG settings, this responsibility falls on the DG units, and this is a core function of the inverters [49]. Figure 2.5 presents a simplified diagram of VSI control, excluding the current control loop represented by dashed lines, although certain limitations of this configuration have been noted in [50], as outlined below:

- i. Without a current control mechanism in place, there's a risk of substantial transient current surges that could potentially harm semiconductor components in case of faults.
- ii. Relying solely on voltage measurements across the capacitor may not offer precise insights into the network.

In light of the limitations associated with a basic VSI control approach, an alternative cascaded control strategy is presented in Figure 2.5, encompassing both voltage and current controls. Notably, the current control loop, centered around the inductor, exhibits a relatively swifter response time compared to the voltage control loop, enabling more

rapid current regulation. This strategy offers the advantage of restricting excessive current within the voltage control loop. Furthermore, the reference current generated by the voltage control loop can also be employed as a reference for power sharing across parallel modules [51]. Thus, while utilizing the voltage controller alone within the inner-loop

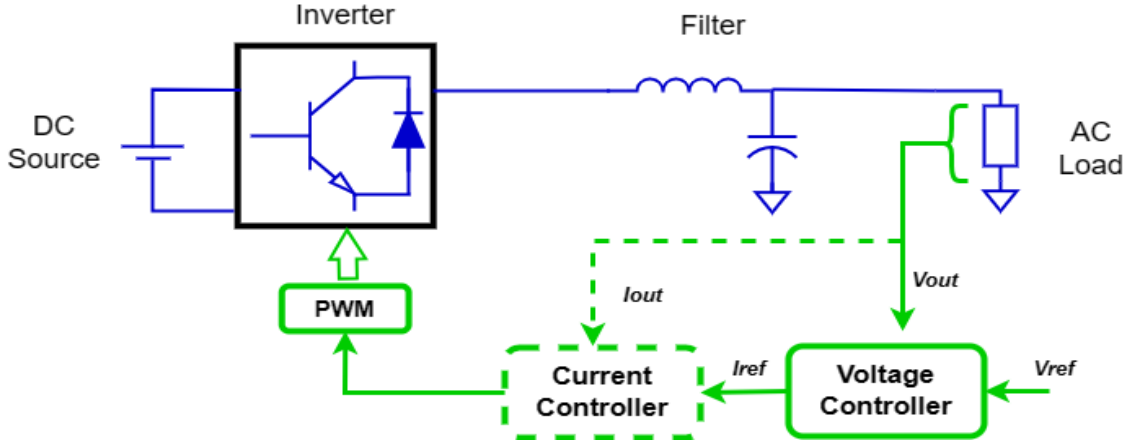


Figure 2.5: Voltage Source Inverter with Control

control, certain desired attributes are anticipated [52], including: 1) A high loop gain at DC to effectively regulate voltage magnitude with minimal error. 2) A high bandwidth to eliminate harmonics. A high loop gain at the fundamental frequency to maintain balance. 3) Robust performance even in the presence of uncertainties in plant models. 4) A rapid response with minimal overshoot. Minimal coupling between active and reactive power. 5) High stability, even when dealing with nonlinear network conditions. It's noteworthy that, in voltage source inverters, inner-loop current control is generally not obligatory for voltage regulation. However, incorporating current control within a voltage control loop enhances inverter performance and ensures compliance with current limitations.

2.3 Classification of VSIs

Based on role of VSI in AC MG, VSI can be categorized into following three types:

2.3.1 Grid Forming Voltage Source Inverters (GF-VSI)

The concept of Grid Forming Voltage Source Inverters (GF-VSIs) has been introduced to provide ideal voltage sources with predefined fixed values of voltage amplitude and frequency through closed-loop control systems. To function in parallel with other GF-VSIs, these inverters require extremely accurate synchronization, as they serve as voltage sources with low-output impedance. The output impedances of GF-VSIs connected in parallel determine the power-sharing function [53]. An instance of the real-world utilization of GF-VSIs can be observed in Uninterrupted Power Supply (UPS) systems. Under specific operational conditions, the UPS remains isolated from the main grid. However, in the event of a grid outage, the power inverters within the UPS system assume the responsibility of generating grid-like voltage. In the context of MG systems, GF-VSIs play

a crucial role by providing an AC voltage reference for other power inverters connected to the grid [6].

The feedback control system for GF-VSI is depicted in Figure 2.6. It employs cascaded voltage and current control loops operating in the dq reference frame. The GF-VSI receives reference inputs for voltage (V^*) and frequency (ω^*) and generates an output voltage at the point of common coupling to align with the desired reference values. The outer voltage loop controls the grid voltage, ensuring it matches the reference value. Meanwhile, the inner current control loop regulates the current produced by the inverter, maintaining it within the desired parameters [54]. The regulated current flows through the filter inductor L_f to charge the filter capacitor C_f to ensure the tracking of the reference voltage provided at the input of the voltage control loop [6]. In most industrial applications, the primary source used to feed GFIs is based on stable DC sources with batteries, fuel cells, etc. It is worth highlighting that precise synchronization among

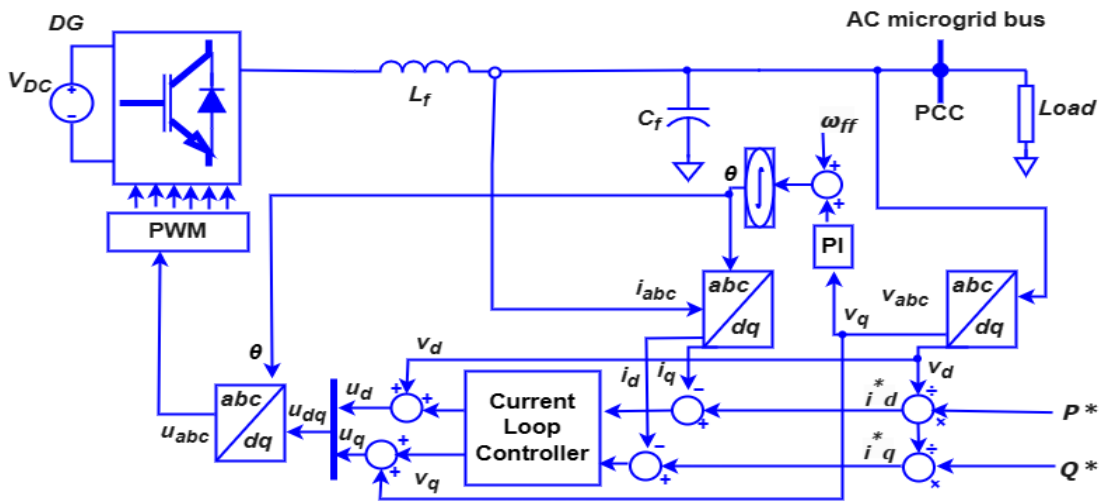


Figure 2.6: Grid Forming Inverter [6]

GF-VSI is vital for their parallel operation, facilitating optimal power sharing among the inverters. The output impedance of the GF-VSI is key in achieving this power sharing objective. Furthermore, these inverters play a critical role in providing continuous power supply during grid outages, underscoring their significance in MG systems. The control mechanism employed in GF-VSI involves a hierarchical structure consisting of cascaded voltage and current control loops. The outer voltage control loop is designed to align the grid voltage with the desired reference value, while the inner current control loop governs the inverter's current output. To ensure accurate voltage tracking, filter inductors and capacitors are incorporated, enabling precise adjustment based on the reference voltage input. This control system configuration ensures the maintenance of voltage and current at the PCC, contributing to the reliable operation of GF-VSIs [55].

2.3.2 Grid Feeding Voltage Source Inverters (GFe-VSI)

The second category of VSIs comprises Grid-Feeding Voltage Source Inverters (GFe-VSI), which function as current sources and exhibit higher value of impedance

at output. In grid-connected mode, they can operate in parallel with other grid-feeding inverters. In the context of DG systems, such as PV or wind energy systems [56], the majority of AC power inverters operate as grid-feeding power inverters. The core objective of these inverters is to regulate the amplitude of AC output voltage along with the frequency by adjusting the reference values of the active along with reactive powers, shown as P^* and Q^* , respectively (refer to Figure 2.7). GFe-VSI serves a pivotal role in the operation of AC microgrids in grid-connected mode, as they are responsible for controlling the voltage and frequency parameters through the precise manipulation of active and reactive power delivery, as described in references [57] and [58].

GFe-VSI differs from grid-forming/grid-supporting inverters primarily in their operational characteristics. Notably, grid-feeding power inverters operate as current sources and possess a higher output impedance [59]. They have limited flexibility in operating in an islanded mode, which means they need to coordinate with grid-forming or grid-supporting inverters. An alternative option for setting the voltage and frequency of a MG is the use of synchronous generators as grid-forming and supporting power inverters [60]. In a MG system, a high-level controller, which could be a power plant controller or a maximum power point tracking controller, is responsible for regulating the operations of the grid-feeding power inverters by setting the reference values of active and reactive power, denoted as P^* and Q^* , respectively. The grid-feeding power inverter's control structure is shown in Figure 2.7 In the context of a MG system, the regulation of grid-feeding power

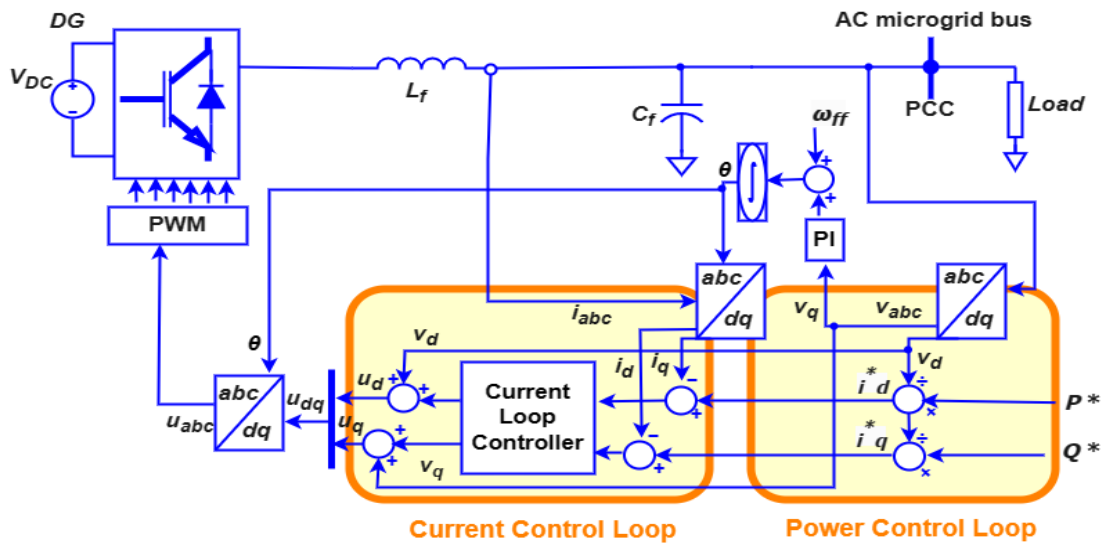


Figure 2.7: Grid Feeding Inverter [6]

inverters is overseen by a higher-level controller, such as a power plant controller or a maximum power point tracking controller. This controller is responsible for determining the reference values of active power (P^*) and reactive power (Q^*). Figure 2.7 illustrates the control structure employed by grid-feeding power inverters, which consists of a current control loop, a voltage control loop, and a high-level controller. The current control loop ensures that the output current of the inverters tracks the reference value of active power (P^*), while the voltage control loop maintains the output voltage at the desired

level corresponding to the reference value of reactive power (Q^*). The high-level controller adjusts the reference values of P^* and Q^* based on the demand of the MG [60], [6].

2.3.3 Grid Supporting Voltage Source Inverters (GS-VSIs)

The stability of a MG relies on the Grid Supporting Voltage Source Inverter (GS-VSI), which plays a crucial role in controlling the voltage and frequency of the grid. This inverter effectively regulates the active and reactive power supplied to the grid, operating in two modes: as a voltage source with link impedance shown in Figure 2.9 and as a current source with parallel impedance shown in Figure 2.8 [6].

- **Current Source:**

The Grid Supporting Current Source inverter plays a critical role in regulating the voltage and frequency of the MG, while also ensuring that the MG operates within the limits set by the utility. By regulating the current output of the inverter, the voltage across the load can be maintained within acceptable limits, preventing over-voltage or undervoltage conditions that can damage connected devices or disrupt the grid operation [61]. Moreover, the Grid Supporting Current Source inverter has

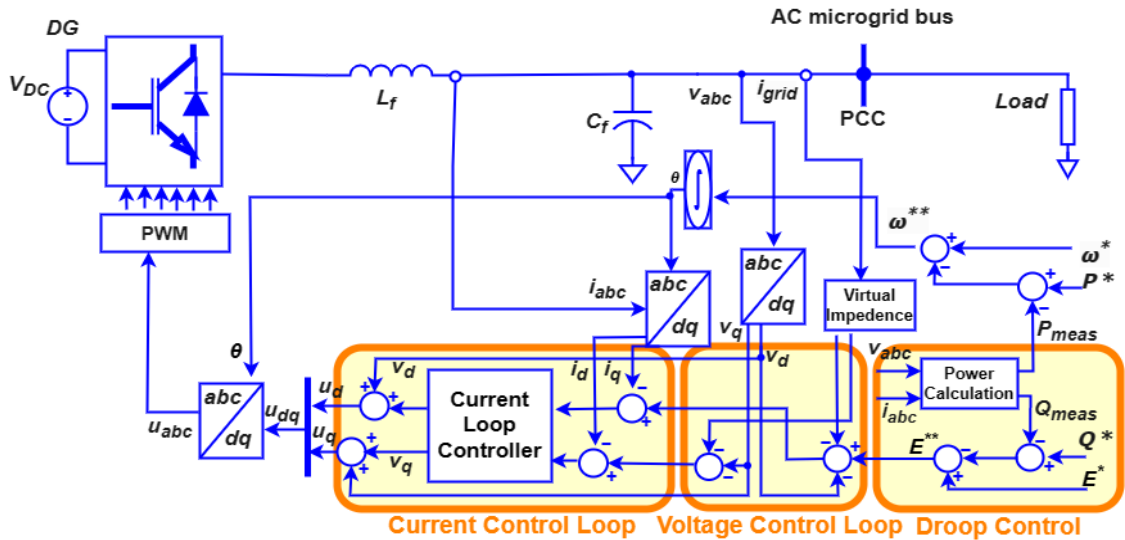


Figure 2.8: Grid Supporting Inverter-Current Source [6]

the capability to offer reactive power support to the grid, resulting in an enhanced power factor for the MG. This is accomplished by regulating the inverter's reactive power output, ensuring that the grid voltage remains at the desired level. The Grid Supporting Current Source inverter must comply with grid codes and regulations, such as those governing the connection of wind turbines to the grid [62]. To ensure that the MG operates within the limits set by the utility, the inverter must be designed to provide a specific amount of power to the grid.

- **Voltage Source:** A voltage source inverter designed to replicate the traits of an AC voltage source is the Grid Supporting Voltage Source Inverter, as depicted in Figure

2.9. This particular inverter is commonly applied for regulating both the voltage level and frequency in scenarios involving grid connections or standalone operations. In contrast to Ground Fault Interrupters (GFIs), the Grid Supporting Voltage Source Inverter operates autonomously in establishing grid voltage and frequency, detached from the functioning of other inverters within the MG system [6].

The control strategy employed by the Grid Supporting Voltage Source Inverter incorporates a link-impedance connection to the grid, resembling the simplified schematic of a synchronous generator [63]. According to [64], the inverter delivers active and reactive power based on the AC grid voltage, the AC voltage of the voltage source, and the link impedance. The link impedance can either be virtual, functioning as a mirror within the current control loop, or it can be a physical device directly connected between the voltage source inverter and the grid. One of the key

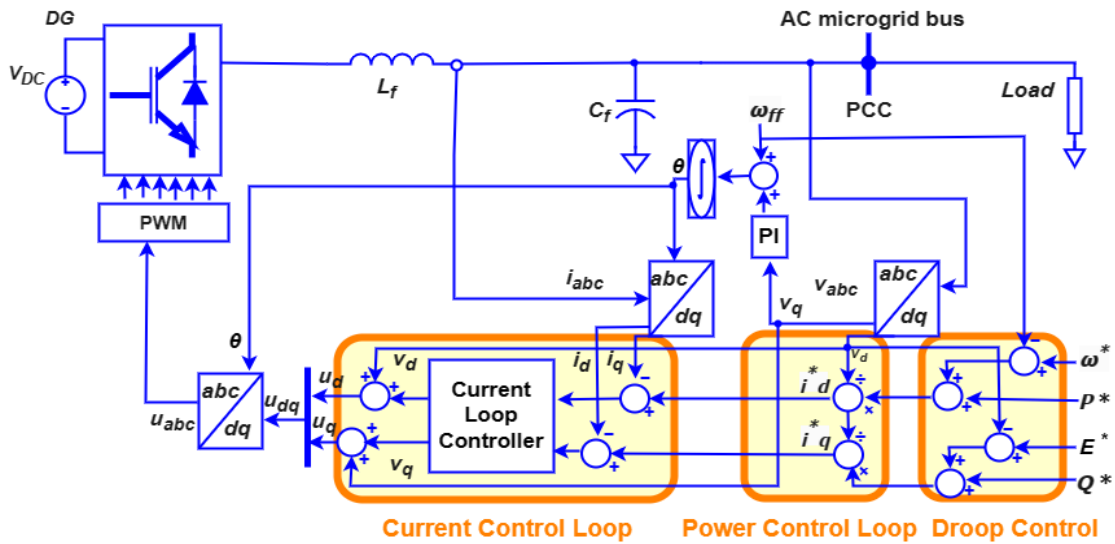


Figure 2.9: Grid Supporting Inverter-Voltage Source [6]

advantages of the Grid Supporting Voltage Source Inverter is its ability to regulate the amplitude and frequency of the voltage in a MG, without the need for additional GFIs. This makes it a cost-effective and efficient solution for MG applications, especially in situations where additional inverters would not be practical or feasible [65]. A comprehensive comparative analysis of specific properties of grid-forming, grid-feeding, and grid-supporting VSIs is presented in Table 2.1.

2.4 Robust Control

The importance of robust control for VSIs cannot be overstated. The primary challenge facing VSIs is the issue of power quality. The intermittent nature of renewable energy sources and the dynamic behavior of loads can lead to unwanted fluctuations in voltage and frequency, which can result in equipment malfunction and decreased reliability. To ensure stable and reliable power supply to consumers, proper control methods are essential [66].

Table 2.1: Comparison of Grid Forming (GS), Grid-Feeding (GFe) and Grid Supporting (GS)-VSIs

Parameters	GF-VSIs	GFe-VSIs	GS-VSIs
Purpose	To establish a stable and reliable grid without external connections	To feed power into the grid	To support the grid by providing ancillary services
Inverter type	Voltage source inverter (VSI)	Current Source Inverter(CSI)	Voltage Source Inverter(VSI)
Control Strategy	Primary control for voltage and frequency regulations, secondary control for droop-based power sharing, and tertiary control for economic dispatch.	Primary control for active and reactive power sharing, secondary control for frequency and voltage regulation, and tertiary control for economic dispatch.	Primary control for voltage and frequency regulation, secondary control for power quality improvement, and tertiary control for ancillary services.
Energy Storage Devices	Essential for grid-forming VSIs to provide power in the absence of external grid.	Optional but can enhance the stability of grid.	Essential to provide ancillary services and support the grid.
Resilience	Grid-forming VSIs are more resilient due to their ability to their ability to operate independent of external grids.	Grid-feeding VSIs are less resilient as their operation rely on external grids.	Grid-supporting VSIs are less resilient as they rely on stability of external grid.
Applications	Remote area islands, vehicle-to-load(V2L), data storage centers, military bases, emergency response systems etc.	Solar and wind farms, electrical vehicles, energy storage systems	Industrial plants, data centers, electrical vehicles charging stations.
Positives	Ability to operate in isolation, faster response time, high level of control.	Ability to integrate renewable energy sources, support the grid during peak demand, reduce transmission losses.	Ability to provide ancillary services, improve power quality, reduce system losses.
Challenges	Higher initial cost, need storage devices, complex control systems	Limited capability to operate in isolation, dependance on the external grid.	Need advanced control algorithms, less control over active and reactive power.

Traditional control methods often fail to address the inherent variability and unpredictability of renewable energy sources and dynamic loads. Robust control methods, on the other hand, are designed to account for uncertainties and disturbances, making them well-suited for the complex coordination of DERs in VSIs. By accounting for uncertainties in renewable energy sources and dynamic loads, robust control methods can effectively address the challenges associated with MG control and ensure the stability and reliability of the MG [67].

In addition, the implementation of robust control methods can help to mitigate the risk of power system blackouts caused by MG issues. The complex coordination of generators, storage devices, and loads in VSI systems requires the use of sophisticated algorithms and models, as well as advanced communication and sensing technologies [68]. Robust control methods provide an effective means of coordinating these resources, making them essential for the proper operation of VSIs.

Therefore, the importance of robust control in VSIs cannot be overemphasized. The inherent variability and unpredictability of RES and dynamic loads require the use of sophisticated control methods that can account for uncertainties and disturbances. Robust control methods offer promising solutions to the challenges associated with MG control and are essential for ensuring the stable and reliable operation of VSIs.

2.4.1 Robust Control vs Conventional Control:

Thus, the robust controllers have been extensively studied in the literature, and their ability to handle uncertainty, provide improved performance, and adaptability have been identified as key features that make them suitable for AC MG applications [69]. Following are the worth mentioning positives of the robust controllers that make them a special and most favoured choice to cater aforementioned issues related to ac MG:

i. Capability to handle uncertainties:

VSIs are complex systems made up of various distributed energy resources, including loads, renewable energy sources, and energy storage equipment. These resources exhibit dynamic behavior and are subject to uncertainties, which can introduce disturbances and unpredictability into the power system. Conventional control methods may struggle to effectively handle such uncertainties, potentially resulting in system instability and compromised performance [70]. Due to their capacity to deal with uncertainties and disturbances, robust control methods have attracted a lot of attention for controlling VSIs.

The utilization of feedback control is prevalent in robust control techniques, offering an effective approach in various systems. This control strategy involves measuring the system's output and comparing it with the desired output to determine the error. By utilizing this error signal, the controller adjusts the system inputs to minimize the error, ensuring stability and desired performance [71]. For controlling the voltage and frequency of the power system in VSIs, feedback control is widely used.

Adaptive control is a robust technique that effectively deals with uncertainties and disturbances within a system. Adaptive control assures peak performance by con-

tinuously adjusting the controller parameters in accordance with the changing system conditions. In VSI applications, this technique is particularly valuable for controlling the power output of generators and energy storage devices [72]. It gives the system the ability to react and change dynamically to changes, enhancing stability and effectiveness.

Intelligent control is a robust control technique that uses artificial intelligence and machine learning algorithms to learn the system behavior and generate optimal control actions. Intelligent control can handle uncertainties and disturbances in the system by adapting to the changing system conditions. Intelligent control has been successfully applied in VSIs for energy management, fault diagnosis, and power quality control [73].

The H_∞ norm, the μ -synthesis technique, and the small-gain theorem are some of the techniques used to quantify the robustness of controllers. The H_∞ norm is a measure of the maximum energy that can be transferred from the disturbance to the output of the system. The μ -synthesis technique is a mathematical framework for designing robust controllers based on the μ -analysis. The small-gain theorem is a mathematical theorem that provides a sufficient condition for the stability of a system under feedback control [74].

Thus, the robust control methods are critical for ensuring the stability and performance of VSIs. These techniques can manage system uncertainties and disturbances while ensuring steady and dependable performance under a variety of operational circumstances. Modern robust control methods utilized in VSIs include feedback control, adaptive control, sliding mode control, model predictive control, and intelligent control. Techniques such as the H_∞ norm, the μ -synthesis technique, and the small-gain theorem provide a rigorous framework for designing and quantifying the robustness of controllers. The successful deployment of VSIs depends on robust control techniques, which can also assist in overcoming the difficulties posed by the integration of renewable energy sources and load fluctuations in the power system [75].

ii. **Adaptability:**

As we have already established, robust control is a crucial component of MG control, but what makes it even more crucial is its capacity to respond to changes in the dynamics of the system. In an AC MG, renewable energy sources and fluctuating loads can cause changes in the system operating conditions, making it a dynamic system. Robust controllers can adapt to these changes by adjusting their control action accordingly [76]. This adaptability feature of robust control is particularly useful in dynamic systems where the system parameters may change over time.

Adaptive robust control techniques have been developed to address the challenges associated with changes in system dynamics. Model Reference Adaptive Control (MRAC) [77], Adaptive Sliding Mode Control (ASMC) [78], and Adaptive Backstepping Control (ABC) [79] are some of the techniques used to design adaptive robust controllers. MRAC is a control technique that adjusts the system's parame-

ters to match those of a reference model. The controller learns the system dynamics and adapts accordingly to achieve the desired control objectives. ASMC is another adaptive robust control technique that uses a sliding surface to control the system's output. Based on the dynamics of the system and its state, the sliding surface modifies itself. A recursive algorithm is used in the ABC control technique to create a feedback control rule that can manage uncertainties and disturbances. It operates by iteratively creating a control law based on the error dynamics of the system.

Adaptive robust control techniques offer several benefits in VSIs. They can handle changes in system dynamics, uncertainties, and disturbances, making them well-suited for VSIs with renewable energy sources and fluctuating loads. These methods are more dependable than conventional controllers since they aim to preserve system performance and stability under a variety of operating situations [80]. Moreover, these techniques can improve the energy efficiency of MG by optimizing the use of renewable energy sources and storage devices.

In summary, robust control techniques are essential for ensuring the stability and reliability of VSIs. The ability to handle uncertainties and adapt to changes in system dynamics makes robust controllers unique and effective in addressing the challenges associated with MG control. Adaptive robust control techniques, such as MRAC, ASMC, and ABC, have been developed to enhance the performance of robust controllers and provide more reliable solutions for MG control. The significance of reliable control methods cannot be overstated given the increase in the usage of renewable energy sources in VSI systems. [80].

iii. **Improved Performance:**

Robust control, a powerful form of control, enables high-performance control even in the presence of uncertainties and disturbances. It is capable of delivering a superior control performance when compared to conventional controllers. Robust control aims to achieve the desired control objectives while simultaneously being able to adapt to the uncertainties and disturbances that are present in the system. This is accomplished by designing the controllers to meet specific performance specifications such as settling time, overshoot, and tracking error [81].

The μ -synthesis technique is a widely used approach for designing robust controllers, especially for systems with multiple input and output channels. It has gained popularity due to its ability to address uncertainties arising from modeling errors, external disturbances, and parametric variations. By employing a structured singular value (μ) analysis, the μ -synthesis technique quantifies the system's sensitivity to these uncertainties. It then formulates a controller that optimizes performance across a range of operating conditions, ensuring robustness. The μ -synthesis technique has been successfully applied to various systems, including VSIs, demonstrating its effectiveness in robust control design [82, 83].

Another popular technique used to design robust controllers is the H_∞ control technique. This technique is a powerful method of control that aims to minimize the maximum gain of the system transfer function while satisfying a set of performance

specifications. The H_∞ control technique is particularly useful in systems where the uncertainties and disturbances are difficult to model or quantify. The technique provides a systematic way of designing a robust controller that is able to handle uncertainties and disturbances that are present in the system. The H_∞ control technique has been applied to a wide range of systems, including VSIs [84].

Another method for designing reliable controllers is structured singular value μ analysis. By examining a control system's susceptibility to uncertainties and disturbances, the μ analysis is a potent technique for determining how robust it is. The method gives a measurement of the largest system transfer function gain that can be attained without leading to instability. It is feasible to construct a controller that is resilient to uncertainties and disturbances and is capable of attaining the intended control objectives by applying the μ analysis. For the construction of reliable controllers for a variety of systems, including AC MG, the μ analysis has been employed widely [85].

Thus, robust control is a powerful method of control that offers superior performance compared to conventional controllers, even under the condition of unwanted disturbances and uncertainties. The μ -synthesis technique, H_∞ control technique, and the structured singular value (μ) analysis are some of the popular techniques used to design robust controllers. Numerous systems, notably VSIs, have successfully used these principles. It is possible to achieve the required control objectives while also being able to manage the uncertainties and disturbances that are present in the system by creating resilient controllers employing these strategies [83].

Robust controllers are designed to deliver high performance as compared to other conventional controllers, even in the presence of uncertainty. To achieve improved performance of the robust controller, the controllers are designed particularly to meet specific performance specifications, like settling time, overshoot, and tracking error. In this regard, several techniques have been developed to design robust controllers to achieve these specifications, including the μ -synthesis technique [86], the H_∞ control technique [87], and the structured singular value (μ) analysis.

iv. **Flexibility in design:**

Robust controllers offer a great deal of flexibility in design, allowing for the tailoring of control systems to meet specific performance specifications. VSIs are complex systems, and conventional controllers may not be well-suited to the task of controlling them. With their ability to account for uncertainties and disturbances, robust controllers provide an excellent alternative for controlling VSIs.

The flexibility of robust controllers is due to their ability to incorporate uncertainty models into the design process. One such approach is the Linear Matrix Inequality (LMI) method, which provides a framework for designing robust controllers that meet specific performance specifications [88]. The LMI technique uses a collection of linear matrix inequalities to specify the limits on the system's performance. The controller is then designed using these boundaries in order to achieve the desired level of performance while taking uncertainty and disturbances into account. An-

other advantage of the LMI approach is its ability to handle multiple performance specifications simultaneously. For example, a controller can be designed to simultaneously achieve fast response, low overshoot, and high tracking accuracy. The LMI approach provides a framework for designing robust controllers that meet these multiple performance specifications while accounting for uncertainties and disturbances [85].

Furthermore, robust controllers offer flexibility in the choice of the control law. The control law can be selected based on the specific needs of the system, such as the type of renewable energy source being used or the type of load being served. This flexibility allows designers to choose the most appropriate control law for the system being controlled, thereby achieving better performance [84].

In summary, the flexibility of robust controllers makes them an attractive option for controlling VSIs. With their ability to incorporate uncertainty models, handle multiple performance specifications, and offer flexibility in the choice of the control law, robust controllers provide an excellent alternative to conventional controllers for controlling complex systems such as VSIs.[89].

v. **Reduced Tuning Effort:**

One of the significant benefits of robust control is its reduced tuning effort. With traditional controllers, tuning can be a time-consuming and challenging process, which can become more complicated when dealing with uncertain and dynamic systems like VSIs. However, robust controllers eliminate the need for extensive tuning efforts, saving valuable time and resources. This is because the controllers are designed to be inherently stable, and once the controller has been designed and tuned for a particular application, it can be used in different systems and operating conditions without requiring significant modifications [90].

Furthermore, the reduced tuning effort of robust controllers is a result of their adaptability and flexibility in design. Robust controllers are designed to account for uncertainties and disturbances in the system dynamics, allowing them to be tailored to specific performance specifications. This means that they can adapt to changes in the operating conditions of VSIs, making them suitable for use in dynamic systems [76].

The incorporation of uncertainty models, such as the Linear Matrix Inequality (LMI) approach, into the controller design process further contributes to the reduced tuning effort of robust controllers. The LMI approach allows the controller design to be formulated as a convex optimization problem, which can be solved using efficient numerical algorithms. This eliminates the need for tedious and time-consuming trial-and-error tuning methods, making the design process more efficient and streamlined [88].

Overall, the reduced tuning effort of robust controllers is a significant advantage that makes them highly attractive for use in VSIs. The ability to achieve superior control performance while minimizing the time and resources required for tuning makes robust controllers a valuable tool for system designers and engineers. The

flexibility and adaptability of the controllers, combined with their reduced tuning effort, make them an excellent choice for controlling complex systems like VSIs.

To reduce the amount of effort required to tune robust controllers, two techniques have been developed: the Genetic Algorithm (GA) approach and the Particle Swarm Optimization (PSO) approach. [91].

Thus, Robust controllers provide numerous benefits over conventional controllers when applied to VSIs:

- Firstly, they are designed to handle uncertainties and disturbances that are commonly present in the MG, resulting in a more stable and reliable control performance. This is essential for VSIs since their operating circumstances may fluctuate as a result of the fluctuation of renewable energy sources and the existence of loads with variable power requirements. Robust controllers guarantee that the system maintains its stability and performance in a variety of operating conditions by being able to handle such uncertainties. [62], [63].
- Secondly, robust controllers can be designed and implemented using automated tuning techniques. This greatly reduces the need for expert user input, making the tuning process more efficient and effective. Automated tuning techniques can also improve the performance of the controller by reducing the likelihood of errors that may occur during the tuning process. With automated tuning techniques, the implementation of robust controllers can be completed in a shorter time and with greater precision, resulting in a more optimal control performance [90].
- Thirdly, robust controllers can be easily adapted to changes in the MG using machine learning techniques. By incorporating machine learning techniques into the controller design process, the controller can learn and adjust to changes in the system dynamics. This makes the controller more scalable and adaptable, allowing it to handle variations in the MG that may occur over time. Additionally, machine learning techniques can improve the controller's performance by enabling it to learn from past experiences and make predictions about future events [76], [80].
- Finally, robust controllers can be implemented using standard hardware and software with some modifications. This eliminates the need for specialized hardware and software, reducing the overall cost of implementation. Additionally, using standard hardware and software ensures that the controller is compatible with existing systems, making it easier to integrate into the MG [85].

Overall, these benefits make robust controllers a promising solution for achieving stable and reliable control performance in VSIs. With their ability to handle uncertainties and disturbances, automated tuning techniques, adaptability using machine learning techniques, and compatibility with standard hardware and software, robust controllers are a flexible and powerful method of control that can improve the performance of VSIs. this discussion leads to a comprehensive comparative analysis of robust and conventional controllers is showcased in Table 2.2.

Table 2.2: Comparison of robust controllers and conventional controllers

Features	Robust Controllers	Conventional Controllers
Design approach	Model-based, optimization-based, or data-driven techniques that consider uncertainties and disturbances.	Based on simplified models and do not account for uncertainties or disturbances.
Performance	Provide robust and stable performance under various operating conditions and disturbances. Latest research shows that robust controllers achieve higher power quality and stability than conventional controllers under uncertainties and disturbances [92], [93] and [94].	Performance can deteriorate under uncertainties and disturbances. Latest research shows that conventional controllers may not perform well under uncertainties and disturbances, leading to decreased power quality and stability [95] , [96].
Complexity	Can be more complex and require more computational resources. Latest research shows that the complexity of robust controllers can be reduced using data-driven techniques, such as machine learning [97].	Typically simpler and require fewer computational resources. Latest research shows that conventional controllers can be made more complex to improve their performance, such as using adaptive control methods [98]
Tuning	Tuning is typically automated and requires less user expertise. Latest research shows that robust controllers can be designed using automated tuning techniques, such as genetic algorithms and particle swarm optimization [99], [100].	Tuning requires user expertise and may require trial and error. Latest research shows that conventional controllers still require expert tuning to achieve optimal performance [101].
Scalability	Can be easily scaled up or down to accommodate changes in the MG. Latest research shows that robust controllers can be easily adapted to changes in the MG using machine learning techniques [102].	May not be easily scalable to accommodate changes in the MG. Latest research shows that conventional controllers may not be easily adaptable to changes in the MG without significant modifications [103].
Implementation	May require specialized hardware and software. Latest research shows that robust controllers can be implemented using standard hardware and software, with some modifications [102].	Can be implemented using standard hardware and software. Latest research shows that conventional controllers can be implemented using standard hardware and software, with some modifications [104].

2.4.2 Robust Control Methods for VSIs

The development of VSIs has become a potential strategy for enhancing the dependability and efficiency of power systems in the search for sustainable energy solutions. Due to the previously described uncertainties and disturbances, integrating renewable energy sources and dynamic loads into VSIs presents considerable control issues. As a result, robust control techniques have gained popularity as a way to guarantee the steady and dependable operation of VSIs. This is as a result of robust control systems' ability to give high-performance control under various operating situations while handling uncertainty and disturbance. In this regard, the section that follows offers a summary of the advantages and uses of robust control approaches for VSIs.

2.4.2.1 State Space Control Methods

Robust control methods play a vital role in ensuring the reliability and stability of performance in VSIs. An effective approach in this regard involves the utilization of robust PID controllers to regulate voltage, with the goal of minimizing steady-state errors and enhancing transient response. Several tuning methods, such as Chien-Hrones-Reswick (CHR), CC, and Wang-Juang-Chan, have been explored, but CC-based PID controllers have exhibited superior performance in controlling VSIs according to previous research findings. To tackle the issue of measurement noise impacting DGs, a distributed controller based on SMC is proposed in [105], accompanied by an extended state observer for a multiagent system. In [106], a dynamic event-triggered scheme is suggested for a secondary controller, aiming to manage frequency control in an isolated AC MG while effectively handling uncertainties originating from Renewable Energy Sources (RESs). However, achieving frequency control in islanded VSIs remains a challenging task due to the absence of power grids, which means none of the agents is grid-forming. To tackle this issue, virtual inertia controllers based on robust H_∞ control are designed in [107] to enhance frequency profiles and overcome undesired fluctuations caused by the application of a Phased-Locked Loop (PLL) for frequency measurement.

As a matter of fact, VSIs are complex systems that present many challenges in terms of control and operation. A critical challenge in islanded VSI control is the distributed design secondary robust voltage and frequency fully distributed design. To address this issue, a multi-agent consensus-based control strategy is proposed in [108]. The main aim of the controller is to attain robustness by considering factors such as model uncertainty, changes in parameters, and unaccounted dynamics. To achieve this, the controller's design ensures that each individual distributed generator (DG) unit relies solely on its local information as well as the information obtained from a small number of neighboring units. This feature helps to reduce the system's bandwidth requirements and minimize communication costs. The result is a more reliable and flexible MG.

A research study in [109] proposes a secondary control approach for islanded VSIs, referred to as the "stochastic consensus-based control approach". The proposed method takes into account both system and communication noises, aiming to achieve precise estimation while minimizing complexity and computational load for the restoration of frequency and voltage. Its effectiveness is proven by its capability to achieve mean-square

synchronization, surpassing existing approaches, in the restoration of voltage and frequency for DGs. Overall, distributed controllers offer many benefits but need to be carefully designed to be robust and handle uncertainties, while centralized controllers offer accuracy but may not be as flexible as distributed controllers. To minimize the communication burden between agents in a MG, a secondary control scheme is proposed in [110]. This approach leverages scattered communication patches to gather information only from neighboring DGs. The active disturbance rejection control (ADRC) technique is employed to address model uncertainties and unknown disturbances, resulting in a more robust control scheme.

The article [111] introduces a unique method called Robust Fractional-Order Control (RFOC) to overcome the issues caused by nonlinearities and uncertainties in Hybrid Energy Storage Systems (HESSs) for Electric Vehicles (EVs). To effectively address the nonlinearities and model uncertainties, this method uses a fractional-order proportional integral derivative (FOPID) controller as an additional input. Additionally, the suggested NRFOC method's control cost is contrasted with that of existing control methods as PID control, feedback linearization control, and SMC. This thorough assessment sheds light on how the NRFOC method performed.

2.4.2.2 Hierarchical control methods:

The development of reliable and effective power-sharing control schemes that can guarantee the steady and dependable functioning of distributed energy resources (DERs) has attracted increasing interest in the field of MG control. Several hierarchical control strategies have been put out in recent years to deal with this problem. A two-layer based hierarchical control technique for power sharing in MGs is provided in [112] as one such method. Information exchange between DG units is handled by the secondary control layer of the scheme, which operates more slowly than the primary level of control. The inverter output voltage's magnitude and angle must be controlled at the initial level of control in order for it to track the reference power and follow specified reference points. One of the main goals of this approach is to reduce information flow within the grid's many agents while maintaining precise voltage and frequency regulation, as well as effective power-sharing control.

In addition to these hierarchical control techniques, another promising approach is the use of harmonics mitigation techniques for frequency control in MGs. This is the focus of the hierarchical control technique presented in [113], which aims to control active power sharing at the secondary level and handle frequency with harmonics mitigation at the primary level. By using this approach, the authors were able to achieve improved frequency control and reduced harmonic distortion compared to traditional proportional-integral (PI) control techniques. Overall, these hierarchical control schemes represent promising avenues for addressing the challenges of power sharing and frequency control in MGs.

2.4.3 Robust Proportional Integral Derivative (PID) Controller:

The Proportional Integral Derivative (PID) is widely used in VSI application like AC MGs due to its simple design and functionality [114]. Its application does not require much of information, and it proves effective in minimizing steady-state error while enhancing both transient and steady-state responses [115]. The selection of parameters of PID controller is the challenging task, the performance of the PID controller is directly related to its parametric values. Robustness of PID controller is ensured through the integration of methods adapted for the selection and tuning of the values of PID controller parameters. Many parameter tuning methods encounter the challenge of plant model mismatch, leading to poor performance and low bandwidth of PID controllers across a broad range of operating conditions [116]. To add robustness through the selection of parameters and handle the impact of mismatched uncertainties, various solutions adopting the Linear Quadratic Regulator (LQR) and Linear Matrix Inequality (LMI) as a foundation for the robust PID controller design [117]. However, with robustness these strategies leads to computation burden.

2.4.3.1 H_∞ based control method:

Numerous robust control approaches based on H_∞ have been proposed to address various control problems in VSIs. The reference [118] provides a nonfragile robust H_∞ control method for an islanded MG under unbalanced and nonlinear loads. The DC bus voltage must be regulated while guaranteeing robustness in the face of external disruptions and model uncertainty. The coefficients of a set of nonlinear stochastic differential equations describing the dynamics of the system have been altered to allow for parametric uncertainty.

The ability of a H_∞ resilient controller to control the AC voltage and frequency in an MG under various loading conditions is evaluated in reference [119]. The implemented control strategy comprises of several hierarchical control levels, where each level performs a specific task in the overall system functioning. These levels include a specific control loop for the LCL filter and coupling circuit as well as droop, voltage, current, and current control loops. The Harmony Search Algorithm (HSA) is also implemented into the controller design for better adjustability.

The study cited in [120] introduces a controller for frequency management of a free-standing PV-diesel hybrid power system. The controller uses a multi-variable H_∞ method and is built using Linear Matrix Inequalities (LMIs). Incorporating μ -analysis, the uncertainties in the State-of-Charge (SoC) of supercapacitors are accounted for, guaranteeing stability even in the face of disturbances and SoC uncertainties.

When it comes to addressing various control difficulties in VSIs, such enhancing power quality, controlling voltage and frequency, and preserving system stability in the face of uncertainties and disturbances, these H_∞ -based control solutions produce good outcomes.

2.4.3.2 Backstepping-Based Control Methods:

In the context of an islanded MG, the implementation of a robust control algorithm that can effectively regulate AC voltage in the presence of faults and disturbances is a key concern. One approach to addressing this issue is the use of a back stepping-based fault-tolerant control algorithm, as proposed in [121]. This method offers robust control and improved reliability of the MG system by regulating the AC voltage despite the occurrence of faults and disturbances. This strategy stands out because it can function without a detailed model of the system, in contrast to many droop and non-droop management systems that rely heavily on the precision of the system model.

In [122], a nonlinear backstepping-based control strategy is proposed as an alternative to the droop and non-droop control approaches. This method takes into account the uncertainties and dynamics of the system by utilizing a disturbance observer. The proposed controller is designed to improve the speed and accuracy of the response in tracking the reference values. Notably, the use of local quantities measurement in this method leads to faster response times, as compared to other control strategies.

In summary, the use of back stepping-based control methods can offer effective solutions to address the challenges associated with regulating AC voltage in an islanded MG system. The proposed control strategies, such as the ones discussed in [121] and [122], can help enhance the reliability of the MG system while accounting for uncertainties and dynamics in the system model.

2.4.3.3 Droop Control Method:

In recent years, a variety of control strategies have been proposed for the integration of renewable energy sources (RESs) into power systems. In this context, droop-based control is a popular method that has gained widespread attention in the control of VSIs. Droop-based control is a distributed control method that is capable of achieving decentralized power management in VSIs.

Numerous research studies have investigated the utilization of droop-based control methodologies to facilitate the integration of renewable energy sources (RESs) into power networks. A notable illustration can be found in the work referenced by [123], which proposes an enhanced droop-based control strategy tailored for the incorporation of RESs into medium- and high-voltage nodes within power systems. This proposed technique employs a triad of controllers, each catering to DC voltage-droop, AC voltage-droop, and frequency-droop, thereby ensuring equitable power distribution among distributed generators (DGs). The meticulous adjustment of the PI controllers further refines the system's operational efficiency. A decentralized droop controller for VSIs is suggested in the article [124] that combines a traditional droop with a robust transient droop function. The controller is designed to address low-frequency oscillations through robust D-stability analysis that incorporates Kharitonov's stability concept. The proposed controller achieves better power-sharing accuracy and demonstrates robustness against parameter uncertainties.

A droop-based control method is presented in [125] for a small-scale MG consisting of heterogeneous battery energy storage systems (BESS). Energy balance, ac-

tive/reactive power dispatch, and voltage/frequency synchronization are all guaranteed by the proposed technique's hierarchical control framework. The fully distributed control is achieved through a sparse communication network without relying on global information. Compared to centralized methods, the proposed approach significantly reduces the computational and communication load.

In conclusion, one of the prevailing control approaches for integrating RESs into power systems is droop-based control. It has the benefit of enabling decentralized power management in VSIs as a distributed control mechanism. It does have certain drawbacks, though, like delayed dynamic operation and communication issues, which put the PCC's constant voltage, frequency, and the distribution of power across DGs in danger. In order to get around these restrictions, a number of research have put forth improved droop-based control algorithms that, by minimizing these restrictions, can increase system performance.

2.4.3.4 Sliding Mode Control (SMC)-Based Control Methods:

The SMC methodology is widely accepted as a trustworthy control method suitable for difficult nonlinear systems affected by uncertainties and disruptions. It originated in the 1950s as a part of variable structure systems, but initially faced challenges related to execution complexity and chattering issues [26]. Despite these difficulties, SMC has considerable benefits since it modifies the system's dynamic behavior by choosing the proper switching functions, rendering the closed-loop response impervious to matched uncertainty. As a result of researchers' interest in this appealing property, SMC design has advanced, enabling the reduction of chattering, correction for unstructured dynamics, flexibility in uncertain systems, and improvement of dynamic performance. The capacity of SMC ensuring stability and resilience in uncertain systems [126].

The basic configuration of SMC tends to exhibit the undesirable phenomenon of chattering, making it impractical for real-world applications. To address the issue of chattering, researchers have proposed a technique known as second-order sliding mode control. This sophisticated approach emerged in the mid-1980s when the concept of "second-order sliding" was introduced [127]. Subsequent advancements in SMC, particularly in the 2000s, focused on higher-order concepts, which gained significant attention [128]. These developments were driven by the need to overcome limitations in the conventional SMC algorithm. The requirement that the system's relative degree be one with respect to the sliding variable and the generation of challenging-to-compensate high-frequency switching control signals are two examples of these limitations.

In recent years, the technological advancements in modern control systems have garnered significant attention, particularly the use of intelligent computers [129]. These advancements have enabled the implementation of complex control algorithms, thanks to the high-speed capabilities of computers. SMC has emerged as a viable option in today's technological landscape, leading to numerous applications documented in the literature [129], [130].

One prominent industrial application where SMC has found extensive use is in robot manipulators. These manipulators are highly regarded in the business since they are es-

sential in processes like laser cutting, welding, welding, painting, and polishing, among others. The dynamics of these manipulator systems are influenced by a variety of factors, including parametric errors, nonlinearities, strong dynamic coupling, and time-varying structures. Industrial robot manipulators have been successfully deployed with a variety of SMC setups, proving the value of SMC in these challenging situations. [131].

In robotics and control theory, a different category of nonlinear systems known as under actuated systems has emerged, having applications in anything from cars to airplanes. Because there are fewer actuators per variable to be controlled, controlling under actuated systems is intrinsically difficult. Robustness becomes a primary concern when dealing with under actuated systems, and SMC has demonstrated its effectiveness in controlling such systems by effectively handling structured and unstructured uncertainties [132].

Overall, the utilization of SMC in various industrial applications, including robot manipulators and underactuated systems, showcases its robustness and adaptability in dealing with complex dynamics and uncertainties. The comparative analysis of the comprehensive comparison of robust control techniques are presented in Table 2.3

- **SMC for VSIs**

In [133], an efficient decentralized resilient control technique is presented to improve power-sharing and stability in a system. Three independent controllers made using different methodologies make up this method, which is tested with unbalanced loads. The controllers' theoretical underpinnings, in particular, are SMC, Lyapunov function theory, and Fractional-Order Sliding Mode Control (FOSMC). The controllers' objectives are to increase power sharing and control the voltage, active power, and reactive power of the system. A decentralized second-order SMC-based boost inverter control technique is presented in [134] in an effort to regulate the DC voltage in a DC MG. The duty cycles of the boost inverters may be continually controlled by the controller using the generated inputs. The effectiveness of the proposed method is assessed in light of foggy modeling and an undefined load demand. LR-[65] offers a dependable control algorithm utilizing the instantaneous power theory for multifunctional grid-tied inverters working in an imbalanced loading situation. The unfavorable load current components, such as harmonics, reactive power, and the negative sequence component, are estimated using a Positive Fundamental Components Estimator (PFCE). The multipurpose grid-tied inverter can regulate reactive power, lessen harmonics, and balance the load in addition to injecting active power. The algorithm ensures that the weighted averages of the MG and the reference voltage converge to one another. The power loss issue the second-order SMC approach confronts is addressed by a different third-order SMC strategy. By using this method, a continuous control signal that can function as a duty cycle is produced. To regulate the AC voltage, frequency, charge balance, and reactive power in an MG while accounting for communication delays, a distributed multiagent fixed-time control technique is put forth in another work mentioned as [135]. The frequency is restored, the average voltage is set to its nominal value, and the proper power-sharing is accomplished using a distributed control system model and a fixed-time observer to preserve the charge balance. The suggested approach

can handle PV systems operating intermittently and changing load conditions. A shipboard MG is subjected to a nonlinear sliding mode control approach in [136] to alter the secondary load frequency. In order to maximize efficiency while minimizing complexity, the Sine Cosine Algorithm (SCA) and Wavelet Mutation (WM) are combined. A dependable control method is suggested by reference [137] for an islanded AC MG with any topology. The system's asymptotic stability is guaranteed by the control strategy, which is based on second-order SMC and AC voltage measurement and eliminates the need for communication networks among DGs.

Table 2.3: Robust Control methods for AC VSIs.

Controller	Advantages	Disadvantages	Applications
State Space Model [138]	Suitable for both linear and nonlinear systems. Allows for control design based on full-state feedback.	May require more computational resources. Can be difficult to design for large-scale systems	Voltage and frequency regulation, active and reactive power control, and islanding detection.
Hierarchical Control [139], [102]	Provides a hierarchical structure that facilitates the control of complex systems.	May not be suitable for highly nonlinear systems. Requires precise knowledge of the system model.	Voltage and frequency regulation, energy management, and power sharing.
H∞ [118], [119]	Provides robust stability for a range of systems. Allows for trade-off between performance and robustness.	Can be computationally intensive. May require specialized software.	Voltage and frequency regulation, power quality improvement, and fault detection.
Backstepping Control [121], [122]	Provides robustness and good tracking performance.	May require extensive system knowledge for control design. Can be sensitive to measurement noise.	Voltage and frequency regulation, power system stabilization, and load following.
Model Predictive Control [140]	Provides optimal performance with constraints. Can handle disturbances and model uncertainties.	May require extensive system knowledge for control design. Can be computationally intensive.	Voltage and frequency regulation, economic dispatch, and demand response.
Sliding Mode Control [133] - [141]	Provides robustness to model uncertainties and external disturbances.	Can produce high-frequency control signals that may be difficult to implement. May require precise knowledge of system parameters.	Voltage and frequency regulation, power sharing, and fault tolerance.
Neural Network [142]	Can approximate nonlinear and unknown system dynamics with high accuracy.	May require extensive training data. Can be sensitive to changes in system dynamics.	Voltage and frequency regulation, power system stabilization, and power quality improvement.
Fuzzy Logic Control [143]	Provides a flexible approach for handling uncertain or imprecise information. Can handle nonlinear systems.	May require more computational resources. Can be difficult to design for large-scale systems.	Voltage and frequency regulation, load balancing, and power quality improvement.

SMC provides the most benefits and the fewest drawbacks among the mentioned robust control techniques for AC MG, according to the comparative analysis given in 2.3. SMC is appropriate for addressing nonlinear systems and offers robustness to model uncertainties and outside perturbations. It can also be used for fault tolerance, power sharing, and voltage and frequency management.

Robust control strategies for VSIs must be taken into consideration in order to handle the issues brought on by the increased penetration of DG in power systems. The design of such control schemes must take into account their complexity, cost, and ability to withstand external disturbances, system operation modes, and the unpredictable behavior of renewable energy sources (RESs). These factors are critical in ensuring the robustness of MG control systems. controllers for VSIs.

While, SMC is considered to be robust due to its ability to achieve perfect tracking

performance despite uncertainties in parameters or models, it has some limitations in real-time applications. One of the main challenges is the phenomenon of chattering, which arises due to the switching control law not being instantaneous and the sliding surface not being perfectly known. As a result, chattering can lead to high-frequency dynamics that may cause significant damage to the system. Despite this, sliding-mode control is still a desirable option from a design standpoint because it can take modeling uncertainties and disturbances into account and is applicable to a variety of nonlinear systems. Along with blessed inherent characteristics of robustness, simple design and easy implementation, SMC faces challenge of unwanted chattering along the sliding surface. Handling which may lead to compromised dynamic response of SMC, as it depends directly upon the sliding surface selection mechanism. Following which many notable scholarly efforts have been made so far, some of which are discussed below. It is also worth mentioning here that SMC has very wide range of applications in almost every field of science and technology, however, the underlying discussion is aimed to focus and review the contributions specific to chattering reduction methodologies and sliding coefficient selection mechanism associated with VSI applications. Furthermore, many state of the art contributions have been made in designing SMC for both discrete and continuous time domain, however, continuous time domain SMC will be the core focus of the discussion of literature review.

- **Challenges Associated with SMC Design for VSIs**

Designing SMC for VSIs offer several benefits, such as robustness and fast dynamic response. However, it comes with its set of challenges:

- i. **Chattering Phenomenon:** SMC is prone to high-frequency oscillations known as chattering in the control signal, which can stress power electronic switches and reduce system reliability [144].
- ii. **Uncertainties and Load Variations:** The uncertainties in system dynamics and fluctuations in load conditions have the potential to impact the performance of SMC, leading to a potential compromise in robustness [145].
- iii. **Power Quality Concerns:** SMC, while offering robustness, may introduce high-frequency components in the control signal, affecting the quality of the output waveform. Increased %THD in the voltage waveform can impact the performance of sensitive loads and lead to power quality issues [146].
- iv. **Balancing Fast Dynamic Response and Low Overshoot:** Achieving a balance between fast dynamic response and low overshoot during transient conditions is challenging. Thus, rapid load changes may lead to aggressive control actions, causing overshooting or undershooting of the desired output, affecting system stability [147].
- v. **Complex Implementation:** Implementing SMC in real-time applications can be complex, requiring a deep understanding of the system dynamics and careful tuning of control parameters. Designing and tuning the sliding surface,

reaching law, and control gains require expertise, making the implementation challenging [7].

2.5 Sliding Mode Control (SMC)

SMC has several intriguing benefits, but it also has some drawbacks. The most noticeable is the chattering along the sliding surface, that results in decreased control precision and greater power losses in VSIs. Unmodeled dynamics and switching time delays are the root causes of chattering, which can lead to oscillations with finite amplitude and frequency. In practical implementations, these oscillations must be reduced to an acceptable level to ensure optimal performance of the system. SMC techniques come in two flavors: continuous-time and discrete-time. The traditional SMC approach and its uses in VSIs in the continuous-time domain will be the main topics of this dissertation. To better understand SMC and its design philosophy, we will also explore the basic concepts of VSS and provide relevant examples. By examining these topics in detail, we can gain a deeper understanding of the challenges and opportunities associated with SMC in VSIs.

2.5.1 Variable Structure Control

Variable Structure Control is a widely researched control technique, which has garnered significant attention since its inception by Emel'yanov and Barbashin in the 1960s, and subsequently presented by Utkin in 1970 [148]. VSS is a form of nonlinear control strategy that relies on employing abrupt control laws to ensure system resilience against disturbances and uncertainties. This approach allows the control system to adjust its dynamics through appropriate switching logic, resulting in a highly robust and adaptable control solution. Due to its attractive features, VSS has found applications in a wide range of fields, including power electronics, robotics, aerospace, and many others. In this chapter, we will explore the basic concepts of VSS, with a particular focus on its use as a foundation for SMC. The basic idea of VSS can be depicted for simplicity in equation 2.3, here the system consists of several structures or subsystems S_i , where $i = 1, 2, \dots, n$. It is worth mentioning here that only one subsystem among all pave path from input to the output at a particular instant. The selection of appropriate structure/subsystem, under particular circumstances is done by VSS control mechanism. Thus, the prime purpose of VSS control is to devise a best possible switching logic under specific conditions. Following second order system can illustrate the control structure shown in equation 2.3:

$$x_1 = y \quad (2.1)$$

$$\dot{x}_1 = x_2 \quad (2.2)$$

where, \dot{x}_2 shown in 2.3 represents the feedback control law that can be explained as:

$$\dot{x}_2 = \begin{cases} -a_1 y & \text{if } y\dot{y} > 0; \quad a_1 > 0 \\ -a_2 y & \text{if } y\dot{y} < 0; \quad a_2 < 1 \end{cases} \quad (2.3)$$

The performance of state space model based system shown in equations 2.1 and 2.2 can be visualised in 2.10 under control law defined in 2.3 It is evident from the equation 2.10 that

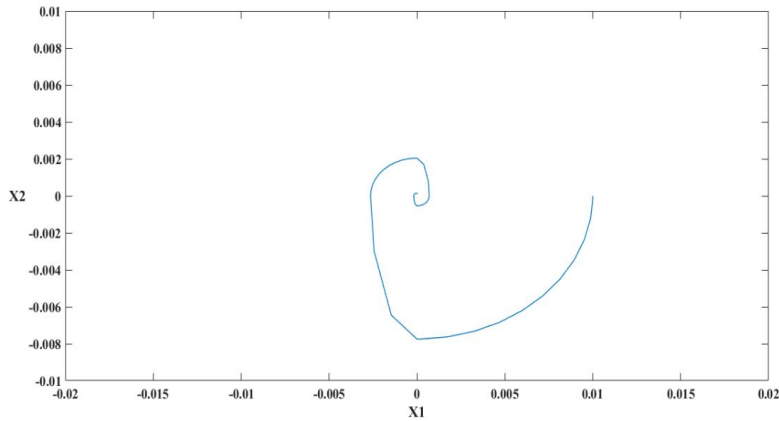


Figure 2.10: Variable Structure Control

switching control law mention in equation 2.3 is asymptotically stable. Moreover, with the help of this example, it can be concluded that besides feedback controller, effective switching strategy plays vital role in determining the system dynamics.

2.5.2 SMC Fundamental Theory and Methodologies

SMC is a powerful control technique that has garnered significant interest among researchers and practitioners due to its inherent non-linear characteristics. Unlike various linear controllers, SMC can handle complex systems with ease, thanks to its ability to adjust the dynamics of the system through appropriate switching logic. However, the prime benefit from the SMC system is achieved when the state variables of the system acquire sliding motion [149].

The fundamental concept underlying SMC design is to create an appropriate feedback controller that pushes the system state trajectories in the direction of a predetermined surface. The state variables stay on the surface once they get there. The SMC mechanism's foundation is made up of this "sliding" motion of the system state variables along the surface. [150].

According to equation 2.11, the SMC mechanism can be roughly categorized as: i) the sliding phase and ii) the reaching phase. The reaching phase remains active until the system state trajectories touches the predetermined sliding surface. The state trajectories follow the surface once they get there and eventually arrive at the equilibrium point. The system's dynamic behavior is heavily influenced by the sliding surface, which distinguishes the SMC from other non-linear controllers of the present in the following two ways [151]:

- Using the SMC technique, one can design a strong controller for complex systems. This controller works effectively even when there are unknown dynamics or uncertainties in the system.
- SMC reduces complexities associated with higher-order systems through order reduction that leads to simple implementation, ensures high level of robustness and shows extremely resilient behaviour to external disturbances.

In the past, several stability criteria were introduced to ensure the controller's stability. However, conventional stability criteria like Routh's and Nyquist's cannot be applied to non-linear systems comprising non-linearities and parametric disturbances [152]. To overcome this challenge, Lyapunov stability criteria were presented by the renowned Russian mathematician and engineer Lyapunov. These criteria provide sufficient prerequisites for stability of non-linear systems [153], [154]. Therefore, Lyapunov stability criteria are employed to guarantee stability of the SMC controller.

2.5.3 Lyapunov Stability Condition

The Lyapunov approach, commonly known as Lyapunov's direct method, offers a distinct advantage in determining system stability without the need for complex mathematical computations. This approach draws its roots from theoretical mechanics, where a stable energy conservation system can be defined as a positive definite scalar function that decreases with time. This fundamental concept is then applied to the study of non-linear systems, which are notoriously difficult to analyze using conventional stability criteria like Routh's or Nyquist's. The Lyapunov Stability function can be used to establish whether the system's equilibrium is either stable or unstable, and to assess the overall system's stability in various operating conditions. By constructing a suitable Lyapunov function, it is possible to obtain valuable insights into the dynamic behavior of a variety of non-linear systems [155].

Let the system domain comprising origin, represented as $D \in \mathbb{R}^2$. Where, $D \rightarrow \mathbb{R}$ is constantly differentiable, thus:

$$V(0) = 0 \wedge V(x) > 0 \quad \forall \quad x \neq 0 \quad (2.4)$$

Consequently, $x = 0$ is stable asymptotically. The sliding mode presence can be demonstrated using Lyapunov's second technique by taking into account a positive definite Lyapunov function with a negative first time derivative, $V(t, x)$. The continuously differential Lyapunov function in the context of Single Input Single Output (SISO) systems can be expressed as:

$$V(t, x) = (1/2)S^2(x) \quad (2.5)$$

Lyapunov function's single derivative can be represented as:

$$\dot{V}(t, x) = S\dot{S} < 0 \quad (2.6)$$

Lyapunov stability function plays major role in setting the foundation for designing sliding mode control. In most cases Lyapunov function mentioned in equation 2.6 is termed as reachability condition.

2.5.3.1 Reachability Condition

The concept of reachability condition can be visualised considering the following case:

$$S\dot{S} < -\gamma^2|S| \quad (2.7)$$

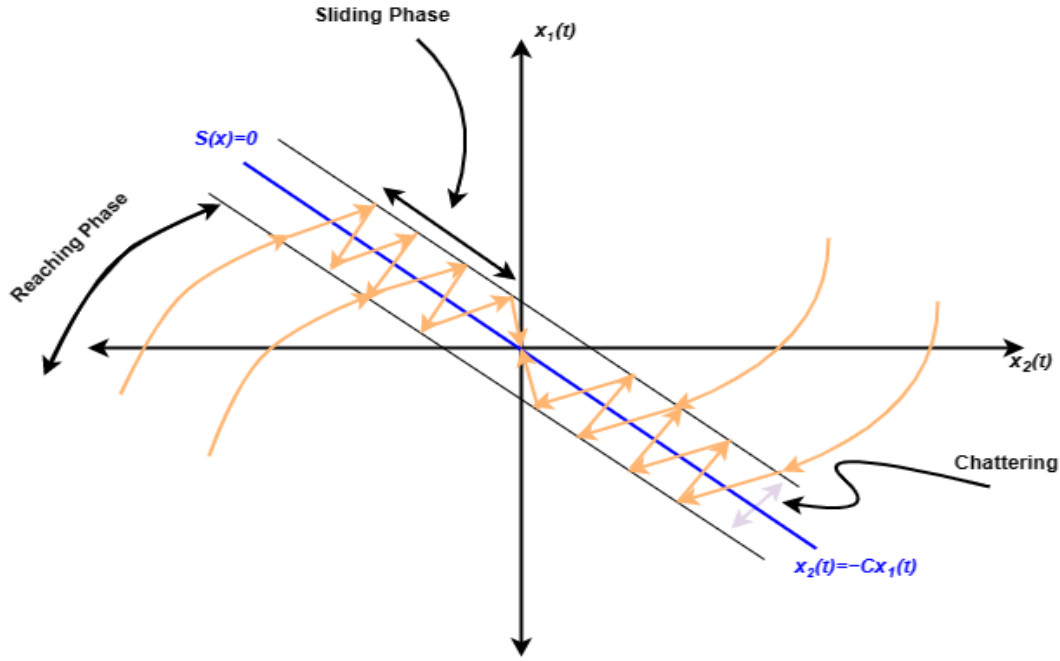


Figure 2.11: Phases Associated With SMC [7]

This implies that,

$$\dot{V}(t, x) = -\gamma^2 \sqrt{2V(t, x)} S \quad (2.8)$$

Now, one can easily find the extreme value of the reaching time through integration of equation 2.5 from t_0 to t_r to achieve following range of reaching phase:

$$t_r \leq |S(t_0)|/\gamma^2 + t_0 \quad (2.9)$$

2.5.4 Sliding Mode Control Design

SMC design can be categorised in following two parts [156]:

- i. Developing of appropriate Sliding Surface is one of the most fundamental step in designing SMC, that plays pivotal role in achieving desired system dynamics during sliding mode.
- ii. An effective feedback control strategy to achieve minimum possible reaching time to ensure robustness. Moreover, control techniques must also have efficient phenomenon to guarantee residing of state variables on the surface during sliding mode.

2.5.4.1 Sliding Surface Design

Appropriate sliding surface plays vital role in sliding mode control design, plus it has the directly effects the controller's dynamic response. Key features associated with sliding surface design can be described through considering following most general Linear Time Invariant(LTI) system model:

$$\dot{x}(t) = Af(x, t) + Bu(t) \quad (2.10)$$

where, $f(x, t) \in \mathbb{R}^n$ represents system state variables, $u(t) \in \mathbb{R}^m$ represents control input, whereas $A \in \mathbb{R}^{n \times n}$ and $B \in \mathbb{R}^{n \times m}$ are constant and controllable matrices with $n > m$. As a matter of fact, we choose sliding surface $S(x) = 0$ as a nonlinear function of the state variable x , it is common practice to define the sliding surface in terms of a linear combination of the states variable, which can be defined as $S(x(t)) = Cx(t) = 0$. Let us define state variable vector $S(t) = Cx(t)$ passing through the point of origin at $x(t) = 0$. Where, $C \in \mathbb{R}^{m \times n}$ with $\|BC\| \neq 0$ is termed as sliding surface coefficient.

2.5.4.1.1 Existence Condition The second crucial stage is to comply with the sliding mode's presence after designing sliding surface. Only when the tangent vector to the trajectory of the controlled system is constantly pointing in the direction of the sliding surface does the necessary condition of the sliding mode exist close to the sliding surface $S = 0$. Additionally, whenever $t > t_r$, the optimal sliding mode can be reached at $S(t) = 0$. where the reaching time is t_r .

It is worth mentioning here, in case of practical scenarios there are many unwanted conditions like switching delays, hysteresis, sampling time etc. system state trajectories cannot reside on the sliding surface, rather they follow zig-zag pattern around the surface, causing phenomenon of unwanted chattering. The concept of chattering will be discussed in later section. The existence problem is primarily concerned with the stability analysis discussed under the section of Lyapunov stability.

2.5.4.1.2 Sliding Coefficient Selection The sliding coefficient is a key factor in determining how dynamically a closed-loop system will respond. It has an impact on the existent region of operation's size in addition to the dynamic response [157]. A larger sliding coefficient results in a faster dynamic response, but it may compromise the system's stability by reducing existence region's size. Conversely, a smaller sliding coefficient slows down the dynamic response. To address these issues, scientists have created mathematical models to ascertain the ideal sliding coefficient value that optimizes the existence region [158]. In this section, we will use a fixed value for the sliding coefficient for the sake of simplicity, but later sections will explore variable sliding coefficient values in detail. The sliding surface rotates with the changing value of the sliding coefficient when the slope is time-varying rather than being fixed [4]. To ensure stability, the following condition for the sliding surface must exist to enforce the state variables to remain on the surface, as soon as they reach it:

$$S(t) = 0 \tag{2.11}$$

Thus, the minimum condition for stability as discussed above in equation 2.11 must be fulfilled. Based on the complexity level and order of the system, state variables can be utilized to design sliding surface. Type and behavior of different sliding surfaces based on sliding coefficient $C_1, C_2, C_3, \dots, C_n$ is shown below. Moreover, in order to fulfill stability condition constraint, value of sliding coefficient must be strictly positive. One can easily visualize positive value constraint of sliding surface coefficient by solving 2.12 for $x_1(t)$, when $x_2(t) = \dot{x}_1(t)$ i.e. $x_1(t) = x_1(0)e^{-Ct}$. Hence, asymptotic stability can

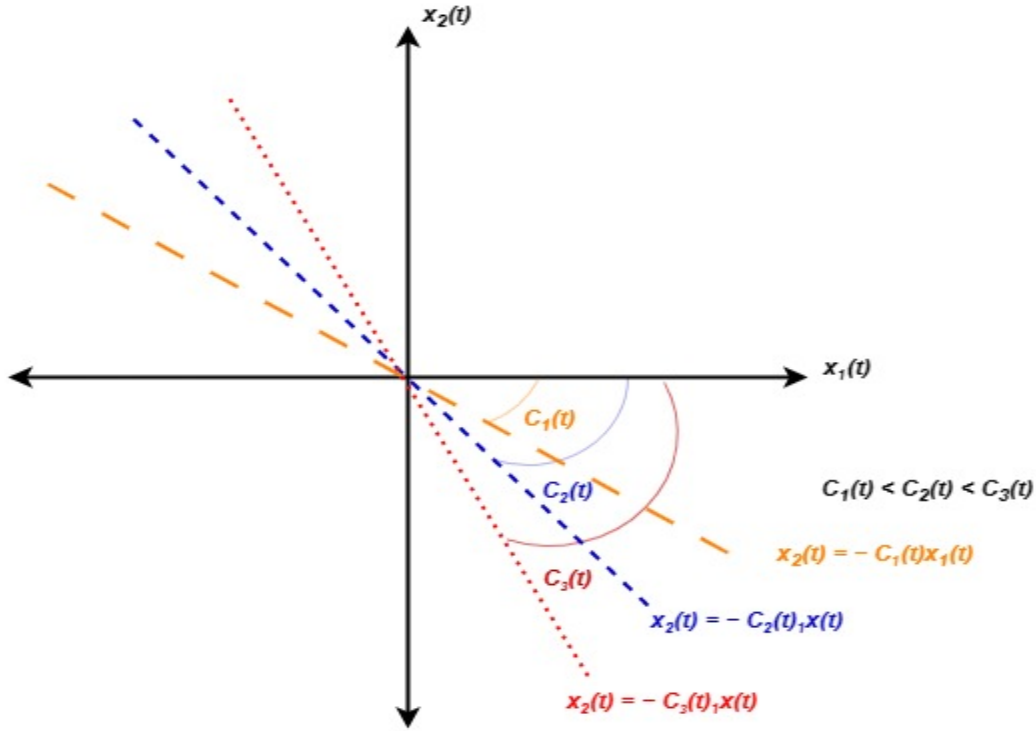


Figure 2.12: Time Varying Sliding Coefficient [7]

only be achieved when $C > 0$.

$$S(x) = \begin{cases} x_1(t) & \text{Linear} \\ C_1x_1(t) + x_2(t) & \text{Linear} \\ C_1x_1(t) + C_2x_2(t) + C_3x_3(t) \dots C_nx_n(t) & \text{Linear} \\ C_1x_1^\gamma(t) + x_2(t); \quad 0 < \gamma < 1 & \text{Non-Linear} \end{cases} \quad (2.12)$$

2.5.4.1.3 Equivalent Control Design: The equivalent control technique is a process of determining motion of the system restricted in sliding mode at $S(x) = 0$. System behavior for second order system mention in 2.13 can be expressed as state space form:

$$\begin{bmatrix} \dot{x}_1 \\ \dot{x}_2 \end{bmatrix} = \begin{bmatrix} a & b \\ c & d \end{bmatrix} \begin{bmatrix} x_1 \\ x_2 \end{bmatrix} + \begin{bmatrix} e \\ f \end{bmatrix} u + \begin{bmatrix} 0 \\ D(t) \end{bmatrix} \quad (2.13)$$

Where, $D(t)$ is disturbance factor and $x_2 = \dot{x}_1$. Stability of SMC is associated with negative rate of change of sliding surface, normally termed as reaching law. Therefore, following conclusions are made for further analysis:

$$S(x) = Cx_1 + x_2 = 0 \quad (2.14)$$

$$\dot{S}(x) = C\dot{x}_1 + \ddot{x}_1 \quad (2.15)$$

$$\dot{S}(x) = (aC + c)x_1 + (bC + d)x_2 + (e + f)u + D(t) \quad (2.16)$$

Let $aC + c = A$, $bC + d = B$, $S(x) = S$, $D(t) = D$ and $e + f = E$, then 2.16 becomes:

$$\dot{S} = Ax_1 + Bx_2 + Eu + D \quad (2.17)$$

Simplifying 2.17, we get following equivalent control function for second order system:

$$u_{eq} = 1/E(\dot{S} - Ax_1 - Bx_2 - D) \quad (2.18)$$

2.5.5 Salient Features of SMC

Upon thorough analysis of SMC's design, it can be observed that it offers several prominent features that make it stand out from other control strategies. These salient features are as follows [151]:

- i. **Order Reduction:** A remarkable characteristic of SMC lies in its capability to diminish the complexity of the controlled system. Through the utilization of an equivalent control function, a second-order system can be transformed into a first-order control function. This approach is universally applicable to systems of varying orders, presenting a notable level of simplicity.
- ii. **Simple Implementation:** SMC operates by forcing the system's state variables to a predetermined sliding surface, where it undergoes a back-and-forth motion under discontinuous control. This methodology of control is relatively simple and straightforward to implement.
- iii. **SMC Phases:** The SMC control process encompasses two distinct stages: the reaching phase and the sliding mode phase. In the reaching phase, the system's state trajectories are guided towards a predefined sliding surface. Upon reaching this surface, the system transitions into the sliding mode phase, where it proceeds to operate along the surface, progressing towards the equilibrium point.
- iv. **Dynamic Response:** Once the system enters the sliding mode, its state trajectory aligns with the sliding surface. Remarkably, this behavior remains unaffected by changes in system parameters and disturbances. Instead, it hinges solely on the value of the sliding coefficient.
- v. **Robustness:** SMC doesn't call for extensive parameterization of the system for precise modeling, making it highly robust. This feature eliminates the need for system parameters that may be difficult to obtain or unavailable, enhancing the control system's overall robustness.

2.5.6 Challenges Associated with SMC Design

Along with the aforementioned advantages of SMC, this control method also presents several challenges that need to be addressed. Therefore, the problem of chattering is considered one of the major hindrances for researchers and engineers in applying SMC to real-time applications. Chattering occurs when the state variable does not stick to the sliding surface, but rather moves back and forth with some magnitude depending upon the

value of control gain magnitude. This phenomenon results in high-frequency oscillations in the control signal and can cause mechanical wear, electromagnetic interference, and acoustic noise, leading to unwanted results in practical systems. Unmodeled dynamics or discrete-time implementation are considered as the prime causes of chattering. Thus, there is a need to develop effective solutions to resolve the problem of chattering and to enhance the performance of SMC in practical applications. Researchers have proposed various methods to reduce or eliminate chattering, including the use of high-order sliding mode control, intelligent techniques, and adaptive control algorithms. Moreover, the development of chattering-free sliding mode control remains an active research area, and further advancements are expected to raise the performance of SMC in practical applications. [159]:

- i. Reduced control accuracy
- ii. Increased heat losses electric switches and circuitry

Furthermore, the occurrence of chattering in SMC can potentially excite unmodeled higher-order dynamics, ultimately resulting in undesirable instability. As a result, researchers have proposed various techniques to mitigate the effects of chattering.

2.6 Chattering Reduction Techniques

2.6.1 Boundary Layer Approach

To mitigate the chattering phenomenon within SMC, a strategy involves implementing a boundary layer in close proximity to the sliding surface. This facilitates the substitution of the discontinuous control action with a continuous one, especially when the system operates within this boundary layer. The modification of the controller's discontinuous element accommodates this adjustment. This technique is introduced as a means of enhancing the efficacy and stability of sliding-mode control, as suggested in [160].

$$u(t) = -K \text{sign}(S) \quad (2.19)$$

where, S is sliding surface and K is a constant. In most of the cases saturation function represented as $\text{sat}(t)$ is adopted, expanded version is shown below:

$$u(t) = -KS / (\|S\| + \alpha) \quad (2.20)$$

where $\alpha > 0$. Since, boundary layer approach has the advantage of easy implementation with fixed frequency characteristics, it has seen widespread use in practical applications. Well, this method also has some downsides, such as

- This method may result in a chattering-free system, it's important to note that a finite steady-state error may still be present.
- The thickness of the boundary layer is important as it affects both the control performance of SMC and the reduction of chattering.
- Once the system enters the boundary layer, it may no longer exhibit the same level of robustness and accuracy as outside the layer.

2.6.2 Dynamic SMC Approach

Incorporating an integrator or a low-pass filter between the SMC and the controlled plant addresses the limitations of the dynamic SMC technique. This approach effectively treats the time derivative of the control input w as a novel input for the expanded system. Introducing a low-pass integrator to eliminate high-frequency chattering within w ,

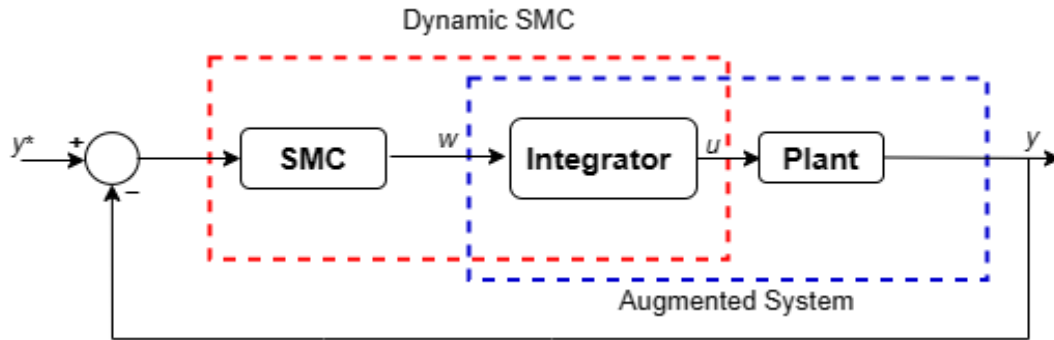


Figure 2.13: Dynamic SMC Approach [8]

transforms the control input u that's directed to the real plant into a continuous form, effectively diminishing chattering. However, it is worth to mention that this approach increases the system order by one and may have an impact on transient responses, even though it successfully eliminates chattering and achieves zero steady-state error. [8].

2.6.3 Second Order SMC (SoSMC)

In recent past, the Second-order Sliding Mode Control (SoSMC) has gained noticeable attention due to its following advantages over conventional first-order SMC:

- i. The SoSMC technique's capability for achieving finite-time convergence in the closed-loop system has been demonstrated in prior studies [161]-[162].
- ii. Yet another notable benefit of the SoSMC strategy is its proficient suppression of the chattering phenomenon, a characteristic commonly linked with first-order SMC. This achievement is realized by employing the derivative of the first-order SMC as a virtual controller, which is subsequently integrated to yield the effective control signal. The adoption of this technique brings about a substantial decline in chattering, resulting in a more seamless and dependable system response [163].
- iii. The SoSMC approach brings an extra edge over traditional SMC by elevating the relative degree of the sliding variable from one to two. This expansion paves the way for developing more precise controllers for closed-loop systems. Additionally, SoSMC adeptly addresses the challenge of chattering, stemming from the amalgamation of a discontinuous virtual controller with the actual control. This is accomplished by employing the derivative of the first-order sliding mode controller as the virtual controller, as expounded in [164].

Over the years, various renowned SoSM algorithms have been developed, building upon the concept initially presented in [165]. In [164], Levant introduced the prescribed convergence law technique, which can be seen as the homogeneous counterpart to the traditional terminal sliding mode algorithm [129]-[166]. It's worth noting that both the twisting and prescribed convergence law approaches necessitate data about the sliding variable S and its derivative \dot{S} . This prompts the question: are there SoSMC algorithms that do not require \dot{S} ? In response to this challenge, a suboptimal algorithm was introduced in [167], grounded in the concept of time-optimal controller design for a double integrator system. Simultaneously, Levant advanced the super-twisting algorithm in [168], enhancing the twisting algorithm by incorporating control input integration. Notably, this augmentation solely relies on information related to the sliding variable s . Furthermore, a study conducted by Perez et al. [169] provides insights into this domain, the super-twisting algorithm demonstrates effectiveness in minimizing chattering even with fast actuators, while maintaining the characteristics of a first-order sliding mode. Other SoSMC algorithms include the quasi-continuous algorithm [170], Lyapunov-based algorithm [171], and more.

The problem of output constraints in control systems has been extensively studied in recent years due to the adverse effects it can have on system performance, safety, and stability. Many practical systems have inherent physical limitations that must be taken into account when designing controllers. For instance, in electric vehicles, the sideslip angle of the vehicle must be constrained to ensure safety. In flapping-wing robotic aircraft, the bending and torsion deformations must be controlled to prevent structural damage. The barrier Lyapunov function method has been proposed as an effective tool for handling output constraints. Tee et al. [172] provided a well-known method for constructing the barrier Lyapunov function, but it has the limitation that the barrier limit must be a constant. To overcome this limitation, [172] proposed a novel barrier function that varies along with the desired trajectory. However, there are few results in the literature related to output constraints in SMC. The application of the barrier Lyapunov function method to SMC was proposed in Obeid et al. [173], where an adaptive strategy was developed for first-order sliding mode controller design. Despite this, there hasn't been much research done on the issue of output limits in SoSMC control. This is so because the majority of SoSM algorithms rely on homogenous closed-loop system features, which output constraints may be violated. The difficulty of stability analysis is also greatly increased by output constraints. Therefore, the design of SoSM controllers subject to output constraints remains an open problem [174].

2.6.4 Super Twisting Algorithm Approach

Super-twisting algorithm is called HoSMC of the second order [175]. The SoSMC approach has received a lot of attention because of its capacity to that are inherent in conventional sliding mode control methods. Compared to the traditional SMC, the SoSMC approach has the potential to reduce chattering without compromising system performance. Several studies, such as [176], [177], have proposed and investigated the effectiveness of SOSMC in various control applications [164]. However, the growing demand

for information compared to the first-order SMC is a limiting factor for its widespread implementation. The super-twisting algorithm is considered particularly effective in dealing with strong nonlinear effects, as it can be viewed as a nonlinear proportional-integral control [9]. The expression of the STA is as follows:

$$u_{STA} = u_{STA1} + u_{STA2} \quad (2.21)$$

$$u_{STA1} = \lambda_1 \text{sign}(S); u_{STA2} = \lambda_2 S^{0.5} \text{sign}(S) \quad (2.22)$$

where, design parameters λ_1 and λ_2 are strictly positive. With advantage of easy im-

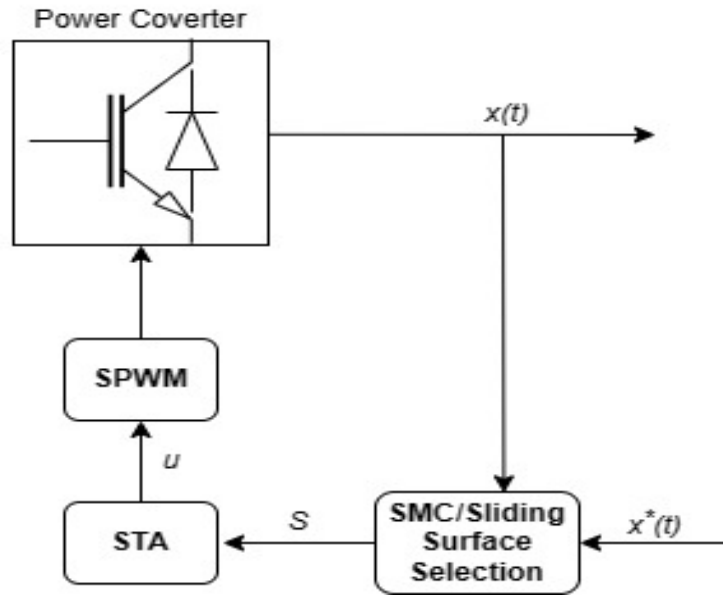


Figure 2.14: Super Twisting Algorithm Approach [9]

plementation of STA, it is also worth-mentioning here that the Theoretical proof of finite time convergence and stability have not been studied in detail yet.

2.6.5 Higher Order SMC (HoSMC)

The idea of HoSMC was introduced as a replacement for the conventional sliding mode (also known as the first order sliding mode). According to the authors of [175], HoSMC has the potential to eliminate the requirement for the relative degree to be equal to one, which is needed in the conventional sliding mode, and can also reduce the chattering effect. The concept of High Order Sliding Mode (HOSM) introduced by Dr. A. Levant has attracted significant attention from researchers, leading to a continuous influx of publications in this area. One such publication,[168], explores the synthesis of a control algorithm for nonlinear systems to steer them to a desired manifold while keeping them within specified constraints. In general, this synthesis often employs sliding mode strategies, known for their frequent and rapid control switching. Yet, the precision of this sliding mechanism, reflecting the system's variance from the set constraints, is intrinsically linked to the duration of switching delays. To address this challenge, a new category of sliding modes and algorithms has emerged, introducing the concept of sliding mode

order. These innovative algorithms showcase a control approach that maintains continuous evolution over time, introducing abrupt changes only in the control derivative. This design guarantees controlled bounds. Furthermore, research highlights that the accuracy of the sliding mode is directly proportional to the square of the switching time delay.

The conclusions drawn through the comparative analysis of conventional and HoSMC by Utkin in [178] are worth mentioning here. While considering whether HoSMC control is a more effective substitute for conventional SMC, it has been found that this is not always the case. Simple demonstration of examples and discussions have shown that the efficacy of HoSMC is dependent on various factors such as system classes, unmodeled dynamics, and disturbances, which have not yet been clearly outlined.

Following are the key conclusions drawn by the comparative study of [178]:

i. **Relative degree**

HoSMC shares a common characteristic with conventional sliding mode in that the relative degree must be equal to one. This means that the number of times the input variable of the system needs to be differentiated to obtain a variable proportional to the output must be equal to one. While HoSMC was introduced as an alternative to conventional sliding mode, it does not remove this requirement for relative degree. Therefore, in terms of relative degree, there is no advantage of HoSMC over conventional sliding mode.

ii. **Finite time convergence**

The concept of finite-time convergence relates to the capacity of a control system to attain the desired state within a defined period. However, in the case of HoSMC control, it has been noted that this property may not hold in the presence of unmodeled dynamics. Hence, even if the control system is designed to exhibit finite time convergence, unmodeled dynamics can cause the system to require an infinite amount of time to attain the desired state.

In addition, it has been noted that if the movement of the control system becomes asymptotically stable after reaching the lower dimensional sliding manifold in HoSMC, then conventional sliding mode control can achieve the same dynamics. In such cases, conventional sliding mode control is a more straightforward and simpler choice for implementation.

iii. **Chattering suppression**

Chattering suppression is a technique used in control theory to reduce the impact of oscillations caused by discontinuous control signals. However, it is important to note that the concept of finite-time convergence, which guarantees convergence in a finite time, is often at odds with chattering suppression. In fact, systems that exhibit finite-time convergence tend to have a higher level of chattering compared to those that exhibit asymptotic convergence. This conflict arises because the discontinuous control signal needed to achieve finite-time convergence can cause high-frequency oscillations in the control signal, resulting in chattering.

Utkin in [178], presents performance analysis of SoSMC with conventional SMC at the condition to achieve same finite time convergence, it is found that the chattering is reduced 8 times incase of conventional SMC. Similarly, the comparison between the super-twisting control and the conventional sliding mode control reveals that the super-twisting algorithm exhibits a significantly higher amplitude of chattering. This outcome is particularly evident in situations with a high level of disturbances.

iv. **Implementation**

From an implementation perspective, the conventional SMC can be modified to incorporate the properties of HoSMC. This modification can be achieved using the same state components for both versions of control, implying that the relative degree remains equal to one in both cases. This provides an advantage in terms of implementation as it eliminates the need for additional hardware or sensors.

2.6.6 Terminal SMC (TSMC)

The concept of Terminal Sliding Mode (TSM) finds its roots in the concept of terminal attractors [179], which initially emerged as a means to investigate content addressable memory within neural networks. This concept was later adapted to the realm of control design in [180]. In this study, the core structure of TSM applicable to second-order systems was employed as follows:

$$s = \dot{x} + \beta|x|^\gamma \operatorname{sgn}(x) \quad (2.23)$$

Where, $x \in \mathbb{R}$ be a variable, $\beta > 0$, and $0 < \gamma < 1$. It is worth noting that in previous studies on TSM, the value of γ was often chosen as $\gamma = q/p$ for the sake of analytic convenience, where p and q are positive odd integers.

The salient characteristics of the Terminal Sliding Mode Control (TSMC) can be demonstrated as:

- i. Unlike the linear sliding surfaces/manifolds of traditional SMC systems [181], the sliding surfaces/manifolds within TSMC systems manifest nonlinearity.
- ii. The TSMC systems differ from the conventional SMC systems in that they achieve finite-time convergence, rather than asymptotic convergence [181].
- iii. Under similar parameter conditions, TSMC systems exhibit lower steady-state errors compared to conventional SMC systems [182].
- iv. The full-order TSMC offers a notable benefit by concurrently addressing two critical obstacles that impede the practical deployment of SMC - the singularity issue and the chattering phenomenon [183].
- v. Continuous TSMC sets itself apart by showcasing a remarkable ability to significantly suppress chattering, all the while ensuring the finite-time convergence of systems featuring bounded uncertainties in relation to the H_2 norm. The employment of this approach not only ensures system stability but also enhances performance, rendering it an optimal solution for real-world applications [184].

Table 2.4: Comparison of three different SMC methods

Parameter	Conventional SMC	HoSMC	TSMC
Sliding Surface	Linear/Nonlinear	Linear/Nonlinear	Fractional Power
Convergence to Sliding Surface	Monotonically	Non-monotonically	Monotonically
Convergence on Sliding Surface	Asymptotic	Finite Time	Finite Time
Chattering (amplitude)[185]	1.27×10^{-4}	4.81×10^{-4}	1.24×10^{-6}
Complexity	Simple	Complex	Complex

TSMC is a versatile technique that finds wide applications in various fields. One of the areas where TSMC has been extensively applied and cover the scope of this dissertation is in voltage source inverters. In this regard, several research works have been conducted to develop and apply TSMC theory and techniques in inverter control.

Moreover, in the study [186], an integral compensation was introduced to the conventional TSMC approach. This addition aimed to eliminate steady-state errors specifically in the context of DC-AC inverters. The diverse applications of TSMC in voltage source inverters attest to the effectiveness and flexibility of the technique in various control scenarios. The comparison of conventional, higher order and terminal SMC techniques is presented in Table 4.7

Numerous TSMC theories have emerged and have been put into practice in diverse applications. Nevertheless, there are certain obstacles in the theoretical and practical realms that require attention for the further growth of TSMC theory and applications. These challenges presented in [181], but are not limited to, the following:

- i. Higher-order SMC technique is used to convert conventional SMC for chattering reduction. However, due to the presence of terms with fractional powers, the derivative of the control signal has the potential to become infinite, which poses a challenge in avoiding singularities.
- ii. This indeed raises a valid concern since the proven finite-time convergence attribute of TSMC systems pertains to continuous-time controllers. However, in practical scenarios, controllers are frequently deployed in discrete-time formats. Consequently, it becomes imperative to explore strategies for conserving or optimizing the finite-time convergence aspect of TSMC systems when actualized with discrete-time controllers. This undertaking presents a notable challenge in the realm of practical implementation.
- iii. One of the challenges in practical applications of the TSMC theories is to determine the optimal parameters of the TSMC controller. This is because the relationship between the controller parameters and the system performance is nonlinear and complex. Optimization algorithms can be used to select the appropriate parameters, but it remains a challenge to find the most efficient and effective optimization methods for TSMC controllers in real-world scenarios.

- iv. The TSMC and its related control strategies are inherently nonlinear, which is different from conventional SMC. Despite their good steady-state and dynamic performances, implementing TSMC controllers can be challenging. In particular, finding a balance between implementation complexity and performance optimization is a practical challenge that needs to be addressed.
- v. The TSMC has found extensive applications in both controllers and observers, with most practical implementations utilizing DSPs, or FPGAs. Yet, the task of implementing TSMC controllers/observers with the intended real-time efficacy on these resource-constrained embedded devices continues to pose a challenge. It requires a delicate balance between the performance requirements and the available computing resources. Addressing this challenge is crucial for the wider adoption of TSMC in various real-world applications.
- vi. In conventional SMC systems, the ideal sliding motion enables certain states to be treated as the linear feedback of the remaining states. Nevertheless, the nonlinearity observed in TSMC systems poses a challenge to their practical implementation in output feedback control applications. Addressing this issue is a significant theoretical challenge for the development and advancement of the TSMC theory.

2.6.7 Intelligent SMC Approach

Intelligent sliding mode control is an approach that involves the integration of fuzzy logic (FL) and intelligent control technologies with SMC and neural networks (NN) etc., to make it smarter and more efficient [187], [188] and [189]. This approach allows for the design of intelligent controllers that can adapt to changing environments and provide improved performance. Based on the technology used, multiple objectives can be defined, such as improving tracking accuracy, reducing chattering, or enhancing robustness. The integration of SMC with intelligent control technologies has received significant attention and has been extensively investigated in recent years, with numerous research papers and applications demonstrating its effectiveness in various fields. follows:

- i. One benefit of using NNs in SMC is their ability to approximate nonlinear functions with high precision. Through this approach, the integration of intelligent control technologies, such as NNs, allows for the compensation of external disturbances and model uncertainties. As a result, chattering is minimized. Furthermore, NNs can be employed to estimate the switching control term, transforming the discontinuous control signal into a continuous one. This effectively reduces chattering within the system.
- ii. The objective of incorporating FL systems into SMC is comparable to the use of NNs. It facilitates the approximation of smooth nonlinear functions with high precision and helps in estimating external disturbances and modeling uncertainties to mitigate chattering.
- iii. Reinforcement Learning (RL) is a machine learning method inspired by psychology, which has gained recognition in game theory, control theory, and optimization

problems. It provides a framework to enable agents to take actions in an environment to maximize a specific reward function. RL has been recognized for its computational efficiency in adaptive optimal control systems, which aim to optimize a function of the controlled process [190].

Researchers have proposed various reinforcement learning algorithms to derive optimal controllers for linear time-invariant deterministic systems without any knowledge of the system dynamics, and only system output feedback is required for convergence to the optimal solution. As an example, in a particular study [191], optimal controllers were obtained using various reinforcement learning techniques for a specific group of linear time-invariant deterministic systems.

The applications of RL extend beyond adaptive optimal control systems to include various areas, such as robotics, finance, and healthcare. RL offers an attractive approach to solve complex problems, and further research is being conducted to develop more efficient RL algorithms that can handle higher-dimensional problems and provide more stable convergence to the optimal solution.

- iv. Evolutionary computation can be considered as a viable alternative to search for optimal control parameters. This approach involves using optimization algorithms that are inspired by biological evolution to find the optimal set of control parameters that can minimize the chattering phenomenon in the SMC system. In addition, machine learning techniques are being integrated with SMC and its various types to extract the inherent characteristics of SMC and apply the effectiveness of machine learning to achieve reduced chattering. This integration involves using machine learning algorithms to model the system dynamics and learn the optimal control parameters that can minimize the chattering effect. The combination of evolutionary computation and machine learning techniques can lead to more efficient and effective SMC systems that are capable of achieving better control performance with reduced chattering. Following are the couple of examples that can be quoted as a reference:

2.6.8 State Observer Approach

A potential approach is to generate an ideal sliding mode by using a control software in the observer loop while excluding the main loop. This method eliminates chattering in the system because the main loop is not required to track the observer loop. State observer approach Provides more flexibility while its implementation is complicated and it requires more effort in the control design. The state-of-the art contributions [192], [193] and [10] applied state observer approaches for chattering reduction in sliding mode control (SMC) for different nonlinear systems. The first paper introduces an SMC approach, free from chattering, that uses an extended state observer to handle matched and mismatched disturbances in nonlinear systems. In the subsequent paper, the authors delve into the application of finite-time adaptive extended state observer, rooted in dynamic SMC, for addressing uncertainties in hybrid robots. In the final paper, they propose a cascaded extended state observer based SMC for an under-actuated flexible joint robot.

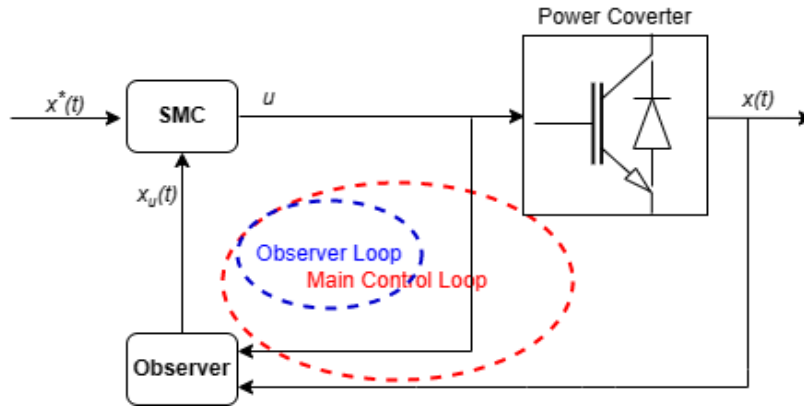


Figure 2.15: State Observer Approach [10]

In this case, the observer plays a role in disturbance estimation and noise reduction. The common thread across all three papers is the demonstration of the efficacy of their respective techniques in curbing chattering and enhancing control performance. These findings underscore the significance of state observer strategies within SMC, underscoring their role in enabling robust control of nonlinear systems grappling with uncertainties and disturbances.

2.6.9 Reaching Law Approach

The conventional approach for designing sliding mode controllers, in either continuous or discrete time, involves formulating the control law and verifying the stability of the system using Lyapunov theorems. However, here is an alternative approach famously termed as reaching law, which is used widely to achieve inherent characteristics of SMC while handling chattering issue.

Considering that chattering's intensity corresponds to the control magnitude, a simple strategy to alleviate chattering is by diminishing the magnitude of the discontinuous control, as noted in [194]. Striking a balance between mitigating chattering and upholding system performance within sliding mode control requires an approach that adapts the magnitude of the discontinuous control signal. This method strives for a middle ground: the magnitude decreases as the system state approaches the sliding surface to curtail chattering, and conversely increases as the system state departs from the sliding surface. This principle has paved the way for numerous contemporary contributions, some of which are discussed below:

2.6.9.1 Seminal Gao and Hung Reaching Laws

The reaching law strategy, initially introduced by Gao and Hung in [195] within the context of continuous-time systems, centers around steering the sliding variable's desired evolution to ensure the stability of the sliding motion. This approach veers away from the need for Lyapunov-based stability analysis, opting instead for the concept of evolution in crafting the control signal. The design of the control signal entails expressing the first derivative of the sliding variable as a function of the variable itself and other pertinent

system parameters. With the passage of time, various scholars have enriched the original methodologies set forth by Gao and Hung [195]. This includes notable contributions such as those by Singh et al. [196] and Liu et al. [197], among others.

In their seminal work [195], Gao and Hung presented three distinct continuous-time reaching law variants. The first among these reaching laws is termed the constant rate reaching law, and its formulation can be articulated as follows:

$$\dot{S} = -K \text{sign}(S) \quad (2.24)$$

where $K > 0$. This approach offers the benefit of simplicity by propelling the sliding variable toward the switching plane at a consistent pace. However, there exists a solitary design parameter that necessitates striking a balance between the convergence speed during the reaching phase and the extent of oscillations during the sliding phase.

Furthermore, Gao and Hung have introduced an alternative reaching law termed the constant plus proportional rate strategy, delineated as follows:

$$\dot{S} = -K \text{sign}(S) - qS \quad (2.25)$$

where $q > 0$ and $K > 0$. By adding the proportional component, the rate of convergence is increased for higher sliding variable values, allowing for smaller constant K values without compromising favorable features in the reaching stage. Conversely, in proximity to the switching surface, the proportional term reduces to prevent an increase in the magnitude of oscillations during the sliding phase.

According to [195], the last approach suggested is the power rate reaching law, which is given as:

$$\dot{S} = -K|S|^\alpha \text{sign}(S) \quad (2.26)$$

where $K > 0$ and $0 < \alpha < 1$. The objective of using this reaching law is to attain rapid convergence to the switching surface while avoiding the undesired oscillations during the sliding phase. Studies have shown that this approach yields a finite reaching time and that the absence of the constant switching term $-K \text{sign}(S)$ reduces chattering.

In order to improve the performance of SMC, various intelligent modifications have been made to Gao and Hung [195] seminal reaching laws. Few of which are discussed below:

2.6.9.2 Exponential Reaching Law

The constant reaching law in [198] is combined with an exponential term to account for the variations in the switching function. This results in the formulation of the Exponential Reaching Law (ERL) as follows:

$$\dot{S} = -(K/\delta_0 + (1 - \delta_0)e^{-\alpha|S|^\gamma}) \quad (2.27)$$

Here, δ_0 , α , and γ represent strictly positive values. It is important to note that the ERL given by 2.27 does not compromise the stability of the control because the denominator of the reaching law is always strictly positive. Looking at the reaching law mentioned in 2.27, one can observe that as the magnitude of $|S|$ increases, the denominator approaches

δ_0 . Consequently, the ERL converges to k/δ_0 , which is greater than K . In this approach, the magnitude of the ERL grows during the reaching phase to expedite the attraction of the sliding surface. As the system approaches the sliding surface and $|S|$ decreases, the ERL gradually diminishes to mitigate chattering. Hence, the ERL enables the controller to adapt to switching function variations by allowing the magnitude of ERL to range between K and K/δ_0 .

This unique control gain adjustment paved new ways for improving the overall performance of SMC. However, ERL still has the limited control gain value at both extreme ends, while it is desired to achieve highest possible gain value when system states are away from sliding surface, to achieve fast transient response. Similarly, when system states reaches the sliding surface the gain value must diminish, while in case of 2.27 minimum achievable gain value is K/δ_0 , thus results in compromised chattering magnitude along the sliding surface.

To handle this gain adjustment constraints better, multiple variants of ERL are proposed on frequent basis. Few of many are worth to mention here, but not limited to cos-ERL [1], Enhanced ERL[14] and Power Rate ERL[12].

2.6.9.3 Cos-Exponential Reaching Law

The cosine ERL proposed in [1] with slight modification to ERL is shown below:

$$\dot{S} = -(K/\delta_0 + (1 - \delta_0)e^{-\alpha|S|^\gamma} \cos(\beta|S|)) \quad (2.28)$$

The term $e^{-\alpha|S|^\gamma} \cos(\beta|S|)$ exhibits the capability to cross the zero multiple times before reaching the origin or equilibrium point. This characteristic allows this term to approach the origin faster than any exponential function. It is important to note that exponential functions tend to approach the equilibrium point asymptotically over time. However, the challenge of adjusting the gain remains unresolved.

2.6.9.4 Power Rate Exponential Reaching Law

In a recent study [12], a modified version of the Extended Reaching Law (ERL) called Power Rate ERL (PRERL) has been proposed, shown in 2.29. PRERL incorporates a "power rate" modification to ERL and has been found to be effective in reducing chattering and generating smooth control. The power rate method was initially introduced in another study [12] as a means to achieve fast response without chattering..

$$\dot{S} = -(K|S|^\alpha/\delta_0 + (1 - \delta_0)e^{-\alpha|S|^\gamma}) \quad (2.29)$$

The power rate law, although effective in reducing chattering and enabling fast response, has the drawback of bypassing most of the sliding mode motion, which compromises the robustness property [199] and [200]. In contrast, the proposed reaching law integrates the power rate principle with ERL, resulting in a balance between reaching speed, chattering reduction, and sliding mode motion. The power rate aspect of the law enhances robustness by reducing the reaching phase, but using a high value of α close to one can result in fast reaching without the sliding mode phase. Conversely, choosing small values of α allows sliding mode motion, but at the cost of chattering.

2.6.9.5 Enhanced Exponential Reaching Law

In [14], Enhanced ERL (EERL) is proposed to handle chattering. If we analyse EERL shown in equation 2.30 the gain adjustment following distance of system state variables from the sliding surface, extra term is added to further reduce the gain value near the equilibrium point.

$$\dot{S} = -G|S| - (K/\delta_0 + (1 - \delta_0)e^{-\alpha|S|^\gamma}) \quad (2.30)$$

The EERL is modified well to handle chattering magnitude by lowering the gain magnitude near the surface, however, since the constant value of G limits reduction of control gain magnitude capability. Though the chattering is reduced but it further requires reduction while ensuring fast minimum reaching time.

2.6.9.6 Fractional Power Rate Reaching Law

In [2], intelligently modified Fractional Power Rate Reaching Law (FPRRL) is proposed to get maximum advantage from inherent characteristics of SMC.

$$\dot{S} = -[G|S|^t/(\delta + \gamma^{|S|})] \quad (2.31)$$

Where, $0 < t < 1$ and γ and δ are strictly positive. The performance analysis of FPRRL shows that it has high gain value when system state variables are far away from the surface, that ensures high level of robustness with minimum reaching time. However, when state variables are near to the sliding surface that gain magnitude is not reduced comprehensively. Therefore, existence of chattering along the surface is highly expected.

2.6.9.7 Hybrid Reaching Law

In order to further reduce sliding chattering, a Hybrid Reaching Law (HRL) incorporating a terminal reaching part control is proposed. The HRL is formulated as follows:

$$\dot{S} = -m|x|^a S^{q/p} - (b/k)(e^{k|x|} - 1)S \quad (2.32)$$

In the given expression 2.32, a , m , b , and k are positive parameters with specific constraints: $a > 0$, $m > 0$, $b > 0$, and $0 < k < 1$. The variable denoted as x symbolizes the system's state variable. The parameters p and q are positive odd integers, with the condition that p surpasses q . The Hybrid Reaching Law (HRL) comprises two constituent parts: the terminal reaching component and the exponential plus proportional rate reaching component. The terminal reaching part incorporates a variable terminal approaching approach, achieved by combining the power function of the system state variable based on the terminal sliding mode. It can be represented as $m|x|^a S^{q/p}$. On the other hand, the exponential plus proportional rate reaching section is denoted by $-(b/k)(e^{k|x|} - 1)S$ and introduces the exponential function of the system state variable using the pure exponential reaching law. This formulation results in a variable exponential reaching mode, allowing for adaptive behavior based on the magnitude of the system state. Advantages of different functions are tailored well in proposed HRL to achieve fast transient response

with minimum possible existence of chattering along the surface. However, the decision maker for adjusting the gain value is the state variable x , while sliding surface along with state variable and its derivatives is dependent upon the sliding coefficient that determines the dynamic response of SMC. Therefore, for second order system the HRL proposed here may not perform well. Adding to this, resultant value of sliding surface may result in negative, that can alter the whole objective of reaching law approach.

2.6.9.8 Piecewise Double Power Reaching Law

Aiming to enhance the system's convergence rate and decrease chattering, a reaching law known as Piecewise Double Power Reaching Law (PDPRL) has been proposed in 2.33. This law is capable of achieving fixed-time convergence and allows for the selection of different stages of the reaching law without any mutual impact.

$$\dot{S} = \begin{cases} k_1|S|_1^{\alpha_1} \text{sign}(S) - k_2|S|_2^{\alpha_2} \text{sign}(S_1) - k|S|_1 & |S| \geq 1 \\ k_3|S|_1^{\beta_1} \text{sign}(S) - k_4|S|_2^{\beta_2} \text{sign}(S_1) & |S| < 1 \end{cases} \quad (2.33)$$

where, k_1, k_2, k_3 and K_4 are strictly positive. Moreover, $0 < \alpha_1 < 1$, $\alpha_2 \geq 1$, $\beta_1 > 1$, and $0 < \beta_2 < 1$.

The basic concept of PDPRL is to divide the reaching process into two stages using 1 as the dividing point. The first stage is when the system is far from the sliding mode surface, i.e., $|S_1| \geq 1$, where the reaching law is mainly governed by the first term. On the other hand, in the second stage, when the system is near the sliding mode surface, i.e., $|S_1| < 1$, the second term dominates the reaching law. This division of stages helps to improve convergence speed and reduce chattering. The main idea behind the concept of PDPRL is to take maximum benefit from the from the SMC inherent properties without compromising on chattering. This technique can work well on specific system and can be designed accordingly. However, the relation of gain adjustment is done in very close margins, normally less than 1. Therefore, in extremely sensitive system the proposed cannot be much beneficial.

2.7 SMC for AC VSIs

The inherent characteristics of SMC have made it a preferred choice for various applications. One such application is the use of SMC in the generalized VSI system, which can be depicted using a generalized block diagram 2.16. The VSI can be categorized into two major types: i) stand-alone inverter that is designed to supply power to a load, and ii) grid-tied inverter that is designed to inject energy from an available input DC source to the grid. SMC has been successfully employed in various applications of DC/AC voltage source inverters, some of which are listed below:

2.7.1 Stand-alone VSI

The use of SMC has been widely studied in single-phase VSIs in recent years. Various studies have presented novel and effective approaches to applying SMC to different VSIs. For example, conventional SMC has been used in single-phase H-bridge inverters

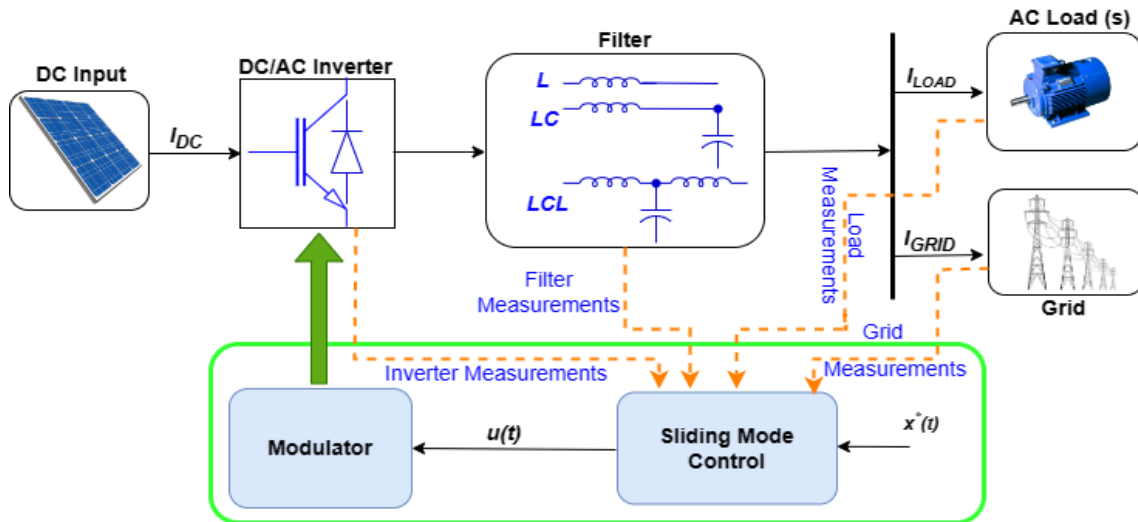


Figure 2.16: Block Diagram of AC Microgrid with SMC System [11]

with fixed, linear, and varying sliding surfaces [201], showing the versatility of SMC in different VSI applications.

Terminal SMC has also been utilized in a single-phase H-bridge inverter with a non-linear sliding surface [202]. In another study, integral SMC was applied to a single-phase quasi-switched boost inverter with linear and fixed sliding surfaces, showing the effectiveness of different SMC techniques [203]. Furthermore, a three-phase voltage source inverter was integrated with conventional SMC, which had linear and fixed sliding surfaces [204].

The aforementioned studies showcase the effectiveness of SMC in diverse applications of single-phase VSIs. Implementing SMC can enhance the overall performance and robustness of VSIs. By employing different sliding mode control techniques, it becomes feasible to effectively regulate the voltage and frequency of VSIs, ultimately enhancing the stability and reliability of the VSI.

In summary, the utilization of SMC has proven to be a versatile and effective approach for the regulation and control of single-phase VSIs. Various SMC techniques have been successfully employed in different VSIs, highlighting the adaptability of SMC in diverse VSI applications. By implementing SMC, the overall performance and robustness of VSI systems can be improved, leading to enhanced reliability and stability.

2.7.2 Grid-tied AC VSIs

The application of SMC in grid-tied inverters has garnered significant attention in the recent past due to its numerous advantages. A plethora of research work has been carried out on the application of SMC in single-phase H-bridge grid-connected DC/AC inverters with fixed, linear, and varying sliding surfaces, respectively. Specifically, conventional SMC has been utilized in [205] and [206] on single-phase H-bridge grid-connected DC/AC inverters with fixed and linear sliding surfaces, whereas conventional SMC is used as feedback control for grid-connected three-phase H-bridge voltage source inverter in [207] and [147]. Under similar conditions, integral and observer-based SMC is applied

with linear and fixed sliding surfaces in [208] and [209], respectively.

Furthermore, conventional SMC with linear and fixed surfaces is applied to three-phase neutral-point-clamped (NPC) inverters in [210]. In [211], a three-phase modulator multilevel inverter (MMC) with conventional SMC comprising linear and fixed sliding surfaces is presented. Integral SMC with linear and fixed sliding surface is applied to single-phase Z-source inverter in [212]. Similarly, conventional SMC with linear and fixed sliding surface is implemented on a single-phase quasi-Z-source inverter in [213].

The literature clearly indicates that SMC is a widely favored option for grid-tied inverters, primarily because of its capability to effectively handle system disturbances and uncertainties. The numerous applications of SMC in grid-tied inverters with varying sliding surfaces highlight its versatility and efficacy in a wide range of applications.

Table 2.5: SMC applications for VSIs (islanded and grid-connected).

References	Application	SMC Type	Sliding Surface
[202] and [214]	1-Phase Islanded	Terminal SMC	Non-Linear/Fixed
[203]	1-phase Islanded	Integral SMC	Linear/Fixed
[201],[215] and [216]	1-phase Islanded	Conventional SMC	Linear/fixed
[204]	3-phase Islanded	Conventional SMC	Linear/Fixed
[205] and [206]	1-phase Grid Connected	Conventional SMC	Linear/Fixed
[207] and [147]	3-phase Grid Connected	Conventional SMC	Linear/Fixed
[208]	3-phase Grid Connected	Integral SMC	Linear/Fixed
[147]	3-phase Grid Connected	Observer based SMC	Linear/Fixed
[210],[211] and [213]	3-phase Grid Connected	Conventional SMC	Linear/Fixed
[212]	3-phase Grid Connected	Integral SMC	Linear/Fixed

2.7.3 Critical Review

As voltage source inverter-based systems have become increasingly prevalent in today's society, ensuring a stable, reliable, and effective voltage source inverter's output for sensitive systems has become a challenging task. This is because these systems operate near stability constraints due to financial and environmental concerns. Therefore, a control system for single phase voltage source inverters (SPVSI) must be designed to achieve the aforementioned objectives.

SMC is a widely adopted technique in several non-linear systems, including voltage source inverter applications [217]. This is due to SMC's inherent properties such as simple design, reduced order, exceptional robustness, insensitivity to external disturbances and parametric variations, finite time convergence, and excellent dynamic behavior [218].

The sliding surface in SMC is selected in a way that states of the system are compelled to reach the sliding surface in a limited time, making system dynamics linear time-varying stable, with negligible internal or external disturbances [219]. Despite asymptotic convergence of states to the sliding surface, conventional SMC, like other non-linear control techniques, suffers from many imperfections [220].

Therefore, in the context of voltage source inverter applications, research has focused on developing and improving SMC for single-phase and three-phase voltage source inverters to mitigate these imperfections. These improvements have led to the development of different SMC techniques such as integral SMC, terminal SMC, and adaptive SMC, which aim to address the limitations of conventional SMC. In the upcoming critical review chapter, we will examine these various SMC techniques and their effectiveness in voltage source inverter-based systems, with a focus on their applications in ac VSIs and Voltage Source Inverters. In this perspective, following are the two major areas that needs utmost attention.

2.7.3.1 Sliding Surface Design/Sliding coefficient Selection

First, the major shortcoming that SMC suffers is related to a fixed sliding surface that restricts the dynamic behavior of the feedback system. The fixed value of the sliding surface slope is a compromise between tracking time under output current disturbances and the reaching time of the system states to the sliding surface [4].

In their work [221], Gudey and Gupta introduced a control strategy for VSI called Fast Terminal Sliding Mode Control (FTSMC). This approach utilizes a recursive technique to adjust the inverter bus voltage, enabling it to converge towards the main grid in grid-connected mode and move away from the micro source in islanded operation. The dynamic performance of the controller is highly commendable, exhibiting low total harmonic distortion and minimal steady-state error, even under abrupt load changes during islanding. An advantageous aspect of the FTSMC algorithm is its reliance on a single voltage sensor, thereby reducing the number of sensors required for control operations. However, the study lacks a detailed comparison with other control strategies and performance benchmarks, limiting the scope of the findings. Moreover, the proposed FTSMC approach is an extension of the work by Gudey and Gupta, which used a sliding surface design based on both linear and nonlinear characteristics. Although this nonlinear surface design reduced the tracking and sliding time, it failed to significantly reduce the tracking error.

Therefore, further research is required to compare the proposed FTSMC approach with other control strategies, identify its limitations, and explore ways to improve its performance. The text provided in [222] proposes a control mechanism for a distributed energy resource system using FoSMC. The aim of the proposed control is to ensure a stable and regulated voltage output, even in case of unbalanced and distorted load conditions. Additionally, the control offers black start functionality and provides protection against external faults to the power electronic interface of the DER system. However, the text points out that these advantages come at the cost of increased computational burden and complexity in implementation. This implies that the proposed control may not be

practical for systems that require simpler and more efficient control strategies. Overall, while the proposed control in [222] offers several desirable features, its implementation may require careful consideration of the trade-off between control complexity and system performance.

In the published work [223], innovative techniques are presented for online tuning of the slope of the linear sliding surface in sliding mode controllers. The aim is to achieve more efficient control for a specific class of second-order systems. The approaches are developed for two new coordinate axes, where one axis represents the classical sliding surface and the other is orthogonal to it. By employing the Lyapunov stability condition, adjustments are made to the control input within the sliding mode control law. To adapt the slope of the linear sliding surface in the updated coordinate axes, a fresh parameter is fine-tuned through diverse approaches. Simulation experiments are conducted on a nonlinear second-order model with bounded external disturbance and parameter uncertainties. A comparison is made between the performance of classical sliding mode controllers that use a constant sliding surface and the delta neighborhood approach in the classical coordinate axes, and the proposed methods that dynamically adjust the slope of the linear sliding surface. The results demonstrate that the proposed approaches outperform the classical sliding mode controller in terms of reduced reaching and settling times, as well as improved robustness to disturbances. The study also highlights that the fixed value of the sliding surface coefficient represents a trade-off between the tracking time under current disturbances and the time taken for system states to reach the sliding surface.

To improve response speed, adjustable sliding surface techniques have been proposed, as discussed in [224]. These methodologies are designed to attain swift and robust tracking within a particular group of uncertain second-order dynamic systems by incorporating a time-varying sliding surface for VSI control. The sliding surface initially traverses arbitrary initial states and gradually moves towards a predefined surface through rotation and/or shifting. The presence of sliding mode using the time-varying sliding surface is demonstrated in the paper, which also provides detailed procedures and notable characteristics of the proposed surface. By utilizing this surface, favorable performance in terms of fast and robust tracking is achieved without amplifying the magnitude of the discontinuous control gain, thereby mitigating undesirable chattering. To illustrate the benefits of the proposed method, the article applies it to a simple second-order nonlinear system subjected to parameter variations and external disturbances, as mentioned in [224]. Additionally, in [223] and [225], two-dimensional (2-D) and one-dimensional (1-D) fuzzy-based rules were adopted, respectively.

The study presented in [226] introduces a novel method for sliding mode control that incorporates a RSS to attain rapid and robust tracking in a specific class of second-order nonlinear systems. In this approach, the rotation of the sliding surface is determined through a linear function approximation derived from the input-output relationship, utilizing a 1-D fuzzy rule. Furthermore, the approach is expanded to encompass a single-input fuzzy logic controller (SIFLC), which utilizes error variables to dynamically adjust the time-varying slope of the sliding surface. This leads to the RSS, which provides a fast transient response for single phase voltage source inverters [4]. Despite the advan-

tages and simplicity of designing sliding surfaces using these techniques, there are some limitations. Firstly, the above-mentioned techniques rely on a linear approximation for nonlinear state space variables, which may result in inaccurate control in some cases. Secondly, only the surface rotation mechanism is adopted, overlooking the significance of the switching gain of the reaching law, which is an important factor in ensuring robustness and stability of the system. These limitations should be considered when applying the proposed methods in practical applications. Nevertheless, the approach presented in [226] provides a promising direction for developing efficient and effective sliding mode control strategies.

In [214], TSM based on fraction power non linear sliding surface selection mechanism is presented for power converters. The presented approach primarily focuses low %THD and fast transient response, while other vital parameters of interest for power converters are overlooked. Similarly, [227] introduced Direct Power SMC for islanded VSIs, based on distributed linear sliding surfaces to handle improve voltage regulation and robustness. Likewise, Linear Matrix Inequalities (LMIs) sliding surface is introduced in [145] to reduce voltage tracking error and low %THD. STA is used in [228] to design a sliding surface to achieve dynamic performance with reduced chattering for single phase VSI application. Moreover, Extended State Observer based on integral sliding surface is proposed in [229] to achieve better dynamic response for VSIs. In order to achieve robustness, dynamic performance, fast transient response and low %THD for VSIs, SMC with switching function based sliding surface is introduced in [146].

2.7.3.2 Reaching Law Design

SMC is commonly employed to achieve robust control of uncertain systems. However, one challenge with SMC is the need to use high switching gains to ensure robustness. The use of high gains, in turn, can result in chattering, a phenomenon where the control signal switches rapidly between high and low values, leading to undesirable high-frequency oscillations. In [230], the authors highlight the problem of chattering in SMC and propose the use of a saturation function instead of a switching function to overcome this issue. The saturation function restricts the control signal within a certain range, thus reducing the high-frequency oscillations and mitigating the chattering problem. The use of a saturation function can be a favorable choice in SMC to achieve robustness without compromising on the control performance. Although, chattering catered through this choice still results in a steady-state error due to boundary layer choice.

A novel approach for controlling a low-voltage VSI system is proposed by Gudey and Gupta et al.[221], which operates in both grid-connected and islanding modes. The VSI system is considered a higher order distribution system, and the proposed control strategy is based on the recursive fast terminal sliding mode control (FTSMC) approach. The application of the FTSMC approach to the VSI allows for precise regulation of the bus voltage, ensuring it stays closer to the main grid during grid-connected operation and farther away during islanding mode. This proposed methodology exhibits excellent tracking performance for the bus as well as the output voltage, achieving faster convergence. Furthermore, the controlled voltage exhibits a low level of %THD and minimal steady-state

error, effectively improving the overall performance of the system. Notably, the proposed algorithm achieves these outcomes while only necessitating a single voltage sensing requirement for control operation. Moreover, this investigation underscores the limitations of the classical sliding mode control approach in regulating the bus voltage, particularly when the bus voltage is located at the far end of the VSI system [221]. However, the proposed recursive FTSMC control for single phase VSI with a condition to avoid singularity, which leads to shortening tracking and sliding time with a merely noticeable reduction in tracking error. Moreover, tuning constants to avoid singularity conditions and sliding coefficients for sliding surfaces designs are selected randomly. The effect of the FTSMC on the chattering problem on the sliding surface is also ignored in the analysis.

Numerous strategies have been adopted to overcome the aforementioned problem, like second-order sliding mode control (SoSMC) [231],[232]. The primary purpose of using SoSMC is to eliminate chattering by allowing the switching function and its derivatives to converge to equilibrium point through integral function. In order to enhance the performance of SoSMC, the super twisting control technique was employed, as described in [233] and [234]. Further improvements were made by integrating modified super twisting algorithms into SoSMC, as mentioned in [235] and [236]. However, despite the benefits achieved through these enhancements, there is an increased risk of system instability due to the second-time derivative of the switching surface, amplifying the vulnerability to external disturbances.

To overcome aforementioned problems, worth mentioning innovative techniques have been proposed, like higher-order sliding mode control (HoSMC) [237], [238]–[239], complementary sliding mode control [240], and the most popular reaching law technique (RL) [241]. HoSMC is preferred to use in higher order multiple input multiple output (MIMO) systems [242]. Since SPVSI is a second order single input single output(SISO) system, therefore due to high level of complexities associated with implementation of HoSMC [243], it is not preferred to use in second order systems like SPVSI.

The reaching law technique directly correlates with the convergence rate of system states to the equilibrium point. Therefore, reaching time of SMC along with chattering reduction can be achieved through intelligent design of a reaching law. Gao et al. [244] proposed a switching function associated with variable structure control and reaching laws such as constant reaching law, proportional reaching law, and power reaching law. However, sliding surface design is also one of the essential parameters in designing SMC SPVSI systems. In most cases, a sliding surface function comprises a linear combination of the error and its derivative.

Several approaches have been proposed in the existing literature to minimize reaching time while taking care of chattering on the sliding surface. Fixed gain reaching law enforces system states to converge on sliding surface ($S=0$) infinite reaching time [245]. The time required to converge the surface depends on the value of the control gain value. Thus, a higher value of gain ensures faster convergence while giving rise to chattering along the sliding surface. Fixed with proportional gain reaching law employs faster convergence, however, lack in mitigation of chattering along the surface. A breakthrough in tackling the issue occurs with the advent of power gain reaching law [246], in which reaching time speed is adjustable with the distance of states from the sliding surface.

Hence, ensuring fast convergence with reduction of chattering. However, very near the surface, the value of gain is not eliminated, thus causing chattering. Through analysis of three reaching gain laws, it can be easily deduced that these laws are beneficial in achieving better results through simple designing of sliding mode control. However, each control gain reaching law has its merits and minor demerits, which always leads to a compromise between reaching speed and chattering mitigation or control robustness and chattering reduction. The commonality among these laws is that convergence time to reach the desired sliding surface is directly dependent upon the value of reaching law gain. The higher value of gain always leads to chattering along the surface that has higher frequency dynamics.

To handle this compromise better, exponential reaching law (ERL) was introduced [247]. That, proves efficient in handling trade-offs between reaching time, chattering, and robustness of control. Interestingly, the E-RL has catered the trade-off by allowing the controller to adjust the gain value according to the surface variation. The idea has been widely accepted and adopted since then and applied to robust control in several non-linear systems of various fields. In [248] along with achieving robustness and reduced overshoot, chattering along the sliding surface is also reduced through applying slight changes to exponential reaching law. A modified E-RL proposed in [14] results in reduced chattering and lower total harmonic distortion value. Discrete-time repetitive sliding mode control based on E-RL with bi-power characteristics applied to three-phase voltage source inverters to achieve better steady-state response with robustness [248]. In [1], using the cos function with exponential and power term (Cos-ERL) further improves the reaching time with a noticeable reduction in chattering across the surface. However, a lower bound of the control gain is maintained at $L_{\text{sign}}(S)$, limiting the convergence behavior of a reaching law. It's observed that the system's state variables do not follow the system trajectory perfectly following the lower value of chattering. In [236], slight modifications to E-RL proved beneficial in achieving reduced chattering with low THD. Moreover, the Enhanced Exponential Reaching Law (EERL) was proposed in [237] to achieve a fast transient response with reduced chattering. Cos function integrated with power function was used to modify E-RL in [240] and [241] to achieve an improved convergence rate with evident chattering reduction along the surface. However, the restricted control gain magnitude limits the reaching time and chattering reduction capacity. The power rate exponential reaching (PRERL) and fractional power rate reaching law (FPRRL) were proposed in [244] and [245], respectively. Both reaching laws have succeeded in achieving marginal improvement in a reduction to the reaching time, robustness, and chattering. Moreover, in [246], the discrete time repetitive reaching law (RRL) based SMC was proposed for three phase VSI to achieve an improved steady state response with reduced chattering. Likewise, discrete time repetitive SMC composed of exponential bi-power reaching is presented in [249] to achieve dynamic response along with robustness for VSIs. Similarly, fast reaching Law is proposed for finite time convergence SMC for VSIs to achieve fast reference tracking and extreme robustness in [250]. In another scholarly effort to achieve fast dynamic response with enhanced robustness for VSIs, super twisting based reaching law is introduced to formulate finite time convergent SMC.

2.7.4 Practical Applications of SMC based VSIs

The practical applications of the SMC technique for VSIs are broad and offer substantial advantages across multiple fields:

- i. **Uninterruptible Power Supplies (UPS):** An improved SMC method can be used to enhance the reliability and efficiency of UPS systems, ensuring continuous and stable power supply during outages. This is especially important for critical facilities such as hospitals, data centers, and telecommunications infrastructure where power stability is crucial [19].
- ii. **Electric Vehicles (EVs):** The SMC with its inherent characteristics can enhance the performance of power conversion systems in EVs, leading to more efficient battery management, longer driving ranges, and improved vehicle reliability [251]. The reduced chattering and high voltage regulation can also improve the overall driving experience and longevity of EV components.
- iii. **Renewable Energy Systems:** The SMC technique can be applied to grid-tied solar inverters and wind turbine converters, ensuring efficient and stable integration of renewable energy into the grid. This helps in maintaining grid stability, reducing energy losses, and maximizing the use of clean energy sources [33].
- iv. **Industrial Motor Drives:** The SMC can be implemented in industrial motor drives to achieve precise control over motor speed and torque, improving the efficiency and performance of machinery in manufacturing, robotics, and automation [252]. This can lead to energy savings and increased productivity in industrial settings.
- v. **Power Quality Improvement:** The advanced VSI with SMC method can be used in power conditioning equipment, such as active power filters, to improve power quality by reducing harmonics, voltage sags, and other disturbances in the electrical grid. This is vital for sensitive equipment in industries and commercial buildings that require clean and stable power.
- vi. **Microgrids and Distributed Generation:** The SMC technique is well-suited for managing MGs, where it can ensure stable operation under varying load conditions and disturbances. This is particularly beneficial in remote areas, disaster recovery sites, and military applications where reliable power supply is essential [23].
- vii. **Emergency and Lifesaving Equipment:** The reliable power regulation offered by the SMC is critical for lifesaving equipment used in hospitals, emergency response units, and mobile medical facilities. The ability to maintain high voltage regulation and low THD ensures that sensitive medical devices operate without interruption.
- viii. **Communication and IT Infrastructure:** The improved SMC for VSI can be applied to power systems in communication networks and IT infrastructure, where stable power is essential to prevent data loss and maintain network reliability. The reduced chattering and high efficiency of the proposed method can enhance the resilience of these critical systems.

- ix. **Laboratory and Research Applications:** The robust control offer SMC technique can be applied in laboratory power supplies, providing researchers with stable and distortion-free power for experiments and testing. This is particularly useful in research environments where accuracy and reliability are paramount.
- x. **Defense and Aerospace Applications:** The robust control offered by the SMC can be used in defense and aerospace systems, where power systems must operate reliably under extreme conditions. The ability to maintain performance in harsh environments makes this technique suitable for military vehicles, aircraft, and space missions.

2.7.5 Summary

When it comes to controlling VSIs, various techniques are available, and each comes with its advantages and limitations. A comparative analysis of these techniques helps in identifying their benefits and drawbacks, and one technique that stands out as being highly advantageous with fewer disadvantages is SMC. SMC is well suited for managing nonlinear systems due to its tolerance to uncertainty and outside disturbances, which is one of its main advantages. Additionally, SMC is a versatile technology that has numerous uses, including fault tolerance, power sharing, and voltage and frequency management.

SMC's resilience to uncertainties and disturbances has shown to be a key factor in its success in regulating VSIs. Even under challenging operating conditions, this robustness helps it to preserve the system's stability. In addition, SMC is highly effective in controlling nonlinear systems, which are becoming increasingly common in VSIs. With rise in the integration of DG sources into the power grid, such as renewable energy sources, it becomes essential to have a control system that can handle the fluctuating power supply. SMC provides the necessary robustness to the system to ensure its stability under such conditions.

Additionally, there are numerous applications for SMC in managing VSIs. It is extremely successful at controlling the VSI's voltage and frequency, ensuring that the system runs within the set parameters. Additionally, SMC can be used to make sure that the loads receive an equal part of the power produced by the dispersed sources, preventing overloading or underloading of the system. SMC is also very good at keeping the system stable when there are faults, making sure that the system keeps working even when there are failures.

To further enhance our understanding of SMC and its behavior in VSIs, it is crucial to undertake an in-depth study of this control technique. In the next chapter, we will delve into the working principle of SMC and explore its behavior under various conditions to improve its performance in the context of VSIs. We will discuss different chattering reduction methodologies and sliding coefficient selection techniques, as well as their practical implementation in real-time applications. Through this chapter, we aim to establish a solid foundation for the effective utilization of SMC in the control of VSIs. SMC has been a favourable choice for VSI systems due to its distinguished features including fast dynamic response, high degree of robustness and order reduction. Variable Structure Sys-

tems (VSS) theory sets the foundation for SMC and has been a popular control method for VSIs for several decades. This is highlighted in a review article by Komurcugil et al. [7]. In order to devise an improve SMC approach, the following chapter discusses SMC theory, basic design principles, challenges we might encounter, and solutions. This will pave the way for introducing proposed SMC technique. Based on which, mathematical modeling shall be designed for single phase and three phase VSIs

CHAPTER 3

RESEARCH METHODOLOGY

In this chapter, a comprehensive study is presented on an improved SMC incorporating a composite reaching law technique paired with an adaptive RSS mechanism, specifically designed for VSIs. The primary objective of the proposed technique is to enhance the robustness and reliability of VSIs with reduced chattering and %THD, particularly in the presence of variable load conditions. The section begins by introducing a sliding surface selection design mechanism, which ensures an optimal choice of the sliding surface for effective control. Following that, the composite reaching law technique is presented, detailing its working principle and its ability to regulate the system's behavior. A thorough stability analysis is conducted to testify the effectiveness of the proposed technique in achieving robustness against load variations. Furthermore, a comparative performance analysis is performed, comparing the proposed SMC technique with other state-of-the-art SMCs. The comparative analysis demonstrates the superior performance and efficiency of the proposed technique in challenging conditions. Significantly, the proposed technique is specifically developed to accommodate the needs of both single-phase and three-phase VSIs, thereby enhancing its versatility and applicability. This design consideration ensures that the proposed technique can be effectively employed in a wider range of VSI configurations, providing flexibility and adaptability to various system requirements and configurations. The proposed technique's effectiveness and reliability are thoroughly examined by evaluating its performance under challenging conditions. To validate the results, a comparative analysis is conducted using MATLAB Simulink, comparing the proposed technique with other state-of-the-art SMC techniques. This analysis provides a comprehensive understanding of the capabilities and advantages of the proposed technique. Furthermore, experimental assessments are conducted for single-phase and three-phase VSI on the MicroLabBox-dSPACE 1202, further affirming the improved performance of the suggested technique in real-world scenarios. The SMC design primarily followed by following two steps i.e. Sliding Surface Design and Reaching Law Design:

3.0.1 Step-I : Sliding Surface Design

In [2], the theory of SMC for non-linear systems is well explained. The general equation for a dynamic non-linear second order system is given below:

$$\ddot{x} = f(x, \dot{x}) + b(x, \dot{x})u \quad (3.1)$$

where, $f \in \mathfrak{R}^n$ and $b \in \mathfrak{R}^{n \times n}$ are non-linear functions, u is the control input and b is an inevitable matrix. The tracking output error that ultimately goes to zero can be defined as $x_e(t) = x - x_d$, where $x_d \in \mathfrak{R}^n$ is the desired output. The first step to design SMC is always to start selecting appropriate sliding surface function S that depend on tracking error. Generally, the sliding surface equation is described as:

$$S = \dot{x}_e + \lambda_s x_e \quad (3.2)$$

where λ_s is termed as the slope of sliding surface or sliding surface coefficient and must be strictly positive, the value of λ_s plays a very significant role in the convergence of tracking output error to zero.

3.0.1.1 Optimal Surface based on Rotating Sliding Surface (RSS)

To achieve RSS, the value of sliding surface coefficient λ_s is set by using time-varying slope of a sliding surface. The adaptation of the time-varying slope is achievable through the utilization of fuzzy logic rules that are applied to the error variables x_e and \dot{x}_e . Thus, different values of λ_s can be achieved during transient and steady-state operations. The outcome yielded by the fuzzy logic controller manifests as a coefficient that varies with time, denoted by λ_s , which must consistently remain positive to ensure the system's stable operation. In reference [225], it has been demonstrated that an appropriate 2-D rule base comprising 49 rules can generate λ_s . Although this rule base operates effectively, it brings about higher computational complexity due to its larger number of rules. Moreover, the same source highlights that the 2-D rule base can be simplified to a 1-D version consisting of only seven rules. This reduction becomes achievable through the utilization of the insight that the 2-D rule base yields an indistinguishable output when at least one input changes its sign in the neighboring quadrant. The study presented in [4] demonstrates that a sliding surface featuring a varying slope λ_s can be rotated within the phase plane, adapting to changes in load conditions. It is worth mentioning here that VSI operates with a greater value of λ_s during a transient caused by load variation to achieve faster voltage convergence. However, the value of λ_s returned back to its original value and remains unchanged during steady-state. This dynamic characteristic of time-varying slope can be achieved simply by adopting a function of first order using error variables of the system. Thus, the function based on Single-Input Fuzzy Logic Controller (SIFLC) rules using error magnitude applied in [225] shown below is used to achieve RSS:

$$\lambda_s = -0.45X_d + 0.5 \quad (3.3)$$

$$X_d(t) = |X_1(t)| - |\dot{X}_2(t)| \quad (3.4)$$

Where, $X_1(t) = K_1 x_e$ and $\dot{X}_2(t) = K_2 \dot{x}_e$, and the values of scaling gains K_1 and K_2 are selected as 2×10^{-3} and 2.4×10^{-5} , respectively [4].

3.0.2 Step-II : Reaching Law Design:

Reaching Law design is the second vital step in to cater while designing SMC. the level of robustness with extremely undesired magnitude of chattering along the sliding

surface can only be managed by properly designed reaching law. The proposed reaching law design is crucial in achieving this objective and is presented as follows:

3.0.2.1 Proposed Composite Exponential Reaching Law(C-ERL)

The mathematical development of the proposed control gain reaching law is presented here. The proposed control gain reaching law links the advantages mentioned in referenced reaching laws and guarantees a better convergence rate than previously presented ERL. The proposed Control Gain Reaching Law uses sinusoidal damping concept from [1] and using exponential term tailored with difference function, and is stated as:

$$\dot{S} = \left[D(S) - \frac{|G \times S|}{E(S)} \right] \text{sign}(S) \quad (3.5)$$

$$D(S) = |S|(\gamma + (1 - \gamma)e^{-\varphi|S|^\phi}) \quad (3.6)$$

$$E(S) = (\gamma + (1 - \gamma)e^{-\varphi|S|^\phi} \cos(\beta(|S|))) \quad (3.7)$$

3.0.2.2 Working Principle

The working principle of the proposed control gain reaching law can be explained as follow:

- i. Initially at $S \gg 0$, value of control gain reaching law will be maximum following initial control loop system conditions.
- ii. Values of φ , ϕ and β are selected in such a way that for $e^{-\varphi|S|^\phi} \cos(\beta(|S|)) \approx 0 \Rightarrow E(S) < 1$ leads to higher value of $\frac{G(S)}{E(S)}$, where $D(S) < \frac{G(S)}{E(S)}$ ensures gradual system convergence to $S = 0$.
- iii. At $S \approx 0 \rightarrow E(S) \approx 1$ leads to $\frac{G(S)}{E(S)} < 1$, hence $D(S) < \frac{G(S)}{E(S)}$ leads to negligible control gain of reaching law i.e. $\dot{S} = \left[D(S) - \frac{|G(S)|}{E(S)} \right] \text{sign}(S) \rightarrow 0$ that ensures extremely low chattering along the sliding surface.

Control gain of the proposed reaching law is the most efficient convergence mechanism for system states to reach equilibrium point in finite time. The term $e^{-\varphi|S|^\phi} \cos(\beta(|S|))$ has damping characteristics to cross surface several times and asymptotically coincide to the reference point [1]. Moreover, the difference function $D(S)$ has an added advantage to gain adjustment and ensures negligible control gain value at an equilibrium point.

3.0.2.3 Stability Analysis

The well-known Lyapunov function can be described as $V(S) = 1/2(S^T S)$; by taking derivative, we get the following equation:

$$\dot{V}(S) = 1/2(S^T \dot{S}) \quad (3.8)$$

Thus, the stability condition can be described as:

$$\dot{V}(S) < 0 \Rightarrow \begin{cases} \dot{S} < 0 & \text{if } S > 0 \\ \dot{S} > 0 & \text{if } S < 0 \end{cases} \quad (3.9)$$

The first derivative of sliding surface \dot{S} , defines the reaching law. Therefore, taking the first derivative of 3.2 can be represented as:

$$\dot{S} = \ddot{x}_e + \lambda_s \dot{x}_e \quad (3.10)$$

Equating 3.1 and 3.10 results in the following generic control equation for the system:

$$u = b^{-1}(\dot{S} - f - \lambda_s \dot{x}_e) \quad (3.11)$$

The vital role of \dot{S} in input control function can be observed easily, i-e the rate of change of sliding surface S is determined. So, at $\dot{S} \ll 0$ for $S > 0$ (and vice versa) forces the system trajectories to reach and converge at $S = 0$. Thus, the term \dot{S} is well-known as “reaching law”. Moreover, when states of the system are very close to $S = 0$, $\dot{S} < 0$ determines that system states are near to $S = 0$ while guaranteeing $\dot{V} < 0$. Subsequently, there is a “switching” mechanism arises to maintain the condition: $S\dot{S} < 0$. by \dot{S} . Furthermore, To achieve stability, the Lyapunov function $V(t) = (S^2)/2$ must be minimum, following condition $\dot{V} < 0$. The gain value of proposed reaching law $\left[D(S) - \frac{|G(S)|}{E(S)} \right]$ is strictly negative, warranting $S\dot{S} < 0$.

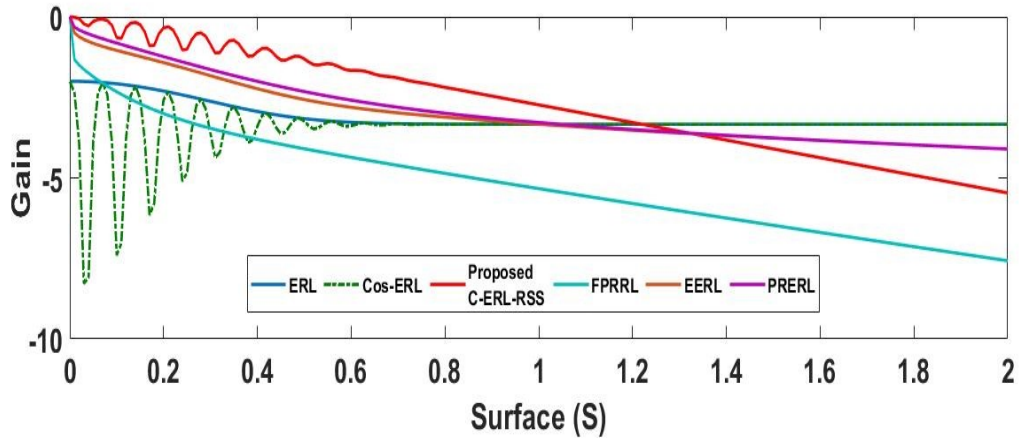


Figure 3.1: Comparison of Reaching Laws Gain variation w.r.t distance from surface.

3.0.3 Comparative Analysis of C-ERL With Other State-of-the Art Reaching Laws

Latest and state of the art reaching laws like Exponential Reaching Law (ERL) [253], Cos-ERL [1], Enhanced Exponential Reaching Law (EERL) [14], Power Rate Exponential Reaching Law (PRERL) [12], Fractional Power Rate Reaching Law (FPRRL) [2] and the proposed C-ERL with Rotating Sliding Surface (C-ERL-RSS) mentioned in Table 3.1 along with comparative analysis of their behavior with changing surface position from the equilibrium point is shown in Figure 3.1, which strongly advocates the

Table 3.1: Reaching Laws with parametric values

	Reaching Law	Parameters
ERL[253]	$\dot{S} = \left[-\frac{G}{(\gamma+(1-\gamma)e^{-\varphi S ^\phi}} \right] sign(S)$	$\gamma = 0.6, \varphi = 10$ $G = 2, \phi = 2$
Cos-ERL[1]	$\dot{S} = \left[-\frac{G}{(\gamma+(1-\gamma)e^{-\varphi S ^\phi} \cos(\beta(S)))} \right] sign(S)$	$\gamma = 0.6, \varphi = 10$ $G = 2, \phi = 2,$ $\beta = 85$
FPRRL[2]	$\dot{S} = \left[-\frac{G S ^\tau}{\delta + \theta S } \right] sign(S)$	$\tau = 0.3, \delta = 0.1$ $G = 2, \theta = 0.01$
PRERL[12]	$\dot{S} = \left[-\frac{G S ^\tau}{(\gamma+(1-\gamma)e^{-\varphi S ^\phi}} \right] sign(S)$	$\gamma = 0.6, \varphi = 10$ $G = 2, \phi = 2,$ $\tau = 0.3$
EERL[14]	$\dot{S} = \left[-KS - \frac{G S }{(\gamma+(1-\gamma)e^{-\varphi S ^\phi}} \right] sign(S)$	$\gamma = 0.6, \varphi = 10$ $G = 2, \phi = 2,$ $K = 200$
Proposed C-ERL-RSS	$\dot{S} = \left[S (\gamma + (1 - \gamma)e^{-\varphi S ^\phi} - \frac{G S }{(\gamma+(1-\gamma)e^{-\varphi S ^\phi} \cos(\beta(S)))} \right] sign(S)$	$\gamma = 0.6, \varphi = 10$ $G = 2, \phi = 2,$ $\beta = 85$

proposed law's effective and adaptive characteristics. It can be seen that when the surface is at $S = 2$ far away from $S = 0$ on the x-axis, at this point magnitude of the control gain on the y-axis must be higher to ensure robustness. At the same time, it is clear from the graph of Figure 3.1 that the value of magnitude of gains for ERL [253], Cos-ERL [1], PRERL [12] and EERL [14] are lesser than the value of gain of proposed C-ERL-RSS. Thus ensuring robustness of the proposed reaching law. Though, the value of gain of FPRRL[2] at $S = 2$ is a bit higher than the proposed reaching law, thus achieving fast response at higher surface value. However, the FPRRL[2] fails to lower its gain value at a higher pace towards the $S = 0$, thus causing extremely higher chattering. Moreover, as the surface moves to the left of the graph, towards the equilibrium point i-e $S = 0$, the value of the magnitude of gain shall be reduced respectively. However, from the graph it is evident that gain magnitude for ERL [253] and Cos-ERL[1] is constant till $S = 0.7$, further to the left on the graph value of gain magnitude reduced to 2 at $S = 0$. This high level of gain magnitude at $S = 0$ results in high chattering. The behavior of EERL [14] and PRERL[12] is improved in comparison to ERL [253] and Cos-ERL[1] in terms of chattering reduction and fast response. However, in the case of the proposed C-ERL-RSS, the value of gain magnitude at $S = 2$ is higher than ERL [253], Cos-ERL[1], EERL[14], PRERL[12], thus ensuring robustness. The value of gain for proposed C-ERL-RSS near to the equilibrium point $S = 0$ is less than all the other reaching laws, thus ensuring extreme chattering reduction. Therefore, the proposed C-ERL-RSS can achieve high ro-

bustness with extremely reduced chattering along the sliding surface, $S = 0$. Comparative analysis summary based on robustness and chattering effect is shown in Table 3.2.

Table 3.2: Comparison of reaching laws in terms of robustness and chattering.

Reaching Law	Robustness	Chattering
ERL[253]	Low	High
Cos-ERL[1]	Low	High
EERL[14]	Moderate	Moderate
PRERL[12]	Moderate	Moderate
FPRRL[2]	High	High
Proposed C-ERL-RSS	High	Low

The reaching law proposed here and reaching laws proposed in [1] and [2] are tested on a second-order system described in Equation 3.1 with the same values of parameters shown in Table 3.1 to examine and analyze the trade-off between tracking time and chattering along the sliding surface at high and low values of gain.

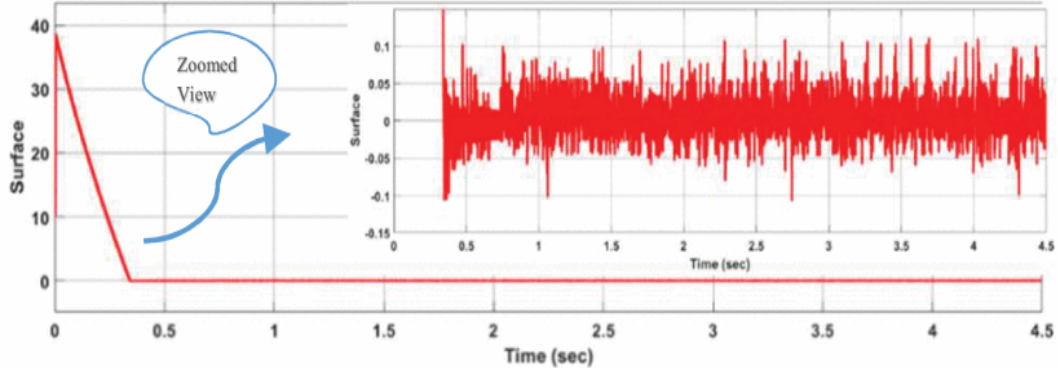


Figure 3.2: Tradeoff-tracking time vs chattering for Cos-ERL[1] with low value of gain.

Another significant aspect in assessing the performance of the reaching law is its examination across varying gain values to scrutinize the balance between chattering and tracking time [254],[255]. This study specifically chooses extreme high and low gain values to explore the trade-off dynamics between reaching time and chattering. The tracking time and chattering response of reaching law proposed in [1] are shown in Figure 3.2 and Figure 3.3 at low and high gain values, respectively. It can be observed from Figure 3.2 that at a low gain value of 50, the tracking time is $0.36sec$ with a chattering of $0.2v$. However, in Figure 3.3, at a high gain value of 5000, the tracking time is extremely reduced to $0.045sec$ with a high rise in the chattering of $1.62v$, which is very undesirable. On the other hand if we observe the behavior of FPRRL [2] under low and high gain shown in Figure 3.4 and Figure 3.5, respectively. It can be observed that the chattering

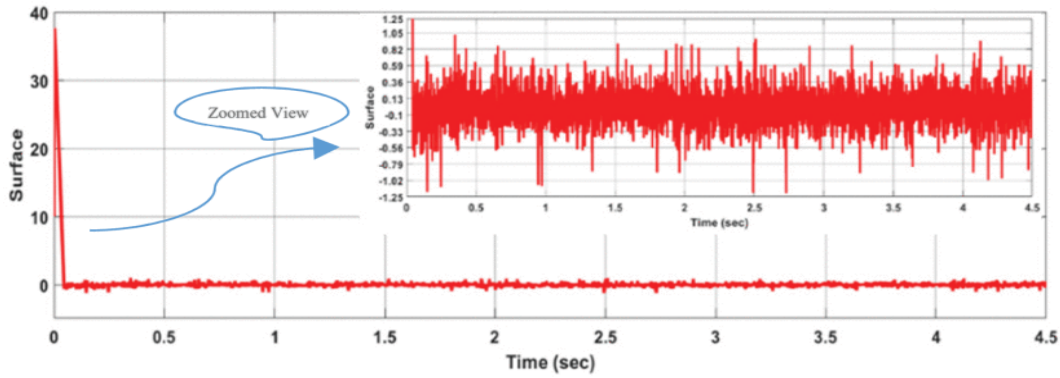


Figure 3.3: Tradeoff-tracking time vs chattering for Cos-ERL[1] with high value of gain.

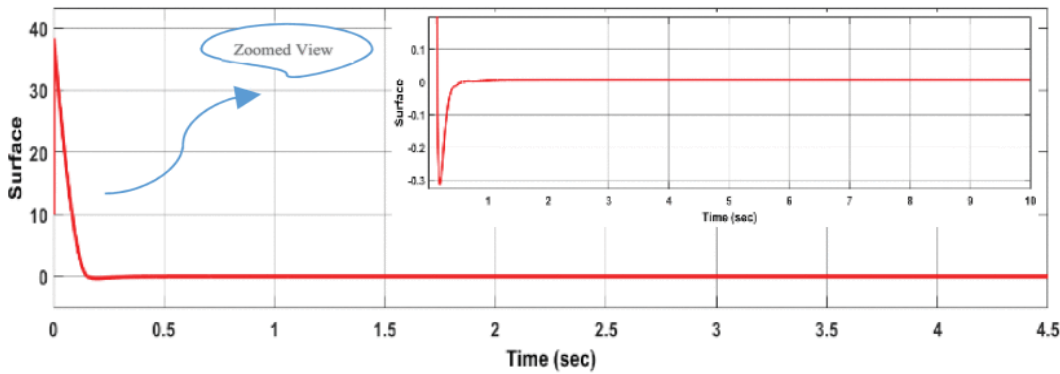


Figure 3.4: Tradeoff-tracking time vs chattering for FPRRL[2] with low value of gain.

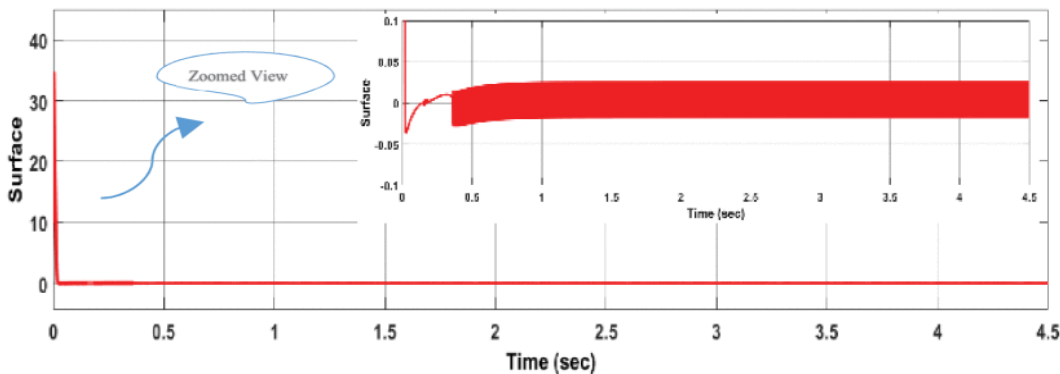


Figure 3.5: Tradeoff-tracking time vs chattering for FPRRL[2] with high value of gain.

is considerably reduced in Figure 3.4, while the overshoot of $0.35v$ occurs which leads to high reaching time of 0.45sec . Moreover, there is a steady state error along the surface and zero crossing doesn't take place after 0.45sec . Moreover, if we observe behavior under high gain value in Figure 3.5, the noticeable increase in chattering takes place and overshoot still occurs that leads to just improved tracking time of 0.2sec . The chattering with overshoot and steady state error with low value of gain is undesirable. However, the response of the proposed reaching law C-ERL-RSS is shown in Figure 3.6 and Figure 3.7 at low and high gain values, respectively. In Figure 3.6 tracking time of 0.4sec is achieved with a chattering of $0.05v$ at a low gain value of 50. While at a high gain value of 5000,

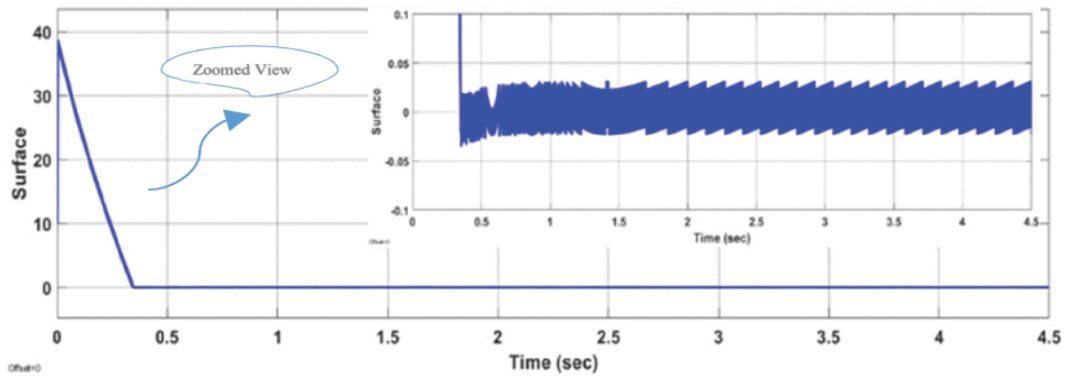


Figure 3.6: Trade-off-tracking time vs chattering for proposed C-ERL-RSS with low value of gain.

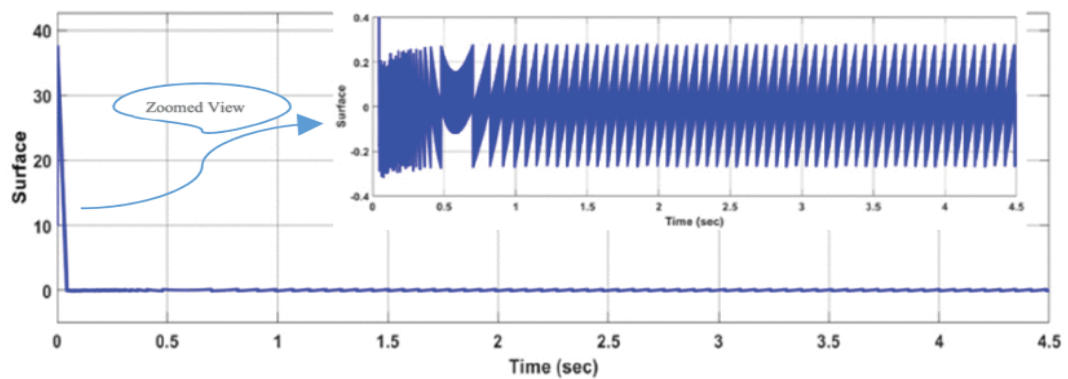


Figure 3.7: Trade-off-tracking time vs chattering for proposed C-ERL-RSS with high value of gain.

tremendous improvement in tracking time can be observed in Figure 3.7 i.e. tracking time is reduced to 0.031sec . At the same time, a slight increase in the chattering of $0.45v$ is observed. The proposed C-ERL-RSS has shown 400% better robustness with 2.34% less chattering than the Cos-ERL reaching law [1]. Thus, the proposed reaching law has proven its capability of assuring robustness with minimum chattering along the sliding surface

3.1 Proposed C-ERL-RSS SMC for single phase VSI

In this section, a novel SMC technique based on C-ERL-RSS is designed for single phase VSIs. The section commences by delving into a conversation regarding the modeling and design of a single phase VSI. Next, the proposed C-ERL technique is designed and implemented on MATLAB/Simulink platform. The performance of the proposed technique is then evaluated under extreme conditions and compared with state-of-the-art SMC techniques. The behavior of the proposed C-ERL-RSS technique is also analyzed through hardware implementation on MicroLabBox dSPACE 1202. The findings of this section offer valuable insights into the potential of the proposed technique to improve the reliability of VSIs.

Table 3.3: Comparison of Proposed C-ERL-RSS With Cos-ERL[1] and FPRRL[2]

Reaching Law	Cos-ERL[1]		FPRRL[2]		Proposed C-ERL-RSS	
	Tracking Time	Chattering	Tracking Time	Chattering	Tracking Time	Chattering
Gain=50	0.36sec	0.2v	0.45sec	0.001v	0.4sec	0.05v
Gain=5000	0.045sec	1.62v	0.2sec	0.05v	0.031sec	0.5v
Effect	800%	12.34%	225%	50%	1212%	10%
	Reduced	Increased	Reduced	Increased	Reduced	Increased

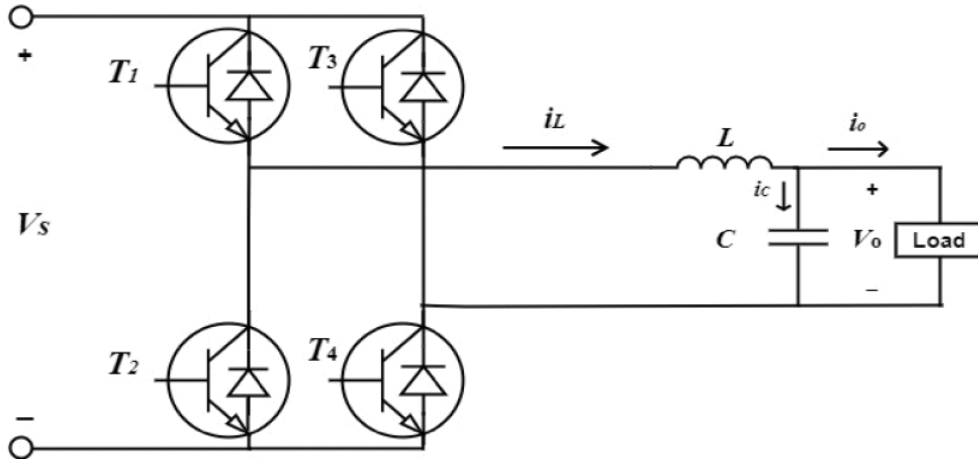


Figure 3.8: Single phase Voltage Source Inverters(VSIs).

3.1.1 System Modeling

The single-phase VSI is shown in Figure 3.8. The system's operation can be described by the following set of state space equations:

$$\frac{d}{dt} \begin{bmatrix} v_0 \\ i_L \end{bmatrix} = \begin{bmatrix} 0 & 1/C \\ -1/L & 0 \end{bmatrix} \begin{bmatrix} v_0 \\ i_L \end{bmatrix} + \begin{bmatrix} 0 \\ v_s/L \end{bmatrix} u + \begin{bmatrix} -i_0/C \\ 0 \end{bmatrix} \quad (3.12)$$

where, u is the control input.

The output voltage error and its derivatives can be defined as:

$$x_1 = v_0 - v_0^* \quad (3.13)$$

$$x_2 = \dot{x}_1 = \dot{v}_0 - \dot{v}_0^* = (i_C - i_C^*)/C \quad (3.14)$$

where v_0^* is the derivative of a reference voltage selected as $v_0^* = V_m \sin(\omega t)$. The dynamics of a system can be represented in the subsequent state space configuration:

$$\begin{bmatrix} \dot{x}_1 \\ \dot{x}_2 \end{bmatrix} = \begin{bmatrix} 0 & 1/C \\ -1/L & 0 \end{bmatrix} \begin{bmatrix} x_1 \\ x_2 \end{bmatrix} + \begin{bmatrix} 0 \\ v_s/LC \end{bmatrix} u + \begin{bmatrix} 0 \\ D(t) \end{bmatrix} \quad (3.15)$$

Where, disturbance term $D(t)$ is given as:

$$D(t) = \begin{bmatrix} 0 \\ -\left(\frac{1}{C}\right) \frac{di_0}{dt} - \left(\frac{1}{LC}\right) v_0^* - \frac{dv_0^*}{dt} \end{bmatrix} \quad (3.16)$$

It is worth noting that due to the derivative of load current, $D(t)$ is not bounded

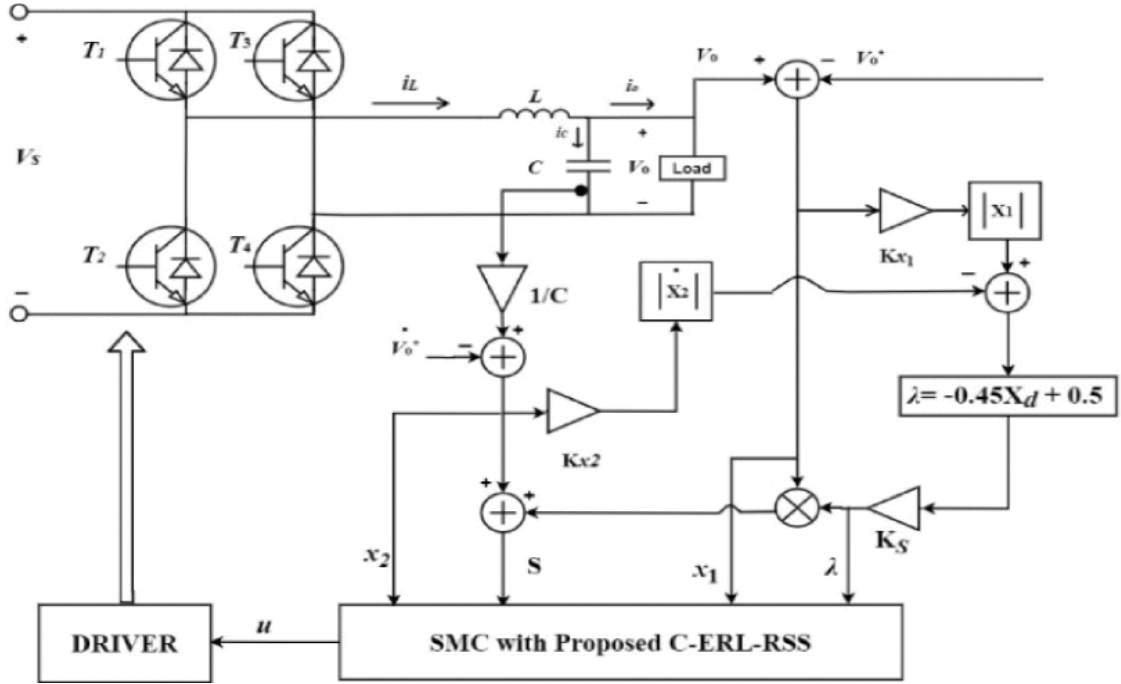


Figure 3.9: Block diagram of single phase VSI with proposed C-ERL-RSS.

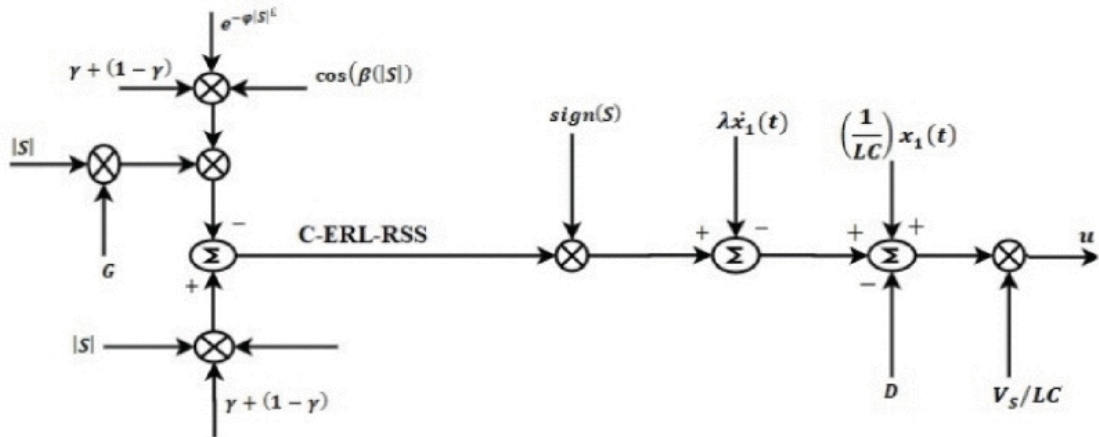


Figure 3.10: SMC with proposed C-ERL-RSS.

3.1.2 Proposed SMC with C-ERL-RSS

The sliding surface equation for a given system is given as:

$$S = \lambda x_1 + x_2 \quad (3.17)$$

Where,

$$x_2(t) = \dot{x}_1(t) \quad (3.18)$$

Substituting equation 3.13 and equation 3.14 in equation 3.17

$$S = \lambda(v_0 - v_0^*) + \left(\frac{i_C}{C} - \dot{v}_0^*\right) \quad (3.19)$$

$$\dot{S} = \lambda\dot{x}_1(t) + \ddot{x}_1(t) \quad (3.20)$$

Substituting equation 3.6 in equation 3.20

$$\begin{aligned} \left[|S|(\gamma + (1 - \gamma)e^{-\varphi|S|^\phi} - \frac{|G(S)|}{(\gamma + (1 - \gamma)e^{-\varphi|S|^\phi} \cos(\beta(|S|)))} \right] \text{sign}(S) \\ = \lambda\dot{x}_1(t) + \ddot{x}_1(t) \end{aligned}$$

where, $0 < \gamma < 1, \varphi > 0, \phi > 0, \beta > 0, \lambda > 0, G > 0$ and $\ddot{x}_1(t) = \dot{x}_2(t)$. In order to achieve RSS, the value of sliding surface coefficient λ is set by using time-varying slope of a sliding surface. Hence, varying values of λ can be attained during both steady-state and transient operations. In [4], it is demonstrated that a sliding surface with a time-varying slope λ can be rotated in the phase plane under changing loads. It is noteworthy that in the case of a single-phase VSI, a higher value of λ is employed during transients caused by load variations to facilitate faster voltage convergence. However, during steady-state, the value of λ returns to its initial value and remains constant. This dynamic characteristic of a time-varying slope can be achieved simply by utilizing a first-order function based on the error variables of the system. Consequently, the function described in [225], which employs SIFLC rules with the magnitude of the error applied, is utilized to achieve the RSS:

$$\lambda = -0.45X_d + 0.5$$

Where,

$$X_d(t) = |X_1(t)| - \dot{X}_2(t) \quad (3.21)$$

Thus, the control function in equation 3.15 with proposed reaching law can be described as equation 3.22 and equation 3.23:

$$\begin{aligned} \left[|S|(\gamma + (1 - \gamma)e^{-\varphi|S|^\phi} - \frac{|G(S)|}{(\gamma + (1 - \gamma)e^{-\varphi|S|^\phi} \cos(\beta(|S|)))} \right] \text{sign}(S) = \lambda\dot{x}_1(t) \\ - \frac{1}{LC}x_1(t) + \frac{V_s}{LC}u \end{aligned} \quad (3.22)$$

$$\begin{aligned} u(t) = \frac{LC}{V_s} \left(\left[|S|(\gamma + (1 - \gamma)e^{-\varphi|S|^\phi} - \frac{|G(S)|}{(\gamma + (1 - \gamma)e^{-\varphi|S|^\phi} \cos(\beta(|S|)))} \right] \text{sign}(S) \right. \\ \left. - \lambda\dot{x}_1(t) + \frac{1}{LC}x_1(t) - D \right) \end{aligned} \quad (3.23)$$

3.2 Proposed C-ERL-RSS SMC for three phase VSI

The proposed control system design with H-bridge circuit topology for three phase VSI is shown in Figure 3.11. The filter inductor, capacitor, and inductor's parasitic resistance is represented as L , C , and r , respectively. The input DC voltage from the DC source and three phase load connected at output is shown as V_S and Z , respectively. Control feedback variables of interest are the voltage across capacitor and current through the filter capacitor, which are shown as $V_{c(abc)}$ and $i_{c(abc)}$, respectively. The control scheme of the proposed law was designed in a stationary (α, β) reference frame.

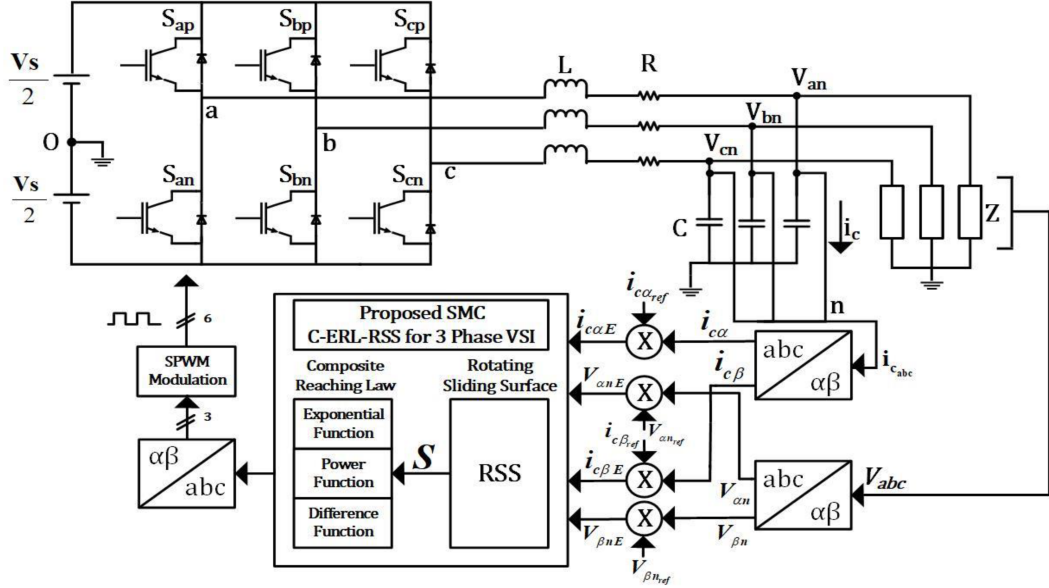


Figure 3.11: Three phase VSI with the proposed reaching law based SMC.

3.2.1 System Modeling

Applying energy conservation laws (KVL/KCL) on the circuit shown in 3.11, the following equalities can be deduced:

$$\begin{cases} C\dot{v}_{jn} = i_{Cj}; & j = a, b, c \\ L\dot{i}_{Lj} + ri_{Lj} = u_{j0} - v_{jn} - v_{n0}; & v_{n0} = 0 \\ i_{Lj} = i_{Cj} + \frac{v_{jn}}{Z_j} \\ v_{j0} = v_{jn} + v_{n0} \\ \sum_j i_{Lj} = \sum_j v_{jn} = 0 & \text{Energy conservation Laws} \end{cases} \quad (3.24)$$

where each phase is represented by $j = a, b, c$. The capacitor voltage and current are represented by v_{jn} and i_{Cj} , respectively. In order to decouple the abc axes, abc is transformed into a stationary $\alpha\beta$ reference frame coordinate system. The following is the $abc \sim \alpha\beta$ transformation matrix [256]:

$$T_{abc \sim \alpha\beta} = \frac{2}{3} \begin{bmatrix} 1 & -\frac{1}{2} & -\frac{1}{2} \\ 0 & -\frac{\sqrt{3}}{2} & \frac{\sqrt{3}}{2} \end{bmatrix} \quad (3.25)$$

The state space equation for three phase VSI with state variables v_{kn} and i_{Ck} in the stationary $\alpha\beta$ reference frame can be derived as:

$$\begin{bmatrix} \dot{v}_{kn} \\ \dot{i}_{Ck} \end{bmatrix} = A \begin{bmatrix} v_{kn} \\ i_{Ck} \end{bmatrix} + Bu_k + D; \quad k = \alpha, \beta \quad (3.26)$$

where u_k represents the control input and after simplifying 3.24, matrices A and B are derived as:

$$A = \begin{bmatrix} 0 & \frac{1}{C} \\ -\frac{Z_j+r}{Z_jL} & -(\frac{1}{Z_jC} + \frac{r}{L}) \end{bmatrix} \text{ and } B = \begin{bmatrix} 0 \\ -\frac{V_s}{2L} \end{bmatrix} \quad (3.27)$$

Representing state variables $\begin{bmatrix} v_{kn} \\ i_{Ck} \end{bmatrix}$ by x , 3.24 can be simplified as:

$$\dot{x} = Ax + Bu_k + D \quad (3.28)$$

Thus equation 3.28 represents the state space model of the system that is same for both axes, moreover, the following control design is valid to apply on any axes. In previous studies such as Liu et al. [257], Mozayan et al. [14], and Shen et al. [258], a second-order SMC with intelligent modifications was proposed for a three-phase nonlinear system. Following a similar approach, a second-order SMC can be designed for a three-phase VSI with a nonlinear load.

3.2.2 Proposed SMC with C-ERL and RSS

Taking into account the properties of a three-phase voltage VSI, the capacitor current serves as a dependable indicator of variations in the output voltage. Consequently, the capacitor current and voltage errors are selected as state variables, offering an optimal foundation for designing control systems that target voltage regulation. The connection between the voltage error and capacitor current can be expressed in the following manner:

$$e = x_{ref} - x = \begin{bmatrix} e_1 \\ e_2 \end{bmatrix} \quad (3.29)$$

$$e_1 = v_{kref} - v_{kn} \quad (3.30)$$

$$e_2 = i_{Ckref} - i_{Ck} = \frac{1}{C} \dot{e}_1 \quad (3.31)$$

$$x_{\alpha ref} = \begin{bmatrix} v_{\alpha ref} \\ i_{C\alpha ref} \end{bmatrix} = \begin{bmatrix} v_0 \sin(\omega t) \\ \omega v_0 \cos(\omega t) \end{bmatrix} \quad (3.32)$$

$$x_{\beta ref} = \begin{bmatrix} v_{\beta ref} \\ i_{C\beta ref} \end{bmatrix} = \begin{bmatrix} v_0 \sin(\omega t - 90^\circ) \\ \omega v_0 \cos(\omega t - 90^\circ) \end{bmatrix} \quad (3.33)$$

where V_0 is the amplitude of the required output voltage and ω is the angular frequency. From 3.29– 3.31, state space form 3.28 can be represented as:

$$\dot{e} = Ae + Bu_k + D \quad (3.34)$$

where $D(t)$ is the disturbance term derived as a similar disturbance matrix D for the three phase VSI derived in [13]:

$$D(t) = \begin{bmatrix} 0 \\ C\ddot{v}_{kref} + \frac{\dot{v}_{kref}}{Z_k} + \frac{v_{kref}}{L} \end{bmatrix} \quad (3.35)$$

In SMC, two operational modes are typically observed: the sliding mode and the reaching mode. The reaching law is employed in the reaching mode to expedite the system state's convergence to the sliding surface. Therefore, an effective reaching law that considers the gap between the system states and the sliding surface is essential for ensuring stability, as will be discussed later in this paper. When the system states align with the sliding surface, it indicates that the system has transitioned into the sliding mode of operation. Within the sliding mode, robustness is assured, and the dynamics of the three-phase VSI can be described using 3.28. An equivalent control law is applied to direct the system states along the sliding surface. However, due to the switching frequency constraint specific to a three-phase VSI, the system states exhibit a zigzag movement along the sliding surface, ultimately leading to chattering. Alongside the stability achieved in the sliding mode and the robustness achieved in the reaching phase, the steady-state and dynamic performance of the system can only be optimized by considering both the reaching law and the selection of the sliding surface. Hence, both the reaching law and sliding surface simultaneously contribute to enhancing the performance of the SMC.

Therefore, in order to design a SMC for three phase VSIs, the following are the two most important parameters of interest:

Appropriate sliding surface selection is ranked among the foremost vital concerns to address. Normally, the sliding surface corresponds to a linear combination of state variables and can be denoted as:

$$S = \begin{bmatrix} \lambda & 1 \end{bmatrix} \begin{bmatrix} e_1 \\ e_2 \end{bmatrix} = Ce; \quad \lambda > 0 \quad (3.36)$$

where, λ is the coefficient of the sliding surface. The dynamic behavior of the sliding surface 3.36, in the absence of external disturbances on a surface, can be shown as:

$$S_\alpha = \lambda e_{1\alpha} + e_{2\alpha} = \lambda e_{1\alpha} + \dot{e}_{1\alpha} = 0 \quad (3.37)$$

$$S_\beta = \lambda e_{1\beta} + e_{2\beta} = \lambda e_{1\beta} + \dot{e}_{1\beta} = 0 \quad (3.38)$$

In the phase plane $(e_1 e_2)$, $S = 0$ represents a sliding line passing through the origin having slope of λ .

$$\dot{e}_{1\alpha\beta} = -\lambda e_{1\alpha\beta} \quad (3.39)$$

First order equation 3.39 can be solved to express the output voltage error as:

$$e_{1\alpha\beta}(t) = e_{1\alpha\beta}(0)e^{-\lambda t}; \quad \lambda > 0 \quad (3.40)$$

Strictly positive real value of λ ensures asymptotic stability. With this, the significance of λ is well proven. Thus, the optimal value of λ can easily be determined, which depends upon the system state variables $\dot{e}_{1\alpha\beta}$ and $e_{1\alpha\beta}$. The single input fuzzy logic (SI-FLC) adopted by Komurkugil in [225] for a single phase VSI was modified with minor adjustments to make it viable to apply on three phase VSI. Therefore, the following linear function is used to rotate the surface with changing state space variables:

$$\lambda_\alpha^R(t) = -0.45E_{d\alpha}(t) + 0.5 \quad (3.41)$$

$$\lambda_\beta^R(t) = -0.45E_{d\beta}(t) + 0.5 \quad (3.42)$$

where $\lambda_\alpha^R(t)$ and $\lambda_\beta^R(t)$ are the rotating sliding coefficient for the α and β stationary frame, respectively, and

$$E_{d\alpha}(t) = |E_{1\alpha}(t)| - |\dot{E}_{2\alpha}(t)|; \quad E_{1\alpha}(t) = K_1 e_{1\alpha} \wedge E_{2\alpha} = K_2 e_{2\alpha} \quad (3.43)$$

$$E_{d\beta}(t) = |E_{1\beta}(t)| - |\dot{E}_{2\beta}(t)|; \quad E_{1\beta}(t) = K_1 e_{1\beta} \wedge E_{2\beta} = K_2 e_{2\beta} \quad (3.44)$$

where K_1 and K_2 are the scaling gains. Based on this, the equation for the sliding surface can be adapted to the form of a rotating sliding surface equation, which can be represented as follows:

$$S_\alpha = \lambda_\alpha^R(t)e_{1\alpha} + e_{2\alpha} = 0 \quad (3.45)$$

$$S_\beta = \lambda_\beta^R(t)e_{1\beta} + e_{2\beta} = 0 \quad (3.46)$$

For simplicity, let us take $S = S_{\alpha\beta}$, $e_1 = e_{1\alpha\beta}$, $e_2 = e_{2\alpha\beta}$ and $\lambda = \lambda_{\alpha\beta}^R$. Thus, taking the derivative of sliding surface we get following relation:

$$\dot{S} = \dot{e}_1\lambda + \dot{e}_2 = \dot{e}_1\lambda + \ddot{e}_1 \quad (3.47)$$

using 3.34,

$$\dot{S} = \dot{e}_1 K \frac{(r+Z)}{ZL} e_1 - \left(\frac{1}{ZC} + \frac{r}{L} \right) e_2 - \frac{V_s}{2L} u_k \quad (3.48)$$

From 3.5, the C-ERL can be described as:

$$\dot{S} = \left[|S|(\gamma + (1-\gamma)e^{-\varphi|S|^\phi} - \frac{|G(S)|}{(\gamma + (1-\gamma)e^{-\varphi|S|^\phi} \cos(\beta(|S|)))} \right] \text{sign}(S) \quad (3.49)$$

where, $0 < \gamma < 1$, $\varphi > 0$, $\phi > 0$, $\beta > 0$, $\lambda > 0$ and $G > 0$. Equating 3.48 and 3.49, we get following relation:

$$\left[|S|(\gamma + (1-\gamma)e^{-\varphi|S|^\phi} - \frac{|G(S)|}{(\gamma + (1-\gamma)e^{-\varphi|S|^\phi} \cos(\beta(|S|)))} \right] \text{sign}(S) = \dot{e}_1 K \frac{(r+Z)}{ZL} e_1 - \left(\frac{1}{ZC} + \frac{r}{L} \right) e_2 - \frac{V_s}{2L} u_k \quad (3.50)$$

Rearranging,

$$u_k = -\frac{2L}{V_s} \left(\left[|S|(\gamma + (1 - \gamma)e^{-\varphi|S|^\phi} - \frac{|G(S)|}{(\gamma + (1 - \gamma)e^{-\varphi|S|^\phi} \cos(\beta(|S|)))} \right] \text{sign}(S) - \dot{e}_1 \lambda + \frac{(r + Z)}{ZL} e_1 + \left(\frac{1}{ZC} + \frac{r}{L} \right) e_2 \right) \quad (3.51)$$

The control input for the stationary frame can be segregated as 3.52 and 3.53:

$$u_\alpha = -\frac{2L}{V_s} \left(\left[|S|(\gamma + (1 - \gamma)e^{-\varphi|S|^\phi} - \frac{|G(S)|}{(\gamma + (1 - \gamma)e^{-\varphi|S|^\phi} \cos(\beta(|S|)))} \right] \text{sign}(S) - \dot{e}_{1\alpha} \lambda + \frac{(r + Z)}{ZL} e_{1\alpha} + \left(\frac{1}{ZC} + \frac{r}{L} \right) e_{2\alpha} \right) \quad (3.52)$$

$$u_\beta = -\frac{2L}{V_s} \left(\left[|S|(\gamma + (1 - \gamma)e^{-\varphi|S|^\phi} - \frac{|G(S)|}{(\gamma + (1 - \gamma)e^{-\varphi|S|^\phi} \cos(\beta(|S|)))} \right] \text{sign}(S) - \dot{e}_{1\beta} \lambda + \frac{(r + Z)}{ZL} e_{1\beta} + \left(\frac{1}{ZC} + \frac{r}{L} \right) e_{2\beta} \right) \quad (3.53)$$

3.3 Summary

Due to its remarkable dynamic response, ease of implementation and robust behavior, SMC has gained widespread adoption and has been extensively studied for controlling VSIs. However, despite its numerous advantages, SMC still encounters certain challenges. These include inaccuracies within the control loop and the switching frequency that changes over time in VSI applications, which are caused by chattering along the sliding surface. Chattering occurs due to the inherent discontinuous control applied to the system, which aims to drive the system states towards the sliding surface within a finite time. The design of the reaching law in the control scheme plays a critical role in minimizing the chattering effect while ensuring the shortest possible reaching time.

Despite numerous scholarly works that focus on individual components of SMC for specific VSI systems, such as the sliding surface or a reaching law, there are several constraints associated with previously proposed SMCs. These constraints include a high level of chattering with a slow transient response, and vice versa. Similarly, voltage regulation and %THD are compromised when both sliding surface and reaching law techniques are not addressed simultaneously. Therefore, the level of sensitivity associated with today's VSIs based systems, demands the development of a more efficient SMC comprising state-of-the-art reaching law with optimal sliding surface to ensure an improved convergence rate, enhanced robustness of a system with a reduced level of chattering, and %THD. Thus, a comprehensive approach to design SMC is necessary to achieve optimal performance in VSI systems.

Following which, a composite Exponential Reaching Law integrated with Rotating Sliding Surface (C-ERL-RSS) SMC technique for VSI systems is introduced. The

proposed technique C-ERL-RSS, addresses the challenges associated with variable load conditions and aims to enhance the system's robustness and reliability. It combines a RSS selection mechanism for sliding surface design and a composite reaching law, C-ERL-RSS, that intelligently adjusts the gain values based on the distance of the state variable from the sliding surface. The proposed technique is validated through stability analysis, which confirms its effectiveness in achieving robustness against load variations. Comparative analysis against other state-of-the-art reaching laws demonstrates its potential for improved efficiency and performance. Moreover, C-ERL-RSS SMC is designed for single phase and three phase VSIs.

CHAPTER 4

RESULTS AND ANALYSIS

In this chapter, the proposed C-ERL-RSS SMC strategy formulated and discussed in the preceding chapter for single and three-phase VSIs, is assessed and analyzed. The evaluation is conducted for both single-phase and three-phase VSI configurations. The initial section assesses the performance of single-phase and three-phase VSI models, followed by the experimental validation of proposed SMC for VSI model in the subsequent segment. To carry out the simulations, MATLAB Simulink serves as the platform, while the experimental validation employs HiL setup comprising of Opal-RT and MicroLabBox dSPACE 1202.

4.1 Performance analysis of the proposed C-ERL-RSS SMC for VSIs under disturbance conditions

The performance of the proposed C-ERL-RSS is analysed for single phase and three phase VSIs on MATLAB Simulink. Furthermore, the proposed C-ERL-RSS is validated experimentally using HiL setup using Opal-RT and MicroLabBox dSPACE 1202.

4.1.1 Performance Analysis of Single Phase VSI on MATLAB Simulink

The performance characteristics of the control function presented in equation 3.23 are evaluated under disturbance conditions e.g sudden load variant i.e. from full load to no load and from no load to full load conditions. Additionally, the performance of two other state-of-the-art control functions, namely Cos-ERL [1] and FPRRL [2], are also assessed on the same system. A comprehensive comparative analysis is conducted to verify the superior performance of the proposed SMC. In this section, demonstrates the implementation of reference voltage trajectory tracking using three state-of-the art SMCs: Cos-ERL [1], FPRRL [2], and the proposed (C-ERL-RSS). The implementations are carried out in the Matlab/Simulink software for a single-phase VSI system operating under variable load conditions i.e. no load to full load and full load to no load. A non-linear diode rectifier load of $1kW$ is applied at $0.045sec$ to test the behavior of proposed control scheme along with Cos-ERL[1] and FPRRL[2] under sudden load variations. The control parameters and circuit specifications are shown in 4.1 and 4.2, respectively. In figure 4.1, SPVSI is tested under load varying condition of full load to no load, followed by the behavior of output voltage tracking the reference voltage is shown in figure 4.2. Here, the Cos-ERL SMC [1] is tested and its is shown that the SMC technique performs

just well in terms of voltage tracking and transient response, however, improvement in voltage regulation is required. This argument can easily be verified through the zoomed version of the same SPVSI system shown in Figure 4.3. It is observed that the Cos-ERL SMC takes $1.43ms$ to track the reference voltage when system is subjected to sudden load variation at $0.045sec$. In zoomed view, prior to the load variation point at $0.045sec$ Cos-ERL[1] needs improvement in terms of voltage regulation.

Likewise, the similar system tested for FPRRL SMC [2] under same load varying conditions i.e. from full load to no load at same time of $0.045sec$. Step response of the system for voltage and current is shown in Figure 4.5 and the behavior of the output voltage tracking the reference voltage is depicted in Figure 4.6. The transient response and the voltage regulation can be observed from the zoomed view of the SPVSI under FPRRL SMC [2], shown in Figure 4.7. The system under consideration exhibits a notably slow transient response of $2ms$. Additionally, the voltage regulation demonstrates better performance when compared to Cos-ERL[1].

Table 4.1: Parameters of controllers.

Gains	Cos-ERL[1]	FPRRL[2]	Proposed C-ERL-RSS
γ	0.6	—	0.6
φ	10	—	10
ϕ	02	—	02
G	500	500	500
τ	—	0.3	—
δ	—	0.1	—
θ	—	0.01	—
β	85	—	85

Nevertheless, when subjected to identical operating conditions involving an abrupt load change from full load to no load at $0.045sec$, the proposed C-ERL-RSS demonstrates favorable outcomes. This is in contrast to the performance of Cos-ERL[1] and FPRRL[2] SMCs. The response of output voltage and current is depicted in Figure 4.9. The voltage tracking behavior of the identical system is illustrated in Figure 4.11, demonstrating encouraging outcomes. To gain a more detailed understanding of the performance of the proposed C-ERL-RSS SMC, a closer examination of voltage regulation and reference tracking is provided in Figure 4.12. It is evident that the proposed technique exhibits robust and rapid response in tracking the reference voltage during sudden load variations. It achieves this in just $1ms$, showcasing a notably enhanced voltage regulation compared to

the Cos-ERL[1] and FPRRL[2] SMCs.

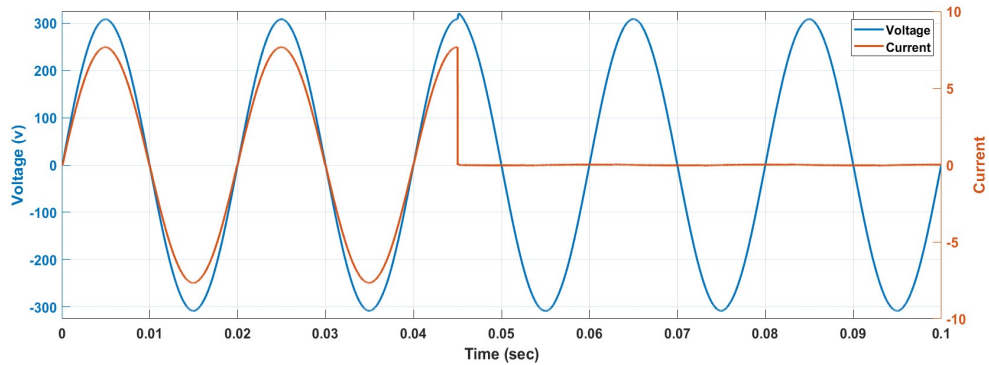


Figure 4.1: SPVSI output voltage and non-linear load current with Cos-ERL (Full Load to No Load) [1].

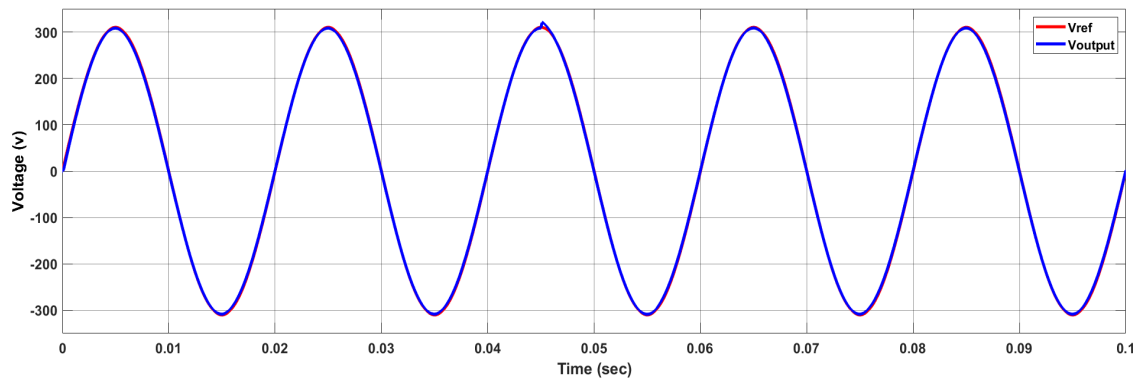


Figure 4.2: Voltage output reference tracking with Cos-ERL (Full Load to No Load) [1].

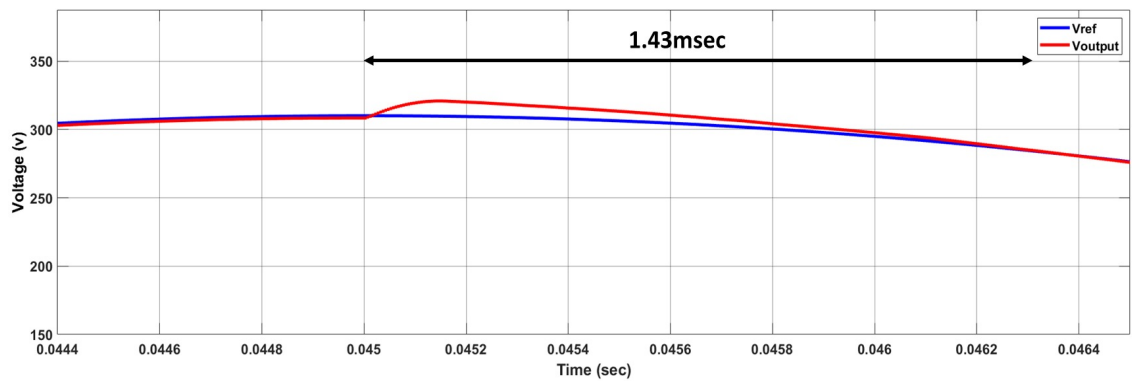


Figure 4.3: Output Voltage waveform-Tracking Evolution with Cos-ERL (Full Load to No Load Zoomed View) [1].

Likewise, the SPVSI with a non-linear rectifier load, using the same circuit parameters, is exposed to an abrupt load change from no load to full load conditions. This scenario is employed to assess and evaluate the effectiveness of the FPRRL[2] and Cos-ERL[1] SMCs, as well as the proposed C-ERL-RSS SMC. In the initial phase, the performance of the Cos-ERL[1] technique is examined by introducing a full load to the system

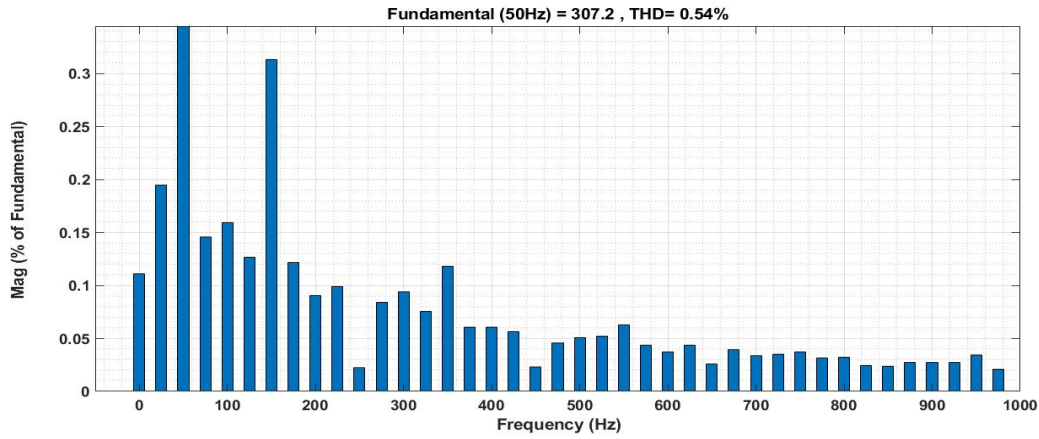


Figure 4.4: FFT analysis of output voltage with Cos-ERL[1].

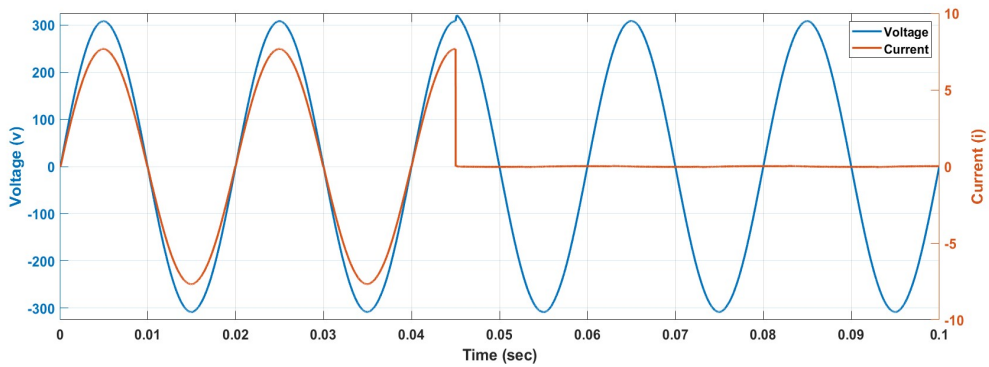


Figure 4.5: SPVSI output voltage and non-linear load current with FPRRL (Full Load to No Load) [2].

from a no-load condition at 0.045 seconds. The transient response of this specific SMC for both voltage and current is displayed in Figure 4.13. Also, reference voltage tracking of said system is shown in Figure 4.14. To analyse the performance of Cos-ERL[1] SMC for SPVSI under no load to full load condition, zoomed view of the Figure 4.14 is shown in Figure 4.15. Which clearly shows that, it takes $5ms$ to regain its reference trajectory.

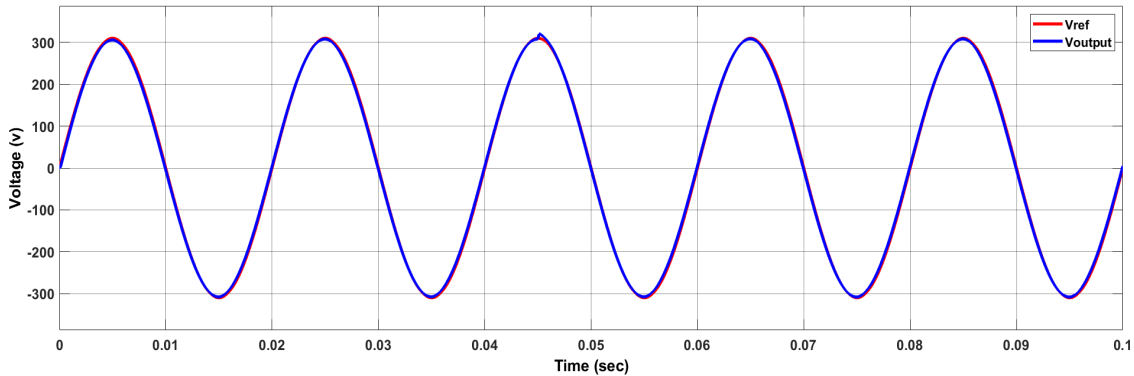


Figure 4.6: Voltage output reference tracking with FPRRL (Full Load to No Load) [2].

Similarly, following the same circumstances, the FPRRL SMC [2] is exposed to a

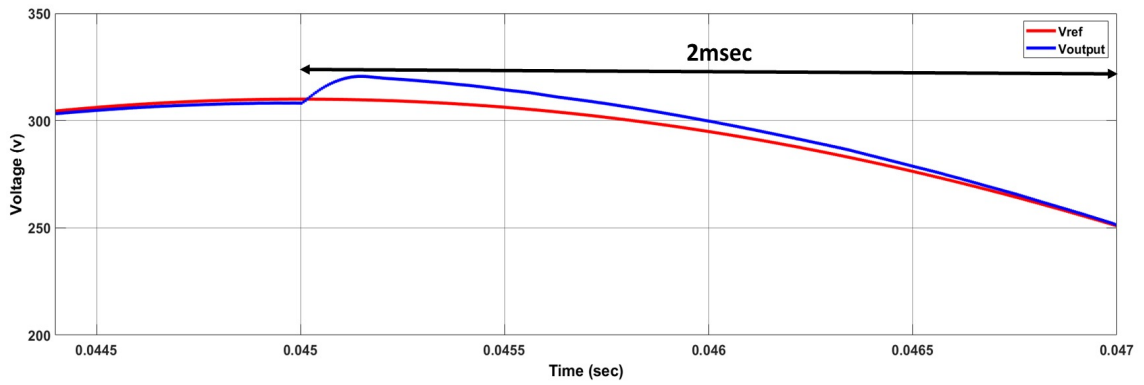


Figure 4.7: Output Voltage waveform-Tracking Evolution with FPRRL (Full Load to No Load Zoomed View) [2].

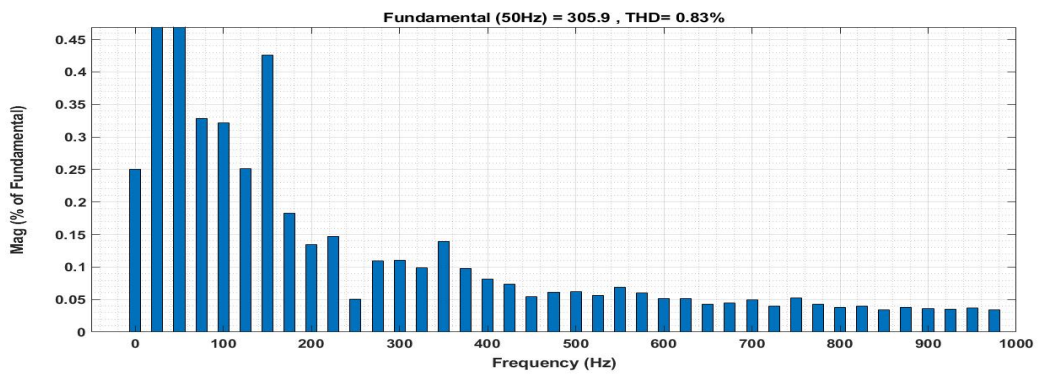


Figure 4.8: FFT analysis of output voltage with FPRRL [2].

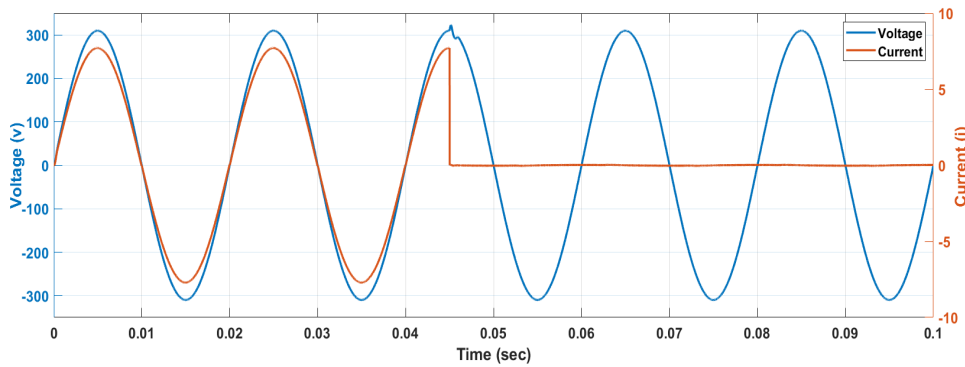


Figure 4.9: SPVSI output voltage and non-linear load current with proposed C-ERL-RSS [3] (Full Load to No Load)

scenario of transitioning from no load to full load. The behavior of the output voltage and current under this abrupt load change is illustrated in Figure 4.16. Figure 4.17 displays the reference voltage tracking performance of the FPRRL SMC [2]. A closer view of this behavior is presented in Figure 4.18, where a notably slower transient response of $9ms$ is evident. The behavior of the proposed C-ERL-RSS SMC is similarly examined for SPVSI under the conditions of transitioning from no load to full load. The response of output voltage and current for the proposed SMC when subjected to a sudden load

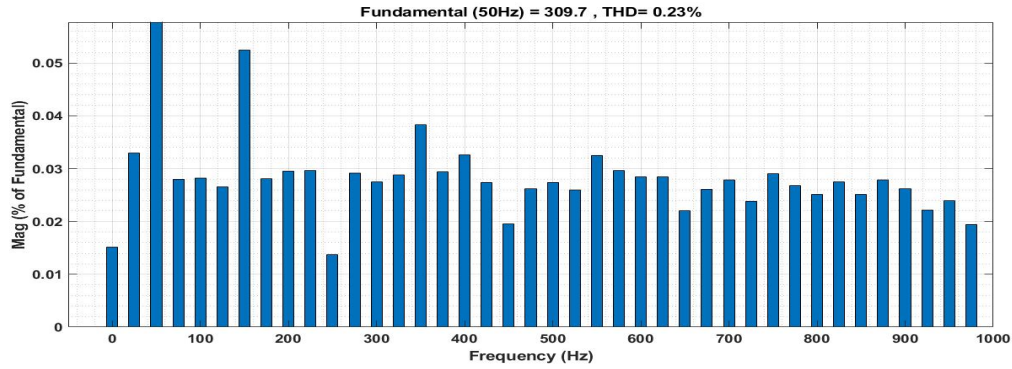


Figure 4.10: FFT analysis of output voltage with CERLRSS [3].

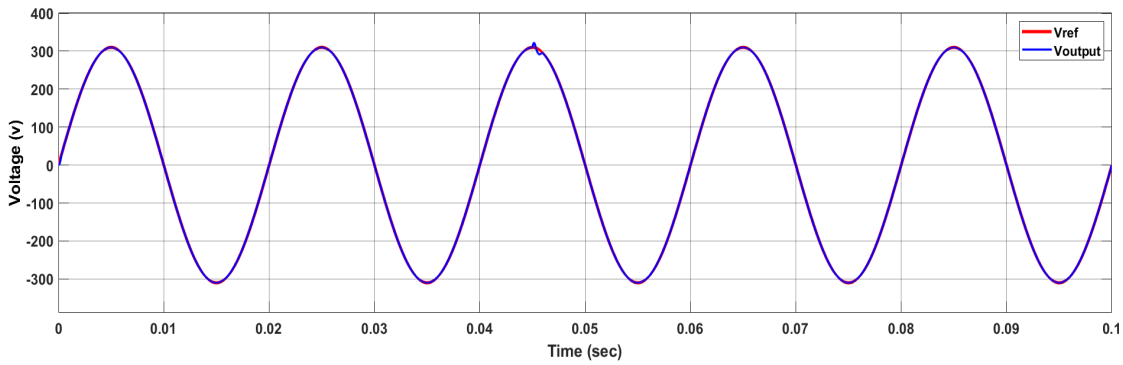


Figure 4.11: Voltage output reference tracking with proposed C-ERL-RSS [3] (Full Load to No Load).

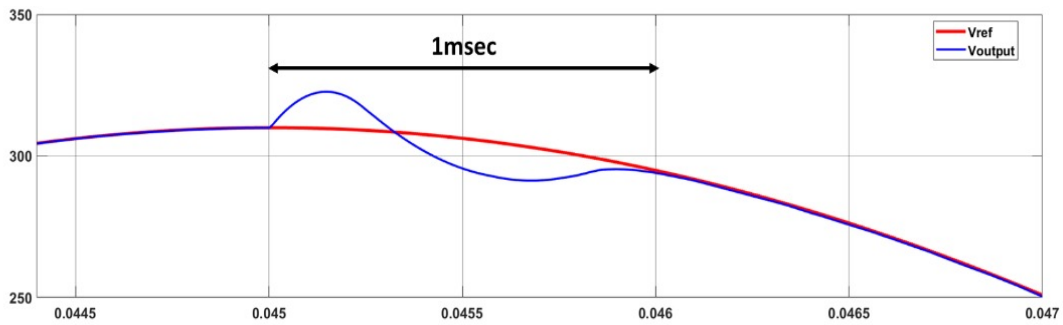


Figure 4.12: Output Voltage waveform-Tracking Evolution with proposed C-ERL-RSS [3] (Full Load to No Load Zoomed View)

variation at 0.045sec is illustrated in Figure 4.19. The Figure 4.20 presents the reference voltage tracking attributes of the examined system with the proposed C-ERL-RSS SMC. Notably, the zoomed view showcased in Figure 4.21 highlights a remarkably swift transient response of only 1.1ms . Furthermore, the proposed C-ERL-RSS SMC exhibits significantly enhanced voltage regulation.

In addition to assessing transient response and voltage regulation, a comparative analysis of %THD is conducted among the proposed SMC, FPRRL SMC [2], and Cos-

Table 4.2: Circuit Specifications.

Circuit Parameter	Value
Input Source DC voltage V_s	465V
Reference Peak Voltage, V_m	310V
Filter Inductor, L	15mH
Filter Capacitor, C	48 μ F
Scaling Gain, Kx_1	2×10^{-3}
Scaling Gain, Kx_2	2.4×10^{-5}
Scaling Gain, Ks	30×10^4
Non-Linear Rectifier Load	1kW
Switching Frequency[4]	21.67kHz

ERL [1]. Notably, FPRRL SMC [2] and Cos-ERL [1] exhibit %THD values of 0.61% and 0.59%, respectively. Conversely, the proposed C-ERL-RSS SMC demonstrates an exceptionally low %THD of 0.25%.

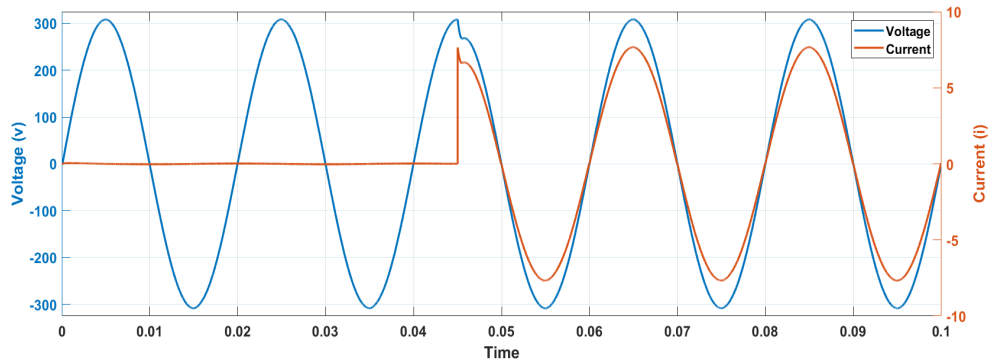


Figure 4.13: SPVSI output voltage and non-linear load current with Cos-ERL (No Load to Full Load) [1]

Table 4.3 shows a comprehensive analysis of four SMC techniques including the proposed one, for SPVSI with diode rectifier non-linear load. The value of the %THD obtained through the proposed technique is much smaller as compared to the other SMC techniques. In addition, under load variation, output voltage starts tracking the reference voltage without any delay. A perfect balance of tracking time and chattering along the sliding surface is attained i-e tracking time along with chattering is considerably reduced

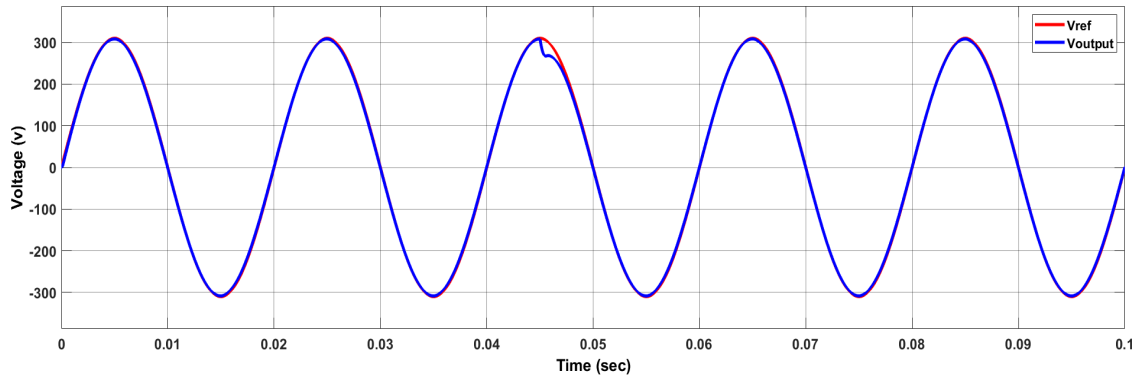


Figure 4.14: Voltage output reference tracking with Cos-ERL (No Load to Full Load) [1].

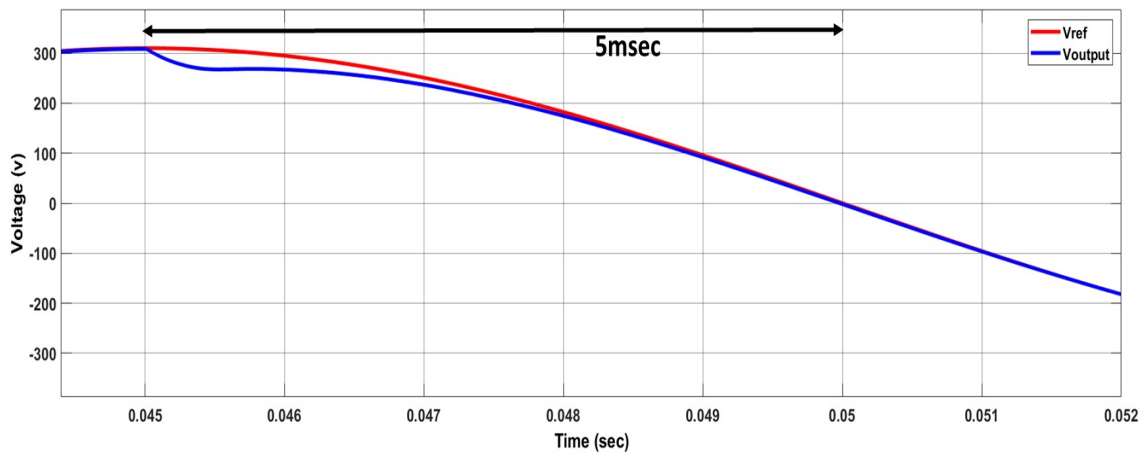


Figure 4.15: Output voltage waveform–Tracking Evolution with Cos-ERL (No Load to Full Load Zoomed View)[1].

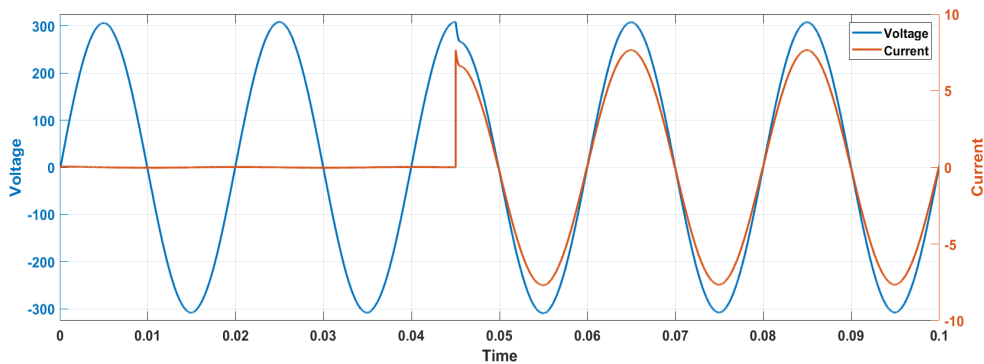


Figure 4.16: Voltage output reference tracking with FPRRL (No Load to Full Load) [2].

even at a higher value of control gain. Table 4.3 shows a comprehensive analysis of four SMC techniques for SPVSI with diode rectifier non-linear load. The %THD obtained through the proposed technique is much smaller as compared to the other reaching law techniques. In addition, under load variation, output voltage starts tracking the reference voltage without any delay. A perfect balance of tracking time and chattering along the sliding surface is attained i-e tracking time along with chattering is considerably reduced even at a higher value of control gain. Table 4.3 shows a comprehensive analysis of

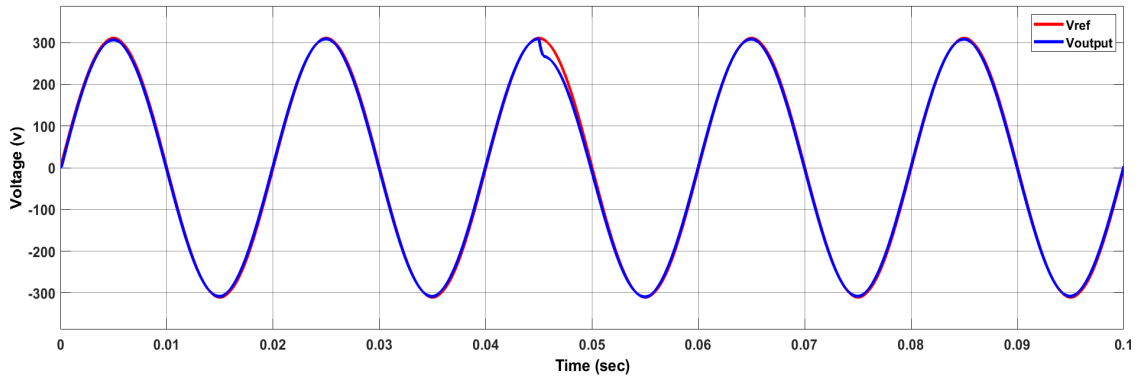


Figure 4.17: Voltage output reference tracking with FPRRL (No Load to Full Load) [2].

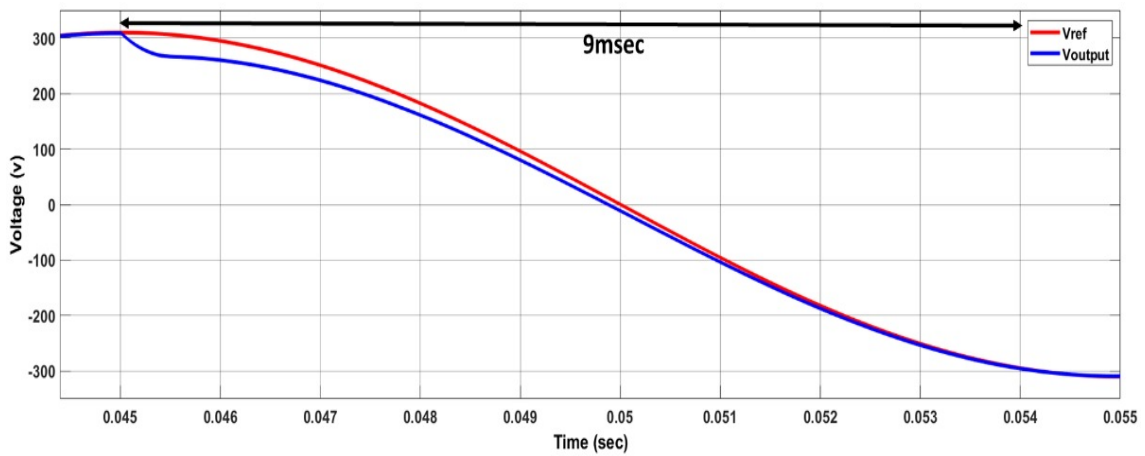


Figure 4.18: Output voltage waveform-tracking evolution with FPRRL SMC [2].

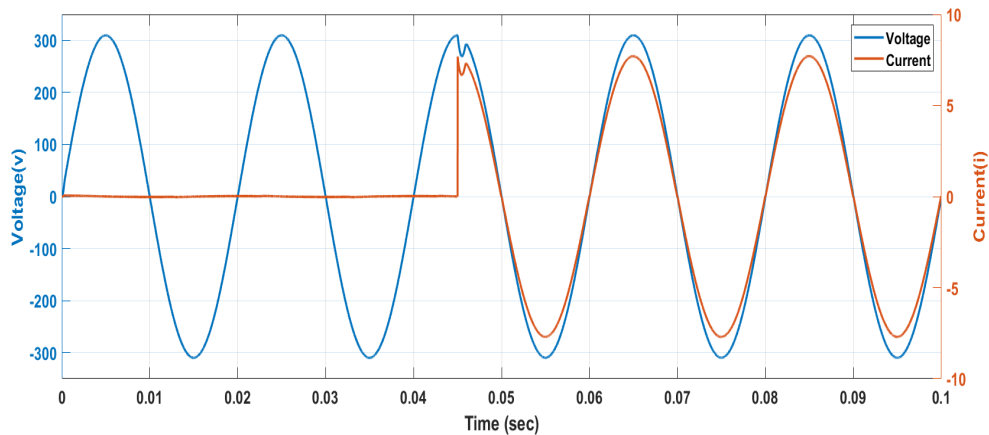


Figure 4.19: SPVSI output voltage and non-linear load current with proposed C-ERL-RSS [3] (No Load to Full Load).

four reaching law based SMC(s) for SPVSI with diode rectifier non-linear load. The %THD obtained through the proposed technique is much smaller as compared to the other reaching law techniques. In addition, under load variation, output voltage starts tracking the reference voltage without any delay. A perfect balance of tracking time and chattering along the sliding surface is attained i-e tracking time along with chattering is considerably

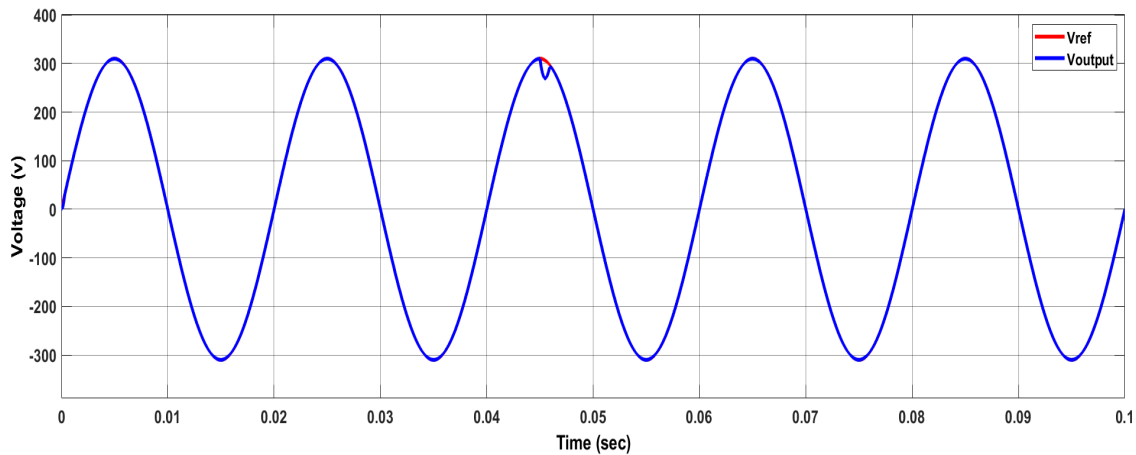


Figure 4.20: Voltage output reference tracking with proposed C-ERL-RSS [3] (No Load to Full Load).

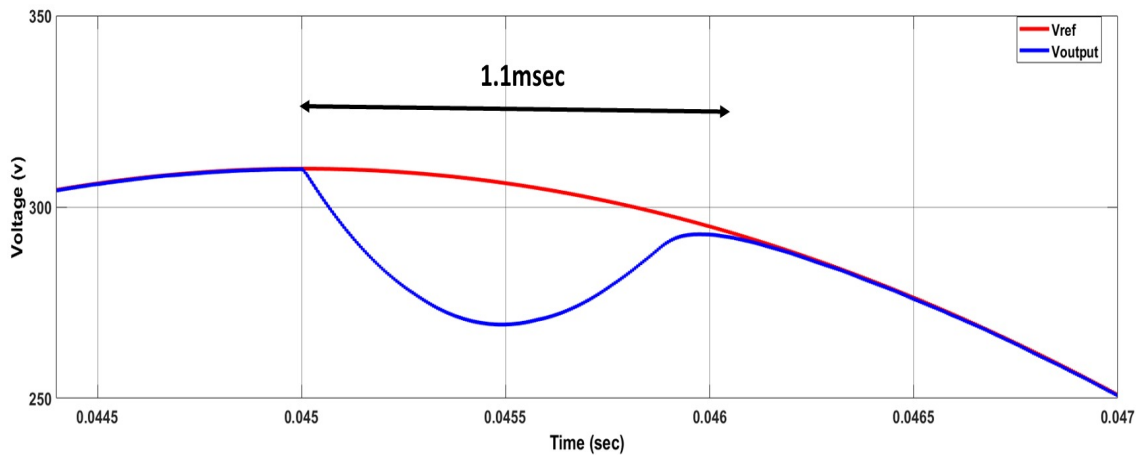


Figure 4.21: Output voltage waveform-tracking evolution with C-ERL-RSS [3]. (No Load to Full Load).

reduced even at a higher value of control gain. Thus, gaining maximum advantage from inherent properties of SMC like robustness.

4.1.2 Performance Analysis of Three Phase VSI on MATLAB Simulink

The performance characteristics of the proposed C-ERL-RSS SMC outlined in equations 3.52 and 3.53 are assessed in the disturbance conditions e.g. sudden load variation i.e. from full load to no load and from no load to full load conditions. Furthermore, the performance of three other state-of-the-art SMC functions, namely RRL [13], PRERL [12], and EERL [14], tested and evaluated on the same system. This extensive comparative analysis is carried out to confirm the superior performance of our proposed SMC approach. In this part of the dissertation, the reference tracking trajectory of output voltage for RRL [13], PRERL [12], EERL [14], and the proposed reaching law is shown through the implementation of three phase VSC in MATLAB/Simulink. The performance of the aforementioned reaching laws along with the proposed reaching law was tested on three phase VSI under a nonlinear rectifier load of 1 kW with circuit parameters and specifica-

Table 4.3: Comparison of proposed C-ERL-RSS SMC [3] with Cos-ERL [1], FPRRL [2] and RSS [4] SMC.

Category	RSS-SMC [4]	Cos-ERL-SMC [1] Implemented with Circuit Specifications (Table 4.2)	FPRRL-SMC [2] Implemented with Circuit Specifications (Table 4.2)	Proposed C-ERL-RSS SMC Implemented with Circuit Specifications (Table 4.2)
%THD	2.66%	0.59%	0.61%	0.25%
Voltage Regulation	98.35%	99.45%	99.15%	99.9%
Tracking Time	<i>Low</i>	<i>5ms</i>	<i>9ms</i>	<i>1.1ms</i>
Chattering	<i>Low</i>	<i>Low</i>	<i>Low</i>	<i>Very Low</i>
Robustness	<i>Good</i>	<i>Good</i>	<i>Good</i>	<i>Best</i>
Steady-State Response	<i>Good</i>	<i>Good</i>	<i>Good</i>	<i>Best</i>

tions shown in Table 4.4. The diode bridge rectifier or DIAC/TRIAC controlled bridge rectifier is regarded as a non-linear load, and the characteristics of the load current are contingent upon the type of component (resistive/inductive) connected at the rectifier's output. In the study conducted by Komurcugil et al. [4], a rectifier was employed as a

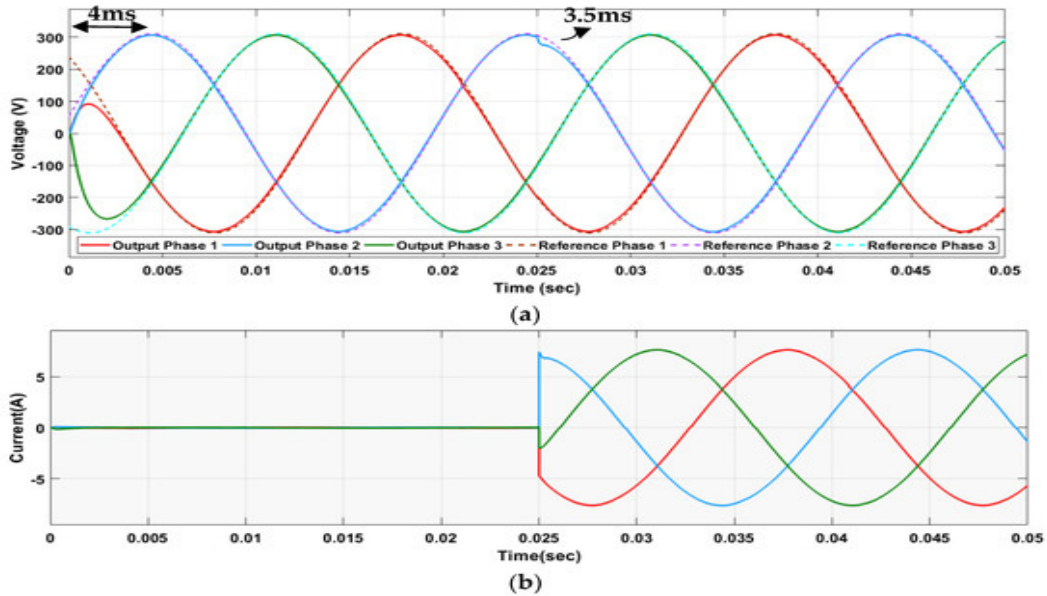


Figure 4.22: (a) PRERL[12], output voltage-reference tracking trajectory and voltage regulation. (b) PRERL[12], load current-step response under no load to full load condition.

nonlinear load with a resistor at its output, resulting in a sinusoidal output current waveform. Conversely, in the study by [35], a rectifier with an inductor at the output was used, leading to a distorted output current waveform. In our proposed approach, we utilized a diode bridge rectifier followed by a resistor as the nonlinear load for testing the SMC

on a three-phase VSC, which resulted as required output current. Having said this, since the load is a rectifier, the load current witnesses zero crossover distortion. In our case, its value is very low, which one can observe as a zoomed view of the current wave form. 4.22 shows the reference tracking trajectory of the output voltage and current response, respectively, from no load to full load condition at 0.025s. It is evident from 4.22 that the output voltage started to track the reference voltage at 4ms under no load condition. Moreover, there was a compromised voltage regulation beyond 4ms. Similarly, the transient time was observed as 3.5ms when the load was applied at 0.025ms.

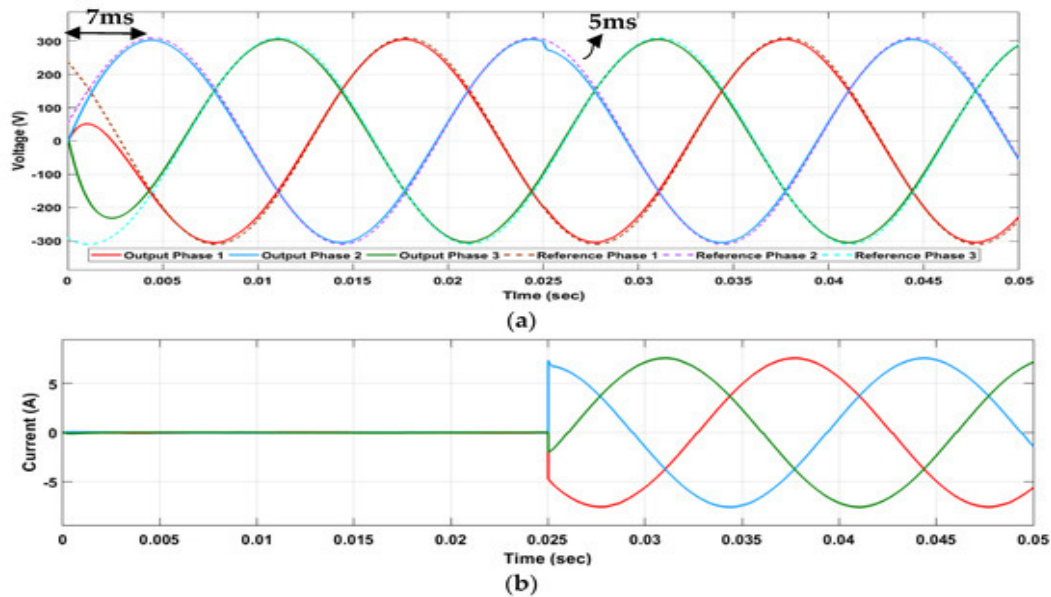


Figure 4.23: (a) RRL[13], output voltage-reference tracking trajectory and voltage regulation. (b) RRL[13], load current-step response under no load to full load condition.

Likewise, the performance of the RRL [13] based SMC under aforementioned conditions is shown in 4.23. The reference tracking time under no load condition was not very encouraging as the output started at the following reference voltage at 7ms with more compromised voltage regulation and comparatively slow transient response of 5ms. However, the response of EERL[14] based SMC, as shown in 4.24 is quite encouraging in terms of the reduced reference tracking time under the no load condition as well as the fast transient response observed. In 4.24, the reference tracking and transient time were observed as 2.5ms and 2ms, respectively. Additionally, a better reference voltage tracking led to improved voltage regulation compared to RRL[13] and PRERL[12]. The performance of the proposed C-ERL-RSS SMC under predefined conditions for voltage regulation and trajectory tracking is shown in 4.25. An enormous reduction in reference tracking time of 0.08ms was achieved with an extremely fast transient response of 0.05ms at 0.025s. Similarly, the prescribed system is tested for load disturbance condition of full load to no load at 0.025sec. In Figure 4.26, the behavior of the system under PRERL SMC [12] is shown. In first part of the Figure reference voltage tracking of the output voltage is presented. It is shown that the three phase VSI with PRERL SMC [12] has the voltage tracking time and transient time of 4ms and 5ms, respectively. The three phase VSI is also tested to analyse the performance of RRL[13] under load disturbance condition of

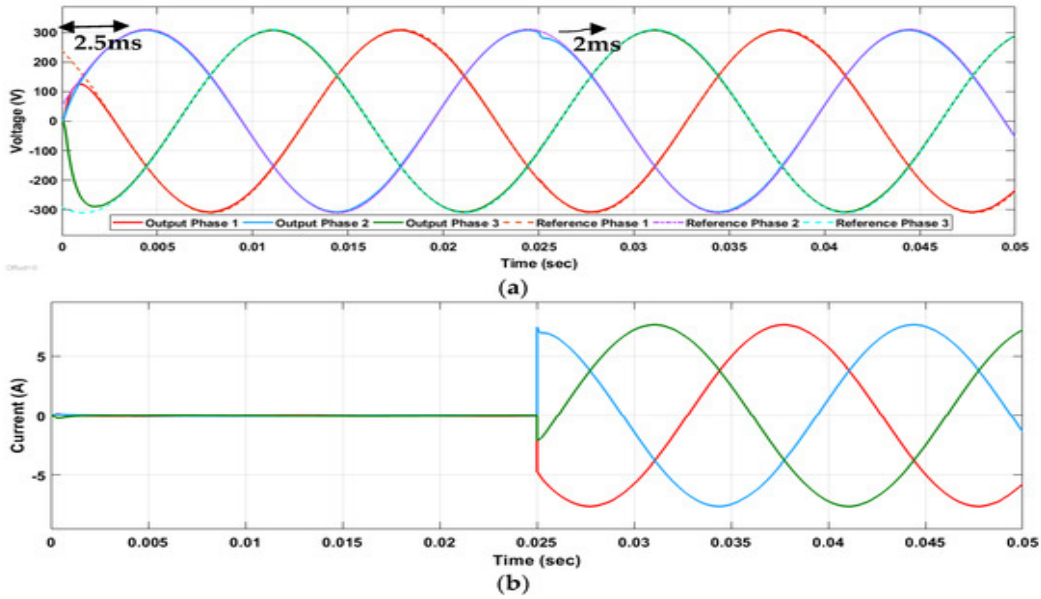


Figure 4.24: (a) EERL[14], output voltage-reference tracking trajectory and voltage regulation. (b) EERL[14], load current-step response under no load to full load condition.

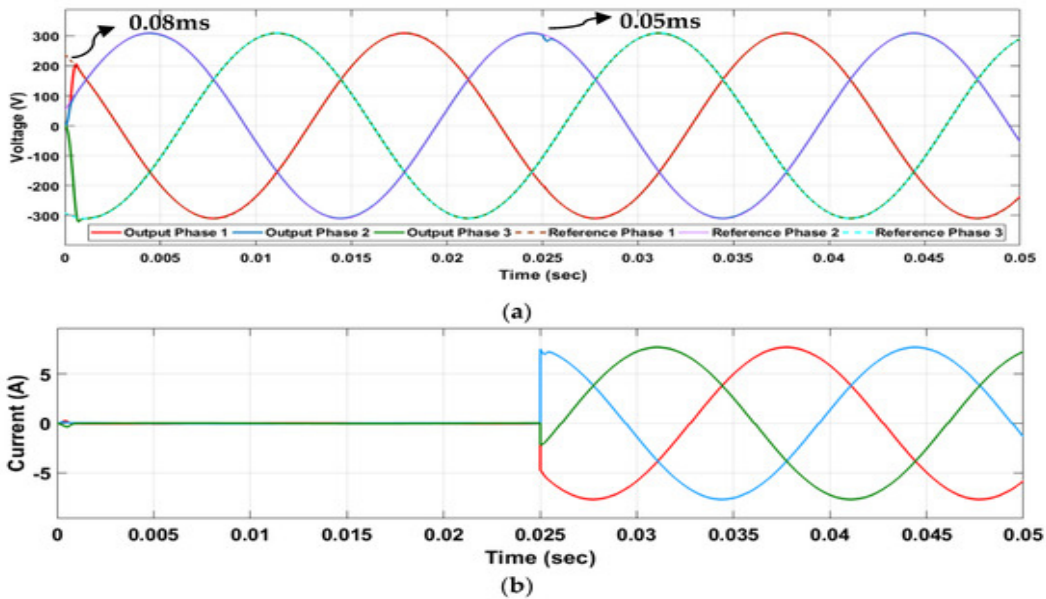


Figure 4.25: (a) Proposed C-ERL-RSS, output voltage-reference tracking trajectory and voltage regulation. (b) Proposed C-ERL-RSS, load current-step response under no load to full load condition [15].

full load to no load applied at 0.025sec. In first part of the Figure , the reference tracking of the output voltage is presented, followed by the current waveform in the second part. It is shown in the Figure the RRL has the tracking time of 7ms and transient time of 6.5ms. Similarly, the behavior of the three phase VSI with EERL[14] control mechanism is presented in Figure . Voltage reference tracking followed by the current waveform in shown in first and second part of the Figure , respectively. It is quite evident that the tracking time consumed by the system under the control of EERL[14] is 2.5ms with the

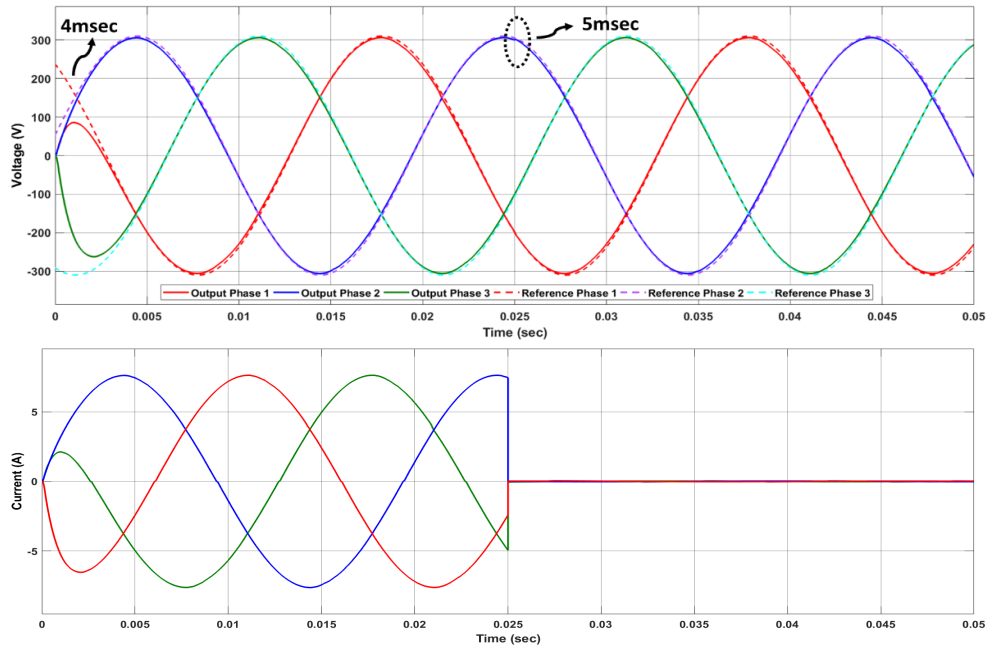


Figure 4.26: (a) PRERL[12], output voltage-reference tracking trajectory and voltage regulation. (b) PRERL[12], load current-step response under full load to no load condition.

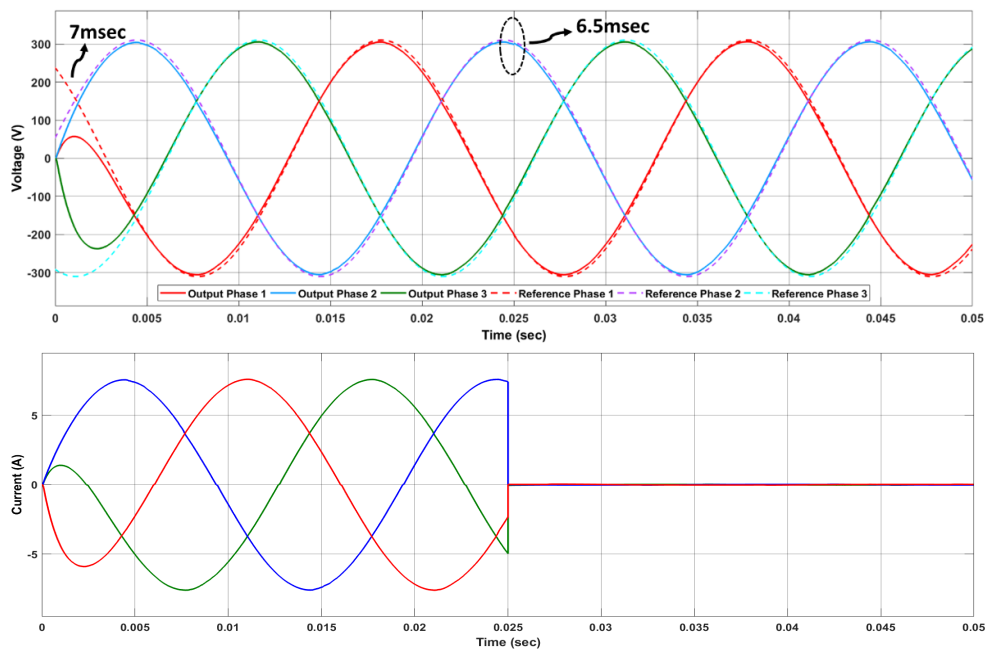


Figure 4.27: (a) RRL[13], output voltage-reference tracking trajectory and voltage regulation. (b) RRL[13], load current-step response under full load to no load condition.

transient response at sudden load variation is 4ms. The performance of the proposed C-ERL-RSS under a load disturbance condition, transitioning from full load to no load, for the same three-phase VSI is depicted in Figure . The performance of this proposed method is notably impressive, achieving a tracking time of 0.08 ms and a transient time of 0.23 ms. This robust behavior of the C-ERL-RSS SMC surpasses the performance of the other state-of-the-art techniques mentioned previously. It is worth mentioning here

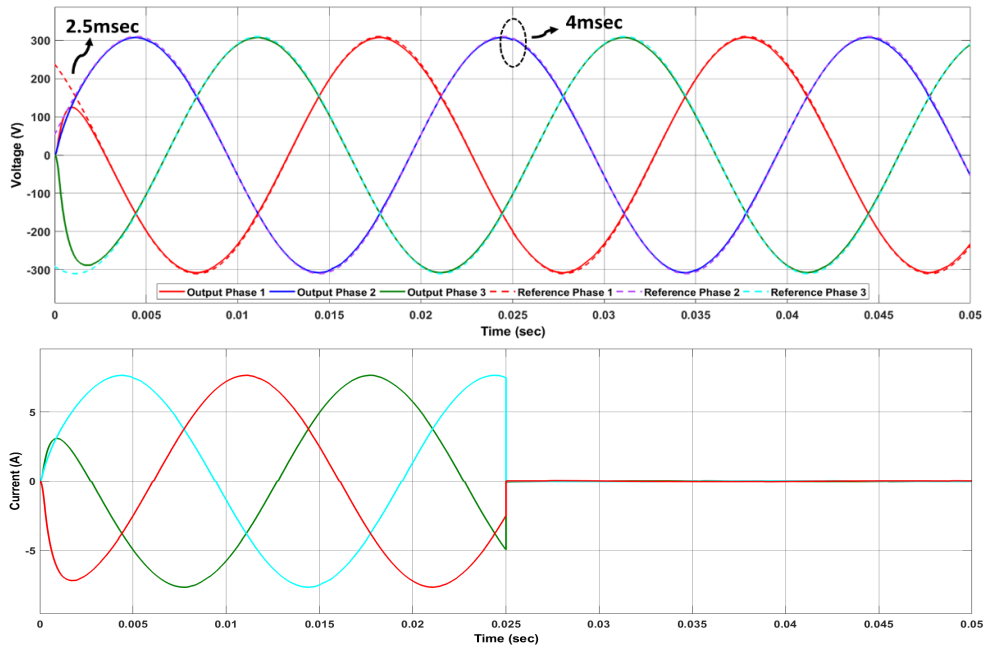


Figure 4.28: (a) EERL[14], output voltage-reference tracking trajectory and voltage regulation. (b) EERL[14], load current-step response under full load to no load condition.

that other techniques exhibit higher steady-state errors, resulting in significantly weaker voltage regulation. In contrast, the proposed C-ERL-RSS technique displays minimal steady-state error, thereby ensuring enhanced voltage regulation.

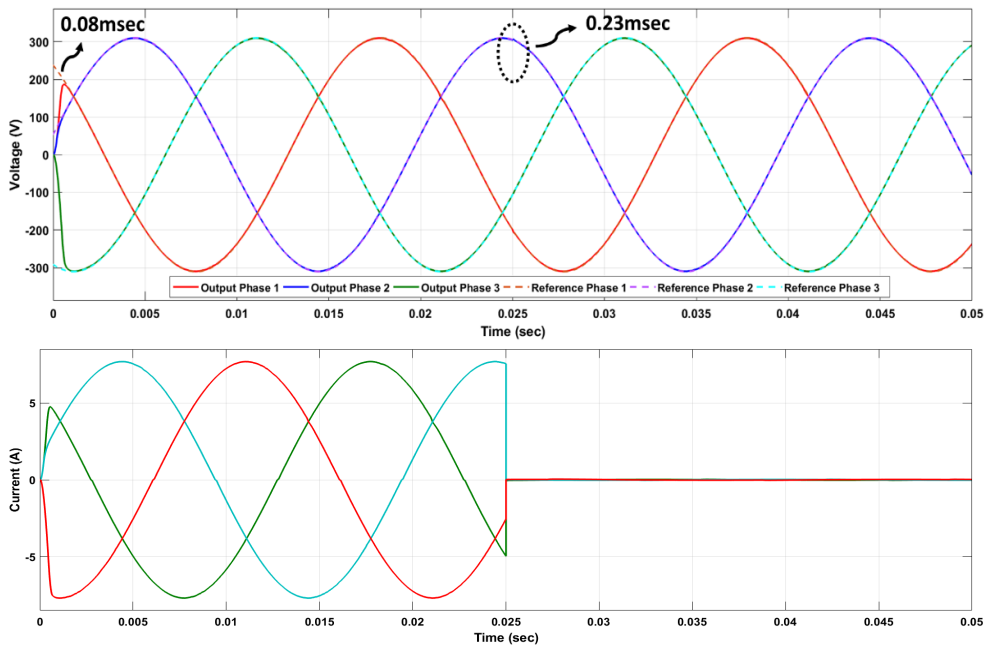


Figure 4.29: (a) Proposed C-ERL-RSS, output voltage-reference tracking trajectory and voltage regulation. (b) Proposed C-ERL-RSS, load current-step response under full load to no load condition [15].

A tremendous improvement in voltage regulation under no load and full load and full load to no load conditions was observed with an extremely low %THD of 1.1%.

Therefore, the proposed SMC with C-ERL and RSS has shown remarkable results to make it the most viable option to be used applications to handle critical loads. A summary of the

Table 4.4: Circuit Specifications for three phase.

Circuit Parameter	Value
Input Source DC voltage from battery, V_s	500V
Reference Voltage, V_{RMS}	220V
Filter Inductor, L	5.4mH
Filter Capacitor, C	30uF
Scaling Gain, K_1	2×10^{-3}
Scaling Gain, K_2	2.4×10^{-5}
Non-Linear Rectifier Load, Z	1kW
Switching Frequency, f_s [259]	9kHz
Fundamental Frequency, f	50Hz

results of the comparative analysis obtained through the implementation of PRERL[12], RRL[13], EERL[14], and the proposed composite reaching law along with other state-of-the-art reaching laws based SMC results obtained from a similar system are shown in 4.5. It can be deduced from Table 4 that the proposed composite reaching law based SMC had extremely resilient behavior against sudden load variations. Moreover, a phenomenal reduction in %THD with a high level of voltage regulation makes the proposed composite reaching law the best among the other reaching laws.

4.1.3 Experimental validation of proposed C-ERL-RSS for VSI on Hardware in Loop (HiL) setup

To demonstrate the competency and authenticity of proposed C-ERL-RSS based SMC for SPVSI system, a proposed control strategy is implemented through a Hardware in Loop (HiL) setup comprising of Opal-RT 4200 and microLabBox dSPACE-1202 with DC input voltage of $V_s = 500V$, reference peak value of $V_m = 100V$, filter inductor $L = 5.4mH$, and capacitor $C = 48\mu F$, shown in 4.30. Value of K_S is selected as 30×10^4 and values of other scaling gains K_{x1} and K_{x2} are selected as 2.4×10^{-5} and 30×10^4 , respectively. Thus, for the purpose of experimental validation, the parametric values remain unchanged from those designed for performance analysis in MATLAB Simulink. The performance of the proposed C-ERL-RSS SMC was evaluated for a single-phase VSI HiL

Table 4.5: Comparison of the proposed composite reaching law with other state-of-the art reaching laws.

Parameters	SMC [260]	SMC [261]	TSMC [262]	PRERL[12] Implemented with Circuit Specifications (Table 4.4)	RRL[13] Implemented with Circuit Specifications (Table 4.4)	EERL[14] Implemented with Circuit Specifications (Table 4.4)	Proposed C-ERL-RSS Implemented with Circuit Specifications (Table 4.4)
Input, $V_{DC}(V)$	360	250	250	500	500	500	500
Ref, $V_{RMS}(V)$	220	110	110	220	220	220	220
Output, $V_{RMS}(V)$	-	-	-	218	217	218.4	219.63
$f_{switching}$ (kHz)	15	10	20	09	09	09	09
% THD	1.7%	1.6%	5.1%	2.3%	3.2%	1.8%	1.1%
% Voltage Regulation	-	-	-	99.09%	98.63%	99.27%	99.83%
Robustness	-	-	-	Good	Good	Better	Best
Tracking Time(ms)	-	-	-	4	7	2.5	0.08
Transient Time(ms)	0.5	2	2	3.5	5	2	0.05

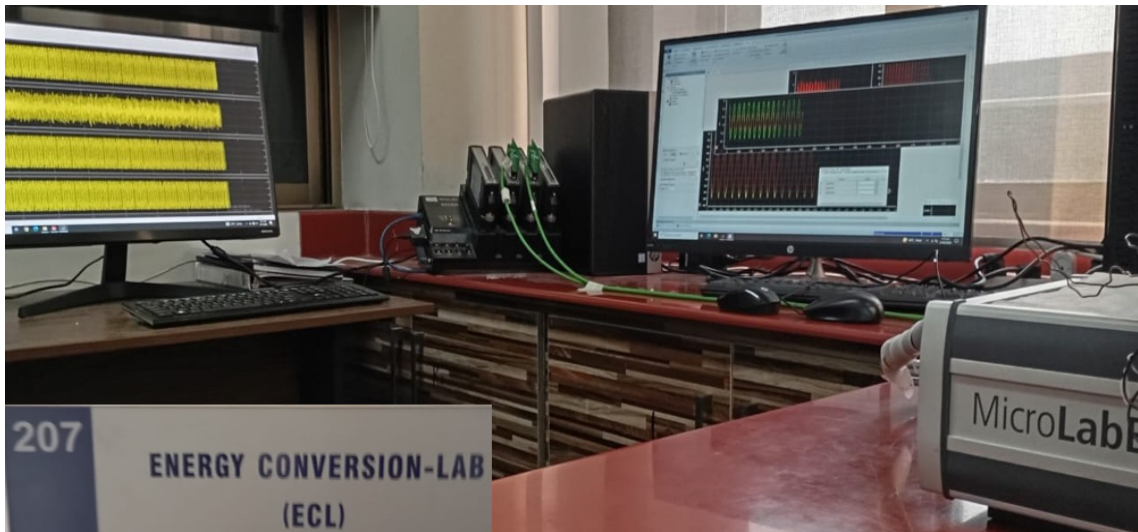


Figure 4.30: Experimental setup: Hardware in Loop (HiL) comprising Opal-RT 4200 and microLabBox dSPACE 1202 .

setup under various disturbance conditions. One such condition involved a sudden reference voltage variation from 200V to 100V at 6.23 seconds as shown in Figure 4.31. The proposed SMC demonstrated highly promising behavior, achieving a voltage regulation of 99.8% with a transient response time of just 0.4632 seconds. Furthermore, the proposed

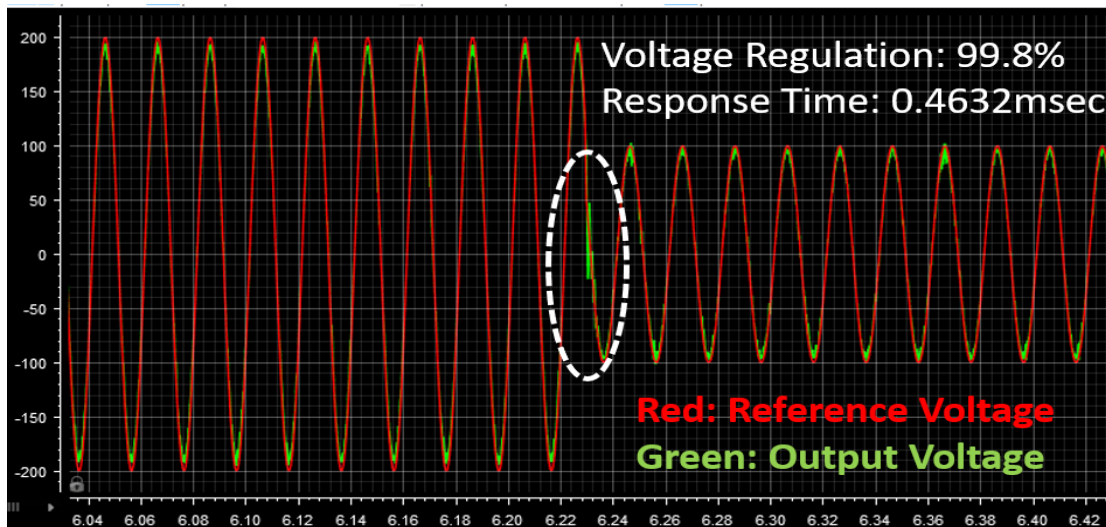


Figure 4.31: Response of the proposed C-ERL-RSS for sudden voltage reference variation from 200v to 100v

C-ERL-RSS SMC for the VSI was subjected to load disturbances ranging from full load to no load at 4.59 seconds, as depicted in Figure 4.32. The response of the proposed SMC was exceptionally promising in terms of both voltage regulation and transient response. Specifically, the system achieved an impressive voltage regulation of 99.8%, with a THD of just 3.32%. This demonstrates the robustness and effectiveness of the proposed control method in maintaining high-quality power output even under significant load variations. Likewise, the proposed C-ERL-RSS SMC for the VSI was tested under load disturbances,

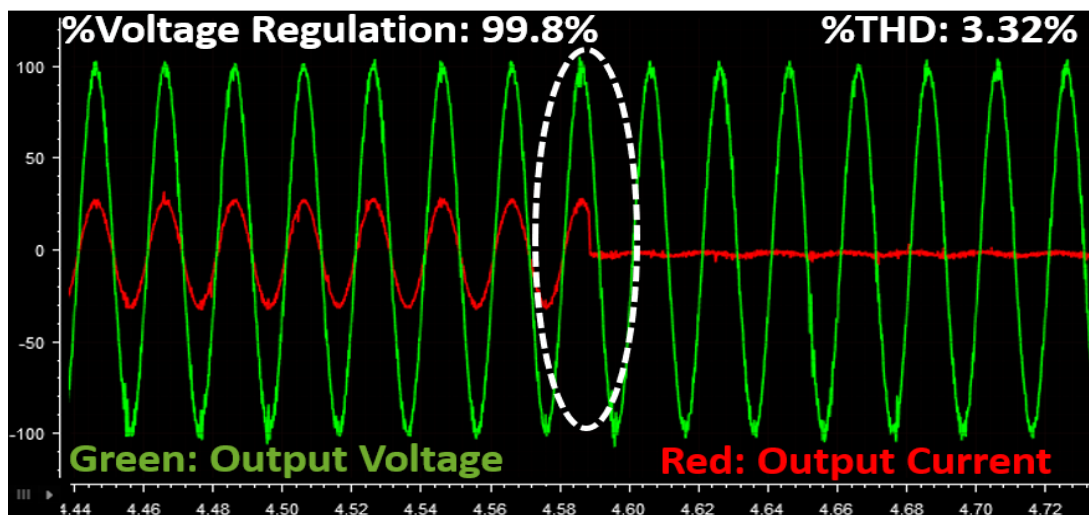


Figure 4.32: Response of the proposed C-ERL-RSS for load disturbance of full load to no load at 4.59 sec.

transitioning from no load to full load at 1.195 seconds, as illustrated in Figure 4.33. The results were exceptionally promising, demonstrating both outstanding voltage regulation and transient response. Specifically, the system achieved an impressive voltage regulation of 99.8% and a THD of just 3.32%. These results underscore the robustness and

efficiency of the proposed control method in maintaining high-quality power output even under substantial load variations. The performance analysis of the proposed C-ERL-RSS

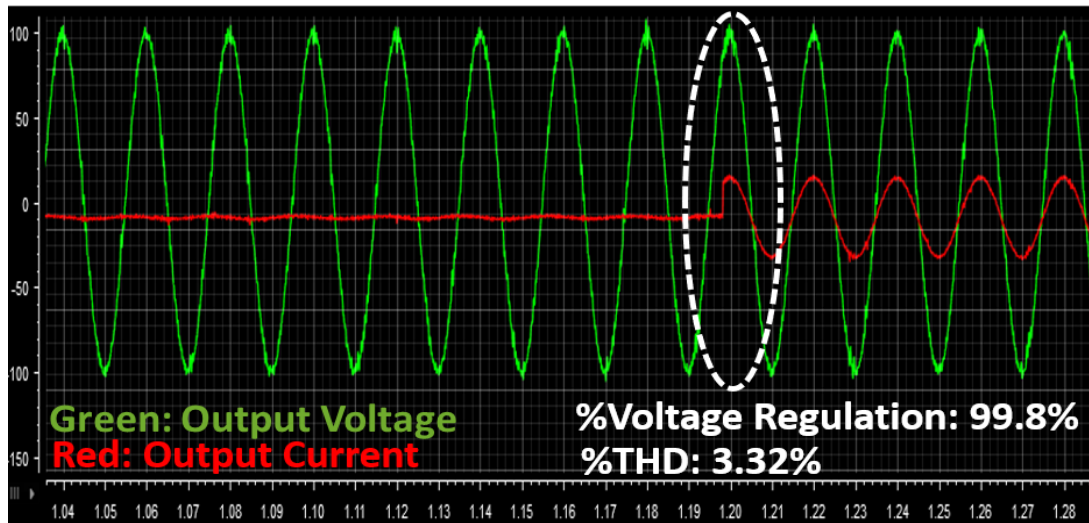


Figure 4.33: Response of the proposed C-ERL-RSS for load disturbance of no load to full load at 1.195 sec

SMC for VSIs, along with experimental validation, demonstrates the effectiveness of the proposed SMC for VSIs under disturbance conditions.

4.2 Performance analysis of optimal surface selection

In this section, the performance analysis for sliding surface selection mechanisms aimed at achieving stability and a fast convergence rate for single-phase and three-phase VSIs is conducted. Furthermore, a comparative analysis is presented, which includes cos-ERL [1] and FPRRL [2], along with the proposed C-ERL-RSS, all evaluated on the same single-phase VSI system. This is followed by a comparative analysis of the performance of surface selection methods, including PRERL [12], RRL [13], and EERL [14], along with the proposed C-ERL-RSS for three-phase VSIs.

4.2.1 Surface selection analysis for Single Phase VSI

The surface selection behaviour of cos-ERL [1] for single phase VSI is shown in Figure 4.34, and Figure 4.35 for no load to full load and full load to no load disturbance conditions, respectively. It can be observed from Figure 4.34 and Figure 4.35 that the zoomed view of surface behaviour is shown at three different points i.e. at 0.045sec when load disturbance takes place, after disturbance and before disturbance. Stability is witnessed to be a compromised before disturbance and after the disturbance, moreover, during disturbance it takes 5ms and 1.43ms to converge to the stable surface for no load to full load and full load to no load conditions, shown in Figure 4.34 and Figure 4.35, respectively.

Likewise, the surface selection behaviour for FPRRL [2] on the same single phase VSI is shown in Figure 4.36 and Figure 4.37 for load disturbance conditions of no load

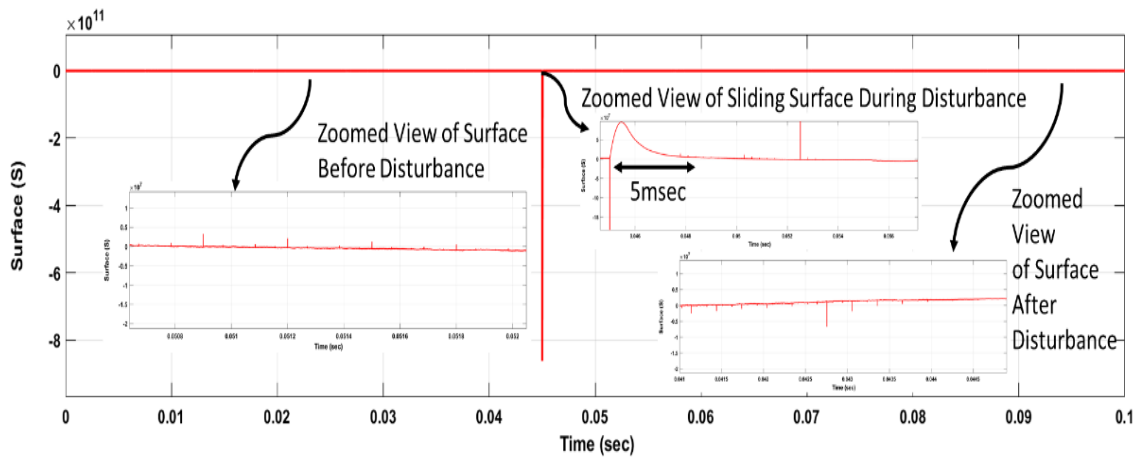


Figure 4.34: Surface selection analysis for cos-ERL [1] (No Load to Full Load).

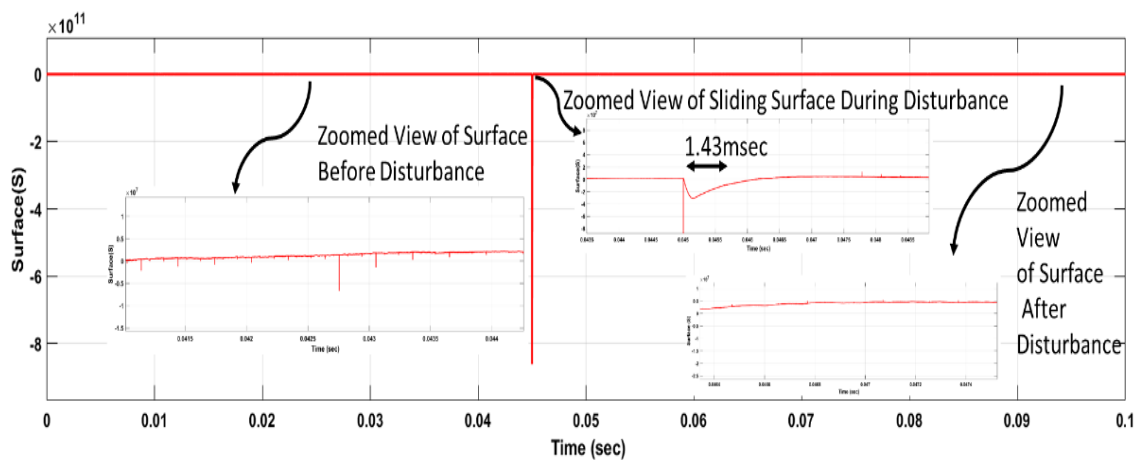


Figure 4.35: Surface selection analysis for cos-ERL [1] (Full Load to No Load).

to full load and full load to no load, respectively. The stability before and after the disturbance point at 0.045sec is not encouraging. Similarly, it takes 9ms and 2ms to converge to the stability condition for no load to full load and full load to no load condition shown in 4.36 and Figure 4.37, respectively.

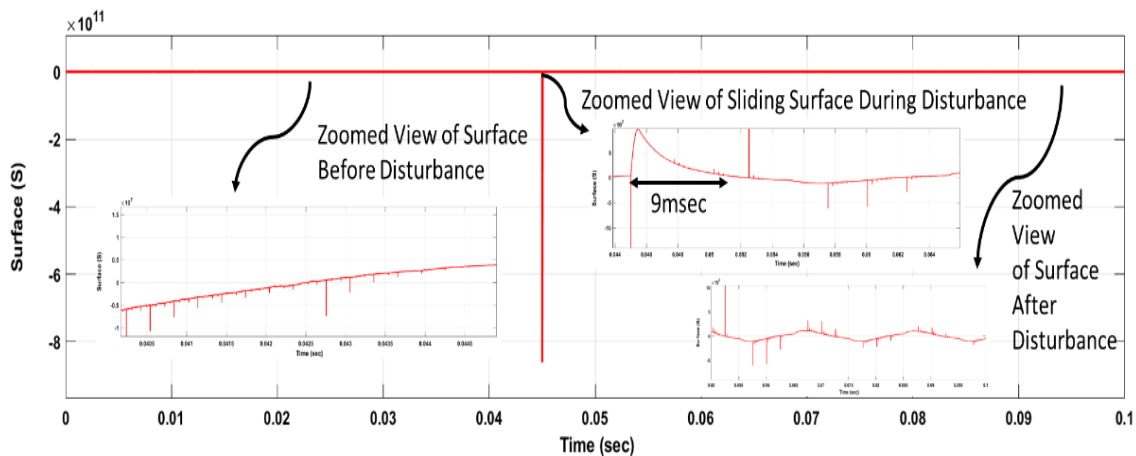


Figure 4.36: Surface selection analysis for FPRRL [2] (No Load to Full Load).

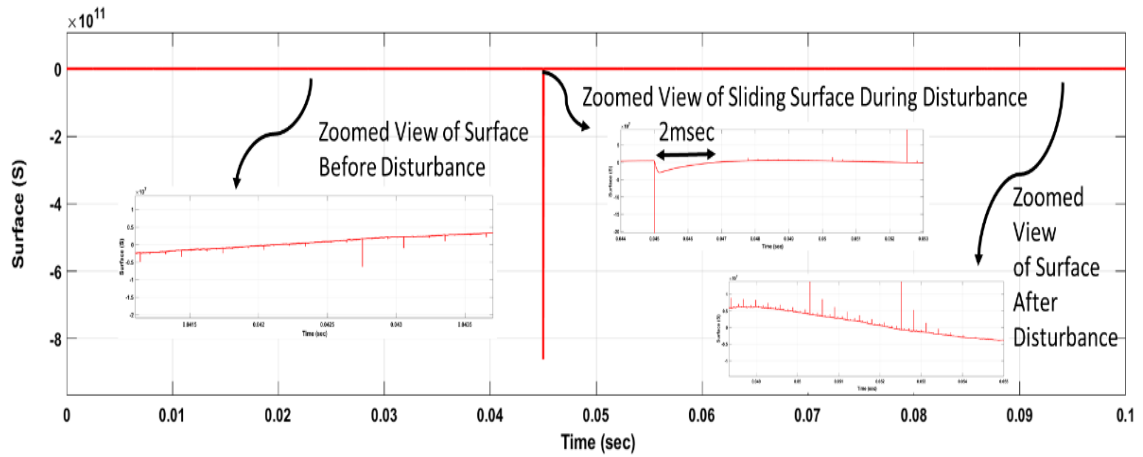


Figure 4.37: Surface selection analysis for FPRRL [2] (Full Load to No Load).

The analysis of the surface selection mechanism's performance, as proposed in C-ERL-RSS, under the same conditions, is depicted in Figure 4.38 and Figure 4.39 for transitions from no load to full load and full load to no load, respectively. Notably, the system exhibits highly favorable behavior in achieving stability both before and after the disturbance conditions. Furthermore, it achieves a rapid convergence rate, namely, 1.2 ms for the no-load to full-load transition and 1 ms for the full-load to no-load transition, as shown in Figure 4.38 and Figure 4.39, respectively.

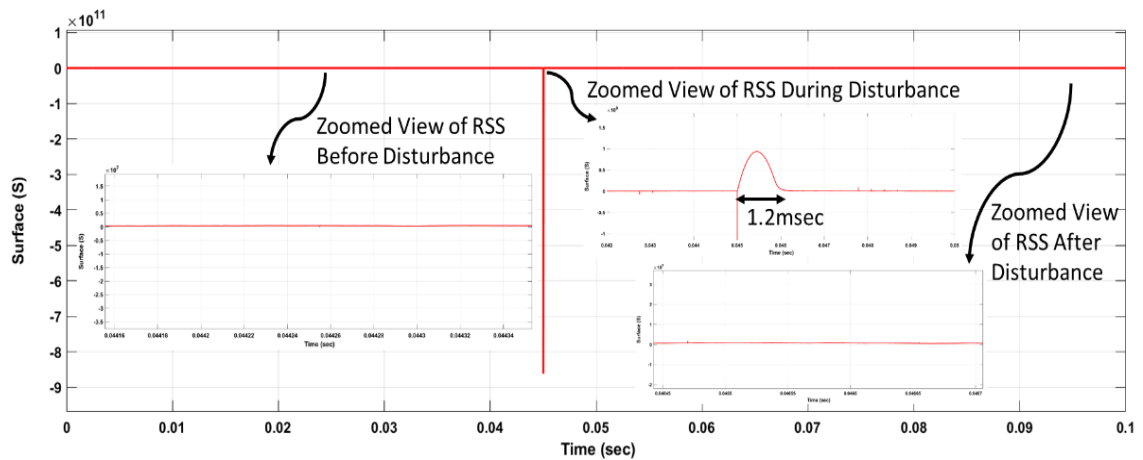


Figure 4.38: Surface selection analysis for proposed C-ERL-RSS (No Load to Full Load).

4.2.2 Surface selection analysis for Three Phase VSI

In this section, performance analysis for the surface selection of PRERL [12], RRL [13], and EERL [14], along with the proposed C-ERL-RSS under load disturbance condition of no load to full load and full load to no load is presented for three-phase VSIs. It starts with the performance analysis of RRL [13] for surface selection is presented in Figure 4.40 and Figure 4.41 for load disturbance condition of no load to full load and full load to no load condition, respectively. It can be observed that stability is compromised in both the cases of load disturbances along with the slow convergence rate of 8.7 ms and 9 ms, respectively.

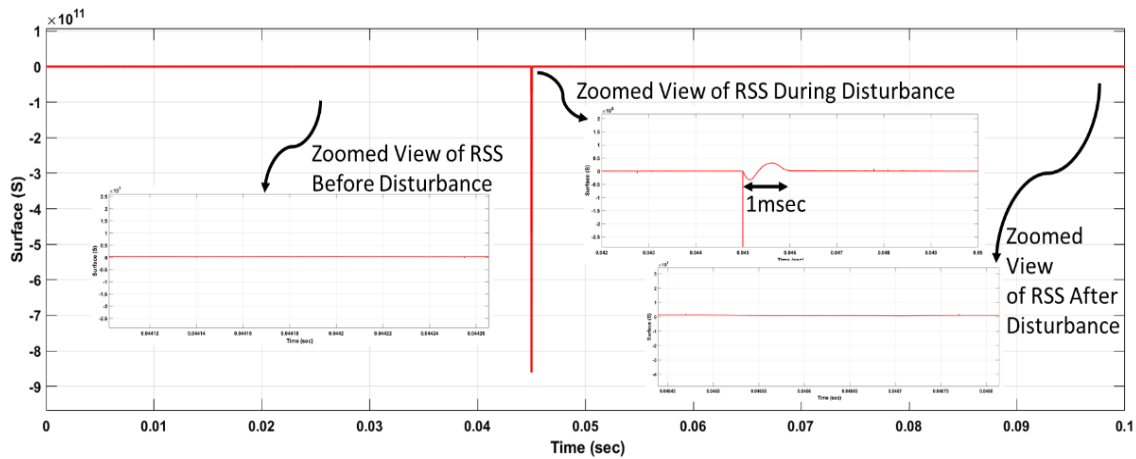


Figure 4.39: Surface selection analysis for proposed C-ERL-RSS (Full Load to No Load).

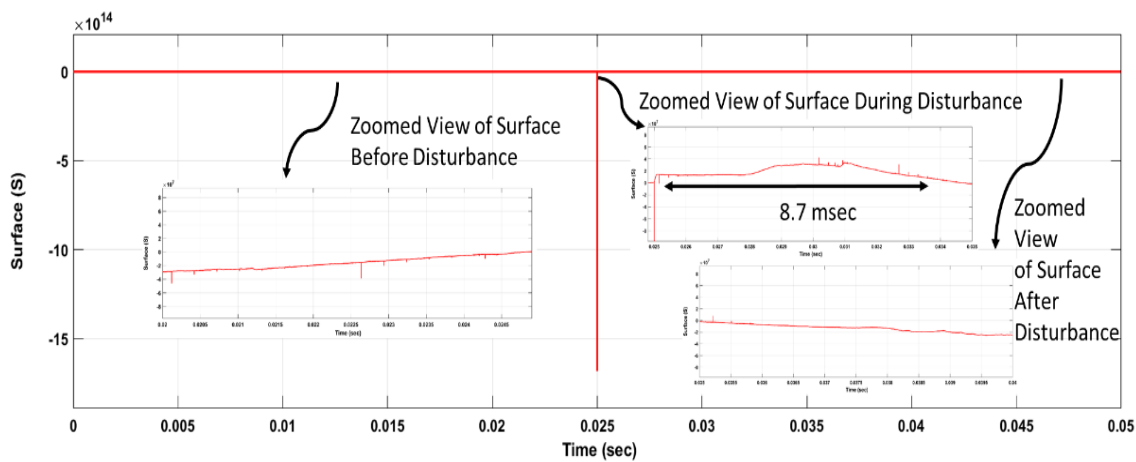


Figure 4.40: Surface selection analysis for RRL [13] (No Load to Full Load).

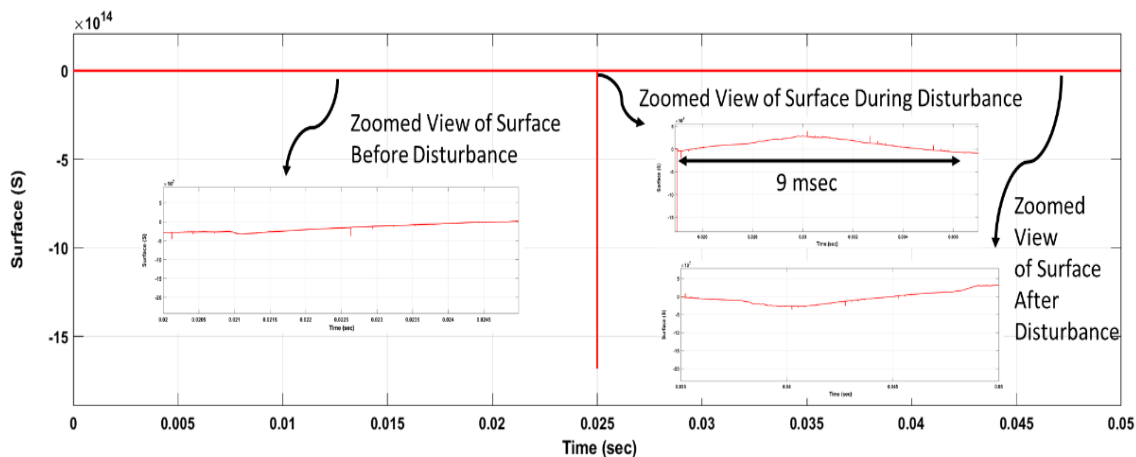


Figure 4.41: Surface selection analysis for RRL [13] (Full Load to No Load).

The surface selection mechanism of PRERL [12] for load disturbance conditions of no load to full load and full load to no load is depicted in Figure 4.42 and Figure 4.43, respectively. The stability attainment of the PRERL [12] needs improvement before and after the disturbance at 0.025sec. While, convergence time of 3.1 ms and 4.7 ms is

achieved, presented in Figure 4.42 and Figure 4.43, respectively.

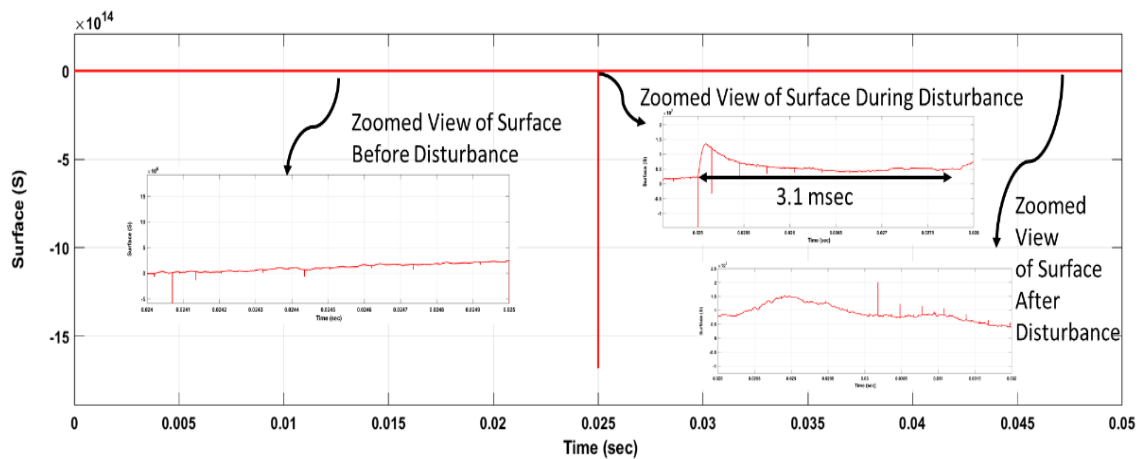


Figure 4.42: Surface selection analysis for PRERL [12] (No Load to Full Load).

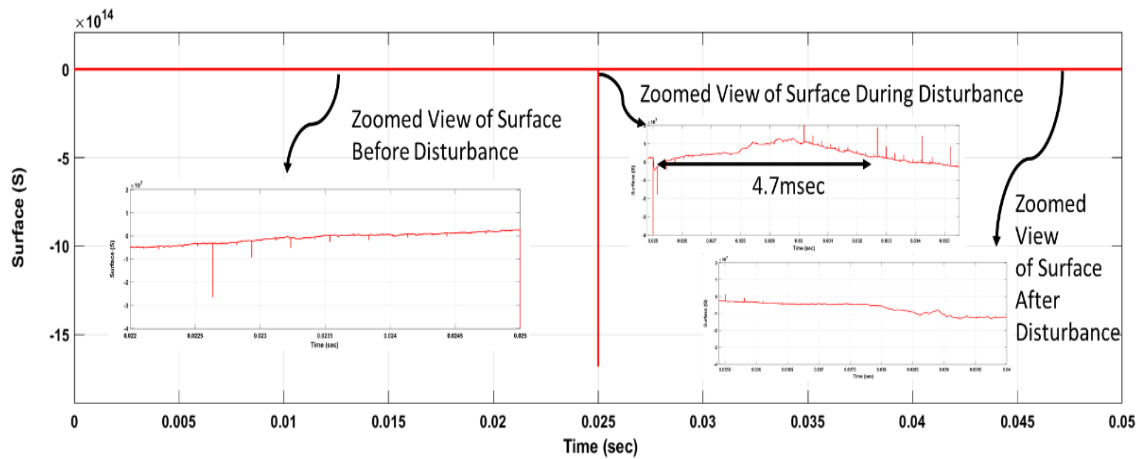


Figure 4.43: Surface selection analysis for PRERL [12] (Full Load to No Load).

the performance analysis of the surface selection for EERL [14] is presented in Figure 4.44 and Figure 4.45 for load disturbance conditions of no load to full load and full load to no load, respectively.

Similarly, the performance analysis of proposed C-ERL-RSS for surface selection under load disturbance conditions of no load to full load and full load to no load is presented in Figure 4.46 and Figure 4.47, respectively. Extremely improved stability condition is achieved before and after disturbance condition along with fast convergence rate of 2 ms and 0.23ms, respectively.

4.3 Performance analysis under input voltage disturbances

In this section, the performance of the proposed SMC is analyzed under input voltage disturbances. The input voltage is selected following the procedure adopted by [4], where the input DC voltage must be 1.5 times the peak value of the output AC voltage. Therefore, an input DC voltage of 450V is chosen to produce a peak output AC voltage

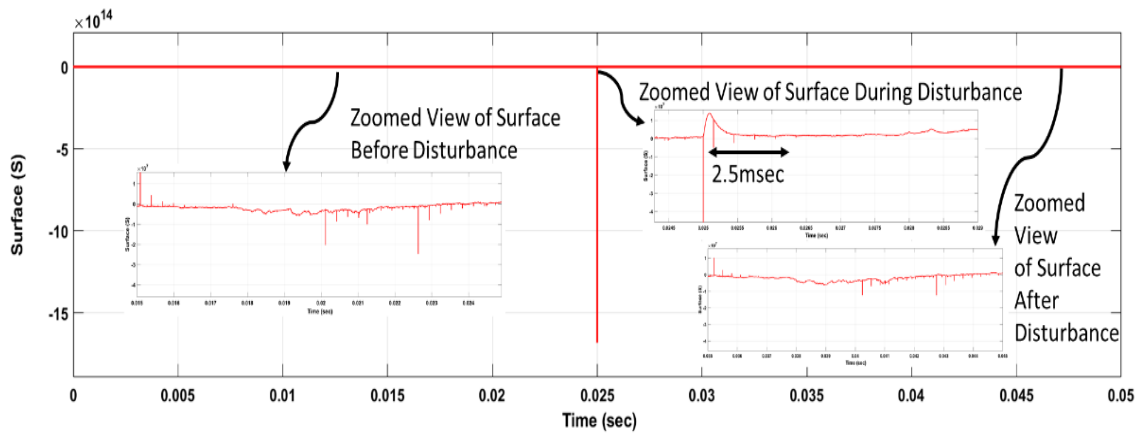


Figure 4.44: Surface selection analysis for EERL [14] (No Load to Full Load).

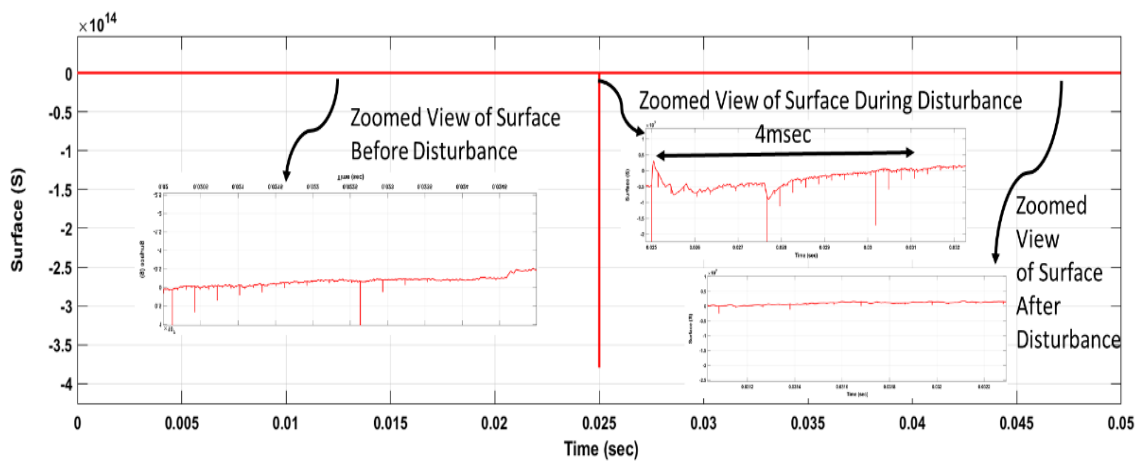


Figure 4.45: Surface selection analysis for EERL [14] (Full Load to No Load).

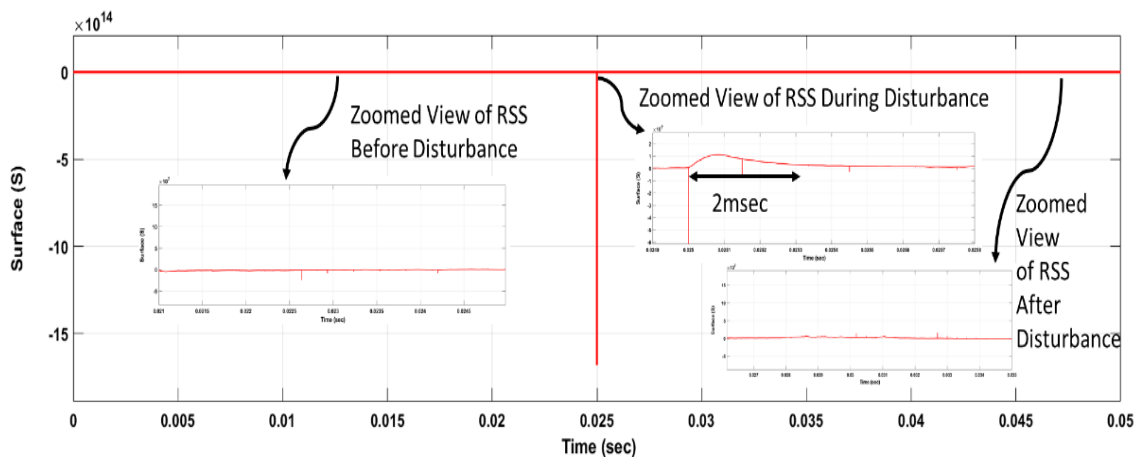


Figure 4.46: Surface selection analysis for proposed C-ERL-RSS (No Load to Full Load).

of 310V. To analyze the behavior of the proposed SMC under input voltage disturbances, the system is tested with a variable input voltage, starting at 400V, which then increases to 450V at 0.045 secs and finally reaches 500V at 0.105 secs. The variable input voltage is illustrated in Figure 4.48, followed by the comparison of the output voltage behavior to the

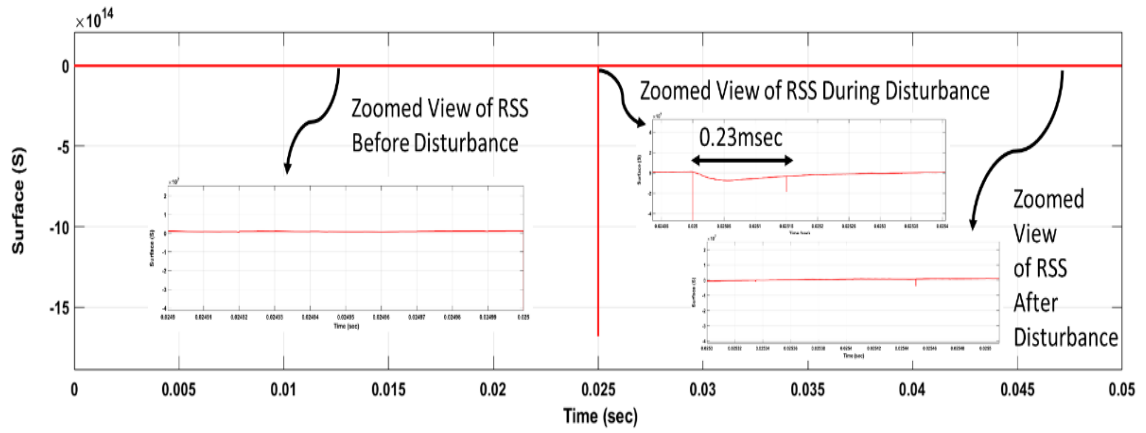


Figure 4.47: Surface selection analysis for proposed C-ERL-RSS (Full Load to No Load).

reference output voltage, as shown in Figure 4.49. It is observed that the proposed SMC has shown extreme resilience to input voltage variation by ensuring voltage regulation of 99.8% and %THD of 0.29%.

Moreover, to further test the performance of the proposed SMC under extreme conditions of load variation, followed by input voltage variation, the VSI system is initially subjected to Full Load to No Load (FN) conditions at 0.045 secs, followed by No Load to Full Load (NF) conditions at 0.105 secs. To gain better insight into the proposed SMC response, other state-of-the-art SMCs are also tested under the same conditions. The performances of the CosERL [1] SMC, FPRRL [2] SMC, and proposed C-ERL-RSS SMC are presented in Figure 4.50, Figure 4.51, and Figure 4.52, respectively. The performance analysis presented in Figure 4.50, Figure 4.51, and Figure 4.52 indicates that the proposed C-ERL-RSS SMC has demonstrated the most impressive robust response under variable load and input voltage conditions, along with promising voltage regulation and low %THD. For CosERL [1] SMC, the transient response from FL to NL condition at 0.045 seconds is observed as 10 milliseconds, and from NL to FL condition at 0.105 secs, the transient response is measured as 2 mss. Additionally, the %THD and output peak voltage are observed as 0.77% and 308V, respectively. Similarly, FPRRL [2] shows a transient response of 20 ms and 25 mss at 0.045 secs and 0.105 secs, respectively. In addition to this, the %THD and output peak voltage are observed as 0.79% and 307.5V, respectively. However, despite achieving quite impressive results in terms of robustness, the transient response at 0.045 secs and 0.105 seconds is observed to be 1 millisecond and 1.1 milliseconds, respectively. Moreover, a low %THD of 0.31% and an output peak voltage of 309.2V are achieved. The detailed comparative analysis of CosERL [1] SMC, FPRRL [2] SMC, and the proposed C-ERL-RSS for FL-NL and NL-FL conditions is presented in Table 4.6. Similarly, the proposed C-ERL-RSS SMC, along with CosERL [1] and FPRRL [2], is also subjected to NL to FL conditions at 0.045 secs and FL to NL conditions at 0.105 secs. Provided that, the VSI is also subject to input voltage disturbances at the same instants, i.e., 0.045 secs and 0.105 secs. The performances of the proposed C-ERL-RSS, along with CosERL [1] and FPRRL [2], are shown in Figure 4.55, Figure 4.53, and Figure 4.54, respectively. Furthermore, the proposed C-ERL-RSS, along with

Table 4.6: Robust behavior under extreme conditions of input voltage disturbances and load disturbances.

Scenario	%THD	V _p (Output Peak Voltage)	Transient Response at 0.045secs	Transient Response at 0.105secs
CosERL [1](FL-NL-FL)	0.77	308.1V	10ms	2ms
FPRRL [2] (FL-NL-FL)	0.79	307.5	20ms	25ms
Proposed C-ERL-RSS (FL-NL-FL)	0.31	309.2	1ms	1.1ms
CosERL [1] (NL-FL-NL)	1.07	308.7V	2ms	0.5ms
FPRRL [2] (NL-FL-NL)	1.3	307.4	15ms	22ms
Proposed C-ERL-RSS (NL-FL-NL)	0.36	309.43	0.5ms	0.3ms

CosERL [1] SMC and FPRRL [2] SMC, is also subjected to NL to FL and FL to NL conditions, along with input voltage disturbances. The transient response of CosERL [1] SMC at 0.045 secs and 0.105 secs is observed as 2 milliseconds and 0.5 ms. Moreover, the %THD and output peak voltage are observed to be 1.07% and 308.7V, respectively. Likewise, the robust behavior of FPRRL [2] SMC is observed to be 15 milliseconds and 22 ms at 0.045 secs and 0.105 secs, respectively. However, the robustness achieved through the proposed C-ERL-RSS SMC is quite impressive, and the transient response at 0.045 secs and 0.105 secs is observed to be 0.5 milliseconds and 0.3 mss, respectively. Also, the low %THD of 0.36% and improved voltage regulation with an output peak voltage of 309.43V are achieved under extreme conditions of input voltage and load disturbances.

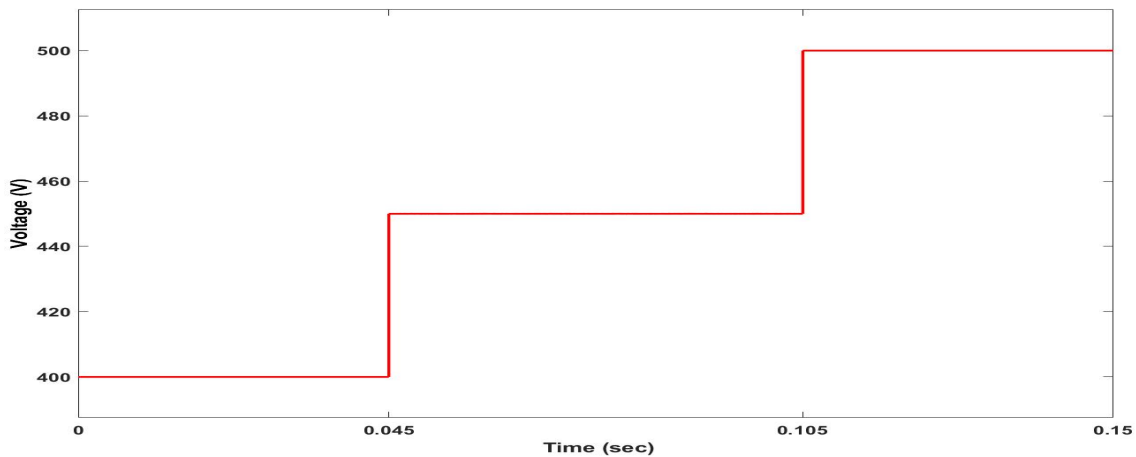


Figure 4.48: Input Voltage with disturbances.

4.4 Performance analysis under filter and input voltage disturbances

In this section of the dissertation, the proposed C-ERL-RSS SMC is subjected under the extreme conditions of input voltage and output load disturbances along with filter

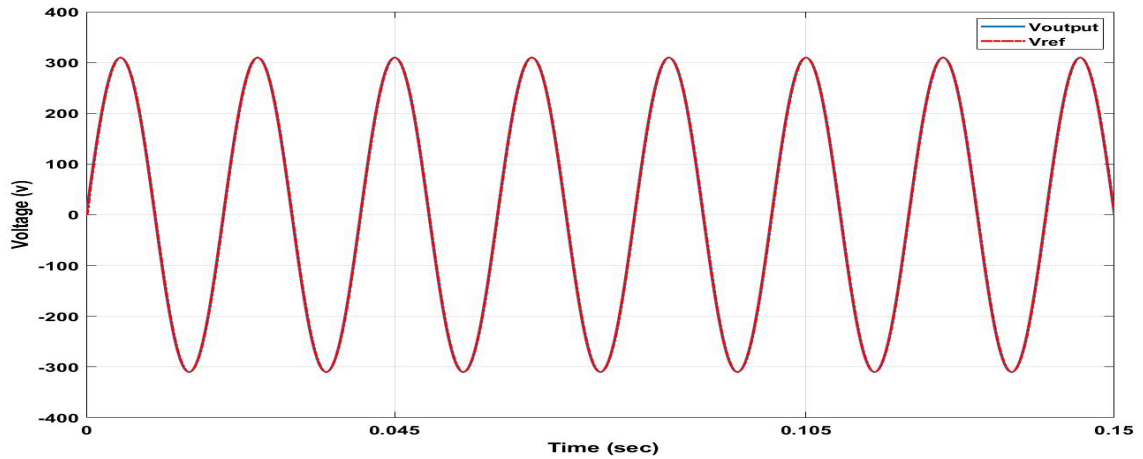
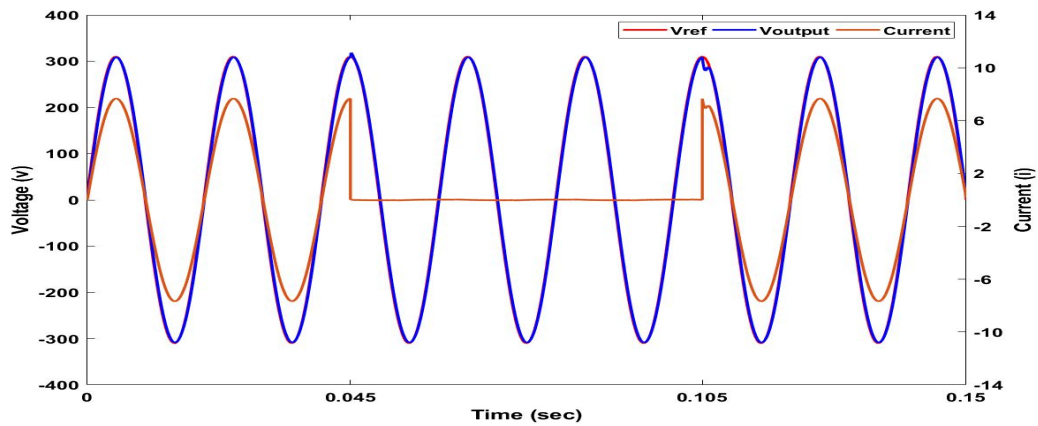
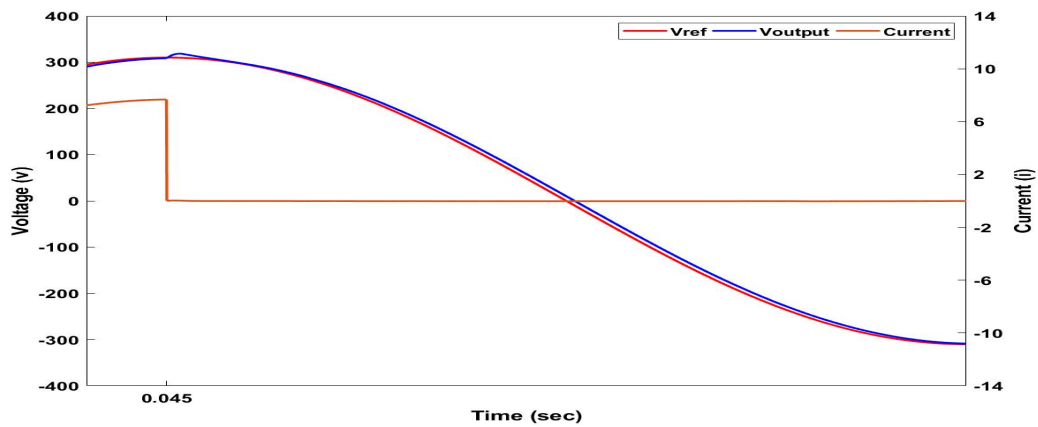


Figure 4.49: Output voltage behaviour under input voltage disturbances i.e. 400 V at 0-0.045 secs, 450V at 0.045 secs to 0.105 secs and 550V at 0.105 secs to 0.15secs

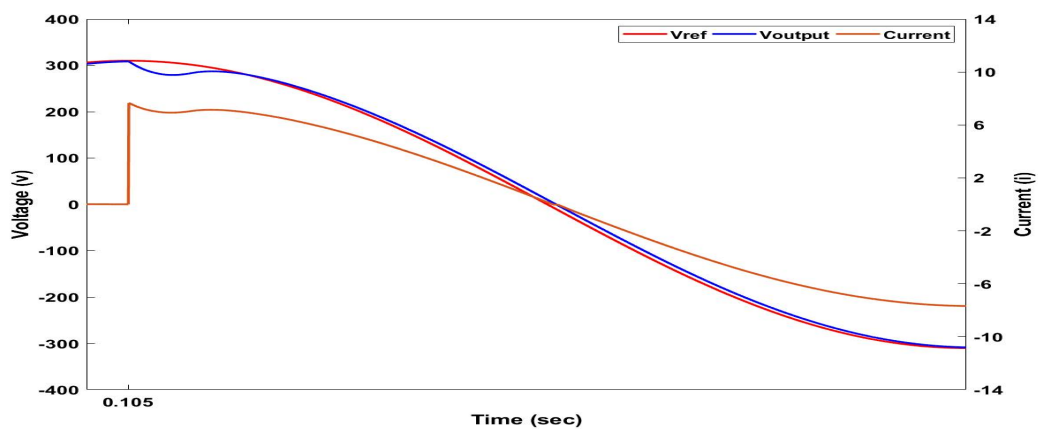
disturbances of $\pm 10\%$ of the rated values of filter inductor and capacitor. The mechanism adopted for testing effect of filter disturbances is driven by the idea implemented in [145] and [263]. The proposed C-ERL-RSS SMC is tested under all possible filter disturbance combinations. In Figure 4.59, the performance of proposed SMC under defined conditions of 15mH inductor and 43.2 μ F capacitor is presented that shows little bit of increase in %THD i.e. 0.73% with voltage regulation of 309.5V and transient time of 1.3 ms and 1.1 ms for FL to NL and NL to FL conditions, respectively. Similarly, proposed SMC is tested at filter values of 15mH and 52.8 μ F, robust response is shown in Figure 4.56. Moreover, %THD and output peak voltage are measured as 0.52% and 309.5V, respectively. The robust response of the proposed SMC is subjected to filter disturbances of 16.5mH and 48 μ F, response of which is presented in Figure 4.57. The transient responses at 0.045 secs and 0.105 secs is observed as 1.3 ms and 1.1 ms, respectively. Moreover, the %THD and output peak voltage is measured as 0.63% and 309.6V, respectively. Furthermore, at the load disturbance conditions of 13.5mH and 48 μ F, the system under proposed C-ERL-RSS shows promising response depicted in Figure 4.58. The transient time measured as 1.1 ms and 1 ms at 0.045 secs and 0.105 secs, respectively. Moreover the values of %THD is observed as 0.46% and output peak voltage is witnessed as 309.6V. Subsequently, the proposed C-ERL-RSS SMC is tested under filter values of 13.5mH and 43.2 μ F on the defined conditions, presented in Figure 4.60. Slight increase in %THD of 0.58% is observed along with output peak voltage of 309.5V and transient responses of 1.7 ms and 1 ms at 0.045 secs and 0.105 secs, respectively. Finally, the filter inductor and capacitor with disturbances are chosen as 16.5mH and 52.8 μ F. %THD is observed to be 0.64% and output peak voltage is measured as 309.5V along with transient responses of 1.1 ms and 1.5 ms at 0.045 secs and 0.105 secs, respectively. Moreover the same scenarios of disturbances are measured under FL conditions, comprehensive summary of comprising transient responses with %THD and voltage regulation is presented in Table 4.7.



(a) Output voltage and current under input voltage variation and FL-NL-FL condition

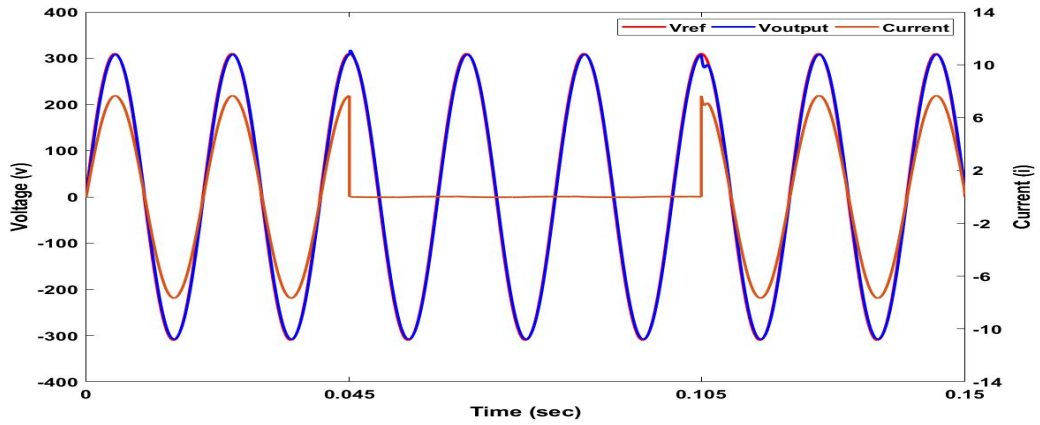


(b) Zoom: Transient response at 0.045 secs FL-NL condition (Transient response= 10ms).

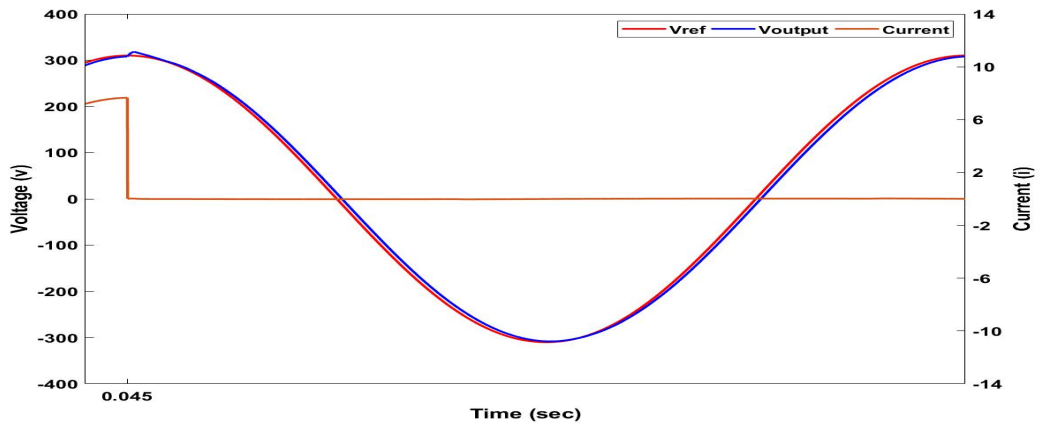


(c) Zoom: Transient response at 0.105 secs NL-FL condition (Transient response= 2ms).

Figure 4.50: Output voltage and current behaviour of the CosERL SMC [1] under input voltage disturbances (400V at (0-0.045secS), 450V at (0.045secs-0.105sec) and 500V at (0.105secs-0.15secs). With FL to NL and NL to FL conditions at 0.045secs and 0.105secs, respectively.



(a) Output voltage and current under input voltage variation and FL-NL-FL condition

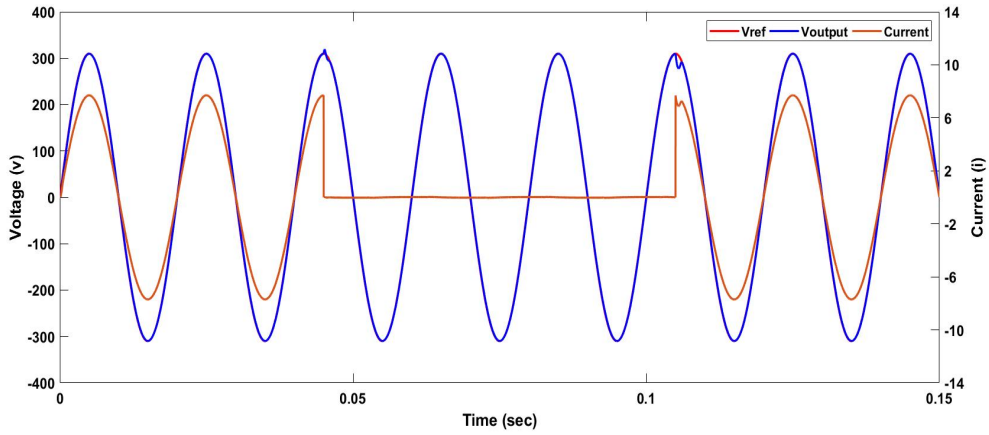


(b) Zoom: Transient response at 0.045 secs FL-NL condition (Transient response= 20ms).

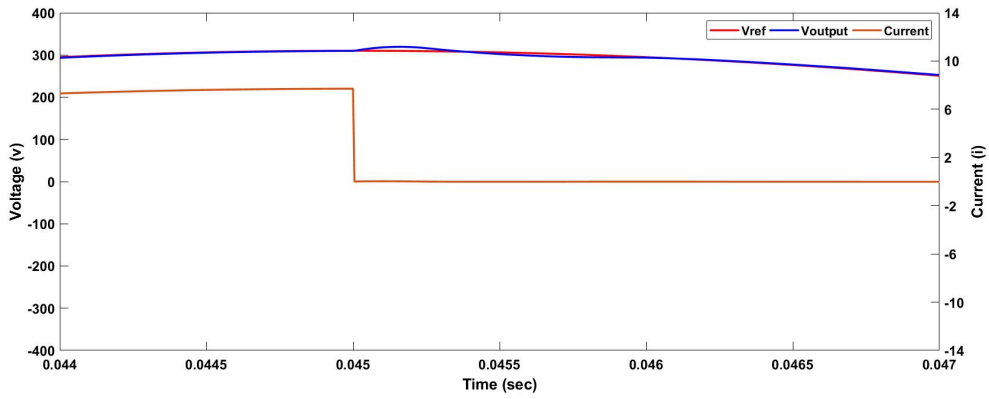


(c) Zoom: Transient response at 0.105 secs NL-FL condition (Transient response= 25ms).

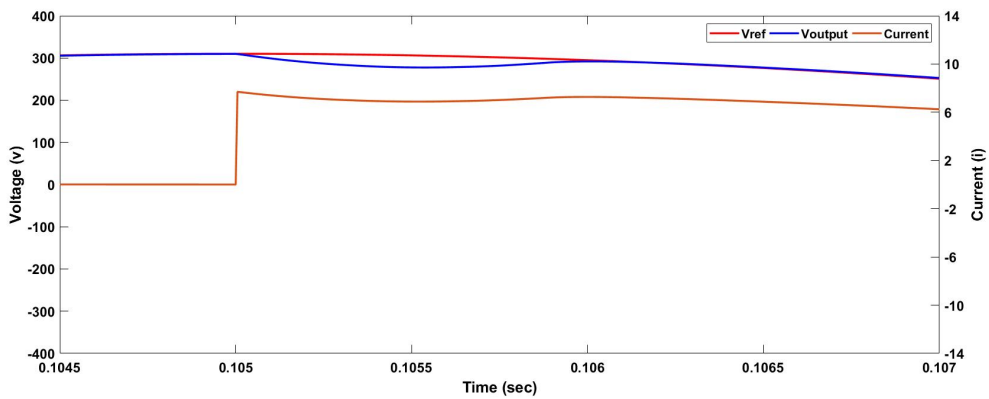
Figure 4.51: Output voltage and current behaviour of the FPRRL SMC [2] under input voltage disturbances (400V at (0-0.045secS), 450V at (0.045secs-0.105sec) and 500V at (0.105secs-0.15secs). With FL to NL and NL to FL conditions at 0.045secs and 0.105secs, respectively.



(a) Output voltage and current under input voltage variation and FL-NL-FL condition

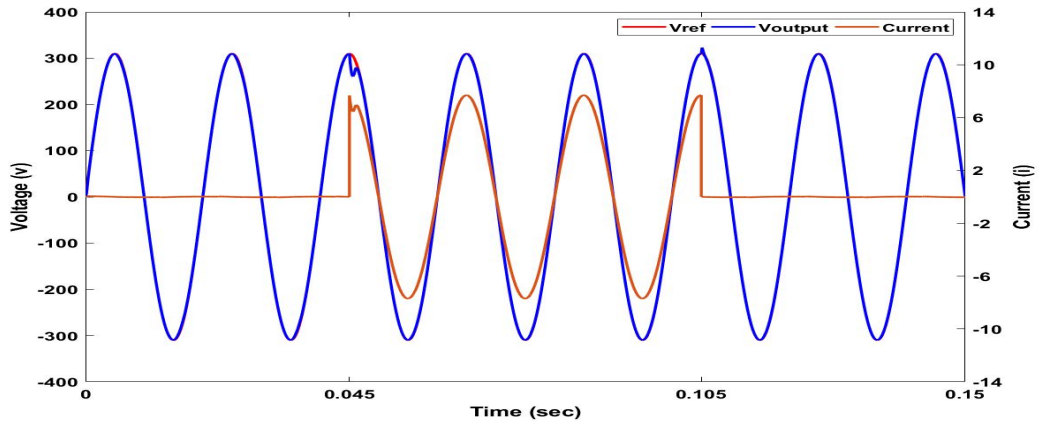


(b) Zoom: Transient response at 0.045 secs FL-NL condition (Transient response= 1ms).

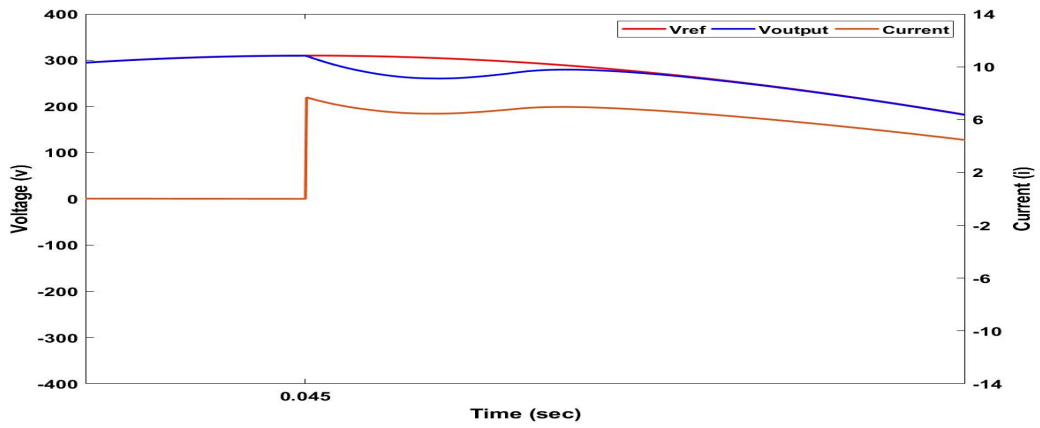


(c) Zoom: Transient response at 0.105 secs NL-FL condition (Transient response= 1.1ms).

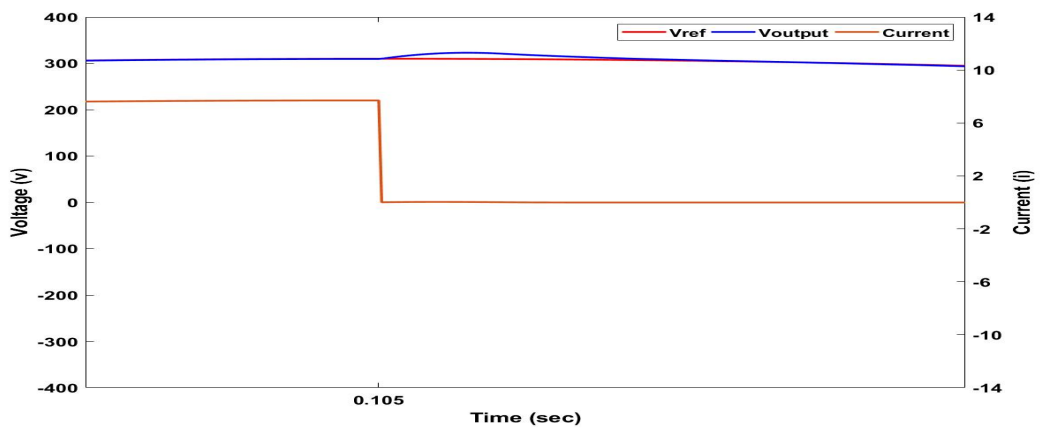
Figure 4.52: Output voltage and current behaviour of the proposed C-ERL-RSS SMC under input voltage disturbances (400V at (0-0.045secS), 450V at (0.045secs-0.105sec) and 500V at (0.105secs-0.15secs). With FL to NL and NL to FL conditions at 0.045secs and 0.105secs, respectively.



(a) Output voltage and current under input voltage variation and NL-FL-NL condition

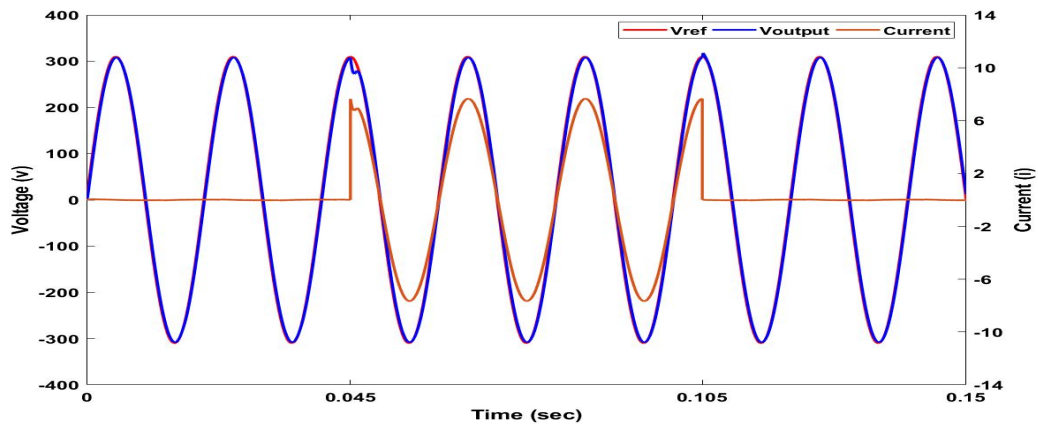


(b) Zoom: Transient response at 0.045 secs NL-FL condition (Transient response= 2ms).

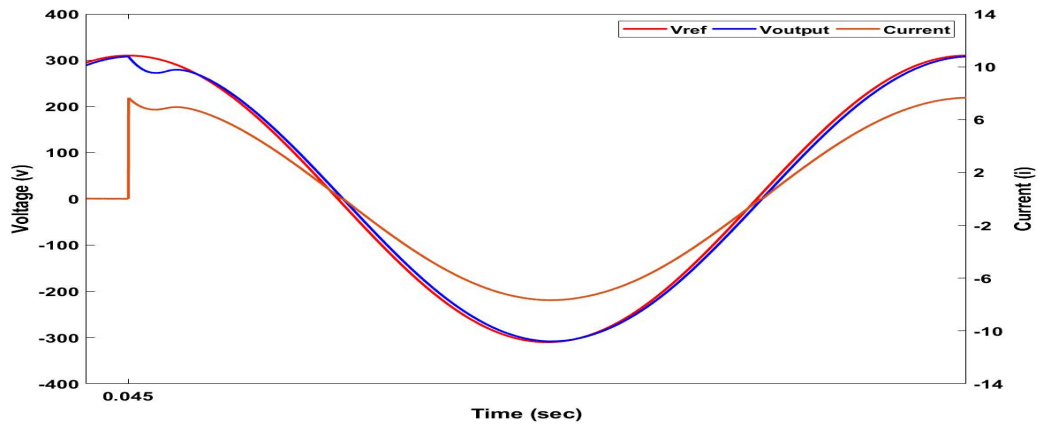


(c) Zoom: Transient response at 0.105 secs FL-NL condition (Transient response= 0.5ms).

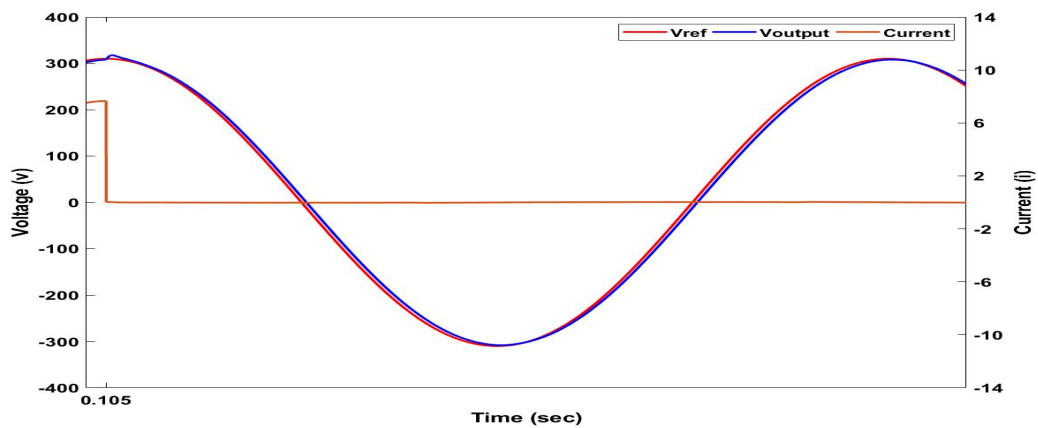
Figure 4.53: Output voltage and current behaviour of the CosERL SMC[1] under input voltage disturbances (400V at (0-0.045secS), 450V at (0.045secs-0.105sec) and 500V at (0.105secs-0.15secs). With NL to FL and FL to NL conditions at 0.045secs and 0.105secs, respectively.



(a) Output voltage and current under input voltage variation and NL-FL-NL condition

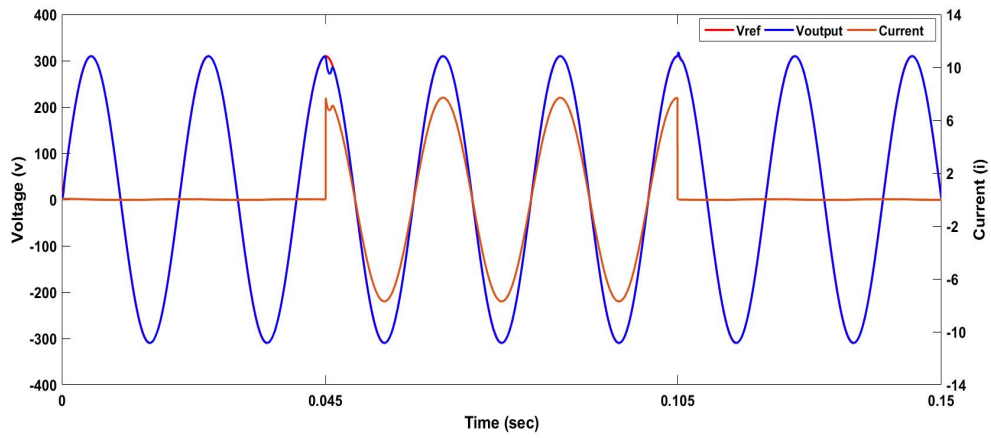


(b) Zoom: Transient response at 0.045 secs NL-FL condition (Transient response= 15ms).

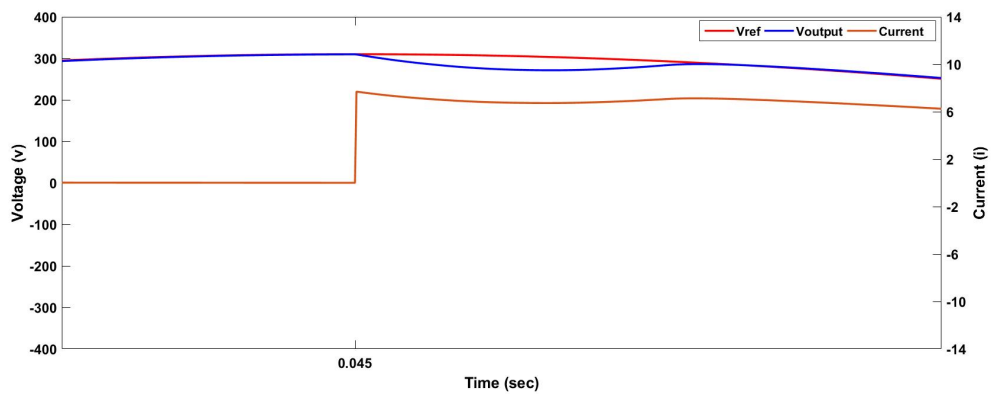


(c) Zoom: Transient response at 0.105 secs FL-NL condition (Transient response= 22ms).

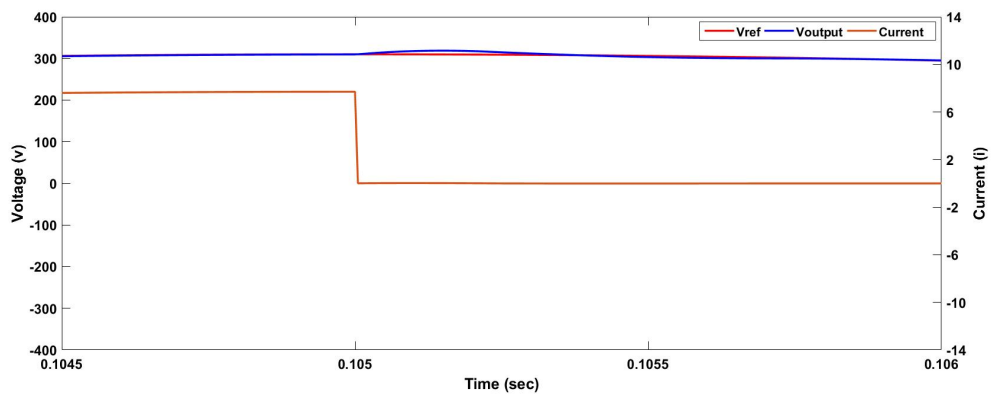
Figure 4.54: Output voltage and current behaviour of the FPRRL SMC [2] under input voltage disturbances (400V at (0-0.045secS), 450V at (0.045secs-0.105sec) and 500V at (0.105secs-0.15secs). With NL to FL and FL to NL conditions at 0.045secs and 0.105secs, respectively.



(a) Output voltage and current under input voltage variation and NL-FL-NL condition



(b) Zoom: Transient response at 0.045 secs NL-FL condition (Transient response= 0.5ms).



(c) Zoom: Transient response at 0.105 secs FL-NL condition (Transient response= 0.3ms).

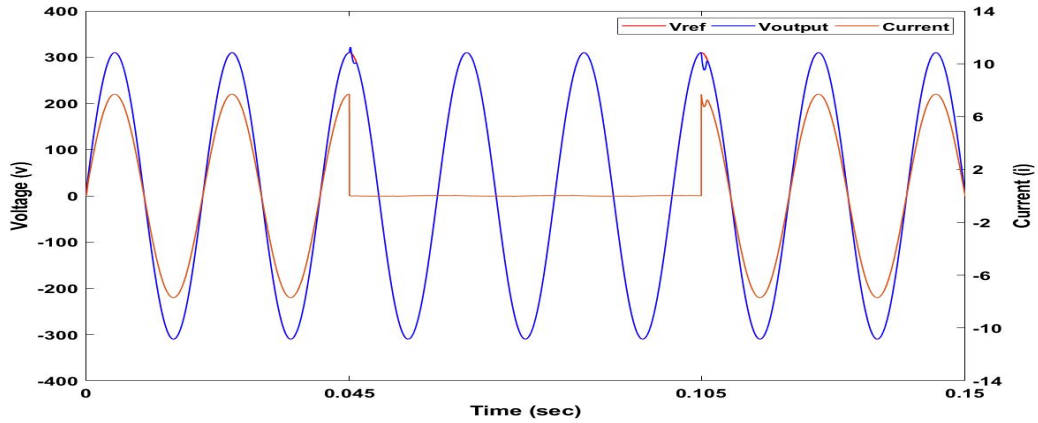
Figure 4.55: Output voltage and current behaviour of the proposed C-ERL-RSS SMC under input voltage disturbances (400V at (0-0.045secS), 450V at (0.045secs-0.105sec) and 500V at (0.105secs-0.15secs). With NL to FL and FL to NL conditions at 0.045secs and 0.105secs, respectively.

Table 4.7: Robust behavior of proposed C-ERL-RSS SMC under extreme conditions of input voltage disturbances of 400V till 0.045 secs that changes to 450V from (0.045 secs to 0.105 secs) and finally shifts to 500V from 0.105 secs to 0.15 secs, load disturbances of FL to NL and NL to FL and filter inductor disturbances of $\pm 10\%$ of rated values of filter capacitor and inductor.

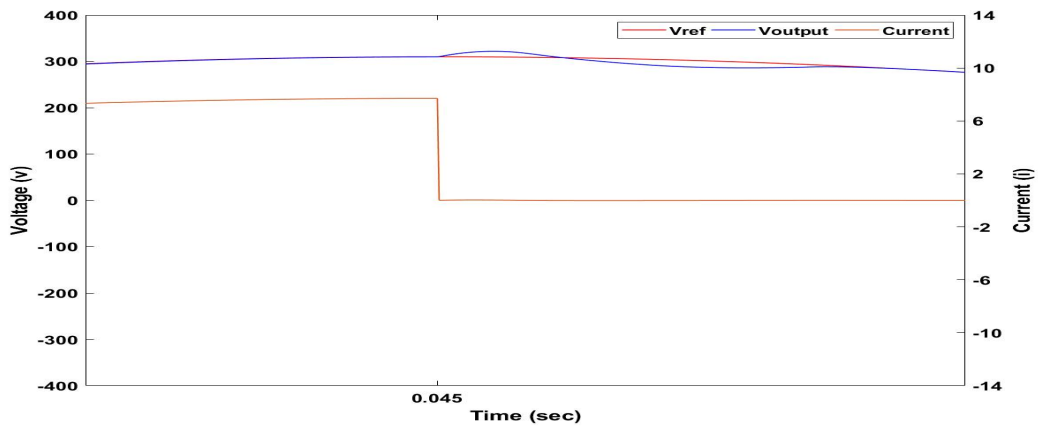
Scenario	%THD	V _p (Output Peak Voltage)	Transient Response at 0.045 secs	Transient Response at 0.105 secs	Value of Filter Inductor	Value of Filter Capacitor
C-ERL-RSS at FL	0.23	309.7V	No Load Variation	No Load Variation	16.5mH	48 μ F
C-ERL-RSS at FL-NL-FL	0.63	309.6V	1.3ms	1.1ms	16.5mH	48 μ F
C-ERL-RSS at FL	0.21	309.7V	No Load Variation	No Load Variation	15mH	52.8 μ F
C-ERL-RSS at FL-NL-FL	0.52	309.5V	1.2ms	1.3ms	15mH	52.8 μ F
C-ERL-RSS at FL	0.39	309.6V	No Load Variation	No Load Variation	13.5mH	48 μ F
C-ERL-RSS at FL-NL-FL	0.46	309.6V	1.1ms	1ms	13.5mH	48 μ F
C-ERL-RSS at FL	0.43	309.6V	No Load Variation	No Load Variation	15mH	43.2 μ F
C-ERL-RSS at FL-NL-FL	0.73	309.5V	1.3ms	1.1ms	15mH	43.2 μ F
C-ERL-RSS at FL	0.39	309.6V	No Load Variation	No Load Variation	13.5mH	43.2 μ F
C-ERL-RSS at FL-NL-FL	0.58	309.5V	1.7ms	1ms	13.5mH	43.2 μ F
C-ERL-RSS at FL	0.52	309.6V	No Load Variation	No Load Variation	16.5mH	52.8 μ F
C-ERL-RSS at FL-NL-FL	0.64	309.5V	1.1ms	1.5ms	16.5mH	52.8 μ F

4.5 Summary

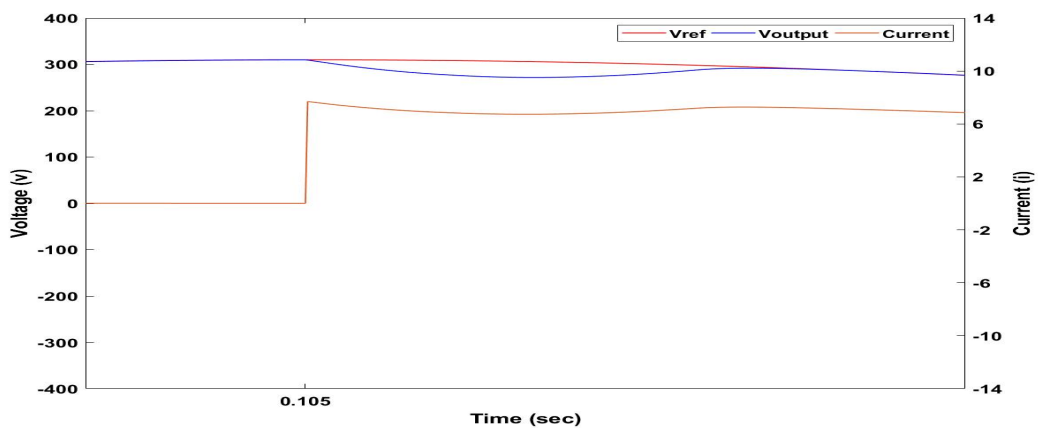
Effectiveness of the proposed C-ERL-RSS SMC is implemented and tested on islanded single phase VSI system to address the needs of a susceptible systems. Through extensive evaluations, the proposed SMC demonstrates its effectiveness in achieving lower %THD of 0.25% with voltage regulation of 99.9% and improved dynamic response with tracking/transient time of 1.1ms. These results validate the advantages of the proposed approach in fulfilling the requirements of susceptible systems, making them more reliable and robust. The successful implementation of the proposed reaching SMC for single-phase VSIs is attributed to the combination of intelligent gain adjustment, effective integration of functions, and the rotating sliding surface selection mechanism. Additionally, the proposed SMC is designed for three phase VSI, to fulfill needs of high power applications. Results reveals the ability of the proposed SMC technique to provide a well-regulated output voltage with minimal %THD of 1.1% and voltage regulation of 99.83%, improved dynamic response with transient response time of 0.08ms, and reduced chattering. Furthermore, the results are validated through comparative analysis of state-of-the art SMCs, implemented on the same systems under extreme conditions. Furthermore, to assess the performance of the proposed SMC technique in practical systems, experimental tests are conducted using the MicroLabBox dSPACE 1202 setup for both single-phase and three-phase VSI. The experimental findings validate the efficiency of the proposed SMC, showcasing fast transient response and low %THD of 1.12% and 2.1% for single phase and three phase, respectively. These promising findings further validate the suitability and robustness of the proposed SMC for real-world applications. Moreover, the optimal behaviour of the proposed C-ERL-RSS is tested and evaluated for single phase and three phase VSIs. Addition to this, the authenticity of the surface selection analysis



(a) Output voltage and current under input voltage disturbances and filter disturbances of rate value of 15mH of inductor and +10% of 48uF (52.8uF) of a capacitor

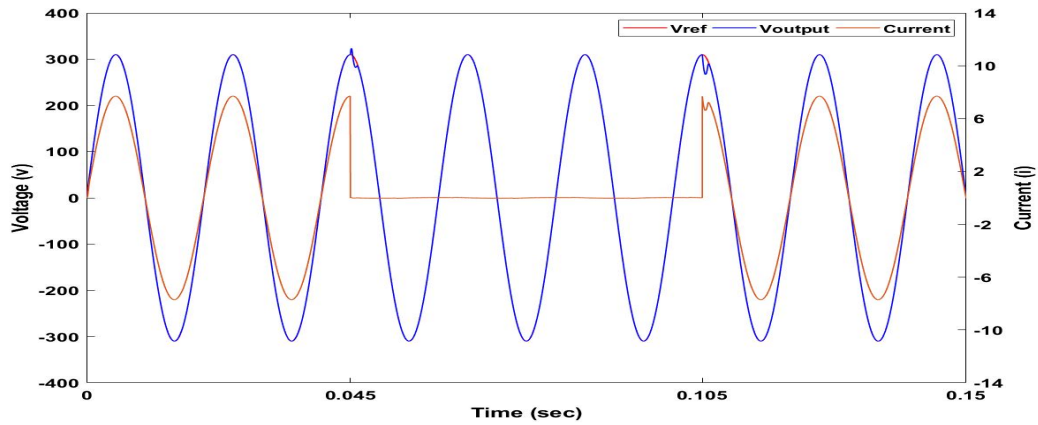


(b) Zoom: Transient response at 0.045 secs FL-NL condition (Transient response= 1.2 ms).

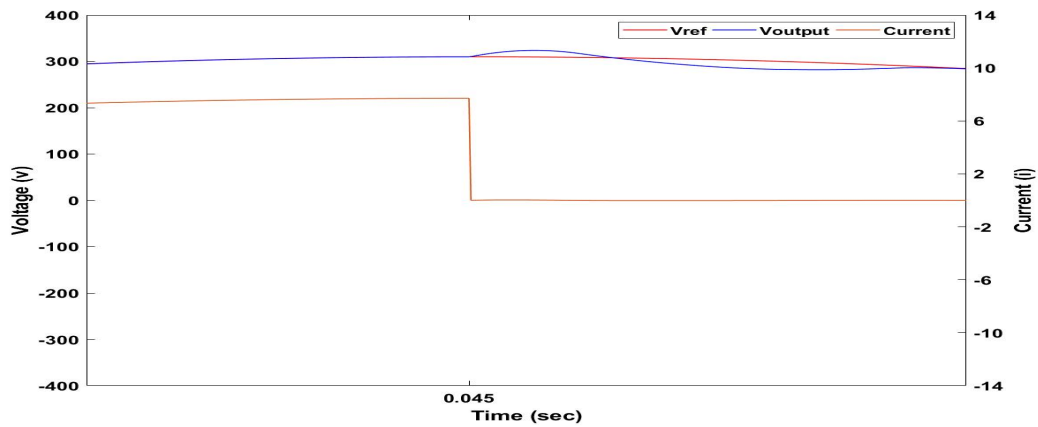


(c) Zoom: Transient response at 0.105 secs NL-FL condition (Transient response= 1.3 ms).

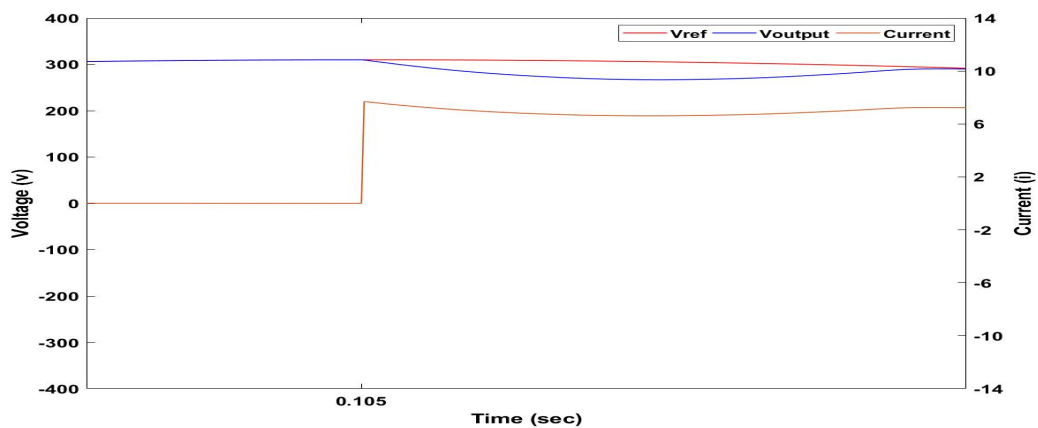
Figure 4.56: Output voltage and current behaviour of the proposed C-ERL-RSS SMC under filter disturbances at rated value of 15mH of inductor and +10% of 48uF (52.8uF) of a capacitor along with input voltage disturbances (400V at (0-0.045secS), 450V at (0.045secs-0.105sec) and 500V at (0.105secs-0.15secs). With FL to NL and NL to FL conditions at 0.045secs and 0.105secs, respectively.



(a) Output voltage and current under input voltage disturbances and filter disturbances of +10% of 15mH (16.5mH) inductor and rated value of 48uF of a capacitor.

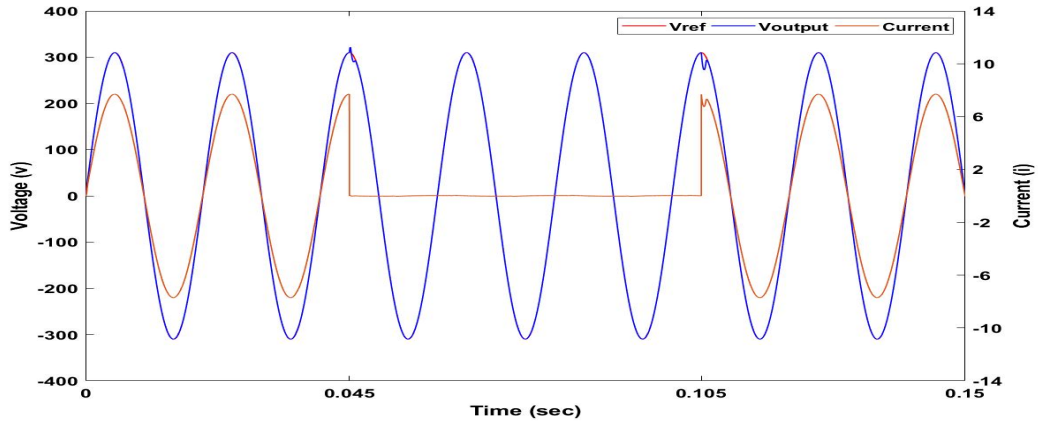


(b) Zoom: Transient response at 0.045 secs FL-NL condition (Transient response= 1.3 ms).

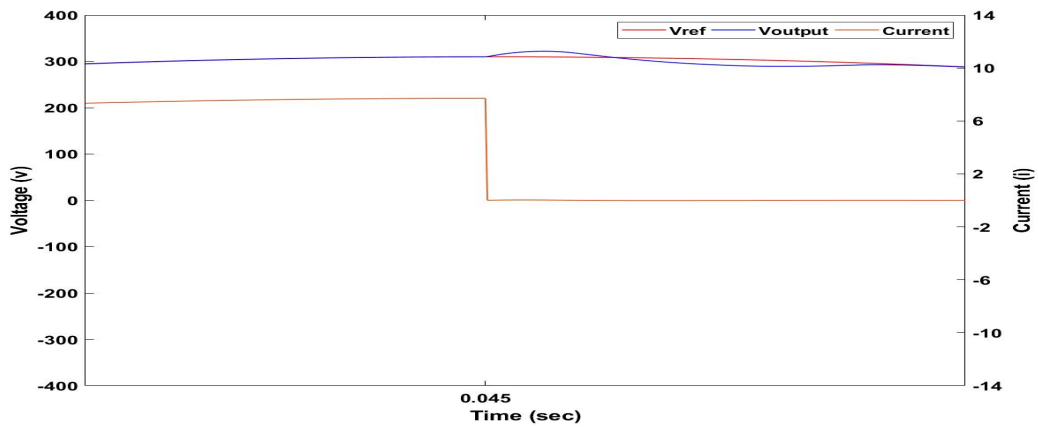


(c) Zoom: Transient response at 0.105 secs NL-FL condition (Transient response= 1.1 ms).

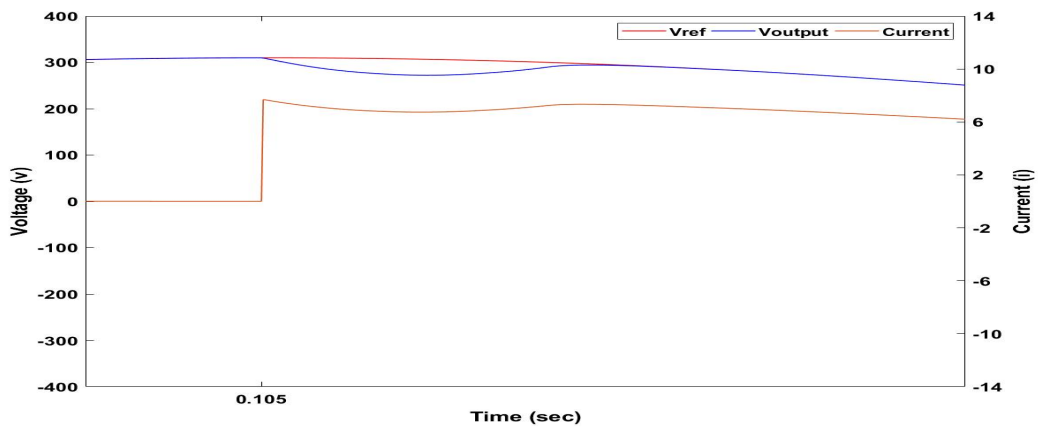
Figure 4.57: Output voltage and current behaviour of the proposed C-ERL-RSS SMC under filter disturbances of +10% of 15mH (16.5mH) inductor and 48uF of rated capacitor along with input voltage disturbances (400V at (0-0.045secS), 450V at (0.045secs-0.105sec) and 500V at (0.105secs-0.15secs). With FL to NL and NL to FL conditions at 0.045secs and 0.105secs, respectively.



(a) Output voltage and current under input voltage disturbances and filter disturbances of -10% of 15mH (13.5mH) inductor and rated value of 48uF of a capacitor.

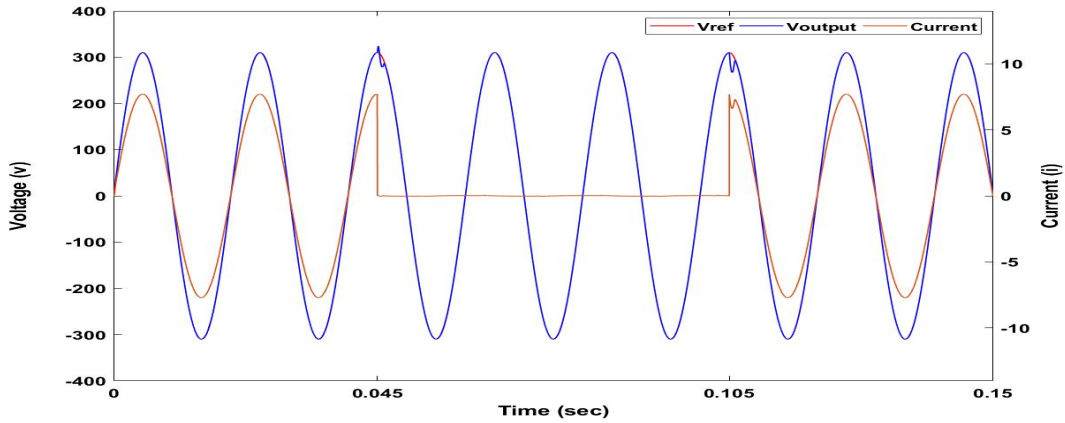


(b) Zoom: Transient response at 0.045 secs FL-NL condition (Transient response= 1.1ms).

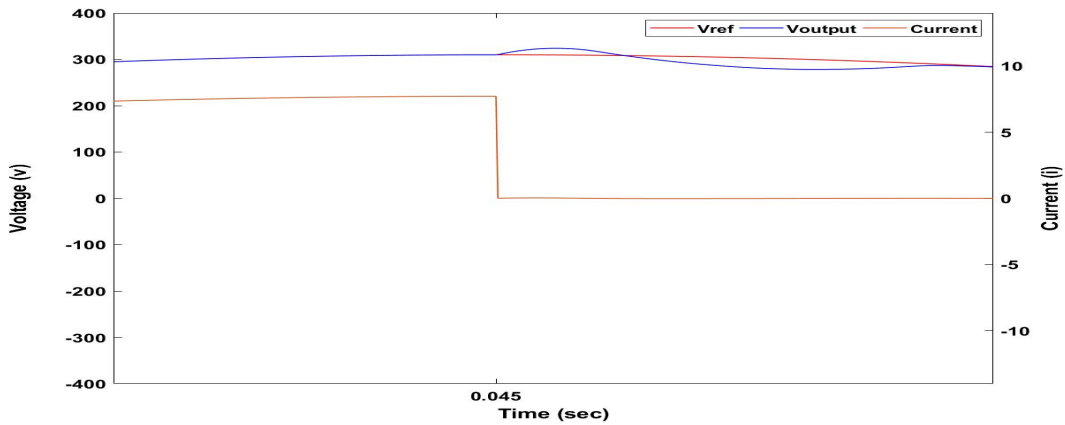


(c) Zoom: Transient response at 0.105 secs NL-FL condition (Transient response= 1 ms).

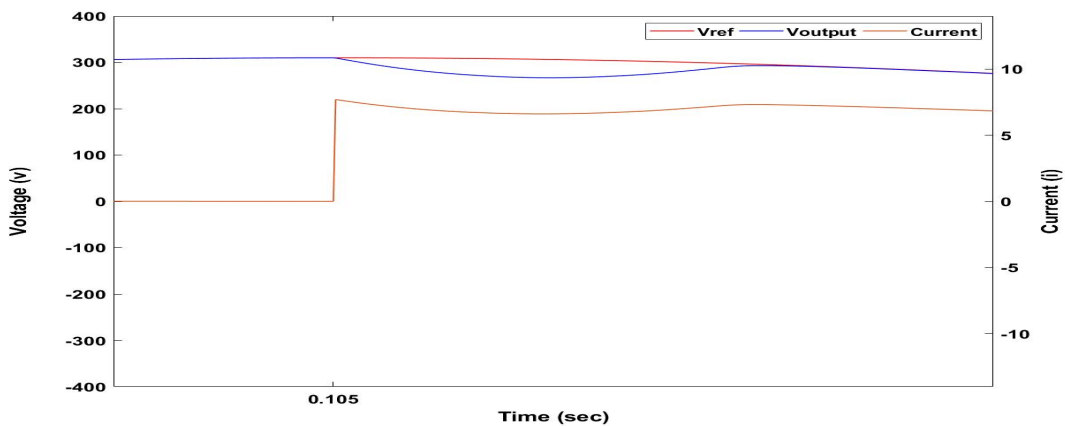
Figure 4.58: Output voltage and current behaviour of the proposed C-ERL-RSS SMC under filter disturbances of -10% of 15mH (13.5mH) inductor and value of 48uF of a capacitor along with input voltage disturbances (400V at (0-0.045secS), 450V at (0.045secs-0.105sec) and 500V at (0.105secs-0.15secs). With FL to NL and NL to FL conditions at 0.045secs and 0.105secs, respectively.



(a) Output voltage and current under input voltage disturbances and filter disturbances of 15mH inductor and -10% of 48uF (43.2uF) of a capacitor.

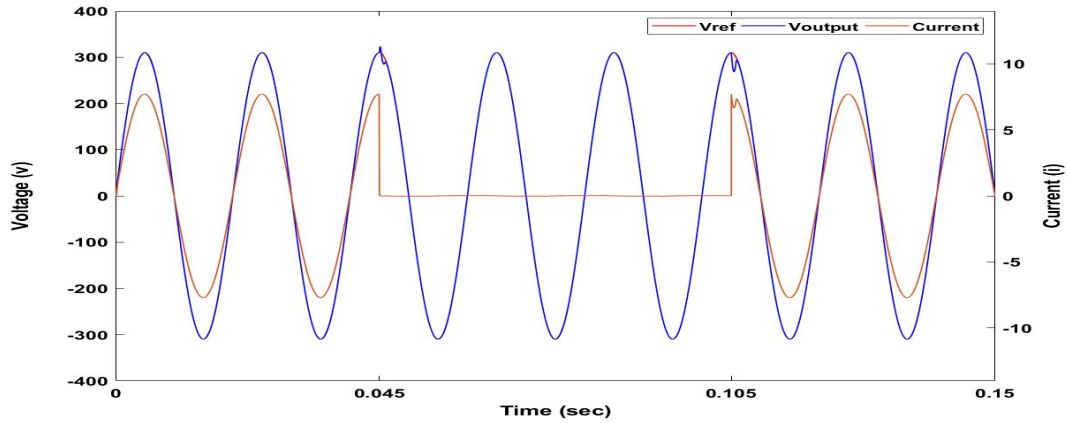


(b) Zoom: Transient response at 0.045 secs FL-NL condition (Transient response= 1.3 ms).

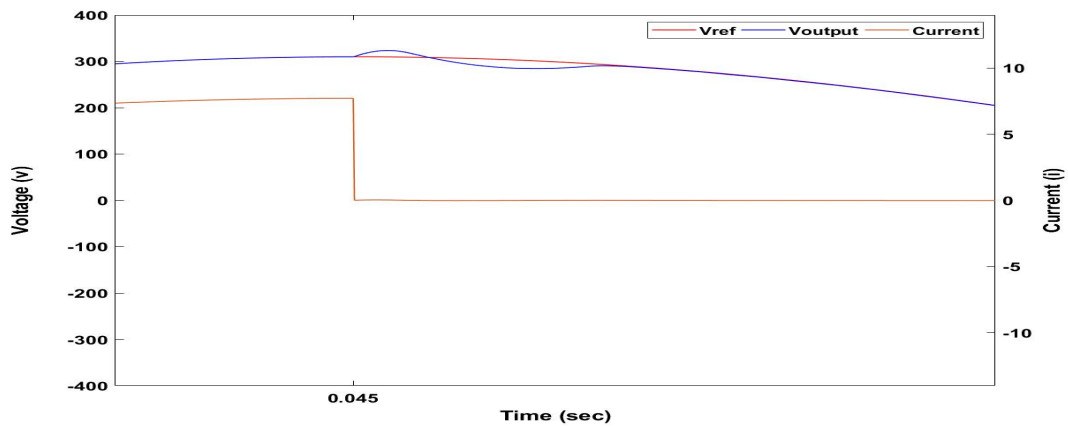


(c) Zoom: Transient response at 0.105 secs NL-FL condition (Transient response= 1.1 ms).

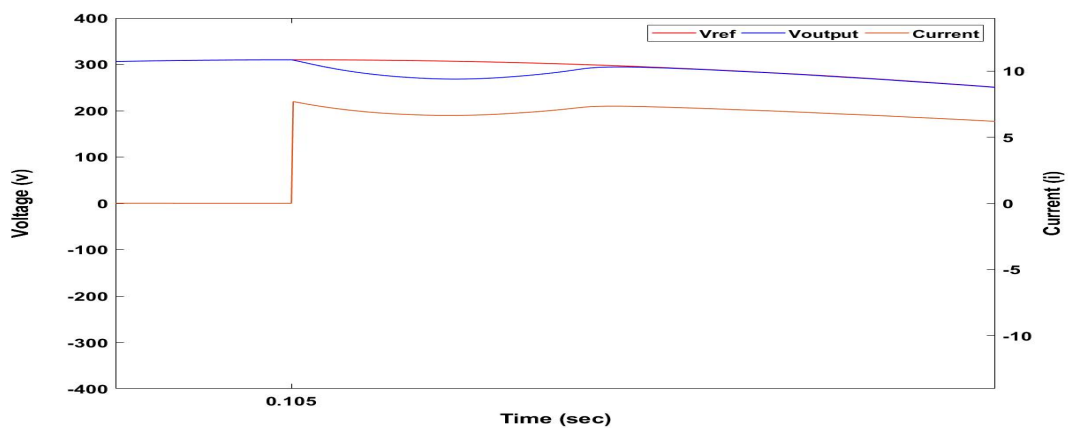
Figure 4.59: Output voltage and current behaviour of the proposed C-ERL-RSS SMC under filter disturbances 15mH inductor and -10% 48uF (43.2uF) of a capacitor along with input voltage disturbances (400V at (0-0.045secS), 450V at (0.045secs-0.105sec) and 500V at (0.105secs-0.15secs). With FL to NL and NL to FL conditions at 0.045secs and 0.105secs, respectively.



(a) Output voltage and current under input voltage disturbances and filter disturbances of -10% of 15mH (13.5mH) inductor and -10% of 48uF (43.2uF) of a capacitor.

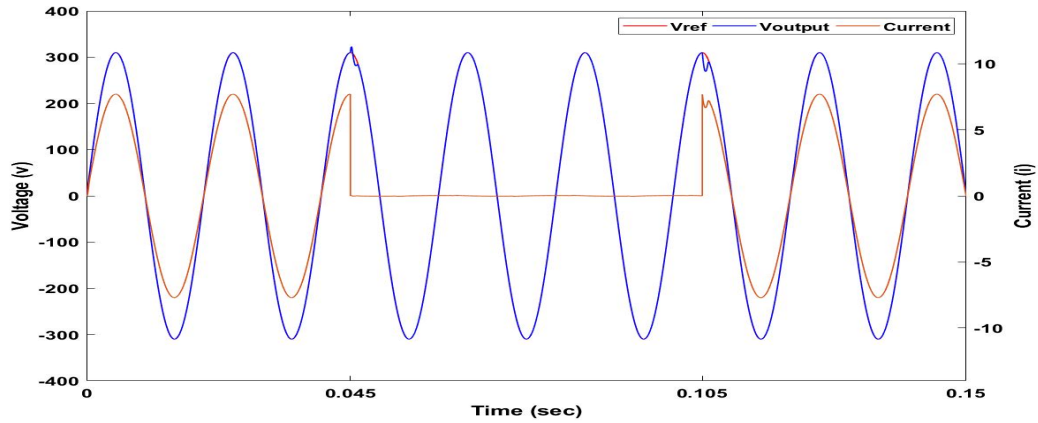


(b) Zoom: Transient response at 0.045 secs FL-NL condition (Transient response= 1.7 ms).

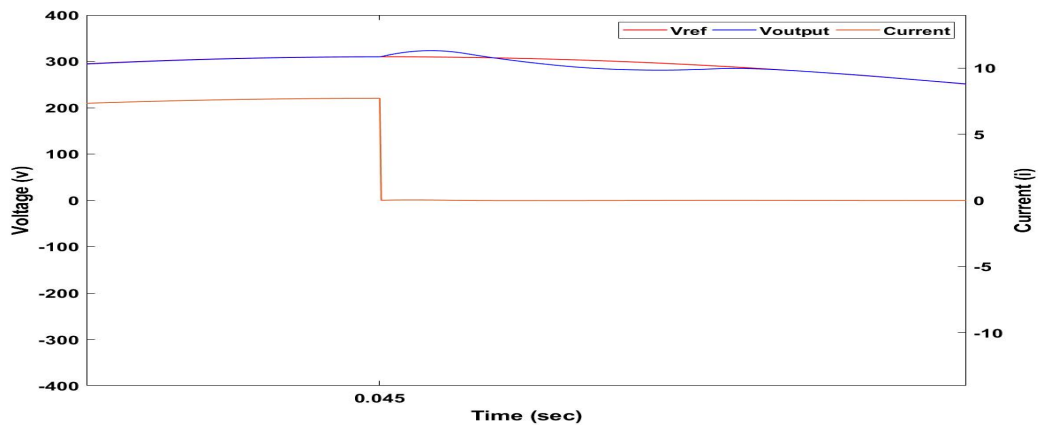


(c) Zoom: Transient response at 0.105 secs NL-FL condition (Transient response= 1 ms).

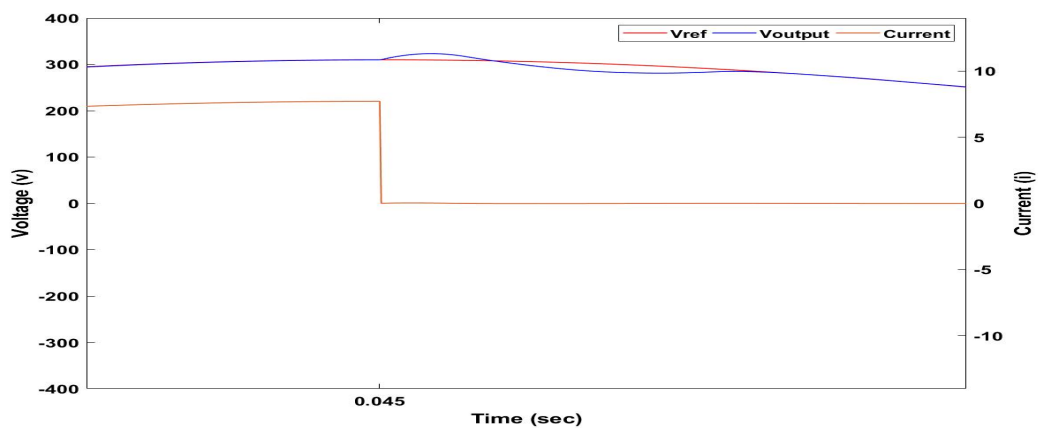
Figure 4.60: Output voltage and current behaviour of the proposed C-ERL-RSS SMC under filter disturbances -10% of 15mH inductor (13.5mH) and -10% 48uF (43.2uF) of a capacitor along with input voltage disturbances (400V at (0-0.045secS), 450V at (0.045secs-0.105sec) and 500V at (0.105secs-0.15secs). With FL to NL and NL to FL conditions at 0.045secs and 0.105secs, respectively.



(a) Output voltage and current under input voltage disturbances and filter disturbances of +10% of 15mH (16.5mH) inductor and +10% of 48uF (52.8uF) of a capacitor.



(b) Zoom: Transient response at 0.045 secs FL-NL condition (Transient response= 1.1 ms).



(c) Zoom: Transient response at 0.105 secs NL-FL condition (Transient response= 1.5 ms).

Figure 4.61: Output voltage and current behaviour of the proposed C-ERL-RSS SMC under filter disturbances +10% of 15mH (16.5mH) inductor and +10% 48uF (52.8uF) of a capacitor along with input voltage disturbances (400V at (0-0.045secS), 450V at (0.045secs-0.105sec) and 500V at (0.105secs-0.15secs). With FL to NL and NL to FL conditions at 0.045secs and 0.105secs, respectively.

of proposed C-ERL-RSS is validated through the comparative analysis of other sliding surface of state-of-the art SMC is also presented. In addition, the performance of the proposed C-ERL-RSS SMC is assessed under input voltage disturbances, load disturbances, and filter disturbances. To gauge the robustness of the proposed C-ERL-RSS SMC under extreme conditions, the proposed SMC is tested under all disturbances simultaneously. The achieved results are highly promising, affirming the robust nature of the proposed SMC for VSIs under extreme conditions.

CHAPTER 5

SUMMARY , CONCLUSION AND FUTURE PROSPECTS

This chapter provides a comprehensive overview of the research study that has been conducted throughout the thesis, followed by a detailed discussion on the conclusions that can be drawn from the research. The chapter also outlines the limitations and challenges that were encountered during the research process. In addition, the chapter provides insights into the future directions and potential research areas that can be explored based on the findings of this study. Overall, the objective of this chapter is to offer a clear and concise summary of the research work presented in the thesis, while highlighting its significance and potential impact on the field.

5.1 Summary

Over the last few years, the spotlight has been cast on VSIs and its extension to formation of AC MGs, owing to their ability to significantly enhance energy efficiency, bolster reliability, and ensure optimal power quality. These compact power networks can operate independently or in conjunction with the primary power grid, usually incorporating various DERs such as solar panels, wind turbines, and ESS, which collaborate to supply energy to local demands. Moreover, the importance of VSIs lies in their multifaceted capabilities, including continuous power supply during outages, delivery of sinusoidal AC voltage with low %THD, precise control over voltage and frequency, disturbance rejection, fast dynamic response, and fault ride through capability. Together, these features safeguard sensitive equipment and critical operations from the adverse effects of power interruptions, variations, and transient faults in the utility grid. To achieve these challenging tasks, various robust control approaches have been suggested to ensure stable and reliable operation of VSIs. Robust control is a branch of control theory that deals with systems subject to uncertainties or disturbances. In the context of VSIs, robust control aims to provide an effective and efficient control strategy that can handle uncertainties and disturbances to ensure stable operation and improve performance.

In the subsequent chapters, the thesis delves deeper into the topic of robust control and specifically discusses the use of SMC as an effective technique for controlling AC MGs. It explains the inherent characteristics of SMC, such as its excellent dynamic response, robust behavior, and insensitivity to parametric variations. However, implementing SMC for VSIs presents several challenges. Foremost among these is the chattering phenomenon, characterized by high-frequency oscillations in the control signal, which can stress power electronic switches and devices, leading to reduced system reliability. In

certain applications of VSIs, uncertainties in the system dynamics, variations in load conditions, and changes in the operating environment can impact the performance of SMC. Additionally, while SMC offers robustness and fast dynamic response, it may introduce high-frequency components in the control signal, thereby affecting the power quality of the output waveform. This introduction of high-frequency components can result in an increased percentage of %THD in the voltage waveform, impacting the performance of sensitive loads. Furthermore, achieving a balance between fast dynamic response and low overshoot during transient conditions is a challenge in SMC. Rapid changes in the load may lead to aggressive control actions, resulting in overshooting or undershooting of the desired voltage output. Last but not least, the implementation of SMC in VSIs can be complex, particularly in real-time applications. Designing and tuning the sliding surface, reaching law, and control gains requires a deep understanding of the system dynamics.

To address these challenges, the thesis proposes an improved SMC technique that comprises state-of-the-art C-ERL reaching law and optimal sliding surface RSS. This technique is designed to ensure improved convergence rate, enhanced robustness of the system with a reduced level of chattering, and low %THD. The C-ERL with RSS is tested on a second-order system to observe its behavior and achieve an optimal balance between robustness and chattering along the sliding surface. Comparative analysis with other state-of-the-art SMC techniques under the same conditions reveals that the proposed SMC exhibits exceptional improvements in transient response. There is a remarkable 1212% reduction in tracking time with only a 10% increase in chattering along the surface. Moreover, the proposed SMC is implemented on MATLAB Simulink and tested for single-phase and three-phase VSI under nonlinear load conditions. The results reveal that the proposed SMC has achieved an exceptionally low %THD of 0.25% with 99.9% voltage regulation and an extremely fast transient response of 1msec under extreme conditions for the single-phase VSI. Similarly, the performance of the proposed SMC for the three-phase VSI is also analyzed, indicating that it has successfully achieved a low %THD of 1.1% with high voltage regulation of 99.83%. Additionally, the proposed SMC exhibits extremely low tracking and transient times of 0.08sec and 0.05sec, respectively. In addition to this, a real-time performance analysis of the proposed SMC for VSI is conducted by implementing it on the HiL setup comprising Opal-RT 4200 and MicroLabBox dSPACE 1202. The analysis, carried out under extreme conditions of load variations, demonstrates a fast transient response with a low %THD of 0.4632 msec and 3.2%, respectively. The dissertation encompasses stability analysis, investigating the sliding surface of the proposed SMC when implemented on both single-phase and three-phase VSIs. The analysis indicates that the surface(s) maintains an equilibrium value of 0. Following extreme load variations, it takes approximately 1msec and 2msec for single-phase and three-phase VSIs, respectively, to reestablish the equilibrium position with a relatively smooth sliding surface.

Overall, the thesis underscores the significance of robust control techniques in AC MGs and introduces an innovative solution to tackle challenges associated with SMC. The proposed SMC incorporates a rotating sliding surface with an optimal reaching law approach, ensuring not only robustness and fast transient response but also minimal chattering across the surface. Consequently, the proposed SMC demonstrates rapid recovery

of the output voltage to the desired reference waveform under extreme load variations, achieving commendable voltage regulation in steady state and a low %THD of the output. This research is expected to contribute significantly to the field of power system's control, paving the way for the development of more efficient and reliable VSI systems in the future.

5.2 Conclusion

This doctoral dissertation introduces an enhanced SMC technique. It involves an optimal sliding surface RSS combined with an adaptive reaching law C-ERL. This approach is based on the state variable's distance from the sliding surface. It enables fast tracking while minimizing chattering, even at the equilibrium point. A RSS selection mechanism is applied to achieve optimal surface based on the input and output relationship using SIFLC and the system's error magnitude. The proposed composite reaching law integrates exponential, power, and difference functions to achieve optimal performance. Moreover, the proposed C-ERL is designed, implemented and tested for single-phase and three-phase VSIs under variable load conditions. The proposed SMC demonstrates remarkable effectiveness, achieving low THD percentages of 0.25%, 0.36%, and 0.73% under conditions of load disturbance, load with input voltage disturbances, and load with input voltage and filter disturbances, respectively. Similarly, voltage regulation is measured at 99.9%, 99.81%, and 99.83% under the same respective conditions. Moreover, a fast transient response is observed, with times of 1.1 ms, 1.1 ms, and 1.7 ms under load disturbance, load with input voltage disturbance, and load with input voltage and filter disturbances, respectively. The effectiveness of the proposed SMC is also verified through experimental results using HiL setup comprising Opal-RT 4200 and MicroLabBox dSPACE 1202, that demonstrated low %THD of 3.23% with improved dynamic response, resulting in a well-regulated output voltage of 99.8%. These findings demonstrate the potential of the proposed techniques to enhance the performance of VSIs under variable load conditions.

5.3 Future Prospects

The future prospects/trends of SMC for VSIs in the coming years look promising. SMC has already gained significant attention in the power system community due to its excellent dynamic response, robust behavior, and insensitivity to parametric variations. However, there is still a need for future research in this field to address some of the challenges associated with SMC for VSIs, such as chattering and inaccuracy in control loops. Therefore, following are the some future directions to be considered in the development of SMC for VSIs and AC MGs:

- i. In the context of grid feeding and grid supporting AC MGs, a major challenge lies in the susceptibility of the system to variable load conditions, potentially leading to reduced system reliability and performance. Given the inherent characteristics of SMC such as extreme robustness, guaranteed stability, and fast transient and dynamic response, it is widely regarded as an effective solution for addressing these challenges. Consequently, many scholarly contributions in the realm of grid feeding

and grid supporting MGs have already employed SMC to enhance MG reliability and sustainability. However, the proposed C-ERL-RSS SMC distinguishes itself with exceptional performance under extreme conditions, making it a favorable option for addressing challenges related to grid-feeding and grid-supporting VSIs. This technique ensures fast tracking and reduced chattering, even at the equilibrium point, with a minimized %THD for grid feeding current. A RSS mechanism has been incorporated to achieve an optimal surface based on the system's error magnitude. The proposed composite reaching law integrates exponential, power, and difference functions, resulting in improved dynamic response with reduced %THD. These findings underscore the potential of the proposed SMC technique with minor modifications in its mathematical model to enhance the performance and reliability of grid feeding and grid supporting AC MGs under variable load conditions, making it an attractive option for future research and development in this field.

- ii. One promising prospect for forthcoming research entails the integration of the proposed reaching law with other advanced control techniques, AI. This integration could potentially result in even more efficient and intelligent control of AC MG systems. For instance, the incorporation of AI could enable the system to learn and adapt to changing operating conditions in real-time. Therefore, the integration of the proposed reaching law with these advanced techniques could offer new possibilities for enhancing the performance, stability, and reliability of AC MG systems.
- iii. While, proposed SMC provides efficient control strategy for AC MG systems, it may face challenges in terms of operational and computational constraints. One potential solution is to integrate machine learning techniques, such as Artificial Neural Networks (ANNs), into the control system. This approach involves training the ANN on the existing SMC design and then replacing it with the proposed SMC. By doing so, the control system can learn from past experiences and adjust to new situations, resulting in improved performance, adaptability, and reliability. This could be an exciting future trend for AC microgrid control, offering a more intelligent and sophisticated approach to system control.

REFERENCES

- [1] B. Brahmi, M. H. Laraki, A. Brahmi, M. Saad, M. H. Rahman, Improvement of sliding mode controller by using a new adaptive reaching law: Theory and experiment, *ISA transactions* 97 (2020) 261–268.
- [2] G. Rohith, Fractional power rate reaching law for augmented sliding mode performance, *Journal of the Franklin Institute* 358 (1) (2021) 856–876.
- [3] F. Haroon, M. Aamir, A. Waqar, Second-order rotating sliding mode control with composite reaching law for two level single phase voltage source inverters, *IEEE Access* 10 (2022) 60177–60188.
- [4] H. Komurcugil, Rotating-sliding-line-based sliding-mode control for single-phase ups inverters, *IEEE Transactions on Industrial Electronics* 59 (10) (2011) 3719–3726.
- [5] D. Jain, D. Saxena, Comprehensive review on control schemes and stability investigation of hybrid ac-dc microgrid, *Electric Power Systems Research* 218 (2023) 109182.
- [6] J. Rocabert, A. Luna, F. Blaabjerg, P. Rodriguez, Control of power converters in ac microgrids, *IEEE transactions on power electronics* 27 (11) (2012) 4734–4749.
- [7] H. Komurcugil, S. Biricik, S. Bayhan, Z. Zhang, Sliding mode control: Overview of its applications in power converters, *IEEE Industrial Electronics Magazine* 15 (1) (2020) 40–49.
- [8] G. Bartolini, A. Ferrara, E. Usai, Chattering avoidance by second-order sliding mode control, *IEEE Transactions on automatic control* 43 (2) (1998) 241–246.
- [9] A. Levant, Principles of 2-sliding mode design, *automatica* 43 (4) (2007) 576–586.
- [10] Q. Qin, G. Gao, J. Zhong, Finite-time adaptive extended state observer-based dynamic sliding mode control for hybrid robots, *IEEE Transactions on Circuits and Systems II: Express Briefs* 69 (9) (2022) 3784–3788.
- [11] J. Singh, S. Prakash Singh, K. Shanker Verma, A. Iqbal, B. Kumar, Recent control techniques and management of ac microgrids: A critical review on issues, strategies, and future trends, *International Transactions on Electrical Energy Systems* 31 (11) (2021) e13035.

- [12] D. KB, S. Thomas, Power rate exponential reaching law for enhanced performance of sliding mode control, *International Journal of Control, Automation and Systems* 15 (2017) 2636–2645.
- [13] L. Zheng, F. Jiang, J. Song, Y. Gao, M. Tian, A discrete-time repetitive sliding mode control for voltage source inverters, *IEEE Journal of emerging and selected topics in power electronics* 6 (3) (2017) 1553–1566.
- [14] S. M. Mozayan, M. Saad, H. Vahedi, H. Fortin-Blanchette, M. Soltani, Sliding mode control of pmsg wind turbine based on enhanced exponential reaching law, *IEEE Transactions on Industrial Electronics* 63 (10) (2016) 6148–6159.
- [15] F. Haroon, M. Aamir, A. Waqar, S. Mian Qaisar, S. U. Ali, A. T. Almaktoom, A composite exponential reaching law based smc with rotating sliding surface selection mechanism for two level three phase vsi in vehicle to load applications, *Energies* 16 (1) (2022) 346.
- [16] W. E. Forum, Electricity generation from renewables is set to increase in 2023, *World Economic Forum* Accessed: 2024-06-05 (2023).
URL <https://www.weforum.org/agenda/2023/03/electricity-generation>
- [17] World Bank, A Renewable Energy Future for Pakistan’s Power System, accessed: 2024-06-05 (2020).
URL <https://www.worldbank.org/en/news/feature/2020/11/09/a-renewa>
- [18] United Nations, Sustainable Development Goals, accessed: 2024-06-05 (2024).
URL <https://sdgs.un.org/goals>
- [19] D. E. Olivares, A. Mehrizi-Sani, A. H. Etemadi, C. A. Cañizares, R. Iravani, M. Kazerani, A. H. Hajimiragha, O. Gomis-Bellmunt, M. Saeedifard, R. Palma-Behnke, et al., Trends in microgrid control, *IEEE Transactions on smart grid* 5 (4) (2014) 1905–1919.
- [20] Z. Shuai, Y. Sun, Z. J. Shen, W. Tian, C. Tu, Y. Li, X. Yin, Microgrid stability: Classification and a review, *Renewable and Sustainable Energy Reviews* 58 (2016) 167–179.
- [21] I. Colak, E. Kabalci, R. Bayindir, Review of multilevel voltage source inverter topologies and control schemes, *Energy conversion and management* 52 (2) (2011) 1114–1128.
- [22] S. Emel’yanov, Theory of variable-structure control systems: Inception and initial development, *Computational Mathematics and Modeling* 18 (4) (2007) 321–331.
- [23] A. I. M. Ali, M. A. Sayed, T. Takeshita, Isolated single-phase single-stage dc-ac cascaded transformer-based multilevel inverter for stand-alone and grid-tied applications, *International Journal of Electrical Power & Energy Systems* 125 (2021) 106534.

- [24] Y. Wu, Y. Ye, Internal model-based disturbance observer with application to cvcf pwm inverter, *IEEE Transactions on Industrial Electronics* 65 (7) (2017) 5743–5753.
- [25] S. Emel'Yanov, S. Korovin, A. Levant, High-order sliding modes in control systems, *Computational mathematics and modeling* 7 (3) (1996) 294–318.
- [26] V. Utkin, Variable structure systems with sliding modes, *IEEE Transactions on Automatic control* 22 (2) (1977) 212–222.
- [27] B. Draženović, The invariance conditions in variable structure systems, *Automatica* 5 (3) (1969) 287–295.
- [28] J. Y. Hung, W. Gao, J. C. Hung, Variable structure control: A survey, *IEEE transactions on industrial electronics* 40 (1) (1993) 2–22.
- [29] F.-J. Lin, Y.-C. Hung, M.-T. Tsai, Fault-tolerant control for six-phase pmsm drive system via intelligent complementary sliding-mode control using tskfnn-amf, *IEEE Transactions on industrial electronics* 60 (12) (2013) 5747–5762.
- [30] S. Jahan, S. P. Biswas, S. Haq, M. R. Islam, M. P. Mahmud, A. Z. Kouzani, An advanced control scheme for voltage source inverter based grid-tied pv systems, *IEEE Transactions on Applied Superconductivity* 31 (8) (2021) 1–5.
- [31] A. Kalair, N. Abas, A. R. Kalair, Z. Saleem, N. Khan, Review of harmonic analysis, modeling and mitigation techniques, *Renewable and Sustainable Energy Reviews* 78 (2017) 1152–1187.
- [32] Ieee standard for harmonic control in electric power systems, *IEEE Std 519-2022 (Revision of IEEE Std 519-2014)* (2022) 1–31doi:10.1109/IEEESTD.2022.9848440.
- [33] F. Katiraei, R. Iravani, N. Hatziaargyriou, A. Dimeas, Microgrids management, *IEEE power and energy magazine* 6 (3) (2008) 54–65.
- [34] F. Katiraei, M. R. Iravani, Power management strategies for a microgrid with multiple distributed generation units, *IEEE transactions on power systems* 21 (4) (2006) 1821–1831.
- [35] C. Jauch, J. Matevosyan, T. Ackermann, S. Bolik, International comparison of requirements for connection of wind turbines to power systems, *Wind energy* 8 (3) (2005) 295–306.
- [36] D. G. Photovoltaics, E. Storage, Ieee guide for design, operation, and integration of distributed resource island systems with electric power systems (2011).
- [37] T. Basso, R. DeBlasio, Ieee smart grid series of standards ieee 2030 (interoperability) and ieee 1547 (interconnection) status, Tech. rep., National Renewable Energy Lab.(NREL), Golden, CO (United States) (2012).

- [38] S. Hazra, A. De, L. Cheng, J. Palmour, M. Schupbach, B. A. Hull, S. Allen, S. Bhattacharya, High switching performance of 1700-v, 50-a sic power mosfet over si igbt/bimosfet for advanced power conversion applications, *IEEE Transactions on Power Electronics* 31 (7) (2016) 4742–4754. doi:10.1109/TPEL.2015.2432012.
- [39] H. A. Sher, A. A. Rizvi, K. E. Addoweesh, K. Al-Haddad, A single-stage stand-alone photovoltaic energy system with high tracking efficiency, *IEEE Transactions on Sustainable Energy* 8 (2) (2017) 755–762. doi:10.1109/TSTE.2016.2616443.
- [40] S. Wang, P. Dehghanian, M. Alhazmi, J. Su, B. Shinde, Resilience-assured protective control of dc/ac inverters under unbalanced and fault scenarios, in: 2019 IEEE Power & Energy Society Innovative Smart Grid Technologies Conference (ISGT), IEEE, 2019, pp. 1–5.
- [41] H. Antunes, S. Silva, R. Ferreira, D. I. Brandao, et al., A new configuration for a grid forming converter in ac islanded microgrid, in: PCIM Europe 2017; International Exhibition and Conference for Power Electronics, Intelligent Motion, Renewable Energy and Energy Management, VDE, 2017, pp. 1–8.
- [42] N. R. Babu, *Smart Grid Systems: Modeling and Control*, CRC Press, 2018.
- [43] A. Yazdani, R. Iravani, *Voltage-sourced converters in power systems: modeling, control, and applications*, John Wiley & Sons, 2010.
- [44] I. D. de Souza, P. M. de Almeida, P. G. Barbosa, C. A. Duque, P. F. Ribeiro, Digital single voltage loop control of a vsi with lc output filter, *Sustainable Energy, Grids and Networks* 16 (2018) 145–155.
- [45] G. Shahgholian, J. Faiz, M. Jabbari, Voltage control techniques in uninterruptible power supply inverters: A review, *International Review of Electrical Engineering* 6 (4) (2011) 1531–1542.
- [46] H. Han, X. Hou, J. Yang, J. Wu, M. Su, J. M. Guerrero, Review of power sharing control strategies for islanding operation of ac microgrids, *IEEE Transactions on Smart Grid* 7 (1) (2016) 200–215. doi:10.1109/TSG.2015.2434849.
- [47] T. Vandoorn, J. De Kooning, B. Meersman, L. Vandeveldde, Review of primary control strategies for islanded microgrids with power-electronic interfaces, *Renewable and Sustainable Energy Reviews* 19 (2013) 613–628.
- [48] A. Bidram, A. Davoudi, Hierarchical structure of microgrids control system, *IEEE Transactions on Smart Grid* 3 (4) (2012) 1963–1976.
- [49] M. A. Hossain, H. R. Pota, Voltage tracking of a single-phase inverter in an islanded microgrid, *International Journal of Renewable Energy Research* 5 (3) (2015) 806–814.
- [50] N. Mohan, T. M. Undeland, W. P. Robbins, *Power electronics: converters, applications, and design*, John wiley & sons, 2003.

- [51] T. C. Green, M. Prodanović, Control of inverter-based micro-grids, *Electric power systems research* 77 (9) (2007) 1204–1213.
- [52] J. Kim, J. Lee, K. Nam, Inverter-based local ac bus voltage control utilizing two dof control, *IEEE transactions on power electronics* 23 (3) (2008) 1288–1298.
- [53] R. Rosso, X. Wang, M. Liserre, X. Lu, S. Engelken, Grid-forming converters: Control approaches, grid-synchronization, and future trends—a review, *IEEE Open Journal of Industry Applications* 2 (2021) 93–109.
- [54] A. Engler, Control of inverters in isolated and in grid tied operation with regard to expandability, in: *Tutorial: Power Electronics for Regenerative Energy at IEEE Power Electronics Specialists Conference (PESC'04) Conference*, Aachen, 2004.
- [55] K. De Brabandere, B. Bolsens, J. Van den Keybus, A. Woyte, J. Driesen, R. Belmans, A voltage and frequency droop control method for parallel inverters, *IEEE Transactions on power electronics* 22 (4) (2007) 1107–1115.
- [56] J. T. Bialasiewicz, Renewable energy systems with photovoltaic power generators: Operation and modeling, *IEEE Transactions on industrial Electronics* 55 (7) (2008) 2752–2758.
- [57] H. H. Zeineldin, A $q-f$ droop curve for facilitating islanding detection of inverter-based distributed generation, *IEEE transactions on power electronics* 24 (3) (2009) 665–673.
- [58] H. Zeineldin, E. El-Saadany, M. Salama, Distributed generation micro-grid operation: Control and protection, in: *2006 Power Systems Conference: Advanced Metering, Protection, Control, Communication, and Distributed Resources*, IEEE, 2006, pp. 105–111.
- [59] T. Bialasiewicz, Renewable energy systems with photovoltaic power generators: Operation and modeling, *IEEE transactions on industrial electronics*, vol. 55, no. 7, pp. 2752-2758 (2008).
- [60] H. H. Zeineldin, A $q-f$ droop curve for facilitating islanding detection of inverter-based distributed generation, *IEEE transactions on power electronics* 24 (3) (2009) 665–673.
- [61] X. Wang, Y. W. Li, F. Blaabjerg, P. C. Loh, Virtual-impedance-based control for voltage-source and current-source converters, *IEEE Transactions on Power Electronics* 30 (12) (2014) 7019–7037.
- [62] N. R. Ullah, T. Thiringer, D. Karlsson, Voltage and transient stability support by wind farms complying with the e. on netz grid code, *IEEE Transactions on Power Systems* 22 (4) (2007) 1647–1656.

- [63] J. Driesen, K. Visscher, Virtual synchronous generators, in: 2008 IEEE power and energy society general meeting-conversion and delivery of electrical energy in the 21st century, IEEE, 2008, pp. 1–3.
- [64] P. S. Kundur, O. P. Malik, Power system stability and control, McGraw-Hill Education, 2022.
- [65] T. Q. Fonseca, R. L. Ribeiro, T. d. O. A. Rocha, F. B. Costa, J. M. Guerrero, Voltage grid supporting by using variable structure adaptive virtual impedance for lcl-voltage source converter dg converters, *IEEE Transactions on Industrial Electronics* 67 (11) (2019) 9326–9336.
- [66] F. Mohammadi, B. Mohammadi-Ivatloo, G. B. Gharehpetian, M. H. Ali, W. Wei, O. Erdiñ, M. Shirkhani, Robust control strategies for microgrids: A review, *IEEE Systems Journal* 16 (2) (2022) 2401–2412. doi:10.1109/JSYST.2021.3077213.
- [67] D. Datta, S. R. Fahim, S. K. Sarker, S. Muyeen, M. R. Islam Sheikh, S. K. Das, A robust control method for damping and tracking of secondary network voltage of a pv based hybrid ac/dc microgrid, *Frontiers in Energy Research* 7 (2020) 580840.
- [68] A. H. Etemadi, E. J. Davison, R. Iravani, A generalized decentralized robust control of islanded microgrids, *IEEE transactions on Power Systems* 29 (6) (2014) 3102–3113.
- [69] K. Zhou, J. C. Doyle, Essentials of robust control, Vol. 104, Prentice hall Upper Saddle River, NJ, 1998.
- [70] D. Xu, G. Wang, L. Qu, C. Ge, Robust control with uncertain disturbances for vehicle drift motions, *Applied Sciences* 11 (11) (2021) 4917.
- [71] A. Pal, J. S. Thorp, S. S. Veda, V. Centeno, Applying a robust control technique to damp low frequency oscillations in the wecc, *International Journal of Electrical Power & Energy Systems* 44 (1) (2013) 638–645.
- [72] G. E. Valderrama, A. M. Stankovic, P. Mattavelli, Dissipativity-based adaptive and robust control of ups in unbalanced operation, *IEEE Transactions on Power Electronics* 18 (4) (2003) 1056–1062.
- [73] M. S. Mahmoud, N. M. Alyazidi, M. I. Abouheaf, Adaptive intelligent techniques for microgrid control systems: A survey, *International Journal of Electrical Power & Energy Systems* 90 (2017) 292–305.
- [74] S. Tahir, J. Wang, M. H. Baloch, G. S. Kaloi, Digital control techniques based on voltage source inverters in renewable energy applications: A review, *Electronics* 7 (2) (2018) 18.
- [75] C. Scherer, P. Gahinet, M. Chilali, Multiobjective output-feedback control via lmi optimization, *IEEE Transactions on automatic control* 42 (7) (1997) 896–911.

- [76] E. Lavretsky, K. A. Wise, Robust adaptive control, in: Robust and adaptive control: With aerospace applications, Springer, 2012, pp. 317–353.
- [77] M. Aquib, A. Vijay, S. Doolla, M. C. Chandorkar, Model reference adaptive system based apparent power sharing in inverter based microgrids, *IEEE Transactions on Energy Conversion* 37 (3) (2022) 1987–1997.
- [78] G. P. Incremona, M. Cucuzzella, A. Ferrara, Adaptive suboptimal second-order sliding mode control for microgrids, *International Journal of Control* 89 (9) (2016) 1849–1867.
- [79] M. Dehghani, T. Niknam, M. Ghiasi, H. R. Baghaee, F. Blaabjerg, T. Dragicević, M. Rashidi, Adaptive backstepping control for master-slave ac microgrid in smart island, *Energy* 246 (2022) 123282.
- [80] T. Söderström, P. Stoica, System identification, Prentice-Hall International, 1989.
- [81] S. Yang, Q. Lei, F. Z. Peng, Z. Qian, A robust control scheme for grid-connected voltage-source inverters, *IEEE transactions on Industrial Electronics* 58 (1) (2010) 202–212.
- [82] K. Torabi-Farsani, M. H. Asemani, F. Badfar, N. Vafamand, M. H. Khooban, Robust mixed μ synthesis frequency regulation in ac mobile power grids, *IEEE Transactions on Transportation Electrification* 5 (4) (2019) 1182–1189.
- [83] H. Bevrani, M. R. Feizi, S. Ataei, Robust frequency control in an islanded microgrid: H_∞ and H_2 -synthesis approaches, *IEEE transactions on smart grid* 7 (2) (2015) 706–717.
- [84] S. Mehta, P. Basak, A comprehensive review on control techniques for stability improvement in microgrids, *International Transactions on Electrical Energy Systems* 31 (4) (2021) e12822.
- [85] F. Mohammadi, B. Mohammadi-Ivatloo, G. B. Gharehpetian, M. H. Ali, W. Wei, O. Erdinç, M. Shirkhani, Robust control strategies for microgrids: A review, *IEEE Systems Journal* (2021).
- [86] M. Chilali, P. Gahinet, P. Apkarian, Robust pole placement in lmi regions, *IEEE transactions on Automatic Control* 44 (12) (1999) 2257–2270.
- [87] J. C. Doyle, B. A. Francis, A. R. Tannenbaum, Feedback control theory, Courier Corporation, 2013.
- [88] M. Armin, M. Rahman, M. M. Rahman, S. K. Sarker, S. K. Das, M. R. Islam, A. Z. Kouzani, M. P. Mahmud, Robust extended h control strategy using linear matrix inequality approach for islanded microgrid, *IEEE access* 8 (2020) 135883–135896.
- [89] M. K. Kumar, T. K. Dash, Hankel norm performance of 2-d digital filters described by roesser model with overflow arithmetic, *Australian Journal of Electrical and Electronics Engineering* (2023) 1–7.

- [90] R. P. Borase, D. Maghade, S. Sondkar, S. Pawar, A review of pid control, tuning methods and applications, *International Journal of Dynamics and Control* 9 (2021) 818–827.
- [91] X. Chen, W. Dong, Q. Yang, Robust optimal capacity planning of grid-connected microgrid considering energy management under multi-dimensional uncertainties, *Applied Energy* 323 (2022) 119642.
- [92] C. Cheng, S. Liu, H. Wu, Sliding mode observer-based fractional-order proportional–integral–derivative sliding mode control for electro-hydraulic servo systems, *Proceedings of the Institution of Mechanical Engineers, Part C: Journal of Mechanical Engineering Science* 234 (10) (2020) 1887–1898.
- [93] F. Fan, R. Zhang, Y. Xu, S. Ren, Robustly coordinated operation of an emission-free microgrid with hybrid hydrogen-battery energy storage, *CSEE Journal of Power and Energy Systems* 8 (2) (2021) 369–379.
- [94] Y. Khayat, Q. Shafiee, R. Heydari, M. Naderi, T. Dragičević, J. W. Simpson-Porco, F. Dörfler, M. Fathi, F. Blaabjerg, J. M. Guerrero, et al., On the secondary control architectures of ac microgrids: An overview, *IEEE Transactions on Power Electronics* 35 (6) (2019) 6482–6500.
- [95] A. A. El-Fergany, Parameters identification of pv model using improved slime mould optimizer and lambert w-function, *Energy Reports* 7 (2021) 875–887.
- [96] M. H. Andishgar, E. Gholipour, R.-a. Hooshmand, An overview of control approaches of inverter-based microgrids in islanding mode of operation, *Renewable and Sustainable Energy Reviews* 80 (2017) 1043–1060.
- [97] J. Xu, W. Liu, Z. Song, Terahertz dynamic beam steering based on graphene coding metasurfaces, *IEEE Photonics Journal* 13 (4) (2021) 1–9. doi:10.1109/JPHOT.2021.3098728.
- [98] V. Sebestyén, Renewable and sustainable energy reviews: Environmental impact networks of renewable energy power plants, *Renewable and Sustainable Energy Reviews* 151 (2021) 111626.
- [99] Q. Shao-ming, L. Liang-cheng, D. Xiu-li, Z. Bin, Whale optimization algorithm based on nonlinear weights and single point crossover, in: *2020 International Conference on Computer Engineering and Intelligent Control (ICCEIC)*, 2020, pp. 179–184. doi:10.1109/ICCEIC51584.2020.00042.
- [100] S. Wu, L. Guo, H. Wang, Z. Wang, Z. Song, T. Shi, Analytical calculation for magnetic field in spoke-type permanent magnet machines based on a rotor magnetic potential model, *IEEE Transactions on Magnetics* 58 (2) (2022) 1–5. doi:10.1109/TMAG.2021.3077917.

- [101] M. Huba, D. Vrancic, Tuning of pid control for the double integrator plus dead time model by modified real dominant pole and performance portrait methods, *Mathematics* 10 (6) (2022) 971.
- [102] F. Mohammadi, B. Mohammadi-Ivatloo, G. B. Gharehpetian, M. H. Ali, W. Wei, O. Erdinç, M. Shirkhani, Robust control strategies for microgrids: A review, *IEEE Systems Journal* 16 (2) (2022) 2401–2412. doi:10.1109/JSYST.2021.3077213.
- [103] M. S. Mahmoud, N. M. Alyazidi, M. I. Abouheaf, Adaptive intelligent techniques for microgrid control systems: A survey, *International Journal of Electrical Power & Energy Systems* 90 (2017) 292–305.
- [104] S. Choudhury, A comprehensive review on issues, investigations, control and protection trends, technical challenges and future directions for microgrid technology, *International Transactions on Electrical Energy Systems* 30 (9) (2020) e12446.
- [105] F. Blaabjerg, R. Teodorescu, M. Liserre, A. V. Timbus, Overview of control and grid synchronization for distributed power generation systems, *IEEE Transactions on industrial electronics* 53 (5) (2006) 1398–1409.
- [106] M. C. Chandorkar, D. M. Divan, R. Adapa, Control of parallel connected inverters in standalone ac supply systems, *IEEE transactions on industry applications* 29 (1) (1993) 136–143.
- [107] P. Rodriguez, A. Timbus, R. Teodorescu, M. Liserre, F. Blaabjerg, Reactive power control for improving wind turbine system behavior under grid faults, *IEEE Transactions on Power Electronics* 24 (7) (2009) 1798–1801.
- [108] E. Clarke, *Circuit analysis of AC power systems: symmetrical and related components*, Vol. 1, Wiley, 1943.
- [109] N. M. Dehkordi, V. Nekoukar, Robust distributed stochastic secondary control of microgrids with system and communication noises, *IET Generation, Transmission & Distribution* 14 (6) (2020) 1148–1158.
- [110] M. Zhang, Y. Li, F. Liu, W.-J. Lee, Y. Peng, Y. Liu, W. Li, Y. Cao, A robust distributed secondary voltage control method for islanded microgrids, *International Journal of Electrical Power & Energy Systems* 121 (2020) 105938.
- [111] B. Yang, T. Zhu, X. Zhang, J. Wang, H. Shu, S. Li, T. He, L. Yang, T. Yu, Design and implementation of battery/smes hybrid energy storage systems used in electric vehicles: A nonlinear robust fractional-order control approach, *Energy* 191 (2020) 116510.
- [112] S. Tabatabaee, H. R. Karshenas, A. Bakhshai, P. Jain, Investigation of droop characteristics and x/r ratio on small-signal stability of autonomous microgrid, in: *2011 2nd Power Electronics, Drive Systems and Technologies Conference*, IEEE, 2011, pp. 223–228.

- [113] W. Yao, M. Chen, J. Matas, J. M. Guerrero, Z.-M. Qian, Design and analysis of the droop control method for parallel inverters considering the impact of the complex impedance on the power sharing, *IEEE Transactions on Industrial Electronics* 58 (2) (2010) 576–588.
- [114] M.-T. Ho, C.-Y. Lin, Pid controller design for robust performance, *IEEE Transactions on Automatic Control* 48 (8) (2003) 1404–1409.
- [115] S. K. Sarkar, F. R. Badal, S. K. Das, A comparative study of high performance robust pid controller for grid voltage control of islanded microgrid, *International Journal of Dynamics and Control* 6 (2018) 1207–1217.
- [116] S. Hafsi, K. Laabidi, R. Farkh, A new tuning method for stabilization time delay systems using $pi\lambda d\mu$ controllers, *Asian journal of control* 17 (3) (2015) 821–831.
- [117] M. Armin, P. N. Roy, S. K. Sarkar, S. K. Das, Lmi-based robust pid controller design for voltage control of islanded microgrid, *Asian Journal of Control* 20 (5) (2018) 2014–2025.
- [118] D. M. Vilathgamuwa, P. C. Loh, Y. Li, Protection of microgrids during utility voltage sags, *IEEE Transactions on Industrial Electronics* 53 (5) (2006) 1427–1436.
- [119] A. Bidram, A. Davoudi, Hierarchical structure of microgrids control system, *IEEE Transactions on Smart Grid* 3 (4) (2012) 1963–1976.
- [120] D. Gaonkar, G. N. Pillai, R. Patel, Seamless transfer of microturbine generation system operation between grid-connected and islanding modes, *Electric Power Components and Systems* 37 (2) (2009) 174–188.
- [121] Y. A.-R. I. Mohamed, H. H. Zeineldin, M. Salama, R. Seethapathy, Seamless formation and robust control of distributed generation microgrids via direct voltage control and optimized dynamic power sharing, *IEEE Transactions on Power Electronics* 27 (3) (2011) 1283–1294.
- [122] F. Wang, J. L. Duarte, M. A. Hendrix, Grid-interfacing converter systems with enhanced voltage quality for microgrid application—concept and implementation, *IEEE Transactions on power electronics* 26 (12) (2011) 3501–3513.
- [123] F. Mohammadi, G.-A. Nazri, M. Saif, An improved droop-based control strategy for mt-hvdc systems, *Electronics* 9 (1) (2020) 87.
- [124] N. M. Dehkordi, N. Sadati, M. Hamzeh, Robust tuning of transient droop gains based on kharitonov’s stability theorem in droop-controlled microgrids, *IET Generation, Transmission & Distribution* 12 (14) (2018) 3495–3501.
- [125] J. Hu, A. Lanzon, Distributed finite-time consensus control for heterogeneous battery energy storage systems in droop-controlled microgrids, *IEEE Transactions on smart grid* 10 (5) (2018) 4751–4761.

- [126] S. Gambhire, D. R. Kishore, P. Londhe, S. Pawar, Review of sliding mode based control techniques for control system applications, *International Journal of dynamics and control* 9 (2021) 363–378.
- [127] A. Hanan, A. Levant, A. Jbara, Low-chattering discretization of sliding mode control, in: *2021 60th IEEE Conference on Decision and Control (CDC)*, IEEE, 2021, pp. 6403–6408.
- [128] S. Laghrouche, M. Harmouche, Y. Chitour, H. Obeid, L. M. Fridman, Barrier function-based adaptive higher order sliding mode controllers, *Automatica* 123 (2021) 109355.
- [129] Y. Feng, X. Yu, Z. Man, Non-singular terminal sliding mode control of rigid manipulators, *Automatica* 38 (12) (2002) 2159–2167.
- [130] C. Liu, Z. Zou, J. Yin, Trajectory tracking of underactuated surface vessels based on neural network and hierarchical sliding mode, *Journal of Marine Science and Technology* 20 (2015) 322–330.
- [131] N. B. Almutairi, M. Zribi, On the sliding mode control of a ball on a beam system, *Nonlinear dynamics* 59 (2010) 221–238.
- [132] R. Xu, Ü. Özgüner, Sliding mode control of a class of underactuated systems, *Automatica* 44 (1) (2008) 233–241.
- [133] D. G. Photovoltaics, E. Storage, *Ieee application guide for ieee std 1547™, ieee standard for interconnecting distributed resources with electric power systems*, IEEE std (2009) 1547–2.
- [134] R. M. Dell, D. A. J. Rand, Energy storage—a key technology for global energy sustainability, *Journal of power sources* 100 (1-2) (2001) 2–17.
- [135] H. J. Laaksonen, Protection principles for future microgrids, *IEEE Transactions on power electronics* 25 (12) (2010) 2910–2918.
- [136] J. Rocabert, G. M. Azevedo, A. Luna, J. M. Guerrero, J. I. Candela, P. Rodríguez, Intelligent connection agent for three-phase grid-connected microgrids, *IEEE Transactions on power electronics* 26 (10) (2011) 2993–3005.
- [137] C. Cho, J.-H. Jeon, J.-Y. Kim, S. Kwon, K. Park, S. Kim, Active synchronizing control of a microgrid, *IEEE Transactions on Power Electronics* 26 (12) (2011) 3707–3719.
- [138] S. Zhao, C. Hao, Z. Jian, M. Li, Energy-efficient phase-aware load balancing on asymmetric multicore processors, in: *2018 IEEE 4th International Conference on Computer and Communications (ICCC)*, 2018, pp. 2575–2579. doi:10.1109/CompComm.2018.8780697.

- [139] M. M. Zaid, J.-S. Ro, Switch ladder modified h-bridge multilevel inverter with novel pulse width modulation technique, *IEEE Access* 7 (2019) 102073–102086. doi:10.1109/ACCESS.2019.2930720.
- [140] J. Hu, Y. Shan, J. M. Guerrero, A. Ioinovici, K. W. Chan, J. Rodriguez, Model predictive control of microgrids—an overview, *Renewable and Sustainable Energy Reviews* 136 (2021) 110422.
- [141] H. Jiayi, J. Chuanwen, X. Rong, A review on distributed energy resources and microgrid, *Renewable and Sustainable Energy Reviews* 12 (9) (2008) 2472–2483.
- [142] L. Djilali, E. N. Sanchez, F. Ornelas-Tellez, M. Belkheiri, Neural network based controller for an ac microgrid connected to a utility grid, in: *2018 IEEE Latin American Conference on Computational Intelligence (LA-CCI)*, 2018, pp. 1–6. doi:10.1109/LA-CCI.2018.8625249.
- [143] J. Chen, F. Gao, J. Yu, D. Liao, S. Wei, D. Ma, Improving dynamic consensus algorithm of ac microgrid with fuzzy logic control, in: *2021 IEEE Sustainable Power and Energy Conference (iSPEC)*, 2021, pp. 2714–2719. doi:10.1109/iSPEC53008.2021.9736025.
- [144] H. Komurcugil, S. Biricik, Time-varying and constant switching frequency-based sliding-mode control methods for transformerless dvr employing half-bridge vsi, *IEEE Transactions on Industrial Electronics* 64 (4) (2016) 2570–2579.
- [145] M. S. Rifaq, S. A. Q. Mohammed, H. H. Choi, J.-W. Jung, An improved sliding mode control technique to mitigate mismatched parameter uncertainties of three-phase voltage source inverters, *IEEE Access* 8 (2020) 81932–81942.
- [146] V. Repecho, D. Biel, J. M. Olm, A simple switching-frequency-regulated sliding-mode controller for a vsi with a full digital implementation, *IEEE Journal of Emerging and Selected Topics in Power Electronics* 9 (1) (2020) 569–579.
- [147] N. Altin, S. Ozdemir, H. Komurcugil, I. Sefa, Sliding-mode control in natural frame with reduced number of sensors for three-phase grid-tied lcl-interfaced inverters, *IEEE Transactions on Industrial Electronics* 66 (4) (2018) 2903–2913.
- [148] A. Bartoszewicz, Discrete-time quasi-sliding-mode control strategies, *IEEE Transactions on Industrial Electronics* 45 (4) (1998) 633–637.
- [149] S. V. Drakunov, V. I. Utkin, Sliding mode control in dynamic systems, *International Journal of Control* 55 (4) (1992) 1029–1037.
- [150] K. Furuta, Sliding mode control of a discrete system, *Systems & Control Letters* 14 (2) (1990) 145–152.
- [151] C. Edwards, S. Spurgeon, *Sliding mode control: theory and applications*, Crc Press, 1998.

- [152] S. P. Bhat, D. S. Bernstein, Continuous finite-time stabilization of the translational and rotational double integrators, *IEEE Transactions on automatic control* 43 (5) (1998) 678–682.
- [153] A. S. Zinober, *Variable structure and Lyapunov control*, Vol. 193, Springer, 1994.
- [154] H. Khalil, J. Grizzle, *Nonlinear systems*, prentice hall, upper saddle river, nj (2002).
- [155] C. Pukdeboon, A review of fundamentals of lyapunov theory, *J. Appl. Sci* 10 (2) (2011) 55–61.
- [156] W. Perruquetti, J.-P. Barbot, *Sliding mode control in engineering*, CRC press, 2002.
- [157] J. Kim, G. Caire, A. F. Molisch, Quality-aware streaming and scheduling for device-to-device video delivery, *IEEE/ACM Transactions on Networking* 24 (4) (2015) 2319–2331.
- [158] S. Biricik, H. Komurcugil, Optimized sliding mode control to maximize existence region for single-phase dynamic voltage restorers, *IEEE Transactions on Industrial Informatics* 12 (4) (2016) 1486–1497.
- [159] H. Lee, V. I. Utkin, Chattering suppression methods in sliding mode control systems, *Annual reviews in control* 31 (2) (2007) 179–188.
- [160] L. Wu, J. Liu, S. Vazquez, S. K. Mazumder, Sliding mode control in power converters and drives: A review, *IEEE/CAA Journal of Automatica Sinica* 9 (3) (2021) 392–406.
- [161] H. Shen, F. Li, H. Yan, H. R. Karimi, H.-K. Lam, Finite-time event-triggered \mathcal{H}_∞ control for t-s fuzzy markov jump systems, *IEEE Transactions on Fuzzy Systems* 26 (5) (2018) 3122–3135. doi:10.1109/TFUZZ.2017.2788891.
- [162] Z.-Y. Sun, M.-M. Yun, T. Li, A new approach to fast global finite-time stabilization of high-order nonlinear system, *Automatica* 81 (2017) 455–463.
- [163] Q. Meng, C. Qian, R. Liu, Dual-rate sampled-data stabilization for active suspension system of electric vehicle, *International Journal of Robust and Nonlinear Control* 28 (5) (2018) 1610–1623.
- [164] A. Levant, Principles of 2-sliding mode design, *automatica* 43 (4) (2007) 576–586.
- [165] S. V. Emelyanov, S. K. Korovin, L. V. Levantovsky, Second order sliding modes in controlling uncertain systems, *Soviet journal of computer and system science* 24 (4) (1986) 63–68.
- [166] M. Zhihong, X. H. Yu, Terminal sliding mode control of mimo linear systems, *IEEE Transactions on Circuits and Systems I: Fundamental Theory and Applications* 44 (11) (1997) 1065–1070.

- [167] G. Bartolini, A. Ferrara, E. Usai, Output tracking control of uncertain nonlinear second-order systems, *Automatica* 33 (12) (1997) 2203–2212.
- [168] A. Levant, Sliding order and sliding accuracy in sliding mode control, *International journal of control* 58 (6) (1993) 1247–1263.
- [169] U. Pérez-Ventura, L. Fridman, When is it reasonable to implement the discontinuous sliding-mode controllers instead of the continuous ones? frequency domain criteria, *International Journal of Robust and Nonlinear Control* 29 (3) (2019) 810–828.
- [170] A. Levant, B. Shustin, Quasi-continuous mimo sliding-mode control, *IEEE Transactions on Automatic Control* 63 (9) (2017) 3068–3074.
- [171] J. A. Moreno, M. Osorio, Strict lyapunov functions for the super-twisting algorithm, *IEEE transactions on automatic control* 57 (4) (2012) 1035–1040.
- [172] K. P. Tee, B. Ren, S. S. Ge, Control of nonlinear systems with time-varying output constraints, *Automatica* 47 (11) (2011) 2511–2516.
- [173] H. Obeid, L. M. Fridman, S. Laghrouche, M. Harmouche, Barrier function-based adaptive sliding mode control, *Automatica* 93 (2018) 540–544.
- [174] S. Ding, J. H. Park, C.-C. Chen, Second-order sliding mode controller design with output constraint, *Automatica* 112 (2020) 108704.
- [175] Y. Shtessel, C. Edwards, L. Fridman, A. Levant, et al., *Sliding mode control and observation*, Vol. 10, Springer, 2014.
- [176] R. Ling, Z. Shu, Q. Hu, Y.-D. Song, Second-order sliding-mode controlled three-level buck dc–dc converters, *IEEE Transactions on Industrial Electronics* 65 (1) (2017) 898–906.
- [177] M. I. Martinez, A. Susperregui, G. Tapia, Second-order sliding-mode-based global control scheme for wind turbine-driven dfigs subject to unbalanced and distorted grid voltage, *IET Electric Power Applications* 11 (6) (2017) 1013–1022.
- [178] V. Utkin, Discussion aspects of high-order sliding mode control, *IEEE Transactions on Automatic Control* 61 (3) (2015) 829–833.
- [179] M. Zak, Terminal attractors for addressable memory in neural networks, *Physics Letters A* 133 (1-2) (1988) 18–22.
- [180] S. Venkataraman, S. Gulati, Control of nonlinear systems using terminal sliding modes (1993).
- [181] X. Yu, Y. Feng, Z. Man, Terminal sliding mode control—an overview, *IEEE Open Journal of the Industrial Electronics Society* 2 (2020) 36–52.

- [182] Y. Feng, X. Yu, F. Han, On nonsingular terminal sliding-mode control of nonlinear systems, *Automatica* 49 (6) (2013) 1715–1722.
- [183] Y. Feng, F. Han, X. Yu, Chattering free full-order sliding-mode control, *Automatica* 50 (4) (2014) 1310–1314.
- [184] S. Yu, X. Yu, B. Shirinzadeh, Z. Man, Continuous finite-time control for robotic manipulators with terminal sliding mode, *Automatica* 41 (11) (2005) 1957–1964.
- [185] V. Utkin, A. Poznyak, Y. Orlov, A. Polyakov, Conventional and high order sliding mode control, *Journal of the Franklin Institute* 357 (15) (2020) 10244–10261.
- [186] F.-J. Chang, E.-C. Chang, T.-J. Liang, J.-F. Chen, Digital-signal-processor-based dc/ac inverter with integral-compensation terminal sliding-mode control, *IET Power Electronics* 4 (1) (2011) 159–167.
- [187] R.-J. Lian, Adaptive self-organizing fuzzy sliding-mode radial basis-function neural-network controller for robotic systems, *IEEE Transactions on Industrial Electronics* 61 (3) (2013) 1493–1503.
- [188] J. Yu, J. Liu, Z. Wu, H. Fang, Depth control of a bioinspired robotic dolphin based on sliding-mode fuzzy control method, *IEEE Transactions on Industrial Electronics* 65 (3) (2017) 2429–2438.
- [189] D. Qian, G. Fan, Neural-network-based terminal sliding mode control for frequency stabilization of renewable power systems, *IEEE/CAA Journal of Automatica Sinica* 5 (3) (2018) 706–717.
- [190] R. S. Sutton, A. G. Barto, *Reinforcement learning: An introduction*, MIT press, 2018.
- [191] F. L. Lewis, K. G. Vamvoudakis, Optimal adaptive control for unknown systems using output feedback by reinforcement learning methods, in: *IEEE ICCA 2010*, IEEE, 2010, pp. 2138–2145.
- [192] K. Rsetam, Z. Cao, Z. Man, Cascaded-extended-state-observer-based sliding-mode control for underactuated flexible joint robot, *IEEE Transactions on Industrial Electronics* 67 (12) (2020) 10822–10832. doi:10.1109/TIE.2019.2958283.
- [193] S.-L. Shi, J.-X. Li, Y.-M. Fang, Extended-state-observer-based chattering free sliding mode control for nonlinear systems with mismatched disturbance, *IEEE Access* 6 (2018) 22952–22957.
- [194] W. Gao, Y. Wang, A. Homaifa, Discrete-time variable structure control systems, *IEEE transactions on Industrial Electronics* 42 (2) (1995) 117–122.
- [195] W. Gao, J. C. Hung, Variable structure control of nonlinear systems: A new approach, *IEEE transactions on Industrial Electronics* 40 (1) (1993) 45–55.

- [196] G. Singh, K. Holé, Guaranteed performance in reaching mode of sliding mode controlled systems, *Sadhana* 29 (2004) 129–141.
- [197] Y. Liu, B. Zhou, H. Wang, S. Fang, A new sliding mode control for permanent magnet synchronous motor drive system based on reaching law control, in: 2009 4th IEEE Conference on Industrial Electronics and Applications, IEEE, 2009, pp. 1046–1050.
- [198] C. J. Fallaha, M. Saad, H. Y. Kanaan, K. Al-Haddad, Sliding-mode robot control with exponential reaching law, *IEEE Transactions on industrial electronics* 58 (2) (2010) 600–610.
- [199] C. J. Fallaha, M. Saad, H. Y. Kanaan, K. Al-Haddad, Sliding-mode robot control with exponential reaching law, *IEEE Transactions on Industrial Electronics* 58 (2) (2011) 600–610. doi:10.1109/TIE.2010.2045995.
- [200] A. Bartoszewicz, A new reaching law for sliding mode control of continuous time systems with constraints, *Transactions of the Institute of Measurement and Control* 37 (4) (2015) 515–521.
- [201] M. Carpita, M. Marchesoni, Experimental study of a power conditioning system using sliding mode control, *IEEE transactions on power electronics* 11 (5) (1996) 731–742.
- [202] E.-C. Chang, T.-J. Liang, J.-F. Chen, F.-J. Chang, Real-time implementation of grey fuzzy terminal sliding mode control for pwm dc–ac converters, *IET Power Electronics* 1 (2) (2008) 235–244.
- [203] A. R. Gautam, D. Fulwani, Adaptive smc for the second-order harmonic ripple mitigation: A solution for the micro-inverter applications, *IEEE Transactions on Power Electronics* 34 (8) (2018) 8254–8264.
- [204] M. Pichan, H. Rastegar, Sliding-mode control of four-leg inverter with fixed switching frequency for uninterruptible power supply applications, *IEEE Transactions on Industrial Electronics* 64 (8) (2017) 6805–6814.
- [205] X. Hao, X. Yang, T. Liu, L. Huang, W. Chen, A sliding-mode controller with multiresonant sliding surface for single-phase grid-connected vsi with an lcl filter, *IEEE transactions on power electronics* 28 (5) (2012) 2259–2268.
- [206] H. Komurcugil, S. Ozdemir, I. Sefa, N. Altin, O. Kukrer, Sliding-mode control for single-phase grid-connected {LCL} -filtered vsi with double-band hysteresis scheme, *IEEE Transactions on Industrial Electronics* 63 (2) (2015) 864–873.
- [207] J. Hu, L. Shang, Y. He, Z. Zhu, Direct active and reactive power regulation of grid-connected dc/ac converters using sliding mode control approach, *IEEE transactions on power electronics* 26 (1) (2010) 210–222.

- [208] L. Shen, D. D.-C. Lu, C. Li, Adaptive sliding mode control method for dc–dc converters, *IET Power Electronics* 8 (9) (2015) 1723–1732.
- [209] R. Guzman, L. G. de Vicuña, M. Castilla, J. Miret, J. de la Hoz, Variable structure control for three-phase lcl-filtered inverters using a reduced converter model, *IEEE Transactions on Industrial Electronics* 65 (1) (2017) 5–15.
- [210] F. Sebaaly, H. Vahedi, H. Y. Kanaan, N. Moubayed, K. Al-Haddad, Design and implementation of space vector modulation-based sliding mode control for grid-connected 3l-npc inverter, *IEEE Transactions on Industrial Electronics* 63 (12) (2016) 7854–7863.
- [211] Q. Yang, M. Saeedifard, M. A. Perez, Sliding mode control of the modular multi-level converter, *IEEE Transactions on Industrial Electronics* 66 (2) (2018) 887–897.
- [212] A. Zakipour, S. Shokri Kojori, M. Tavakoli Bina, Closed-loop control of the grid-connected z-source inverter using hyper-plane mimo sliding mode, *IET Power Electronics* 10 (15) (2017) 2229–2241.
- [213] F. Bagheri, H. Komurcugil, O. Kukrer, Fixed switching frequency sliding-mode control methodology for single-phase lcl-filtered quasi-z-source grid-tied inverters, in: *2018 IEEE 12th International Conference on Compatibility, Power Electronics and Power Engineering (CPE-POWERENG 2018)*, IEEE, 2018, pp. 1–6.
- [214] H. Trazamni, E. Babaei, M. Sabahi, Full soft-switching high step-up dc–dc converter based on active resonant cell, *IET Power Electronics* 10 (13) (2017) 1729–1739.
- [215] L. Malesani, R. Spiazzi, P. Tenti, Performance optimization of cuk converters by sliding-mode control, *IEEE Transactions on Power Electronics* 10 (3) (1995) 302–309.
- [216] O. Kukrer, H. Komurcugil, A. Doganalp, A three-level hysteresis function approach to the sliding-mode control of single-phase ups inverters, *IEEE Transactions on Industrial Electronics* 56 (9) (2009) 3477–3486.
- [217] V. Utkin, Variable structure systems with sliding modes, *IEEE Transactions on Automatic control* 22 (2) (1977) 212–222.
- [218] V. I. Utkin, Variable structure systems: Survey, Coordinated Science Laboratory Report no. T-27 (1976).
- [219] J. Y. Hung, W. Gao, J. C. Hung, Variable structure control: A survey, *IEEE transactions on industrial electronics* 40 (1) (1993) 2–22.
- [220] B. Draženović, The invariance conditions in variable structure systems, *Automatica* 5 (3) (1969) 287–295.

- [221] S. K. Gudey, R. Gupta, Recursive fast terminal sliding mode control in voltage source inverter for a low-voltage microgrid system, *IET Generation, Transmission & Distribution* 10 (7) (2016) 1536–1543.
- [222] M. B. Delghavi, S. Shoja-Majidabad, A. Yazdani, Fractional-order sliding-mode control of islanded distributed energy resource systems, *IEEE Transactions on Sustainable Energy* 7 (4) (2016) 1482–1491. doi:10.1109/TSTE.2016.2564105.
- [223] S. Tokat, I. Eksin, M. GÜZELKAYA, New approaches for on-line tuning of the linear sliding surface slope in sliding mode controllers, *Turkish Journal of Electrical Engineering and Computer Sciences* 11 (1) (2003) 45–60.
- [224] S.-B. Choi, D.-W. Park, S. Jayasuriya, A time-varying sliding surface for fast and robust tracking control of second-order uncertain systems, *Automatica* 30 (5) (1994) 899–904.
- [225] F. Yorgancıoğlu, H. Kömürçügil, Single-input fuzzy-like moving sliding surface approach to the sliding mode control, *Electrical Engineering* 90 (2008) 199–207.
- [226] A. Šabanovic, Variable structure systems with sliding modes in motion control—a survey, *IEEE Transactions on Industrial Informatics* 7 (2) (2011) 212–223.
- [227] C. Alfaro, R. Guzman, L. G. De Vicuna, H. Komurcugil, H. Martín, Distributed direct power sliding-mode control for islanded ac microgrids, *IEEE Transactions on Industrial Electronics* 69 (10) (2021) 9700–9710.
- [228] M. Barzegar-Kalashani, B. Tousi, M. A. Mahmud, M. Farhadi-Kangarlu, Robust nonlinear sliding mode controllers for single-phase inverter interfaced distributed energy resources based on super twisting algorithms, *ISA transactions* 123 (2022) 61–75.
- [229] X. Hao, Y. Luo, An smc-eso-based distortion voltage compensation strategy for pwm vsf of pmsm, *IEEE Journal of Emerging and Selected Topics in Power Electronics* 10 (5) (2022) 5686–5697.
- [230] F.-J. Lin, Y.-C. Hung, M.-T. Tsai, Fault-tolerant control for six-phase pmsm drive system via intelligent complementary sliding-mode control using tskfnn-amf, *IEEE Transactions on industrial electronics* 60 (12) (2013) 5747–5762.
- [231] Q. Tabart, I. Vechiu, A. Etxeberria, S. Bacha, Hybrid energy storage system microgrids integration for power quality improvement using four-leg three-level npc inverter and second-order sliding mode control, *IEEE Transactions on Industrial Electronics* 65 (1) (2017) 424–435.
- [232] H. Wang, X. Ge, Y.-C. Liu, Second-order sliding-mode mras observer-based sensorless vector control of linear induction motor drives for medium-low speed maglev applications, *IEEE Transactions on Industrial Electronics* 65 (12) (2018) 9938–9952.

- [233] L. Derafa, A. Benallegue, L. Fridman, Super twisting control algorithm for the attitude tracking of a four rotors uav, *Journal of the Franklin Institute* 349 (2) (2012) 685–699.
- [234] Y. Kali, M. Saad, K. Benjelloun, C. Khairallah, Super-twisting algorithm with time delay estimation for uncertain robot manipulators, *Nonlinear Dynamics* 93 (2018) 557–569.
- [235] M. Defoort, M. Djemai, A lyapunov-based design of a modified super-twisting algorithm for the heisenberg system, *IMA Journal of Mathematical Control and Information* 30 (2) (2013) 185–204.
- [236] L. Fridman, J. Davila, A. Levant, High-order sliding-mode observation for linear systems with unknown inputs, *Nonlinear Analysis: Hybrid Systems* 5 (2) (2011) 189–205.
- [237] F.-J. Lin, J.-C. Hwang, P.-H. Chou, Y.-C. Hung, Fpga-based intelligent-complementary sliding-mode control for pmlsm servo-drive system, *IEEE transactions on power electronics* 25 (10) (2010) 2573–2587.
- [238] S. K. Kommuri, S. B. Lee, K. C. Veluvolu, Robust sensors-fault-tolerance with sliding mode estimation and control for pmsm drives, *IEEE/ASME Transactions on Mechatronics* 23 (1) (2017) 17–28.
- [239] U. P. Ventura, L. Fridman, Chattering measurement in smc and hosmc, in: 2016 14th international workshop on variable structure systems (VSS), IEEE, 2016, pp. 108–113.
- [240] Y. Feng, X. Yu, F. Han, High-order terminal sliding-mode observer for parameter estimation of a permanent-magnet synchronous motor, *IEEE Transactions on industrial electronics* 60 (10) (2012) 4272–4280.
- [241] X. Zhang, L. Sun, K. Zhao, L. Sun, Nonlinear speed control for pmsm system using sliding-mode control and disturbance compensation techniques, *IEEE transactions on power electronics* 28 (3) (2012) 1358–1365.
- [242] J. D. Li, J. Zhang, Higher order sliding mode control for a class of mimo systems, in: *Advanced Materials Research*, Vol. 834, Trans Tech Publ, 2014, pp. 1105–1109.
- [243] V. Utkin, A. Poznyak, Y. Orlov, A. Polyakov, Conventional and high order sliding mode control, *Journal of the Franklin Institute* 357 (15) (2020) 10244–10261.
- [244] W. Gao, Y. Wang, A. Homaifa, Discrete-time variable structure control systems, *IEEE transactions on Industrial Electronics* 42 (2) (1995) 117–122.
- [245] J. Y. Hung, W. Gao, J. C. Hung, Variable structure control: A survey, *IEEE transactions on industrial electronics* 40 (1) (1993) 2–22.

- [246] J. Pan, W. Li, H. Zhang, Control algorithms of magnetic suspension systems based on the improved double exponential reaching law of sliding mode control, *International Journal of Control, Automation and Systems* 16 (6) (2018) 2878–2887.
- [247] C. J. Fallaha, M. Saad, H. Y. Kanaan, K. Al-Haddad, Sliding-mode robot control with exponential reaching law, *IEEE Transactions on industrial electronics* 58 (2) (2010) 600–610.
- [248] Y. Liu, Z. Wang, L. Xiong, J. Wang, X. Jiang, G. Bai, R. Li, S. Liu, Dfig wind turbine sliding mode control with exponential reaching law under variable wind speed, *International Journal of Electrical Power & Energy Systems* 96 (2018) 253–260.
- [249] L. Zheng, F. Jiang, J. Song, Y. Gao, M. Tian, A discrete-time repetitive sliding mode control for voltage source inverters, *IEEE Journal of emerging and selected topics in power electronics* 6 (3) (2017) 1553–1566.
- [250] Y. S. Abdalla, N. Ali, A. Alanazi, M. Alanazi, H. Armghan, M. A. Sharaf, A. R. Boudabbous, A. Armghan, Fast reaching law based integral terminal sliding mode controller for photovoltaic-fuel cell-battery-super capacitor based direct-current microgrid, *Journal of Energy Storage* 56 (2022) 105915.
- [251] L. K. Yadav, M. K. Verma, P. Joshi, S. Agrawal, M. A. Alotaibi, H. Malik, F. P. G. Márquez, M. A. Hossaini, A framework for qualitative analysis of voltage stability indices (vsi), *IEEE Access* (2024).
- [252] Y. Eldigair, A. R. Beig, J. Alsawalhi, Sensorless dtsmc of a three-level vsi fed pmsm drive, *IET Power Electronics* 13 (4) (2020) 788–797.
- [253] Y. Liu, Z. Wang, L. Xiong, J. Wang, X. Jiang, G. Bai, R. Li, S. Liu, Dfig wind turbine sliding mode control with exponential reaching law under variable wind speed, *International Journal of Electrical Power & Energy Systems* 96 (2018) 253–260.
- [254] A. Bartoszewicz, P. Leśniewski, New switching and nonswitching type reaching laws for smc of discrete time systems, *IEEE Transactions on Control Systems Technology* 24 (2) (2016) 670–677. doi:10.1109/TCST.2015.2440175.
- [255] H. Ma, Y. Li, Z. Xiong, Discrete-time sliding-mode control with enhanced power reaching law, *IEEE Transactions on Industrial Electronics* 66 (6) (2018) 4629–4638.
- [256] S. Tokat, I. Eksin, M. GÜZELKAYA, New approaches for on-line tuning of the linear sliding surface slope in sliding mode controllers, *Turkish Journal of Electrical Engineering and Computer Sciences* 11 (1) (2003) 45–60.
- [257] J. Liu, X. Shen, A. M. Alcaide, Y. Yin, J. I. Leon, S. Vazquez, L. Wu, L. G. Franquelo, Sliding mode control of grid-connected neutral-point-clamped converters

- via high-gain observer, *IEEE Transactions on Industrial Electronics* 69 (4) (2021) 4010–4021.
- [258] X. Shen, J. Liu, A. M. Alcaide, Y. Yin, J. I. Leon, S. Vazquez, L. Wu, L. G. Franquelo, Adaptive second-order sliding mode control for grid-connected npc converters with enhanced disturbance rejection, *IEEE Transactions on Power Electronics* 37 (1) (2021) 206–220.
- [259] S.-B. Choi, D.-W. Park, S. Jayasuriya, A time-varying sliding surface for fast and robust tracking control of second-order uncertain systems, *Automatica* 30 (5) (1994) 899–904.
- [260] A. Merabet, L. Labib, A. M. Ghias, C. Ghenai, T. Salameh, Robust feedback linearizing control with sliding mode compensation for a grid-connected photovoltaic inverter system under unbalanced grid voltages, *IEEE Journal of Photovoltaics* 7 (3) (2017) 828–838.
- [261] O. Lopez-Santos, L. Martinez-Salamero, G. Garcia, H. Valderrama-Blavi, T. Sierra-Polanco, Robust sliding-mode control design for a voltage regulated quadratic boost converter, *IEEE transactions on power electronics* 30 (4) (2014) 2313–2327.
- [262] F.-J. Chang, E.-C. Chang, T.-J. Liang, J.-F. Chen, Digital-signal-processor-based dc/ac inverter with integral-compensation terminal sliding-mode control, *IET Power Electronics* 4 (1) (2011) 159–167.
- [263] F. Mohammadhassani, H. G. Narm, Dynamic sliding mode control of single-stage boost inverter with parametric uncertainties and delay, *IET Power Electronics* 14 (12) (2021) 2127–2138.

APPENDIX A

APPENDIX ONE



MicroLabBox

- Compact all-in-one development system for the laboratory
- More than 100 high-performance I/O channels with easy access
- Comprehensive support for electric motor control
- Three connector panel variants available

MicroLabBox

Compact prototyping unit for the laboratory

Highlights

- Compact all-in-one development system for laboratory purposes
- Dual-core real-time processor at 2 GHz
- User-programmable FPGA
- More than 100 channels of high-performance I/O
- Dedicated electric motor control features
- Ethernet and CAN bus interfaces
- Easy I/O access via integrated connector panel



Application Areas

MicroLabBox is a compact development system for the laboratory that combines compact size and cost-effectiveness with high performance and versatility. MicroLabBox lets you set up your control, test or measurement applications quickly and easily, and helps you turn your new control concepts into reality. More than 100 I/O channels of different types make MicroLabBox a versatile system that can be used in mechatronic research and development areas, such as robotics, medical engineering, electric drives control, renewable energy, vehicle engineering, or aerospace.

Key Benefits

High computation power combined with very low I/O latencies provide great real-time performance. A programmable FPGA gives you a high degree of flexibility and lets you run even extremely fast control loops, as required in applications such as electric motor control or active noise and vibration cancellation.

MicroLabBox is supported by a comprehensive dSPACE software package (p. 5), including, e.g., Real-Time Interface (RTI) for Simulink® for model-based I/O integration and the experiment software ControlDesk, which provides access to the real-time application during run time by means of graphical instruments.

Versatility through Connector Panel Variants

MicroLabBox is available in three connector panel variants (p. 3-4), offering different types and/or positions of the I/O connectors. The front panel variant provides Sub-D connectors at the front to access the connectors of the MicroLabBox when it is included in a stack of laboratory equipment or easily switch between wire harnesses. The top panel variant is available with two different connector types and is ideal for desk use.

Equipped with BNC and Sub-D connectors, the top panel MicroLabBox allows easy access to the analog I/O channels via probes that are typically used in laboratories to offer

high analog signal quality. Additionally, a top panel variant with spring-cage terminal blocks, which are often used in industrial automation, is available. This means, signal connections can be changed very fast and conveniently by means of a common push-in and release mechanism of the clamp with a standard screwdriver. To make wiring and signal tracing as user-friendly as possible, all panel variants show the pinout information on the unit itself. The pinout information is also displayed in the I/O blocks of the implementation software Real-Time Interface (RTI).

Technical Details

Parameter		Specification		
MicroLabBox		Front Panel Variant	Top Panel Variant with BNC Connectors	Top Panel Variant with Spring-Cage Terminal Blocks
Processor	Real-time processor	<ul style="list-style-type: none"> ■ NXP (Freescale) QorIQ P5020, dual-core, 2 GHz ■ 32 KB L1 data cache per core, 32 KB L1 instruction cache per core, 512 KB L2 cache per core, 2 MB L3 cache total 		
	Host communication co-processor	<ul style="list-style-type: none"> ■ NXP (Freescale) QorIQ P1011 800 MHz for communication with host PC 		
Memory		<ul style="list-style-type: none"> ■ 1 GB DRAM ■ 128 MB flash memory 		
Boot time		<ul style="list-style-type: none"> ■ Autonomous booting of applications from flash (depending on application size), ~5 s for a 5 MB application 		
Inter- faces	Host interface	<ul style="list-style-type: none"> ■ Integrated Gigabit Ethernet host interface 		
	Ethernet real-time I/O interface	<ul style="list-style-type: none"> ■ Integrated low-latency Gigabit Ethernet I/O interface 		
	USB interface	<ul style="list-style-type: none"> ■ USB 2.0 interface for data logging ("flight recorder") and booting applications via USB mass storage device (max. 32 GB supported) 		
	CAN interface	<ul style="list-style-type: none"> ■ 2 CAN channels (partial networking supported) 		
	Serial interface	<ul style="list-style-type: none"> ■ 2 x UART (RS232/422/485) interface 		
	LVDS interface	<ul style="list-style-type: none"> ■ 1 x LVDS interface to connect with the Programmable Generic Interface PGI1 		
Programmable FPGA ¹⁾		<ul style="list-style-type: none"> ■ Xilinx® Kintex®-7 XC7K325T FPGA 		
Analog input	Resolution and type	<ul style="list-style-type: none"> ■ 8 14-bit channels, 10 Msps, differential; functionality: free running mode ■ 24 16-bit channels, 1 Msps, differential; functionality: single conversion and burst conversion mode with different trigger and interrupt options 		
	Input voltage range	<ul style="list-style-type: none"> ■ -10 ... 10 V 		
Analog output	Resolution and type	<ul style="list-style-type: none"> ■ 16 16-bit channels, 1 Msps, settling time: 1 µs 		
	Output voltage range	<ul style="list-style-type: none"> ■ -10 ... 10 V 		
	Output current	<ul style="list-style-type: none"> ■ ± 8 mA 		
Digital I/O		<ul style="list-style-type: none"> ■ 48 bidirectional channels, 2.5/3.3/5 V (single-ended); functionality: bit I/O, PWM generation and measurement (10 ns resolution), pulse generation and measurement (10 ns resolution), 4 x SPI Master ■ 12 bidirectional channels (RS422/485 type) to connect sensors with differential interfaces 		
Electric motor control I/O functionality	Separate interfaces	<ul style="list-style-type: none"> ■ 2 x Resolver interface 		
	Functionality on digital I/O channels	<ul style="list-style-type: none"> ■ 6 x Encoder sensor input ■ 2 x Hall sensor input ■ 2 x EnDat interface ■ 2 x SSI interface ■ Synchronous multi-channel PWM ■ Block commutational PWM 		
Sensor supply		<ul style="list-style-type: none"> ■ 1 x 12 V, max. 3 W/250 mA (fixed) ■ 1 x 2 ... 20 V, max. 1 W/200 mA (variable) 		
Feedback elements		<ul style="list-style-type: none"> ■ Programmable buzzer ■ Programmable status LEDs 		
Theft protection		<ul style="list-style-type: none"> ■ Kensington® lock 		
Cooling		<ul style="list-style-type: none"> ■ Active cooling (temperature-controlled fan) 		
Physical connections		<ul style="list-style-type: none"> ■ 4 x Sub-D 50 I/O connectors ■ 4 x Sub-D 9 I/O connectors 	<ul style="list-style-type: none"> ■ 2 x Sub-D 50 I/O connectors ■ 48 x BNC I/O connectors ■ 4 x Sub-D 9 I/O connectors 	<ul style="list-style-type: none"> ■ 2 x Sub-D 9 I/O connectors ■ 27 x spring-cage terminal block connectors with 8 pins each
		<ul style="list-style-type: none"> ■ 3 x RJ45 for Ethernet (host and I/O) ■ USB Type A (for data logging) ■ 2 x 2 banana connectors for sensor supply ■ Power supply 		

¹⁾ User-programmable via RTI FPGA Programming Blockset. Using the RTI FPGA Programming Blockset requires additional software.

Parameter		Specification		
MicroLabBox		Front Panel Variant	Top Panel Variant with BNC Connectors	Top Panel Variant with Spring-Cage Terminal Blocks
Physical characteristics	Enclosure size	■ Approx. 310 x 250 x 110 mm (12.2 x 9.8 x 4.3 in)	■ Approx. 310 x 250 x 115 mm (12.2 x 9.8 x 4.5 in)	■ Approx. 310 x 250 x 110 mm (12.2 x 9.8 x 4.3 in)
	Temperature	■ 0 ... 50 °C (ambient temperature)		
	Power supply	■ 100 ... 240 V AC, 50 ... 60 Hz		
	Power consumption	■ 125 W		

Panel Variants



MicroLabBox, front panel variant



MicroLabBox, top panel variant with BNC connectors



MicroLabBox, top panel variant with spring-cage terminal blocks

Order Information

Products	Order Number
MicroLabBox, front panel variant	■ MLBX_1302F
MicroLabBox, top panel variant with BNC Connectors	■ MLBX_1302T
MicroLabBox with spring-cage terminal blocks	■ MLBX_1302S

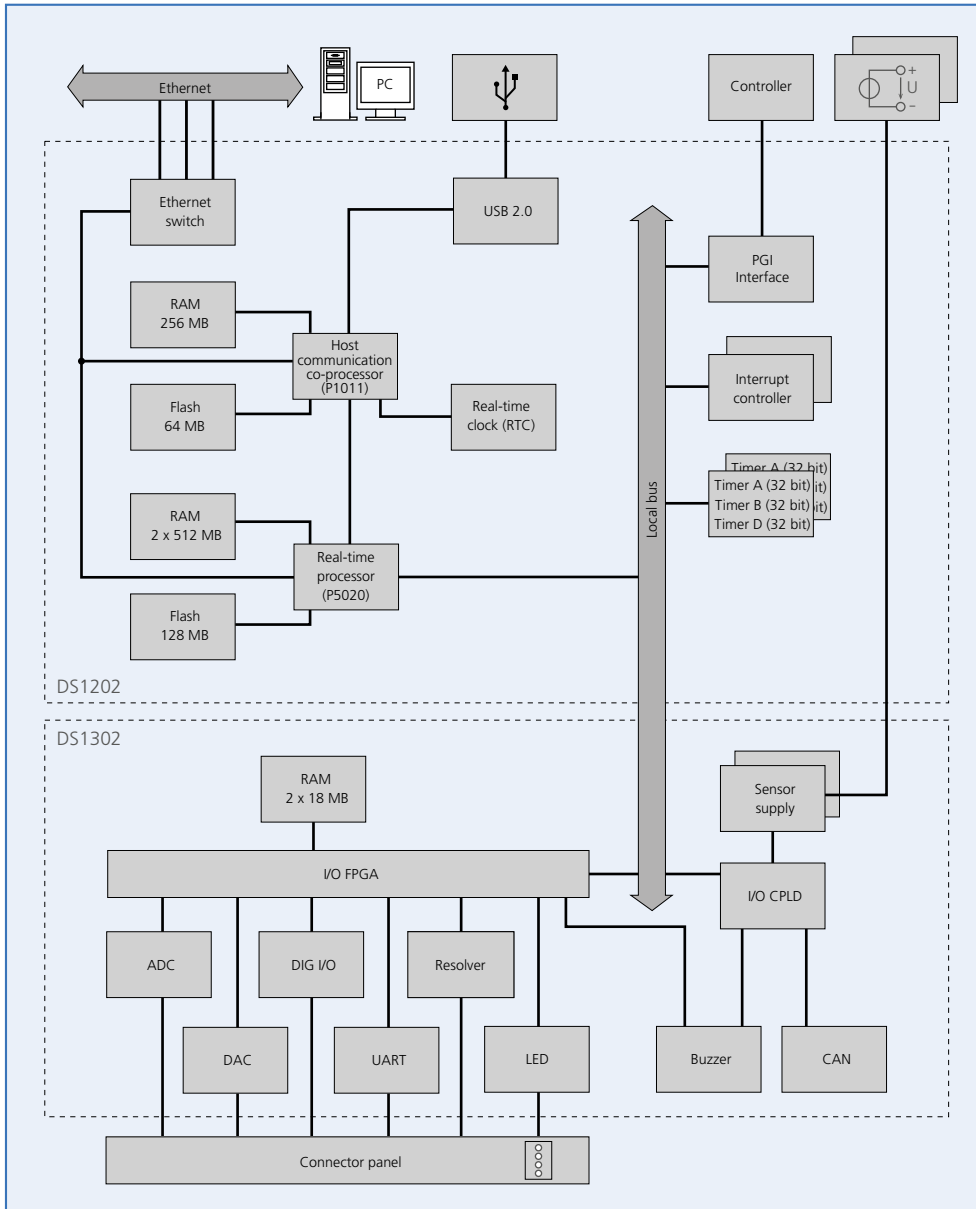
Relevant Software and Hardware

Software	Order Number	
Included	<ul style="list-style-type: none"> ■ Data retrieval utility for flight recorder read-out ■ Comprehensive C libraries (e.g., digital I/O support) 	–
Required	<ul style="list-style-type: none"> ■ For Simulink®-based use cases: Real-Time Interface (RTI) ■ GNU C Compiler for Power PC 	<ul style="list-style-type: none"> ■ RTI ■ MLBX_COMP
Optional	<ul style="list-style-type: none"> ■ ControlDesk ■ For multi-core applications: RTI-MP ■ RTI CAN Blockset ■ RTI CAN MultiMessage Blockset ■ RTI Electric Motor Control Blockset (p. 10-11) ■ RTI USB Flight Recorder Blockset (part of Real-Time Interface) ■ RTI Ethernet Blockset ■ RTI FPGA Programming Blockset ■ Platform API Package 	<ul style="list-style-type: none"> See relevant product information ■ RTI_MP ■ RTICAN_BS ■ RTICANMM_BS ■ RTI_EMCC_BS ■ RTI ■ RTI_ETHERNET_IO See relevant product information ■ PLATFORM_API

Hardware	Order Number	
Included	<ul style="list-style-type: none"> ■ Ethernet patch cable (HSL_PATCH) for host connection ■ Power supply cable ■ Set of Sub-D plugs ■ Case for storage and transportation 	–
Optional	<ul style="list-style-type: none"> ■ Adapter cable 50-pin Sub-D to WAGO terminal panel ■ RapidPro SC Unit ■ RapidPro Power Unit 	<ul style="list-style-type: none"> ■ MLBX_CAB1 See relevant product information See relevant product information

MicroLabBox

Block Diagram

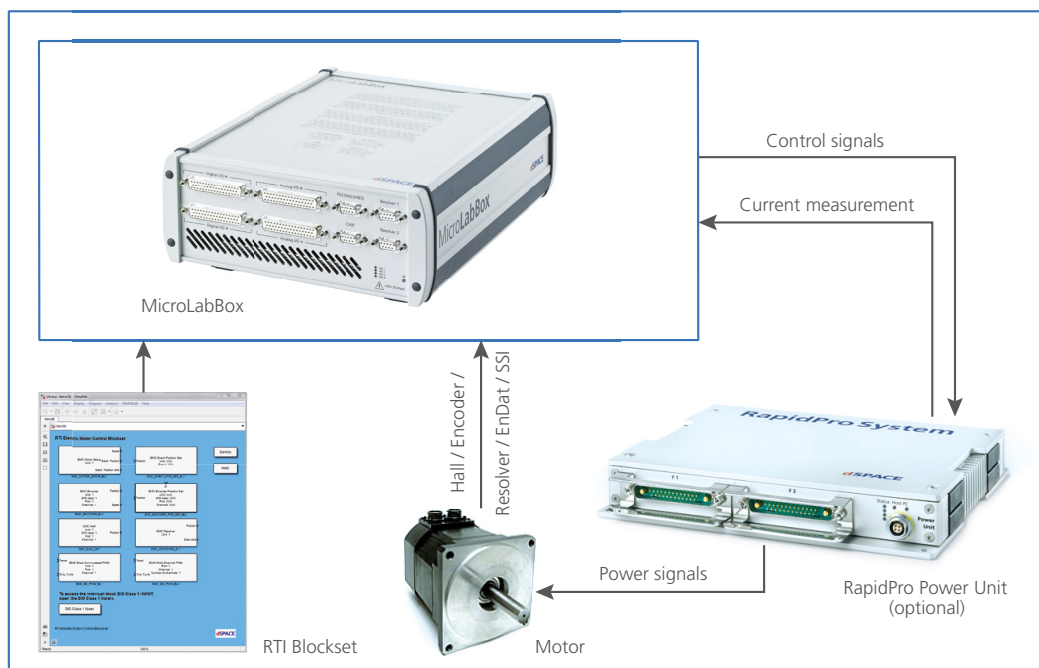


Use Cases (Examples)

Developing Control Strategies for Electric Motors

MicroLabBox is ideal for developing control functions for many different electric motors, such as asynchronous motors, brushless DC (BLDC) motors, and permanent magnet synchronous motors (PMSM). The RTI blocks for electric

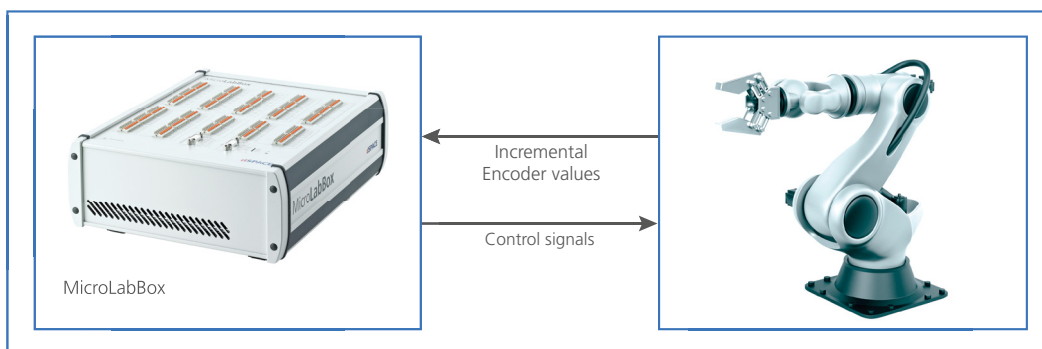
motor control (p. 10, RTI Electric Motor Control Blockset) ensure convenient and comprehensive configuration options for the I/O interfaces.



Rapid Control Prototyping in Robotics

Its numerous interfaces make MicroLabBox ideal for many kinds of robotics applications. In this example, MicroLabBox replaces the robot's position controller and receives the robot's incremental encoder signals for determining the current position of the robot. Then, the real-time processor

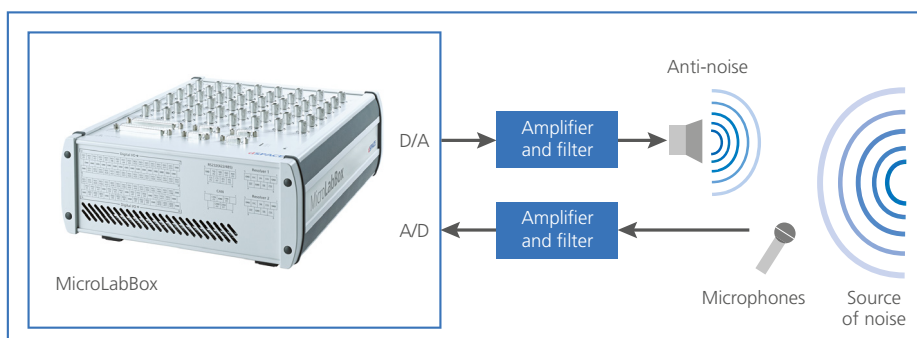
calculates the control algorithm and sends the controller output with position and velocity data back to the robot. Thus, you can implement and test different control algorithms very quickly.



Active Noise Cancellation and Vibration Damping

Applications in active noise cancellation (ANC: e.g., for hi-fi headphones, cell phones or a passenger car cabin) and vibration damping (e.g., for reducing wear and tear or industrial plant noise) pose a particularly great challenge for signal processing. For ANC applications, for example, the anti-noise has to be calculated and generated before the original noise reaches the respective noise cancella-

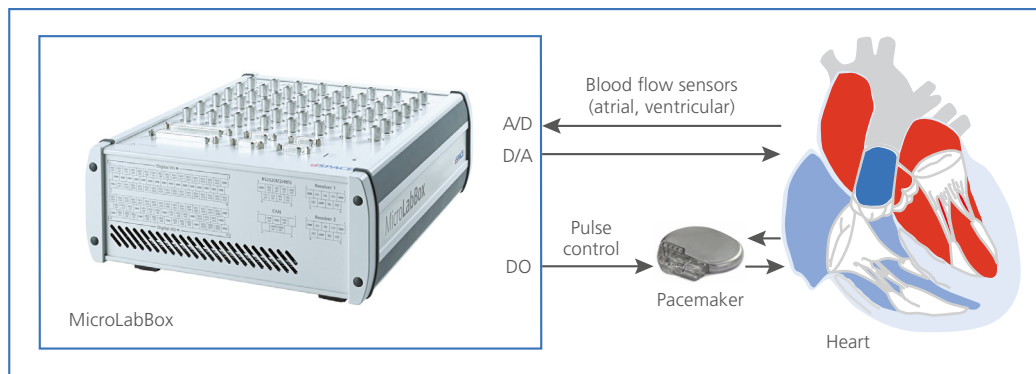
tion speaker or the point in space designated for noise cancelling. MicroLabBox's fast real-time processor and low-latency I/O access make it the right tool for developing new algorithms for active noise reduction and vibration reduction. MicroLabBox achieves control loops of only a few microseconds. If the requirements are even higher, the algorithms can always be offloaded to the integrated FPGA.



Developing and Testing Medical Devices

Safety and reliability play a crucial role in the development of medical devices. New functions must have an optimal design and undergo extensive testing. In many cases, capturing and preprocessing signals is an integral part of function development. With MicroLabBox, you can outsource extensive and computation-intensive signal preprocessing tasks, such as filtering or signal analysis, to an integrated FPGA. Connecting BNC cables directly to MicroLabBox for processing analog signals minimizes the influence of

external errors on the signal and makes it possible to achieve a high signal quality. During or after the development of the medical device, MicroLabBox can also be used as a testing system. With it, you can reproducibly simulate many different environment conditions, e.g., based on test algorithms or existing measurement data. This increases the medical device's maturity, saves time, reduces costs, and minimizes the risks compared to tests on a living organism.

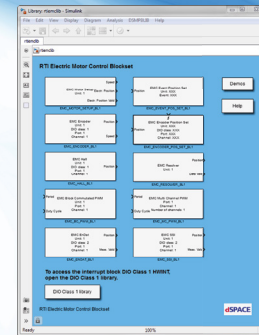


RTI Electric Motor Control Blockset

Configuring electric motor control I/O functions of MicroLabBox

Highlights

- Access to electric motor control specific I/O functionalities of MicroLabBox
- Easy configuration and implementation of Hall sensor inputs, incremental encoder, Resolver, EnDat, and SSI interfaces as well as PWM signal generation
- Automatic calculation and interpolation of the current motor speed, position, and angle, plus generation of asynchronous events



Application Areas

Electric motor controls play an important role in various application fields such as automotive industry, robotics, medical engineering, and many more, e.g., to comply with new, strict emission regulations or to build up more precise machines in industrial environments. Often, the control algorithm for an electric motor is a key point in fulfilling customers' requirements. But the effort of developing, implementing, and validating the required control algorithms in traditional tool chains can be very high, and these tool chains often lack flexibility. The MicroLabBox in combination with the RTI Electric Motor Control Blockset is the ideal system to reduce this effort. Developing and testing new control algorithms takes place in a model-based software environment with a minimum amount of time. The RTI Electric Motor Control Blockset is a user-friendly software interface that provides a link between your real-time hardware platform MicroLabBox and the model-based development software MATLAB®/Simulink®/Stateflow® from Mathworks.

Key Benefits

The RTI Electric Motor Control Blockset provides access to the electric motor control specific I/O functionalities of MicroLabBox and allows you to configure them easily and conveniently. No additional modeling effort is needed to use sensor interfaces commonly applied in electric motor applications such as Hall sensors, incremental encoder, resolver, EnDat, or SSI. In addition, ready-to-use Simulink blocks for generating different synchronous PWM signals are available. The current speed, position and angle of the electric motor are automatically calculated. If sensor interfaces with low resolution such as Hall sensors are used, an automatic interpolation can be enabled to achieve a higher sensor resolution and to improve the quality of the position measurement. When first starting the motor to get the current motor position it is possible to use the Hall sensor interface immediately, and then switch to a sensor with the higher resolution such as the encoder interface after one revolution of the electric motor. With this process, a valid position and the best resolution is always available for the controller. Simulink-based control models can be easily connected with the required I/O interfaces and then be downloaded to the MicroLabBox at the push of a button. The controller can be tested in a real environment with different sensors and actuators, and new motor control strategies can be developed much faster than in traditional tool chains.

Functionality Overview

Functionality	Description
General	<ul style="list-style-type: none"> ■ Accessing and configuring dedicated I/O functions for: <ul style="list-style-type: none"> ■ Resolver interfaces ■ Encoder sensor inputs ■ Hall sensor inputs ■ EnDat interfaces ■ SSI interfaces ■ Synchronous multi-channel PWMs ■ Block commutational PWMs ■ For electric motors with up to 6 phases and 16 pole pairs ■ Controlling 2 or more electric motors at the same time ■ Combining 2 sensors to extrapolate the position of the motor's rotor ■ Generating events for algorithm execution triggered by specified motor positions

Order Information

Product	Order Number
RTI Electric Motor Control Blockset	■ RTI_EMC_BS

Relevant Software and Hardware

Software	Order Number
Required For MicroLabBox ■ Real-Time Interface ¹⁾	■ RTI

Hardware	Order Number
Required For MicroLabBox ■ MicroLabBox ²⁾ with front or top panel	■ See p. 5

¹⁾ For information on standard hardware and software requirements for Real-Time Interface (RTI), please see Real-Time Interface product information.

²⁾ A corresponding compiler is required, please see p. 5.

© Copyright 2020 by dSPACE GmbH.

All rights reserved. Written permission is required for reproduction of all or parts of this publication. The source must be stated in any such reproduction. dSPACE is continually improving its products and reserves the right to alter the specifications of the products at any time without notice. "ConfigurationDesk", "ControlDesk", "dSPACE", "Embedded Success dSPACE", "MicroAutoBox", "MicroLabBox", "ProMINT", "SCALEXIO", "SYNECT", "SystemDesk", "TargetLink", and "VEOS" are trademarks or registered trademarks of dSPACE GmbH in the United States of America or in other countries or both. Other brand names or product names are trademarks or registered trademarks of their respective companies or organizations.

Germany

dSPACE GmbH
Rathenaustraße 26
33102 Paderborn
Tel.: +49 5251 1638-0
Fax: +49 5251 16198-0
info@dspace.de

United Kingdom

dSPACE Ltd.
Unit B7 · Beech House
Melbourn Science Park
Melbourn
Hertfordshire · SG8 6HB
Tel.: +44 1763 269 020
Fax: +44 1763 269 021
info@dspace.co.uk

France

dSPACE SARL
7 Parc Burospace
Route de Gisy
91573 Bièvres Cedex
Tel.: +33 169 355 060
Fax: +33 169 355 061
info@dspace.fr

Croatia

dSPACE Engineering d.o.o.
Ulica grada Vukovara 284
10000 Zagreb
Tel.: +385 1 4400 700
Fax: +385 1 4400 701
info@dspace.hr

China

dSPACE Mechatronic Control
Technology (Shanghai) Co., Ltd.
Unit 01-02,06-09, 19F/L
Middle Xizang Rd. 168
The Headquarters Building
200001 Shanghai
Tel.: +86 21 6391 7666
Fax: +86 21 6391 7445
infochina@dspace.com

Japan

dSPACE Japan K.K.
10F Gotenyama Trust Tower
4-7-35 Kitashinagawa
Shinagawa-ku
Tokyo 140-0001
Tel.: +81 3 5798 5460
Fax: +81 3 5798 5464
info@dspace.jp

USA and Canada

dSPACE Inc.
50131 Pontiac Trail
Wixom · MI 48393-2020
Tel.: +1 248 295 4700
Fax: +1 248 295 2950
info@dspaceinc.com